Novel Quorum Sensing Inhibitors targeting PqsR

Dissertation

Zur Erlangung des Grades des Doktors der Naturwissenschaften

der Naturwissenschaftlich-Technischen Fakultät

der Universität des Saarlandes

vorgelegt von

M. Sc. Christian M. Schütz

Saarbrücken

2020

Tag des Kolloqiums: 20.11.2020

Dekan: Univ.-Prof. Dr. rer. nat. Jörn Walter

Berichterstatter: Prof. Dr. Rolf Hartmann

Prof. Dr. Christian Ducho

Prof. Dr. Stefan Laufer

Akademische Mitarbeiterin: Dr. Angelika Ullrich

Vorsitz: Dr. Andreas Speicher

Die vorliegende Arbeit wurde von August 2016 bis Juni 2020 unter Anleitung von Herrn Univ.-Prof. Dr. Rolf W. Hartmann in der Fachrichtung Pharmazeutische und Medizinische Chemie der Naturwissenschaftlich-Technischen Fakultät der Universität des Saarlandes sowie am Helmholtz-Institut für Pharmazeutische Forschung Saarland (HIPS) in der Abteilung Drug Design and Optimization (DDOP) angefertigt.

"You eat, drink, and sleep your molecule."

Phil S. Baran

Acknowledgement

Ich bedanke mich herzlich bei allen, die zum Gelingen dieser Arbeit beigetragen haben.

Ein besonderes Dankeschön gilt hierbei Dr. Martin Empting, der mir ermöglicht hat meine Promotionsarbeit in diesem interessanten und spannenden Projekt anzufertigen. Darüber hinaus möchte ich mich bedanken für die Unterstützung, sein Vertrauen und damit einhergehend die Freiheiten die ich hatte um eigene Ideen verwirklichen zu können.

Weiterhin gilt mein besonderer Dank Prof. Dr. Rolf W. Hartmann, der mir die Möglichkeit gab, meine Promotionsarbeit in seiner Arbeitsgruppe anfertigen zu dürfen, für die sehr gute Betreuung, seine wissenschaftliche Expertise und Kreativität, als auch für die Übernahme des Erstgutachtens.

Herzlich bedanken möchte ich mich ebenfalls bei Prof. Dr. Christian Ducho für die exzellente wissenschaftliche Begleitung dieser Arbeit und die Übernahme des Zweitgutachtens.

Bei Dr. Angelika Ullrich möchte ich mich für die Übernahme der Aufgabe der akademischen Mitarbeiterin bedanken.

Ganz besonders möchte ich mich bei Simone Amann, Tabea Wittmann, Jeannine Jung, Dennis Jener und Selina Wolter für die Erhebung der biologischen Daten (Pyocyanin Assay, Reportergen Assay, MTT Assay) sowie der Durchführung einiger Löslichkeitsversuche.

Im besonderen Maße möchte ich vor allem dem ganzen PqsR Team danken, ohne welches diese Arbeit nicht zustande hätte kommen können, darunter neben Dr. Martin Empting, Prof. Dr. Rolf Hartmann, Prof. Anna K. H. Hirsch vor allen Dingen Dr. Christine Maurer und Dr. Ahmed Kamal Ashraf, sowie Dr. Mostafa Hamed, Dr. Ahmed Saad Abdelsamie Ahmed und Dr. Samir Yahiaoui danken. Ferner gilt ein ganz besonderes Dankeschön Dr. Teresa Röhrig und Dr. Christian Herr für die Durchführung der *in vivo* target engagement Versuche, sowie Dr. Katharina Rox für die Erhebung der *in vivo* PK Daten. Ebenso möchte ich mich bei unseren Kooperationspartnern von Sygnature Discovery, Dr. Carsten Börger, Dr. Lorenz Siebenbürger und Dr. Marius Wirth von der PharmBioTec, Saretius, Cyprotex und Ascenion bedanken für die Generierung diverser DMPK und safety pharmacology Daten und die Hilfe bei der Anfertigung der Patente. Ein großer Dank gilt auch dem Kristallographie Team um Prof. Dr. Wulf Blankenfeldt, Dr. Stefan Schmelz und Dr. Andrea Scrima. Mein Dank gilt auch Dr. Thomas Hesterkamp, Dr. Marina Steindorff und unserem Projektpaten Dr. Manfred Rössner.

Mein Dank gilt auch besonders meinem Bachelor Studenten Amir Hodzic, der mich bei der Synthese einiger Analoga unterstütze, sowie meinen Vertiefungspraktikanten Maximilian Bauer, Robert Becker und Max Kappus für die synthetische Unterstützung.

Bei Dr. Andreas Kany möchte ich mich weiterhin für Durchführung einiger Experimente zur metabolischen Stabilität bedanken und Dr. Jelena Konstantinovic für die Aufnahme der hochaufgelösten Massenspektren.

Bei Dr. Lukas Junk und Dr. Alexander Kiefer möchte ich mich für das gewissenhafte und zügige Korrekturlesen dieser Arbeit bedanken.

Ein ganz großes Dankeschön an die gesamte DDOP/CBCH Abteilung. Hierbei möchte ich besonders meinen engsten Kollegen Dr. Alexander Kiefer, Dr. Andreas Kany, Valentin Jakob, Dr. Alwin Hartmann, Dr. Isabell Walter, Cansu Kaya und Federica Mancini danken.

Im Besonderen möchte ich bei meiner „Partnerin in crime“ Philine Kirsch a.k.a. beste Laborpartnerin überhaupt bedanken, für die vielen Stunden vor und fernab der Abzüge, für sämtliche wissenschaftliche und nicht wissenschaftliche Diskussionen und vor allem die Freundschaft.

Ein großer Dank gilt vor allem all meinen Freunden und Musikerkollegen die in der ganzen Zeit für die nötige Abwechslung gesorgt haben.

Bei meinen Eltern Harald und Monika Schütz möchte ich mich für die finanzielle Unterstützung während meines Studiums bedanken.

Insbesondere möchte ich mich bei meiner Freundin Belinda König bedanken, die mich vor allem in der Endphase dieser Arbeit motiviert und ertragen hat. Ein großes Dankeschön für die Geduld, sowie für die notwendige Ablenkung und die Unterstützung.

Summary

Pseudomonas aeruginosa, a ubiquitous Gram-negative bacterium is counted among the most clinical relevant pathogens according to the World Health Organization (WHO). The opportunistic pathogen is able to form biofilms and persister cells, which makes it hard to eradicate and renders common antibiotic treatment ineffective. These factors are under control of the Pseudomonas Quinolone Signal (PQS) quorum sensing (QS) system, which thereofre displays an attractive drug target.

This work describes the design and synthesis of novel PqsR inverse agonists based on a previously described hit compound. A highly divergent synthetic route was established and enabled the synthesis of various classes of 2-(trifluoromethyl)pyridin-4-amines providing deep structure-activity relationship (SAR) insights. Lead generation resulted in a highly active optimized compound possessing also good drug metabolism and pharmacokinetic (DMPK) properties. Furthermore, this compound showed *in vivo* target engagement in a murine lung infection model. Based on this lead compound, a medicinal chemistry-driven multiparameter optimization allowed for deeper insights into structure-activity relationship (SAR) and structure-property relationship (SPR). In the course of this thesis, several compounds were synthesized with improved activity, solubility and metabolic stability. In addition, compounds based on computer-aided drug design were synthesized.

Zusammenfassung

Pseudomonas aeruginosa, ein omnipräsentes Gramnegatives Bakterium zählt laut Weltgesundheitsorganisation (WHO) zu den klinisch relevantesten Pathogenen. Dieses opportunistische Pathogen ist in der Lage, Biofilme und Persisterzellen zu bilden, die eine Eradizierung erschweren und übliche Antibiotika Therapien ineffektiv werden lassen. Diese Faktoren unterliegen dem Pseudomonas Quinolone Signal (PQS) Quorum Sensing (QS) System, welches dabei ein attraktives Target zur Behandlung dar.

Diese Arbeit beschreibt das Design und die Synthese von neuen PqsR inversen Agonisten, basierend auf einer bereits beschriebenen hit Verbindung. Eine hoch divergente Syntheseroute wurde dabei etabliert und ermöglichte die Synthese verschiedener Klassen von 2-(Trifluoromethyl)pyridin-4-aminen und lieferte tiefe Einblicke in die Struktur-Aktivitätsbeziehungen. Die Leitstruktur Generierung brachte eine hoch-aktive Verbindung hervor, die ebenso über gute pharmakokinetische Eigenschaften verfügte und in einem murinen Lungeninfektionsmodel *in vivo* target engagement zeigte. Ausgehend von dieser Leitstruktur lieferte eine medizinal-chemische Multiparameter-Optimierung tiefe Einblicke in Struktur-Aktivitätsbeziehungen und Struktur-Eigenschaftsbeziehungen. Im Zuge dieser Leitstruktur Optimierung wurden verschiedene Verbindungen mit verbesserter Aktivität, Löslichkeit und Stabilität synthetisiert. Darüber hinaus wurden Verbindungen basierend auf Computer-gestütztem Wirkstoffdesign synthetisiert.

Abbreviations

°C	degree Celsius
µM	micromolar
9-BBN	9-borabicyclo[3.3.1]nonane
Ac	acetyl
acac	acetylacetonate
AhR	aryl hydrocarbon receptor
AMR	antimicrobial resistance
AUC	area under curve
BALF	bronchoalveolar lavage fluid
Bn	benzyl
Boc	*tert*-butyloxycarbonyl
Boc_2O	*di-tert*-butyldicarbonate
BPI	Benzophenon imine
cat	catalytic
Cbz	carboxybenzyl
CDI	1,1'-carbonyldiimidazole
CF	cystic fibrosis
CFU	colony forming units
cpd	compound
CuAAC	copper(I)-catalyzed azide alkyne cycloaddition
Cy	cyclohexyl
CYP	cytochrom P450
d	days
dba	dibenzylideneacetone
DCM	dichloromethan
DIPEA	*N,N*-diisopropylethylamine
DMAP	4-(dimethylamino)-pyridine
DMEDA	*N,N'*-dimethylethylenediamine
DMF	*N,N'*-dimethylformamide
DMPK	drug metabolism and pharmacokinetics
DMSO	dimethylsulfoxide
DNA	deoxyribonucleic acid
DPPA	diphenyl phosphoryl azide
dppf	1,1'-bis(diphenylphosphino)ferrocene
eDNA	extracellular DNA
ELF	epithelial lining fluid
EPS	extracellular polymeric substances
Et	ethyl
EtOH	ethanol
FDA	Food and Drug Administration
GP	general procedure
h	hour

h S9	human S9 fraction
hERG	human Ether-a-go-go Related Gene
HHQ	4-hydroxy-2-heptylquinoline
HMDS	hexamethyldisilazane
HQNO	2-heptyl-4-hydroxyquinoline N-oxide
HRMS	high resolution mass spectrometry
HTS	high-throughput-screening
IC_{50}	half maximal inhibitory concentration
*i*Pr	isopropyl
i.v.	intravenously
KHMDS	potassium hexamethyldisilazide
LC-MS	liquid chromatography-mass spectrometry
LC-MSMS	liquid chromatography-tandem mass spectrometry
LD_{50}	median lethal dose
LDA	lithium diisopropylamide
M	molarity
mAb	monoclonal antibody
mCPBA	meta-chloroperoxybenzoic acid
Me	methyl
MeCN	acetonitrile
MeOH	methanol
min	minute
MRT	mean residence time
MvfR	multivirulence factor regulator
n.d.	not determined
NHMDS	sodium hexamethyldisilazide
nM	nanomolar
NMP	N-methyl-2-pyrrolidone
NMR	nuclear magnetic resonance spectroscopy
OMPTA	outer membrane protein targeting antibiotics
PA	Pseudomonas aeruginosa
PBS	phopshate-buffered saline
Ph	phenyl
PhCN	benzonitrile
PPB	plasma protein binding
PQS	2-heptyl-3-hydroxyquinolin-4(1H)-one
QS	quorum sensing
rt	room temperature
SAR	structure-activiy relationship
Skin	kinetic solubility
SME	small and medium-sized enterprises
S_NAr	nucleophilic aromatic substitution
SPR	structure-property relationship
$t_{1/2}$	half-life
*t*Bu	tert-butyl

TFA	trifluoro acetic acid
THF	tetrahydrofuran
TLC	thin-layer chromatography
TMEDA	tetramethylethylenediamine
TMP	2,2,6,6-tetramethylpiperidine
TMS	trimethylsilyl
$TMSN_3$	trimethylsilyl azide
TsCl	tosylchloride
UHP	urea hydrogen peroxide
US	United States
WHO	World Health Organization
wt%	weight percent

Table of Contents

The references in chapter 7 refer to chapters 1 – 5, except for chapter 1.6. References referring to the main text of this subchapter are listed at the end of this subchapter.

1. Introduction

1.1. Antibiotic resistance

It is widely acknowledged that the "golden era" of antibiotics is over. Right now, in this time of ever-increasing antimicrobial resistance (AMR), we can no longer take the fruitful efforts, discoveries and developments of early antibiotic research for granted. Annually, the death toll resulting from resistant infections is estimated to be 700,000 and predicted to increase to 10 million deaths per year by 2050.[1] Even though bacterial resistance is increasing, the discovery of novel antibiotics is decreasing. In the past 20 years, only two new classes of antibiotics were introduced whereas all other recently approved antibacterial drugs were derivatives of already known classes.[2,3] Even worse, for Gram-negative bacteria there has been no innovative new antibacterial agent for the past 40 years. As depicted in Figure 1.1.1, there are now resistant strains for most of the commonly used antibiotics. It is worth mentioning, that resistance often occurs already shortly after approval of an antibiotic. There are more reasons for the rise of AMR than economic and scientific barriers in drug discovery.[4–6] The massive overuse of antibiotics in agriculture is alarming. In 2010, 80% of antibiotics sold in the US were used in lifestock either for growth promotion and/or in order to prevent infections. Moreover, there is no data available justifying the abundant use of these preventive measures.[7] The 2018 FDA report on antimicrobials sold or distributed for use in food-producing animals states that 48% of the antibiotics used were not medically required.[8]

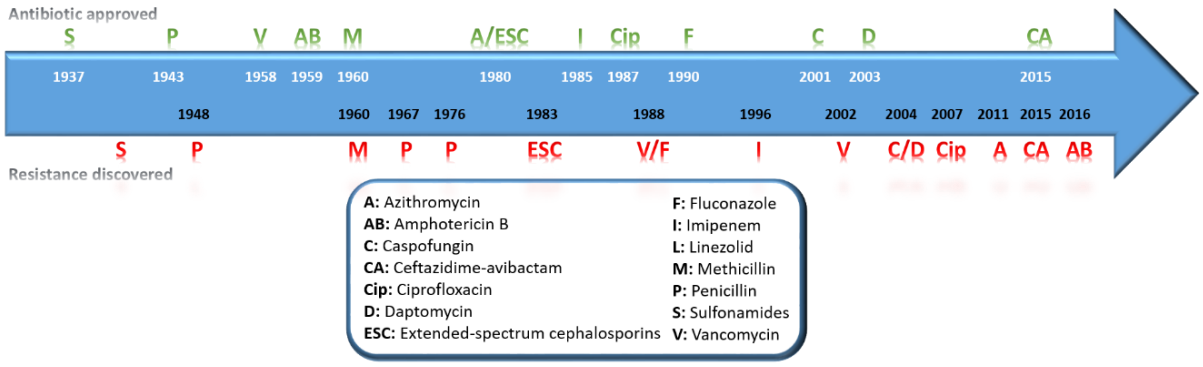

Figure 1.1.1: *Timeline of antibiotics approved and resistances discovered.*[9]

AMR is not only an issue of the possible forthcoming and much-dreaded "post-anitbiotic era" but also a result of natural evolution. Resistance already started occurring ages before humans began using antibiotics to treat infections.[10] Genes transferring resistance are found in 30,000-year-old permafrost samples as well as in bacterial cultures hailing from caves where no human being has set a foot before.[10] The latter proved that for the past four million years resistance against 14 antibiotics has already existed. Moreover, indigenous people in South America were home to a host-associated

microbiome, which proved to encode various genes responsible for antibiotic resistance.[11] The armory of this ancient defense mechanism is vast and resistance is a complex, multifactorial issue. Summarized as the "antibiotic resistome", the concept of understanding and studying origins and evolution of bacterial resistance explains how microbes are able to escape and ultimately survive antibiotic treatment. The term resistome describes the entirety of bacterial resistance genes, known or unknown, and covers both, intrinsic and acquired resistance genes. It also includes proto-resistance genes and silent or cryptic resistance genes.[11–13] Whenever bacteria become resistant towards antibiotics, the mechanism they make use of can be grouped into the following four: (i) the inactivation or modification of the antibiotic, (ii) protection, alteration or overexpression of the target, (iii) efflux pumps, either generalist or antibiotic-specific and (iv) reduced cell wall permeability (Figure 1.1.2).[14]

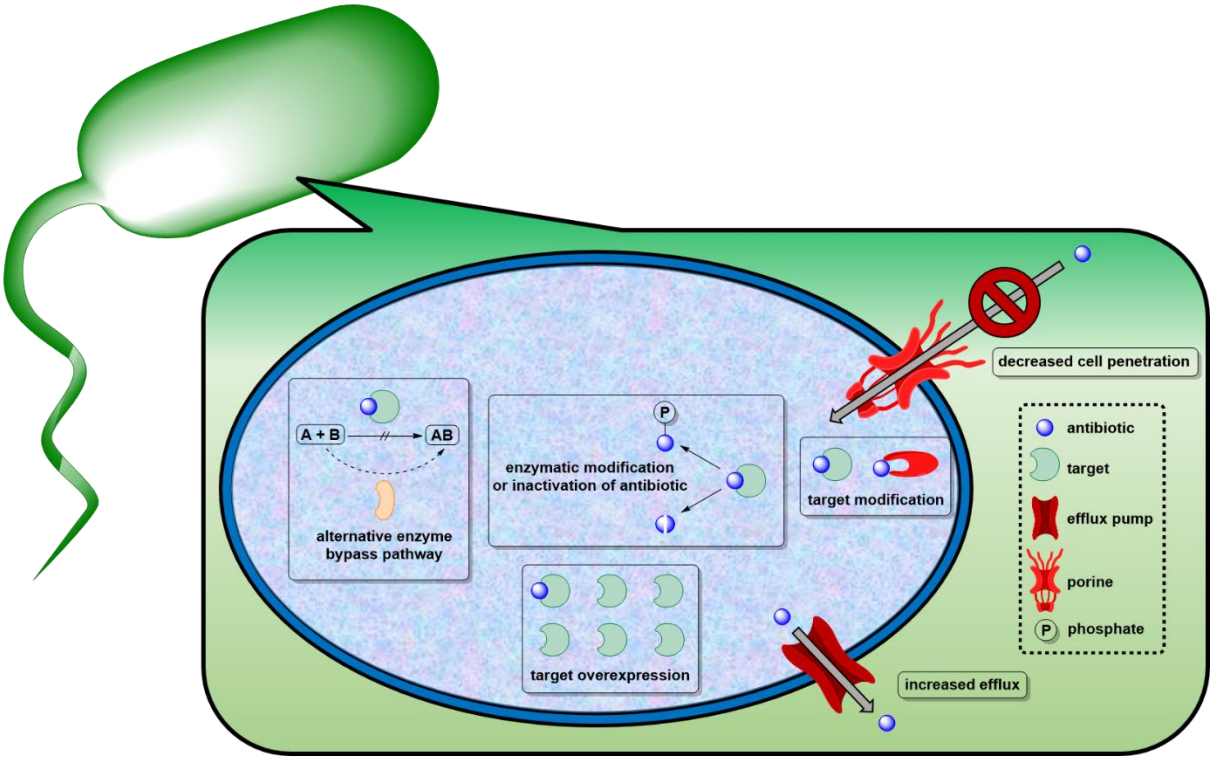

Figure 1.1.2: *Mechanisms of antimicrobial drug resistance.*

P. aeruginosa is, among other bacterial species, capable to form biofilms. In these biofilms, planktonic cells start to stick to each other and adhere to a surface.[15,16] Over time, these cells start to produce extracellular polymeric substances (EPS) which they embed themselves into.[17] These EPS include rhamnolipids, extracellular DNA (eDNA), exopolysaccharides and various proteins and renders antibiotic treatment difficult. Resistance in this biofilm habitat is increased up to 1000-fold compared to planktonic bacteria.[18] This indicates differences in the drug-resistance arsenal of biofilm cultures compared to planktonic cells, making it even more difficult to combat. *P. aeruginosa* biofilms are known to delay penetration and delivery of aminoglycosides, such as tobramycin *via* increased

expression of efflux pumps and eDNA secretion.[19–22] Ciprofloxacin, on the other hand, does not suffer from impaired penetration but rather from an overexpression of efflux pumps and resistance-promoting target-site modification.[23–25] The biofilm architecture creates a nutrient and oxygen gradient and therefore accounts for a high population heterogeneity. Among the bacteria within this construct, metabolic activity fluctuates, leading to differences in their susceptibility towards antibiotic therapy. These "dormant" bacteria significantly enhance biofilm resilience, since most antibiotics aim for metabolically active bacteria. Moreover, the aforementioned oxygen uptake was also found to be crucial when it comes to treatment with ciprofloxacin and tobramycin. It has been observed that these antibiotics killed only bacteria adjacent to the air interface, stressing how important oxygen levels and metabolic activity are for successful treatment.[26] The surviving small fraction of these biofilm cells is referred to as persister cells and further amplifies resistance.[27]

1.2. Pathoblocker approach

Since resistance occurs upon selective pressure, killing bacteria might have some intrinsic flaws. Moreover, most antibiotics do not differentiate between pathogenic strains and the beneficial host microbiome, leading to unwanted side effects of antibiotic therapy. A novel approach to circumvent the aforementioned issues is the so-called "pathoblocker approach" or "antivirulence-therapy". As the name already suggests, antivirulence agents target bacterial virulence factors rather than growth or survival. Virulence is the ability of pathogens to cause diseases making use of virulence factors that actively cause damage to host tissues. Since these are selective for the pathogens but not the microbiome, the latter is preserved, which further helps reducing the pathogens ability to colonize the host. The commensal microbiome protects the host against infections and therefore is of high importance. Because classical bactericidal or bacteriostatic effects are avoided and virulence factors seem to be non-essential, bacteria may experience less selective pressure, ultimately resulting in less sensitivity for resistance development. Attenuating bacterial virulence, which mediates tissue damage in hosts could lead to less morbidity and improved quality of life, especially for patients suffering from chronic infections. Finally, yet importantly, the chemical space for addressing the numerous possible antivirulence targets is vast compared to the limited number of classical antibiotic targets.[28–39] Nevertheless, targeting virulence might not be spared from resistance development as it has been discussed among the scientific community recently, resistance has already been observed.[40,41] The most prominent examples validating this approach are monoclonal antibodies (mAb) with Bezlotoxumab as the spearhead. The FDA approved the *Clostridium difficile* toxin B-targeting agent in 2016 for treatment of recurrent *C. difficile infections*.[42] Moreover, PA virulence factors such as alginate and lipopolysaccharides are addressed by mAbs AR-105 and AR-101, respectively. The latter successfully completed Phase II clinical trials and AR-105 is in Phase II trials. Furthermore, the *S. aureus*

toxin-targeting mAb AR301 is already in Phase III clinical trials.[43] Novel strategies for attenuating virulence in PA have been vastly discussed in literature and emphasize the potential of this new kind of therapy.[16,44]

1.3. Antibiotic Drug Discovery

In the "golden era" of antibiotic drug discovery, many antibacterial agents have been established. Among them are classical mechanisms of actions like inhibition of cell-wall biosynthesis, the ribosome or DNA gyrase. In the 1940s, the so-called "Waksman platform" was giving birth to novel antibiotics for over 20 years. The systematic screening made use of streptomycetes which also earned streptomycin, the first aminoglycoside antibiotic, its name. Nevertheless, the pharmaceutical industry turned its back on the once Nobel Prize awarded technique since streptomycetes as well as other actinomycetes were exploited and only compounds that had already been discovered were obtained. With increasing resistance towards the well-established natural product-derived antibiotics, avenues were opened up for the medicinal chemistry era. Innovative structural modifications of natural scaffolds promoted successful antibiotic treatments again, which at first avoided resistance and expanded the spectrum of antimicrobial drugs. The discovery of the fluoroquinolones as a class of synthetic antibiotics was a breakthrough and displayed the potential of medicinal chemistry in drug discovery projects. Then, the innovation pipeline of antibiotics ran dry and no new class was introduced until 1986, when daptomycin was discovered. However, it took 17 more years for the drug to hit the market and only one year later resistant bacterial strains were already detected. In the 1990s, resistance was spreading faster than new antibiotics were discovered, giving the starting shot for the race against antimicrobial drug resistance. The pharmaceutical industry focused on rational drug design guided by the likes of genomics, high-throughput screenings (HTS) and combinatorial chemistry. Even though at the time it was believed that with the help of genomics, novel targets could be found and thus feeding the HTS machinery would solve the problem, no new antibacterial drug against important pathogens were developed.[45–47] Most of the large pharmaceutical companies left the field of antibiotic research creating a void which could be filled by small and medium-sized companies (SMEs).[48] Nevertheless, economic and regulatory barriers, disregarding scientific ones, make it hard to discover and develop novel antibiotics. Not only the lack of funding as well as the high demand for patients in expensive clinical trials are to mention here. But the main issue might be the limited market potential for newly licensed antibacterial drugs and, hence, lack of economic incentives.[47]

1.4. Importance of drug-like properties

When it comes to lead optimization, focusing on improving only activity alone will not deliver a drug suitable for use in human patients. Various studies suggest that the high attrition rate of compounds in clinical development is due to insufficient pharmacokinetic properties.[49–52] It is believed that physicochemical properties such as size, hydrogen bonding descriptors, pK_a and lipophilicity are essential for promising high-quality drug candidates. As described in Figure 1.4.1, optimizing activity only leads to good ligands, whereas optimization of activity and DMPK (drug metabolism and pharmacokinetics) properties result in good drugs. Some important parameters for successful drug discovery are depicted in Figure 1.4.1 B. Good drugs need to be soluble and chemically stable. Depending on the target, a drug must be active and selective. Safety pharmacology aspects play a significant role and should be considered as early as possible, e.g. when designing libraries for screenings or hit-to-lead/lead optimization. Moreover, a novel structural space should be addressed in order to acquire intellectual property.

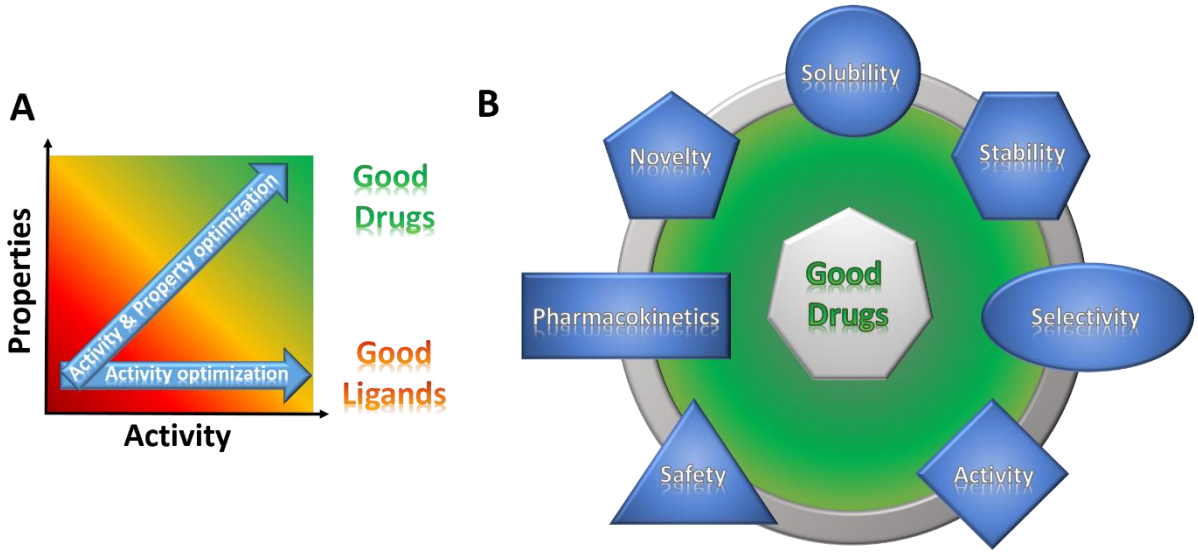

Figure 1.4.1: *A: different optimization aspects yield either good drugs or good ligands. B: Important parameters for successful drug discovery (adapted from [53,54])*

One of the most important properties concerning the quality of a good lead and, in the end, a novel drug is lipophilicity.[55] The role of this important PK parameter is reflected in a study in which compounds that differed in lipophilicity either failed due to clinical safety in Phase I or succeeded and progressed to Phase II. Nevertheless, attrition reasons are manifold and not just one-dimensional.[49] This means that not only SAR should be considered when deciding which way to go in a drug discovery project but also structure-property-relationships (SPR). The combination of both serves as an excellent tool for prioritizing compounds based on multifactorial data sets. This leads to an easier early-stage optimization, thus resulting in better compounds for very expensive *in vivo* studies.[56]

1.5. Role of medicinal chemistry in drug discovery

Medicinal chemistry has always played and is still playing a major role in the process of drug discovery and development. In the past, medicinal chemists focused on semisynthesis of existing natural products, e.g. tetracyclines or aminoglycosides. Since then the focus has shifted more and more and medicinal chemists have become involved in multifactorial and interdisciplinary projects, expanding their role from just synthesizing compounds to their evaluation and multiparameter optimization. Among the highlights of synthetic antibacterial drugs are compound classes such as fluoroquinolones, carbapenems and oxazolidinones, not to mention the first synthetic antibiotics such as arsenicals and sulfa drugs.[57] While in the past, chemists were not in charge of selecting a suitable target, nowadays medicinal chemists are involved in the drug discovery process from the beginning. Starting with selection of biological targets and e.g. the choice of screening-libraries and hit selection, moving to chemical space exploration, interpretation of SAR studies and lead generation, ultimately resulting in scale-up and reaction optimization for a pre-clinical candidate. While in the early days, medicinal chemists more or less focused solely on activity when optimizing a compound, pharmacokinetic properties such as solubility or metabolic stability were often disregarded, resulting in high attrition rates.[52,58] Especially in the discovery phase and early development, medicinal chemists can accelerate the drug discovery process and thus reduce costs (Figure 1.5.1).

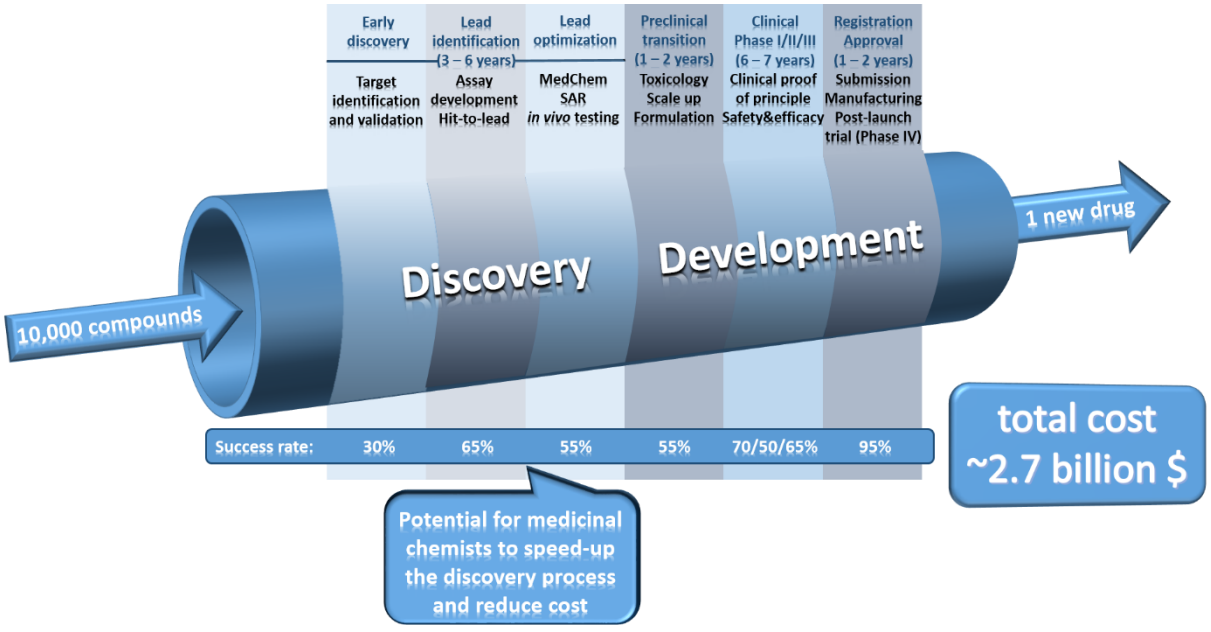

Figure 1.5.1: *Schematic depiction of the drug discovery pipeline.*[59]

The great impact innovation in organic chemistry has had and still has on drug discovery and development ultimately peaked in 2010 when Richard F. Heck, Ei-ichi Negishi and Akira Suzuki were awarded the Nobel Prize in chemistry for their groundbreaking work on “palladium-catalyzed cross

couplings in organic synthesis".[60] These innovations served as a blueprint for medicinal chemists of the 21st century and the Suzuki-Miyaura and Buchwald-Hartwig reactions, besides other Pd-catalyzed cross couplings, are among the most abundant chemical transformations in the medicinal chemists' toolbox.[61–66] The synthesis of the last-resort antibiotic vancomycin makes use of the Suzuki-Miyaura coupling and represents one of many examples.[67–69] Uehling *et al.* recently reported the utilization of the Buchwald-Hartwig coupling as a late modification to access complex molecules in a fast and efficient manner, using oxidative addition complexes.[70] The so-called „click chemistry", a term established by K. B. Sharpless represents another widely used application of organic chemistry in drug discovery.[71–73] One of the most prominent examples is the 1,3-dipolar cycloaddition of alkynes and azides catalyzed by copper(I) (CuAAC = copper(I)-catalyzed alkyne azide cycloaddition) to yield 1,2,3-triazoles. CuAAC not only provides fast access to large compound libraries, as it is perfectly suited for combinatorial chemistry, but also plays an important role in biorthogonal methods.[74–78]

On the one hand, synthetic organic chemistry might be among the most crucial time-consuming and rate-limiting factors within the drug discovery process. On the other hand, medicinal chemists in integrated drug discovery projects serve an important role and can ultimately speed-up especially lead generation and optimization as well as scale-up and process development.[79] Very recently, Russell *et al.* have reported an innovative and fast flow chemistry-based synthesis of linezolid, an antibiotic of last resort.[80] This emphasizes the impact of organic chemistry on the workflow in drug discovery relying on medicinal chemist's in-depth knowledge of state-of-the-art technologies in organic chemistry but also on the ability to tackle eventual DMPK problems. Conclusively, medicinal chemists are still of high importance and play a big role for the establishment of novel drugs.[81]

1.6. Targeting the *Pseudomonas aeruginosa* PQS System

Title:

Targeting the *Pseudomonas* quinolone signal quorum sensing system for the discovery of novel anti-infective pathoblockers

Authors:

Christian Schütz and Martin Empting

Bibliographic Data:

Beilstein J. Org. Chem. **2018**, *14,* 2627–2645. doi:10.3762/bjoc.14.241

BEILSTEIN JOURNAL OF ORGANIC CHEMISTRY

Targeting the *Pseudomonas* quinolone signal quorum sensing system for the discovery of novel anti-infective pathoblockers

Christian Schütz[1,2] and Martin Empting[*1,2,3]

Review

Open Access

Address:
[1]Helmholtz-Institute for Pharmaceutical Research Saarland (HIPS) - Helmholtz Centre for Infection Research (HZI), Department of Drug Design and Optimization (DDOP), Campus E8.1, 66123 Saarbrücken, Germany, [2]Department of Pharmacy, Saarland University, Campus E8.1, 66123 Saarbrücken, Germany and [3]German Centre for Infection Research (DZIF), Partner Site Hannover-Braunschweig, Saarbrücken, Germany

Email:
Martin Empting[*] - martin.empting@helmholtz-hzi.de

* Corresponding author

Keywords:
anti-infectives; pathoblockers; PQS; *Pseudomonas aeruginosa*; quorum sensing

Beilstein J. Org. Chem. **2018,** *14,* 2627–2645.
doi:10.3762/bjoc.14.241

Received: 31 July 2018
Accepted: 28 September 2018
Published: 15 October 2018

This article is part of the thematic issue "Antibacterials, bacterial small molecule interactions and quorum sensing".

Guest Editor: D. Spring

Abstract

The Gram-negative opportunistic pathogen *Pseudomonas aeruginosa* causes severe nosocomial infections. It uses quorum sensing (QS) to regulate and coordinate population-wide group behaviours in the infection process like concerted secretion of virulence factors. One very important signalling network is the *Pseudomonas* quinolone signal (PQS) QS. With the aim to devise novel and innovative anti-infectives, inhibitors have been designed to address the various potential drug targets present within pqs QS. These range from enzymes within the biosynthesis cascade of the signal molecules PqsABCDE to the receptor of these autoinducers PqsR (MvfR). This review shortly introduces *P. aeruginosa* and its pathogenicity traits regulated by the pqs system and highlights the published drug discovery efforts providing insights into the compound binding modes if available. Furthermore, suitability of the individual targets for pathoblocker design is discussed.

Introduction

In recent years, attempts to raise public awareness on antimicrobial resistance (AMR) and the large threat that it poses towards modern health standards have been made [1]. It is an alarming notion that at an increasing rate of available treatment options proves ineffective in eradicating bacterial infections [2]. Especially in the case of Gram-negative bacteria, an urgent need for novel medicines has been identified while the pipeline of drug candidates is literally running dry and a desirable renaissance of the golden age of antibiotic drug research in 'big pharma' is currently not to be seen on the horizon [3,4]. Nevertheless, some innovative strategies to be explored for their clinical applicability in combating bacterial infections have been devised

Beilstein J. Org. Chem. 2018, 14, 2627–2645.

in the last decades mostly driven by academic research [5-7]. In contrast to addressing classical antibiotic drug targets involved in vital processes of the bacterial cell, 'antivirulence' strategies aim at abolishing pathogenic features without affecting cell viability, providing the basis for a lower drug-induced selection pressure [5,8,9]. Hence, a reduced rate of resistance development is expected [9]. A clinical proof-of-concept for this unconventional strategy has been provided recently by the approval of the toxin-neutralizing therapeutic antibody bezlotoxumab, which is henceforth in clinical use for pre-emptive treatment of recurring clostridial infections [10]. So, the potential of active principles, which do not kill the bacteria through bactericidal or bacteriostatic effects, but mediate their effect through pathogen-specific action on virulence mechanisms, has been unveiled. This short review focuses on the current knowledge of one particular antivirulence strategy against the important pathogen *Pseudomonas aeruginosa*, which is based on the disruption of the *Pseudomonas* quinolone signal quorum sensing system (pqs QS).

Review

Antimicrobial resistance and clinical relevance of *Pseudomonas aeruginosa*

P. aeruginosa is one of the threatening ESKAPE pathogens and has regularly been attributed with the label 'superbug' [11]. In 2017, the World Health Organization (WHO) has published a priority list for pathogens with urgent need for novel treatment options and carbapenem-resistant *P. aeruginosa* was ranked in the highest category 'critical' [12]. One of the main problems we face regarding this Gram-negative bacterium is that it shows a prominent ability to resist antibiotic treatment via several mechanisms. First and foremost, it possesses an intrinsic resistance to many antibiotics because of the low permeability of its cell wall and due to the action of a number of efflux pumps as well as β-lactamases. Efflux pumps in particular are nifty molecular machineries consisting of several protein components, which in total span from the inner to the outer side of the cell membrane. Their function is to expel a wide range of xenobiotics, among them antibiotics from the cephalosporin, carbapenem, fluroquinolone and aminoglycoside classes [13]. Through this mechanism, these drugs cannot reach their intracellular targets rendering them ineffective. β-Lactamases, on the other hand, act specifically on compounds which carry the eponymous cyclic moiety as the activity-driving motif and their genes are found to be encoded on the chromosomes of many *P. aeruginosa* strains. Hence, these antibiotic-inactivating enzymes provide resistance against penicillins and cephalosporins [14].

In addition to these intrinsic capabilities, *P. aeruginosa* is able to acquire resistances toward antibiotics it has come in contact with. These acquired resistances can be the result of spontaneous mutations in genes encoding for the target protein. For example, certain mutational changes within DNA gyrase will lead to lowered susceptibility for fluoroquinolones [15]. Other examples are mutants leading to efflux pump overexpression [15]. If the resistance determinant is located on a transferable plasmid, it can be efficiently spread among bacteria via horizontal gene transfer, which is probably the most frequent mechanism for the development of acquired resistances [15]. In these cases, the resistance determinant is inheritable and passed over to the next generation of bacteria.

Furthermore, a mechanism has been discovered, which is referred to as adaptive resistance and describes the observation that a persistent environmental stimulus can induce non-mutational resistances [15]. Under continuous treatment regimes, the antibiotic itself can of course be the stimulus. But, nutrient deprivation, pH, anaerobiosis, as well as biocides, polyamines, cations and carbon sources could also act as external triggers leading to adaptive resistance. The common effect of these stimuli seems to be an alteration in expression patterns ultimately impacting, e.g., efflux pump or enzymatic activity, as well as cell envelope properties or biofilm formation [15].

All the mechanisms described above help to explain the notion that established chronic *P. aeruginosa* infections are notoriously difficult to eradicate. This ubiquitous opportunistic pathogen is able to cause infections basically in every niche of the human body where it finds enough moisture [16]. Common sites of infection are the respiratory and urinary tracts, the eye and wounds, e.g., those resulting from burn injuries [17]. These occur frequently in hospitalized and especially immunocompromised individuals. Patients with chronic lung diseases like cystic fibrosis (CF) or bronchiectasis have a poor prognosis when *P. aeruginosa* colonisation is detected, as this is usually associated with loss of lung function, morbidity, and mortality [18]. In 2013, it has been estimated, that by the age of eighteen 80% of the CF patients are *Pseudomonas* positive. Recently, evidence has been provided that this ratio is reducing [19]. Nevertheless, with progression of age the majority of CF patients will become chronically infected with *P. aeruginosa* and this is still the major cause of death associated with this genetic disorder [20]. Importantly, it has been described that the amount of quinolone-based quorum sensing (pqs QS; vide infra) in those patients correlates with a negative prognosis and might function as a possible biomarker for the severity of the infection [21].

Quroum sensing (QS)

In general, the term quorum sensing describes a population-density-dependent cell-to-cell communication system making use

Beilstein J. Org. Chem. **2018,** *14,* 2627–2645.

of small diffusible molecules as signalling agents. By this means, pathogenic bacteria can coordinate population-wide changes to expression patterns and regulate concerted group behaviours important in the infection process. Critical pathogenicity traits like the production of virulence factors or biofilm formation are under the control of these systems. Actually, title pathogen makes use of four intertwined QS systems, referred to as las, rhl, pqs, and iqs [22]. These subsystems influence each other establishing an intricate regulatory network with compensatory mechanisms ensuring environmental adaptability and fine-tuned control of associated virulence genes (Figure 1). All four have been studied in the pursuit of quorum sensing inhibitors (QSI) to be used as blockers of *P. aeruginosa* pathogenicity [11,23].

Typically, a QS system of Gram-negatives consists of a transcription regulator, the signal molecules and one or several enzymes involved in the synthesis of the latter. The regulator usually controls the transcription of the biosynthetic enzymes and also functions as a receptor for the signal molecules themselves. As these are actually autoinducers (AIs) and, hence, have an agonistic activity toward their receptor, a positive feedback loop is created. In *P. aeruginosa* three different chemotypes of AIs have been identified, to date: alkyl homoserine lactones (AHLs) used by the las and rhl systems, alkylquinolones (AQs) used by the pqs system and 2-(2-hydroxyphenyl)thiazole-4-carbaldehyde used by the iqs system (Figure 1). Strategies addressing las and rhl have been reviewed elsewhere [5,11], while to date one study on iqs inhibition has been reported [23]. Many drug discovery efforts towards effective pathoblockers have been published based on the design and optimisation of pqs targeting QSI, which is the topic of this review.

The biosynthetic cascade of the pqs QS system

PQS is the abbreviation for *Pseudomonas* quinolone signal and actually refers to the signal molecule 2-heptyl-3-hydroxyquinolin-4(1*H*)-one (Figure 2). This quinolone-based AI and its biosynthetic precursor HHQ (2-heptylquinolin-4(1*H*)-one) are ligands of a transcription factor called 'multiple virulence factor regulator' (MvfR), also referred to as PqsR. Through interaction with this receptor, HHQ and PQS induce the transcription of a variety of genes including their own biosynthetic enzyme cascade (PqsABCDE). Together with PqsH and PqsL, which are under the control of LasR from the las QS system, these enzymes manage to build up PQS and related molecules from anthranilic acid (Figure 2). This initial building block can be

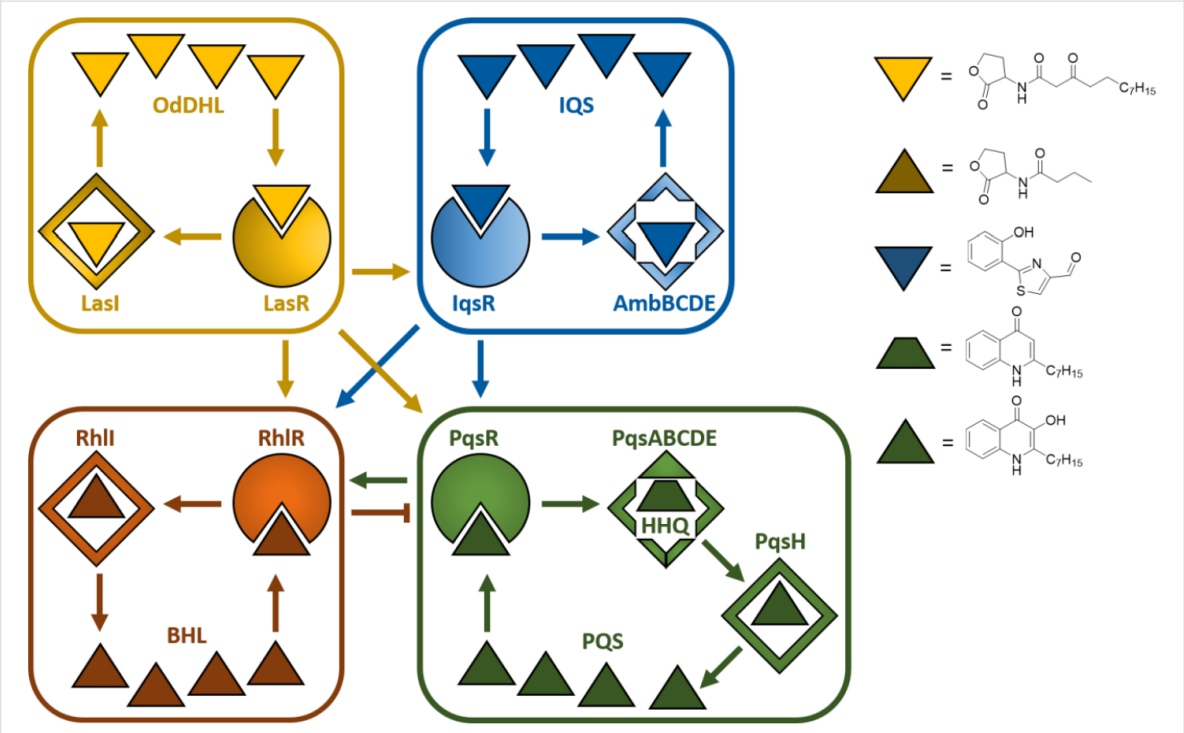

Figure 1: The four quorum sensing systems in *P. aeruginosa las, iqs*, *rhl*, and *pqs*. Abbreviations: OdDHL, *N*-(3-oxododecanoyl) homoserine lactone; IQS, integrating quorum sensing signal; BHL, *N*-butyryl-L-homoserine lactone; PQS, *Pseudomonas* quinolone signal. Positive control is represented by arrows, negative control by blunted arrow.

Beilstein J. Org. Chem. **2018,** *14,* 2627–2645.

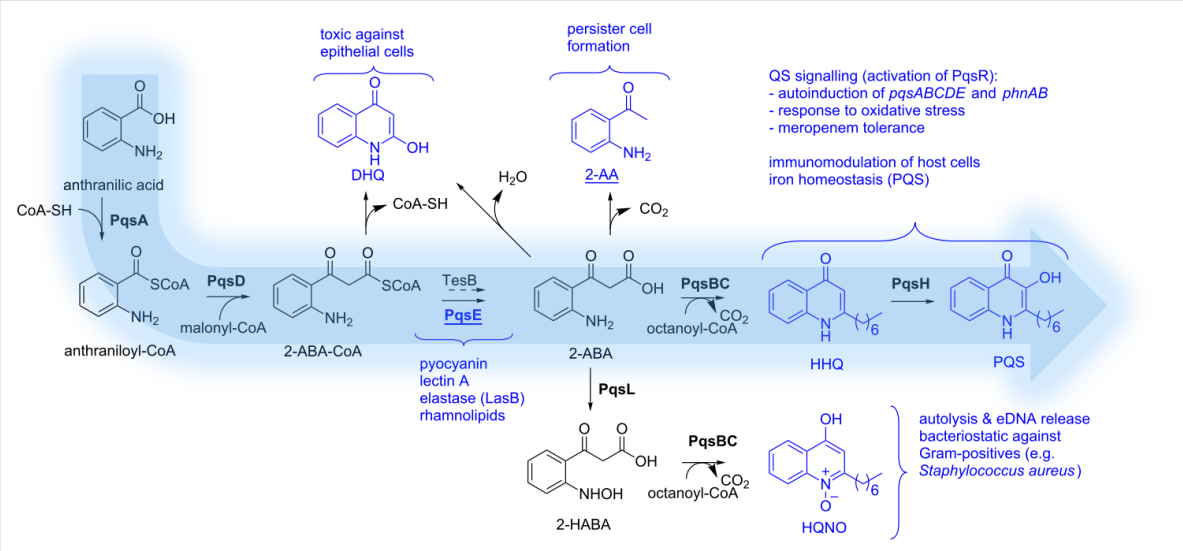

Figure 2: Schematic overview of the PQS biosynthesis and involvement of related metabolites and PqsE in virulence. Effector molecules are highlighted in blue. Enzymes are given in bold. Abbreviations: CoA, coenzyme A; 2-ABA-CoA, 2'-aminobenzoylacetyl-CoA; 2-ABA, 2'-aminobenzoylacetate; DHQ, dihydroxyquinoline; 2-AA, 2'-aminoacetophenone; 2-HABA, 2'-hydroxylaminobenzoylacetate; HHQ, 2-heptyl-4-(1*H*)-quinolone; HQNO, 4-hydroxy-2-heptylquinoline-*N*-oxide; PQS, *Pseudomonas* quinolone signal.

provided either through the kynurenine pathway starting from tryptophan or by anthranilate synthases from the PqsR-controlled phnAB operon starting using chorismic acid as a source [24]. Either way, the ligase PqsA starts PQS synthesis by condensing anthranilic acid with coenzyme A [25]. The resulting activated thioester (anthraniloyl-CoA) is then transferred to an active-site cysteine of the β-ketoacyl-ACP synthase III (FabH)-type enzyme PqsD [26,27]. Subsequently, another CoA-activated substrate comes into play. In analogy to fatty acid synthesis, malonyl-CoA is reacted with the enzyme-bound thioester to yield 2-aminobenzoylacetyl-CoA (2-ABA-CoA) under decarboxylation [28,29]. In a next step, the pathway-specific thioesterase PqsE generates 2-aminobenzoylacetate (2-ABA) [29]. It has been shown, that also the broad-specificity thioesterase TesB present in *P. aeruginosa* can catalyse this reaction [29]. The quinolone core is formed by action of the heterodimeric complex PqsBC. This time, CoA-activated octanoic acid is used to preload an active-site cysteine of PqsC with the fatty acid via a thioester linkage [30,31]. The previously produced 2-ABA is then consumed to from HHQ under decarboxylative condensation [30]. Finally, PQS is produced through hydroxylation of position 3 by the NADH-dependent flavin mono-oxygenase PqsH [32].

This biosynthetic cascade is also responsible for the generation of the pqs-related metabolites DHQ, 2-AA, and HQNO as well as other AQs having different lengths of the alkyl chain [29,30]. Aforementioned enzyme PqsL is needed for the production of HQNO, as it delivers the *N*-oxidised substrate 2-HABA for PqsBC-mediated condensation with octanoyl-CoA analogous to HHQ biosynthesis [27].

PQS-mediated pathogenicity traits and molecular targets

P. aeruginosa makes use of an arsenal of virulence factors and other pathogenicity traits to overwhelm and colonise the host in the infection process [5] and pqs QS plays a crucial role in the regulation of many of those. It is astonishing, that expression of 182 genes is altered in response to exogenous PQS [33]. Evidence has been gathered, that these effects are mediated either through direct PqsR-dependent action or by PqsR-independent mechanisms, which are most likely due to the iron-chelating as well as antioxidant properties of PQS [33]. Furthermore, it has been unravelled that the thioesterase PqsE, whose biosynthetic function is dispensable due to the presence of alternative thioesterases in *P. aeruginosa*, is actually also a major effector molecule of *pqs* QS [33]. Via a yet unknown mechanism, this enzyme regulates 145 genes, while only 30 of these overlap with the PQS regulon. It seems that these two are the main mediators of *pqs* QS response. In terms of pathogenicity traits, they are involved in the regulation of genes encoding for enzymes responsible for phenazine biosynthesis (pyocyanin production), hydrogen cyanide synthesis, Lectins LecA and LecB and additional genes involved in biofilm formation, enzymes for rhamnolipid synthesis, a Resistance-Nodulation-Cell division (RND) efflux pump encoded by *mexGHI-opmD* operon, components of Type 3 and Type 6 secretion as well as the exotoxin ExoS, and siderophore synthases [33].

Beilstein J. Org. Chem. **2018,** *14,* 2627–2645.

In addition to virulence regulation, some remarkable secondary effects have been attributed to the PQS molecule [34]. This autoinducer has been described to mediate iron acquisition, cytotoxicity, outer-membrane vesicle biogenesis, and to exert host immune modulatory effects [34,35]. Interestingly, PQS as well as HHQ are able to interfere with nuclear transcription factor-κB and hypoxia-inducible factor 1 (HIF-1) signaling pathways and, thus, down-regulate host innate immune systems [36,37]. Other PQS-related metabolites have been shown to have additional effects. HQNO, for example, induces autolysis and release of extracellular DNA thereby promoting biofilm formation and increasing meropenem tolerance [38]. HQNO acts through inhibition of complex III in the respiratory chain of bacteria and mitochondria of eukaryotes and, hence, it can be considered a general cytotoxic agent. DHQ, a shunt product of the PQS biosynthetic pathway, is important for *P. aeruginosa* virulence in a *Caenorhabditis elegans* model and also excerts a growth inhibitory effect on epithelial cells [26,39]. Finally, 2-AA has been described to be important for persister cell formation, a very important tolerance mechanism against antibiotic treatment [40].

Among the virulence factors which are directly or indirectly controlled by pqs QS, pyocyanin is one of the most prominent. This redox-active pigment is responsible for the greenish-blueish colour of *P. aeruginosa* cultures. It seems that generation of reactive oxygen species is a major mechanism of pyocyanin cytotoxicity [41]. This tricyclic compound is known to induce apoptosis in neutrophils, but also to enhance neutrophil extracellular trap formation [42,43]. Both mechanisms impair neutrophil-mediated host defenses. Additionally, it has been hypothesised that pyocyanin functions as an extracellular electron shuttle, contributing to redox homeostasis of *P. aeruginosa* cells in biofilms with anaerobic conditions [44].

Due to these important virulence mechanisms, which are under direct or indirect control of pqs QS, targeting this master regulatory system with small molecular compounds, thereby blocking *P. aeruginosa* pathogenicity, is very attractive. However, this complex network of biosynthetic pathways and effector molecules renders selection of the perfect point for intervention difficult. Due to their rather peripheral role in AQ synthesis, PqsH and PqsL, have not been of significant interest for QSI discovery to date. However, all enzymes of the primary biosynthetic cascade pqsA–E as well as the signal molecule receptor PqsR might be valuable drug targets. Also, agents capable of modulating more than one target could be of interest. The question is, which of these targets and/or combinations asserts the most relevant virulence-attenuated phenotype after QSI treatment.

PqsA inhibitors

Anthranilic acid analogues

Since anthranilic acid (**1**) serves as a PqsA substrate, the first compound reported to inhibit PqsA is 6-FABA (**2**, Figure 3), which was able to block this enzyme and successfully suppressed the production of DHQ in PA14 strains at a rather high concentration of 1.5 mM. Moreover, it was shown that 6-FABA had no impact on the bacterial growth. Lépine et al. suggested that **2** competitively occupies the active site of PqsA [45] and therefore serves as a substrate analogue of AA (**1**). It was stated that the introduction of electron-withdrawing substituents could prevent activation of the carbonyl group as a CoA-ester.

In 2017, Witzgall et al. were able to co-crystallize 6-FABA-AMP within the *N*-terminal domain of PqsA (Figure 4) [46].

Key interactions involve a water-mediated hydrogen bond between the amino function of the compound and Q162, as in anthraniloyl-AMP. The reason why the fluorinated anthraniloyl-AMP shows good affinity is the formation of a hydrogen bond of the fluorine with the G279 backbone amide hydrogen and furthermore an interaction with the N7 position of the adenine moiety. Additionally a very typical fluorine/main-chain interaction with G302 could be observed.

Various halogenated derivatives of AA could also reduce HHQ and PQS levels. Especially 4- and 6-CABA (**3**, **4**) showed promising results in the suppression of signal molecules as well as in an in vivo mouse survival model at a concentration of 1.5 mM [47].

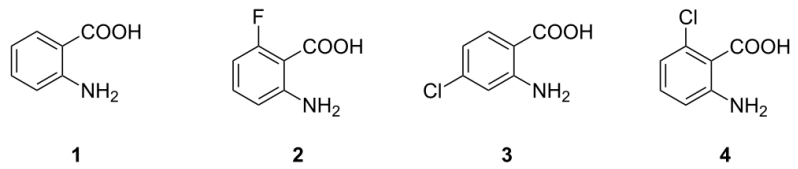

1 **2** **3** **4**

Figure 3: Anthranilic acid (**1**) and derivatives thereof (**2**–**4**).

Beilstein J. Org. Chem. **2018,** *14,* 2627–2645.

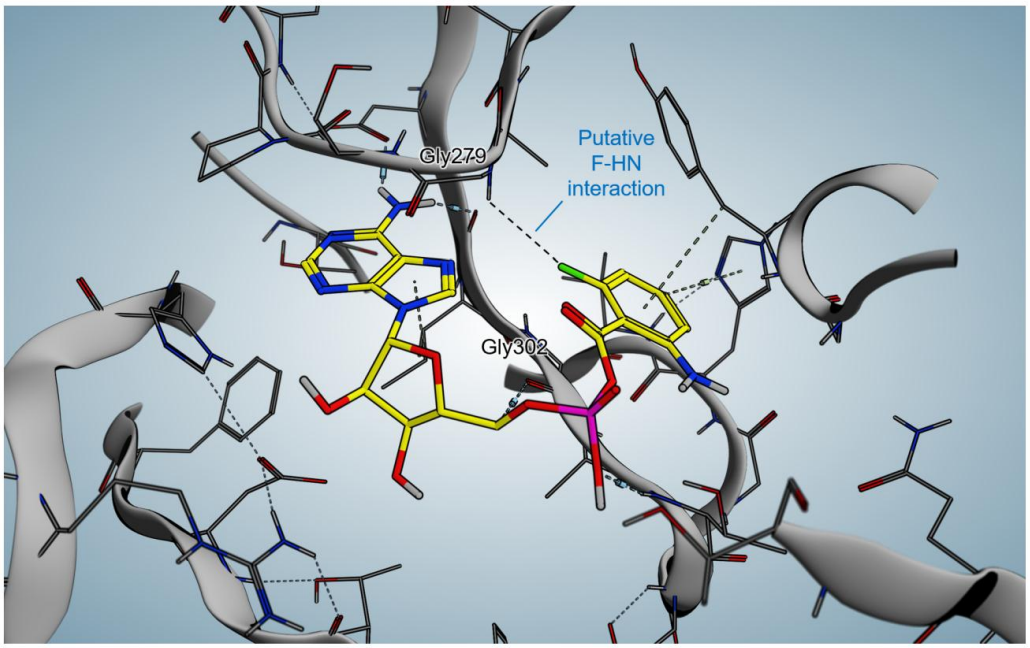

Figure 4: Crystal structure of 6-FABA-AMP in complex with PqsA.

Anthraniloyl-AMP mimetics

More recently, Ji et al. published two classes of sulfonyladenosine inhibitors, more precisely the sulfamate/sulfamide inhibitors **5**–**9** and the vinyl sulfonamide inhibitors **10** and **11** (Figure 5). While the latter showed very low affinity for the protein, the former displayed K_i values between 88 nM for compound **7** and 420 nM for compound **9**. Despite these promising results, the designed molecules were not able to reduce the signal molecules HHQ and PQS at satisfactory levels (300 µM < IC_{50} < 880 µM).

A plausible reason for this outcome might be low cell penetration and/or efflux pump mechanisms, which was supported by compound accumulation studies [48].

PqsD inhibitors

PqsD, the second enzyme in the biosynthetic cascade, has been studied intensely by the Hartmann group. Several design strategies have been pursued leading to diverse structural classes of inhibitors (Figure 6). Unfortunately, for none of these compounds an X-ray structure in complex with PqsD has been reported although the apoenzyme as well as a substrate-bound form has been successfully crystallized [49]. Using these coordinates, employing in silico methods allowed proposing plausible binding poses for prototypic analogues of the respective structural classes.

The first reported inhibitors of PqsD were 2-benzamidobenzoic acids [50]. In a pioneering study on the biosynthetic function of

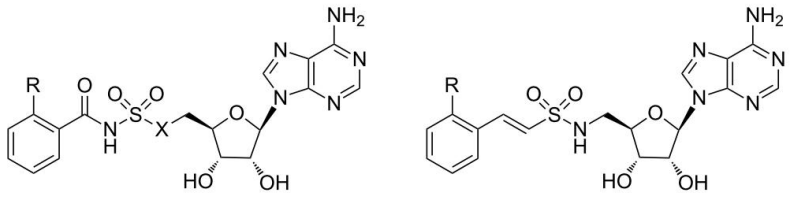

5 R = OH, X = O
6 R = OH, X = NH
7 R = NH_2, X = NH
8 R = NH_2, X = O
9 R = H, X = O

10 R = NH_2
11 R = OH

Figure 5: Structures of substrate mimetic PqsA inhibitors.

Beilstein J. Org. Chem. **2018,** *14,* 2627–2645.

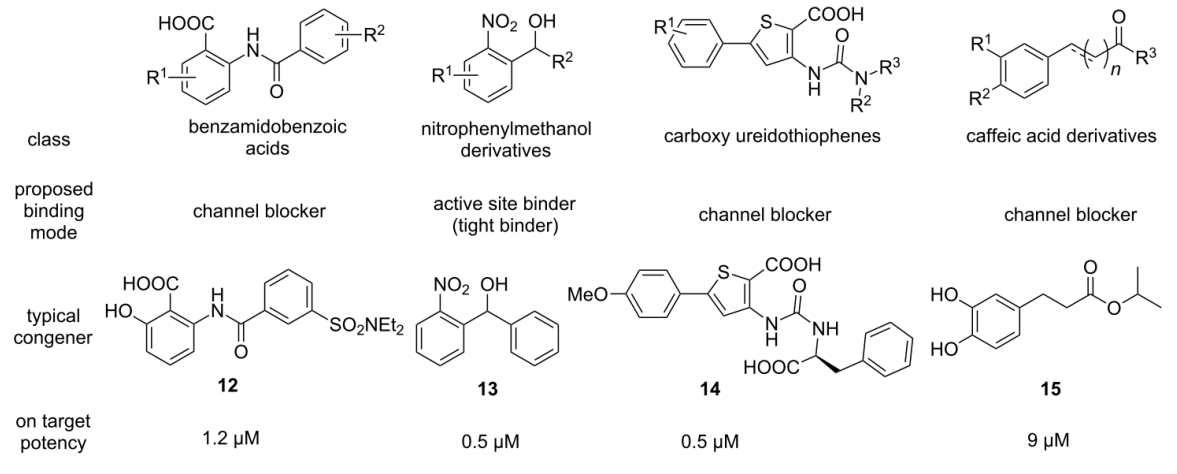

Figure 6: Structures and characteristics of prominent classes of PqsD inhibitors.

this β-ketoacyl-ACP synthase III (FabH)-type enzyme, known blockers of FabH were described to also inhibit this related target [50]. The claim that PqsD is directly responsible for HHQ production by using anthraniloyl-CoA and β-ketodecanoate as substrates, had to be revised later to also include PqsE and PqsBC as participants in AQ biosynthesis in *P. aeruginosa* (vide supra) [27]. Nevertheless, this conversion is indeed catalysed by PqsD in vitro and was successfully exploited for devising a valuable assay, which served as an SAR driver for most of the literature-known PqsD-directed projects. Further benzamidobenzoic acid derivatives were explored for their efficacy and a binding mode was proposed based on SPR- and STD-NMR-assisted docking [51]. These inhibitors appeared to bind in the substrate channel in a slightly remote position from the active site cysteine and, hence, termed channel blockers [51]. Optimised hits exhibited a potency in the single-digit micromolar range (**12**, Figure 6). However, it has been found that similar compounds also showed activity against RNA polymerase, a popular target for the development of new antibiotics [52,53]. Hitting such a target would jeopardise the principle of pathoblockers, which should only disarm the bacteria and not kill them. Hence, a follow-up study on PqsD/RNAP selectivity was conducted providing insights into motifs granting selective PqsD inhibition [52].

In a ligand-based approach, nitrophenylmethanol derivatives were identified as fragment-sized inhibitors of PqsD. Initially, these compounds where designed as transition state analogues mimicking the tetrahedral reaction intermediate between PqsD and anthraniloyl-CoA [54]. Upon simplification and rigidification through reduction in size as well as removal of rotatable bonds inhibitor **13** was obtained carrying the characteristic secondary alcohol of this class. Notably, both enantiomers of **13** show similar potency, but different thermodynamic profiles as measured via isothermal titration calorimetry (ITC) [55]. Despite its low molecular weight, **13** showed tight-binding kinetics and was able to reduce production of HHQ, as well as PQS. Furthermore, it was capable of attenuating biofilm production [54]. All the information gathered via site-directed mutagenesis combined with thermodynamic profiling, as well as surface plasmon resonance (SPR) experiments with and without covalent active site blockade, corroborated that the nitrophenylmethanol class directly binds to the active site near the reactive cysteine of PqsD [55]. This is in line with the initial transition state analogue design principle. Further structural exploration of this class showed that this fragment-like size helps to retain cellular activity [56]. While fragment growing could increase target activity to the nanomolar range, a complete loss of efficacy in the *P. aeruginosa* quorum quenching assays was observed [56]. This highlights a notable issue when addressing intracellular targets of this Gram-negative bacterium, as permeating the outer and inner membrane while escaping efflux and enzymatic deactivation may represent a true challenge.

The elucidation of the binding mode of the nitrophenylmethanol class was then exploited to gain insights into the interaction profile of another chemotype of PqsD inhibitors – the ureidothiophenes (Figure 6) [57,58]. An initial hit showing activity against the enzyme in the single-digit micromolar range was studied using a tailor-made SPR experiment including truncated and elongated derivatives as well as nitrophenylmethanol-based active-site blockers of different size as competitors. These experiments combined with molecular docking (Figure 7) led to the postulation of a plausible binding pose characterising the ureidothiophenes as channel blockers. This model was suc-

Beilstein J. Org. Chem. **2018,** *14,* 2627–2645.

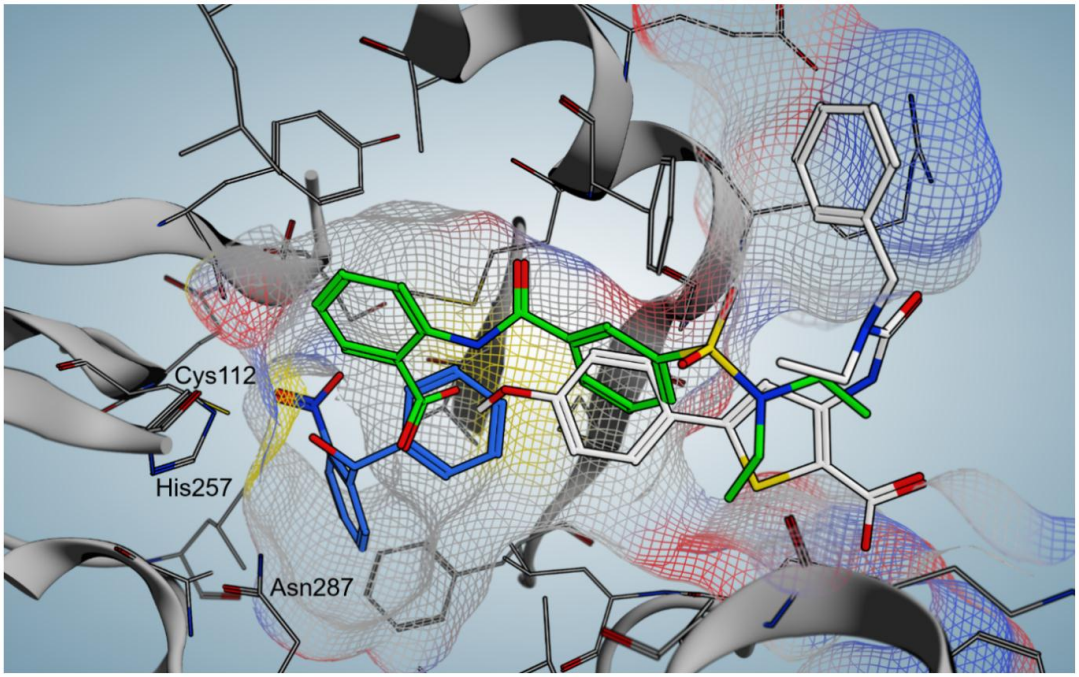

Figure 7: Comparison of docking poses of three prototypic PqsD inhibitors: benzamidobenzoic acid derivative **12** (green), nitrophenylmethanol derivative **13** (blue), carboxy ureidothiophene derivative **14** (white). Active site residues are labelled and the surface of the substrate tunnel is indicated by a mesh.

cessfully used for further optimisation attempts and nanomolar potency in the enzyme assay was achieved (**14**, Figure 6) [57,58]. Notably, a nucleophilic warhead could be introduced specifically reacting with the active-site cysteine through elongation into the substrate tunnel [57]. The binding models of the ureidothiophene and nitrophenylmethanol classes even allowed for the generation of a merged inhibitor [58]. One major liability of this class, however, was the general inefficacy in whole cell assays, which could not be improved, even through the attachment of a cell-penetrating peptide sequence [58].

One additional class, which did show cellular activity, was based on a catechol scaffold [59]. In analogy to the successful discovery of PqsD inhibitors starting from known FabH-targeting compounds (vide supra), ligands of another enzyme with high similarity to the signal molecule synthase were investigated. Here, substrates of chalcone synthase CHS2 from *Medicago sativa* were tested for their ability to block PqsD function. Indeed, caffeic acid analogues, such as **15**, were identified as hits and further characterized as channel blockers as described before [59].

Further interesting starting points for the discovery of PqsD inhibitors have been provided by a dedicated screening campaign involving fragment-based hit discovery, in silico screening and a similarity-guided approach starting from FabH inhibitors [60]. The most potent hit **16** of this study showed activity in the nanomolar range (Figure 8). Furthermore, a tetrazolopyrimidinone scaffold **19** has been reported to inhibit PqsD through a putative blockade of the CoA binding site [61].

The Böttcher group used a library of HHQ as well as PQS analogues to screen for PqsD inhibition [62]. To this end, a novel competition assay employing ‘clickable’ active-site-labelling probes was developed. These compounds contain terminal alkyne moieties, which can be exploited for straightforward decoration via copper(I)-catalyzed alkyne–azide cycloaddition (CuAAC), the prototypic click reaction. This facilitated the discovery of novel PqsD-targeting compounds through CuAAC-mediated conjugation of a fluorescent dye (Figure 9) [62].

Finally, Sangshetti et al. reported the discovery of linezolid-like Schiff bases, which showed promising anti-biofilm activity in the double-digit micromolar range [63]. Notably, their potency in attenuating biofilm formation was more pronounced than ciprofloxacin and linezolid itself. A docking study suggested PqsD to be the target of these compounds like **23** (Figure 10), although this remains speculative.

Beilstein J. Org. Chem. **2018,** *14,* 2627–2645.

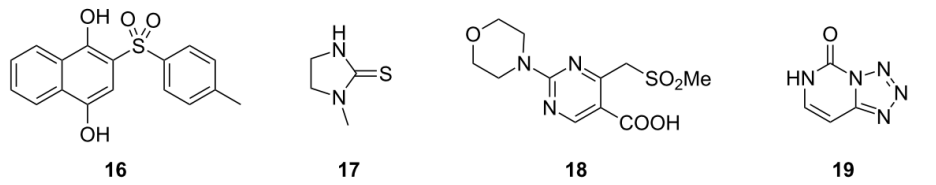

	16	**17**	**18**	**19**
hit identification method	target similarity (FabH inhibitor)	fragment screening	virtual screening	purine base mimic
proposed binding mode	channel blocker	channel blocker	channel blocker	channel blocker
on target potency	0.2 μM	4.7 μM	2.6 μM	9 μM

Figure 8: Structures and characteristics of hits against PqsD identified through different methods.

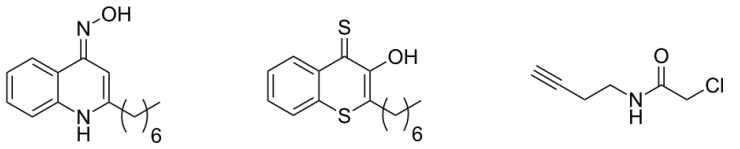

	20	**21**	**22**
type	HHQ derivative	PQS derivative	click probe used for competition assay
activity in competition assay	fully active at 240 μM	fully active at 24 μM	covalent active-site binder

Figure 9: HHQ and PQS analogues as PqsD inhibitors and chemical probe used for screening.

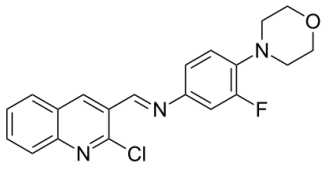

23
linezolid-like Schiff base

Figure 10: Structure of PqsD-targeting biofilm inhibitor derived from linezolid.

PqsE inhibitors

The pathway-specific thioesterase PqsE is not only responsible for hydrolyzing 2-ABA-CoA to form 2-ABA, but moreover also regulates bacterial virulence [29]. It has been shown that PqsE is a key effector of the *pqs* system and required for full *P. aeruginosa* virulence. One of its most prominent functions is the upregulation of pyocyanin, which is mediated through the *rhl* system. Notably, PqsE can still exert its function in absence of an active *pqs* QS [64,65]. Its important role in virulence regulation renders this enzyme an attractive target for pathoblockers.

In 2016, Zender et al. reported their attempt to inhibit PqsE through fragment-based screening. In order to block the thioesterase activity of the enzyme, a library of 500 fragments was screened via differential scanning fluorimetry (DSF) and the hit fragments **24**–**26** (Figure 11) were further validated using isothermal titration calorimetry (ITC) [66]. Binding to PqsE could be confirmed with K_D values of 0.9 ± 0.3 μM for **24** and 19.6 ± 3.7 μM for **26**.

The highly enthalpy-driven binding indicates a specific noncovalent interaction of **24** to the protein. To further investigate the binding mode of the hit fragments in the protein crystallization experiments were performed. Since the native substrate 2-ABA-

Beilstein J. Org. Chem. **2018,** *14,* 2627–2645.

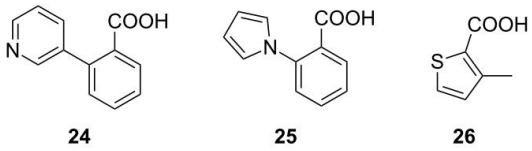

24 **25** **26**

Figure 11: Fragment-based PqsE-inhibitors **24**–**26**.

CoA shows a short half-life, the reaction product 2-ABA was used as a surrogate to compare its binding mode with that of the hit fragments.

Even though the screening hits occupy the same binding site as the native cleavage product 2-ABA, the binding mode is different. The fragments bridge the two metal atoms in the binuclear active center via a water molecule in contrast to 2-ABA, where the carboxylate occupies this position (Figure 12). Moreover both, 2-ABA and the ligands **24**–**26** are stabilized by hydrophobic interactions. Additionally, compounds **24** and **25** are interacting with a histidine (His71) sidechain via π-stacking. For the thiophene-containing fragment **26** a π–π interaction of the sulfur with Phe195 can be observed.

In vitro evaluation was performed using a combined PqsDE assay due to the aforementioned instability of 2-ABA-CoA which in this scenario is generated in situ from anthraniloyl-CoA via PqsD-mediated condensation with malonyl-CoA. The hit fragments were able to block the thioesterase in the micromolar range (e.g., IC_{50} (**24**) = 25 ± 4 μM). When assessing the hits on *Pseudomonas* cultures, thioesterase inhibition remained, whereas none of the compounds had any impact on pyocyanin production at a concentration of 500 μM. This means that the regulatory function of PqsE is not linked to its hydrolase function. Since the regulatory function of the enzyme is not associated to its active site, it was hypothesized that it might be involved in a macromolecule–macromolecule interaction, e.g., protein–protein or protein–DNA/RNA interaction, while the exact molecular mechanism remains unclear. Even though Zender et al. were not able to attenuate PA virulence via blockage of PqsE, important new insights on this target were made. The discovery that pathoblockers targeting PqsE assumedly may not need to target the active site of the enzyme, but rather a different pocket or surface. To this end, further research on the exact molecular mechanism of the regulatory activity of PqsE is needed.

PqsBC

The small molecule 2-AA (**27**), which is also a secondary metabolite generated in the AQ biosynthesis pathway, was reported to inhibit PqsBC [31]. In a PqsBC-based biochemical assay it showed an IC_{50} in the micromolar range and was proven to reduce virulence in an acute mouse infection model [67].

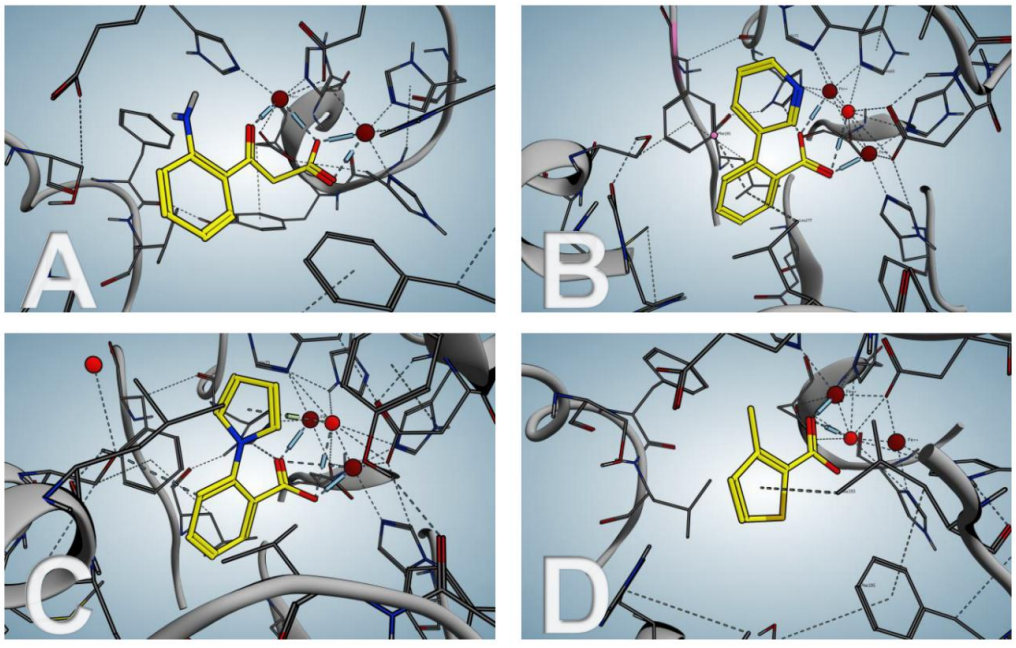

Figure 12: PqsE co-crystal structures. (A) native product 2-ABA; (B–D) hit fragments **24**–**26**.

Beilstein J. Org. Chem. **2018,** *14,* 2627–2645.

In 2017, Maura et al. synthesized inhibitors based on a benzimidazole scaffold (Figure 13) [68]. Starting from a PqsR inhibitor, changes of the electronic properties on the benzimidazole by introducing an electron-donating group led to a higher PqsBC inhibitory activity, while decreasing the affinity to PqsR (compound **28**).

Nevertheless, it was shown that blockage of PqsBC leads to a reduction of HHQ but an accumulation of DHQ, which is reported to be toxic for epithelial cells, and 2-AA, which is involved in formation of persister cells [69]. In the same work, compounds **29** and **30** were evaluated. Compound **29** was first reported in a study aiming at the design of PqsD inhibitors, showing only very weak activity against this target. However, it showed surprisingly good effects on signal molecule production in cell-based assays. Later it was found that this compound actually gains its cellular activity through inhibition of PqsBC [56,70]. As already expected from previous results these compounds also showed a strong increase in 2-AA and DHQ production, while not affecting the overall production of AQ's.

PqsR

In 2017 Kamal et al. investigated the structure–functionality relationship of compounds targeting PqsR. They differentiated between agonists, neutral agonists, inverse agonists and agonistic/antagonistic mixed profile compounds. It was shown that only inverse agonists were able to reduce transcriptional levels below basal and with that the production of pyocyanin. This implies that the aim is to search rather for inverse agonists than for antagonists [71].

Ligand-based design

Following a ligand-based approach Lu et al. modified the native PqsR ligand HHQ (**31**) by introducing a strong electron-withdrawing nitro group in the 6-position (compound **33**) [72]. While displaying an IC_{50} of 51 nM in an *E. coli*-based reporter gene assay, **33** was also able to reduce pyocyanin production to 44% at 15 µM. Further investigations showed that when conducting the reporter gene assay in *P. aeruginosa* instead of using the heterologous *E. coli* system activity of **33** was drastically reduced (only 60% inhibition at 10 µM). The reason for this drop in activity was the cell-mediated oxidation of the 3-position of the quinolone core through action of the *P. aeruginosa* enzyme PqsH (Figure 14), turning the inverse agonist **33** into a strong agonist **34** (EC_{50} = 2.8 nM).

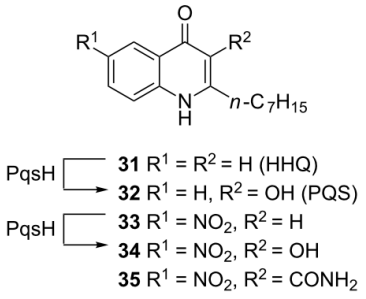

Figure 14: Native PqsR ligand HHQ (**31**) which is converted into PQS (**32**) by PqsH and synthetic inhibitors **33** and **35**, former is also converted by PqsH into the strong agonist **34**.

This phenomenon was overcome by blocking the metabolic susceptible 3-position with various functional groups resulting in **35** which showed good activity in both *E. coli* (IC_{50} = 35 nM) and *P. aeruginosa* (IC_{50} = 404 nM) based reporter gene assays. Furthermore, this compound was able to inhibit pyocyanin production with an IC_{50} of 2 µM and HHQ levels were reduced to 54% at a concentration of 15 µM. Additionally the Hartmann group demonstrated that **35** enables survival of PA14-infected *Galleria melonella* larvae [73]. Moreover, the optimised compound also benefited from a decreased clogP value compared to the parent compound **33**, which is reflected in an improved solubility [74]. In a recent publication by Kamal et al. the pharmacological profiles of several alkylquinolone compounds were investigated in a structure–functionality relationship manner, resulting in four different profiles: (a) agonists, (b) antagonists, (c) inverse agonists and (d) biphasic modulators. These studies revealed that pyocyanin production is only decreased significantly when the QS modulators are inverse agonists. It was hypothesized that the already mentioned 3-position is crucial for the functionality. Depending on the groups installed in this position and, hence, the different ligand–protein interactions they introduce, com-

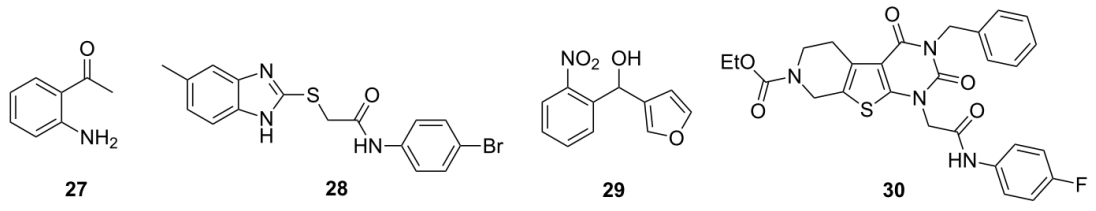

Figure 13: Structurally diverse PqsBC-inhibitors **27**–**30**.

Beilstein J. Org. Chem. **2018,** *14,* 2627–2645.

pounds are either agonists, antagonists, or inverse agonists. This hypothesis was in accordance with a study made by Shanahan et al. who synthesized various other C-3 substituted analogs [75].

Ilangovan et al. discovered a quinazoline scaffold as another class of ligand-based hit compounds. Based on the C9-congener of HHQ several substituted 2-alkyl-4(*H*)-quinazolines were synthesized. The most potent compound **36** (Figure 15) showed micromolar inhibition in *P. aeruginosa* and was able to decrease pyocyanin levels down to less than 0.5 µg/mL at 100 µM. Furthermore, AQ signal molecules could also be suppressed. The crystal structure of the PqsR co-inducer binding site in complex with **36** was solved at 2.95 Å resolution (Figure 16), as well as a co-crystal structure of the native HHQ C9-congener NHQ [76] demonstrating a competitive binding mode.

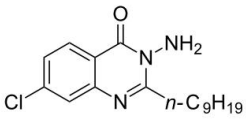

36

Figure 15: Quinazolinone inhibitor **36** (QZN).

When compared to the native ligand NHQ, **36** shows similar hydrophobic interactions (Figure 16). In addition, the chlorine is able to occupy a vacant sub pocket. A hydrogen bond is found between the backbone oxygen of L207 and the 3-NH_2 hydrogen atoms. Interestingly, adding the chlorine substituent in 7-position of PQS leads to a 135 times more potent agonist, indicating the importance of the vacant sub pocket next to T265. This also indicates that the quorum quenching activity of **36** depends on slight conformational changes. The L1 loop main chain and a rotation of the T265 side chain are hypothesized to be important for antagonistic/inverse agonistic functionality of PqsR-targeting QSIs.

More recently the same group used docking studies to select compounds from a quinolone-based compound library (Figure 17). The best fitting compounds **37**–**40** were then evaluated in a whole bacterial cell-based *P. aeruginosa* screening

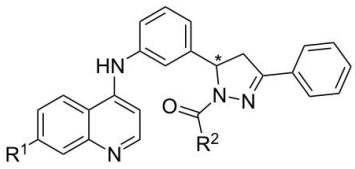

37 R^1 = Cl, R^2 = H
38 R^1 = Cl, R^2 = Me
39 R^1 = CF_3, R^2 = H
40 R^1 = CF_3, R^2 = Me

Figure 17: Structures of best fitting compounds **37**–**40** obtained from docking studies.

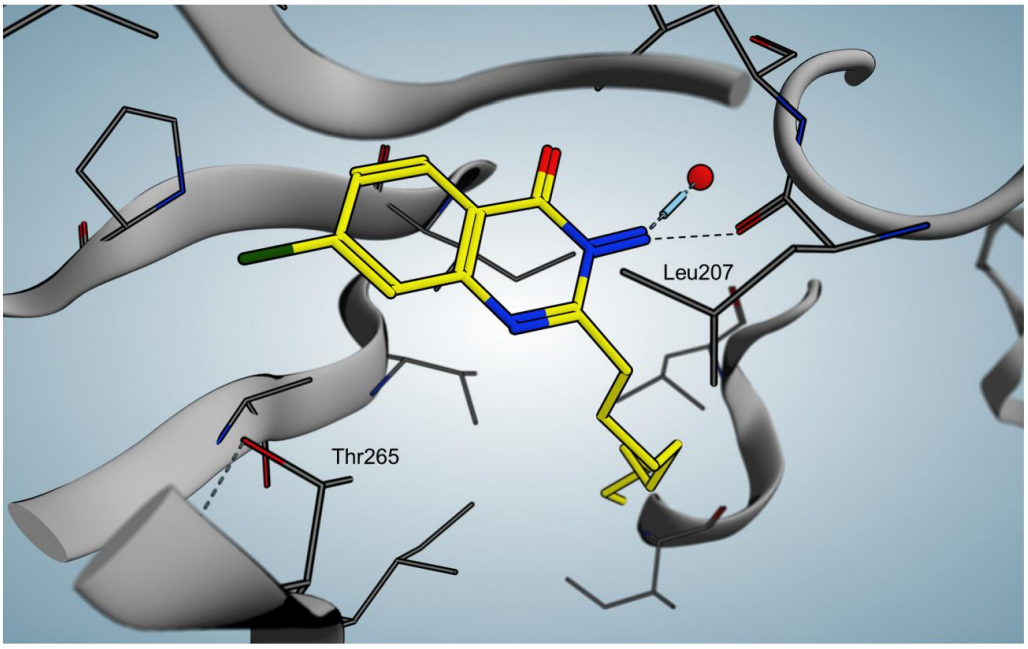

Figure 16: Crystal structure of QZN (**36**) in complex with $PqsR^{CBD}$.

Beilstein J. Org. Chem. **2018,** *14,* 2627–2645.

with IC_{50} values in the low micromolar range. Additionally, they showed that compound **37** emerged as the most potent inhibitor of this series.

Compounds **37** and **39** furthermore exhibited inhibition of HHQ, PQS and HQNO production in PAO1 strains when treated with 3 × IC_{50}, whereas in PA14 a strong decrease in activity could be observed, especially for **39**.

Benzamide-benzimidazole (BB) series

In 2014, Starkey et al. performed a high-throughput whole-cell screening and identified the benzamide-benzimidazole (BB) motif as a promising scaffold for the inhibition of PqsR [77]. Starting from **41**, which was not only able to suppress expression of AQs but also completely blocked pyocyanin production at a concentration of 10 μM. Various analogues were synthesized resulting in compound **42** (M64), where similar as in the quinolones described by Lu et al., introduction of the electron-withdrawing nitro function led to very potent inverse agonist (Figure 18) [72]. M64 (**42**) proved a very potent inhibitor of HAQ and pyocyanin production at 1 μM.

Further investigations revealed that M64 (**42**) also reduces 2-AA levels leading to a decreased rate of persister cells. The compound also proved to be active in burn wound and lung infection models in mice and increased survival rates especially when applied in combination with sub-therapeutic doses of ciprofloxacin. In an analytics-driven study by Allegretta et al., the compound was further profiled regarding suppression of the PQS-related metabolites DHQ, 2-AA, HHQ, PQS and HQNO. In brief, this study demonstrated that PqsR is an excellent target for potent QSI compounds effectively suppressing AQ levels and 2-AA production at reasonable concentrations [69]. Lately, Maura and Rahme were able to demonstrate the effect of M64 (**42**) on biofilm formation [78]. Biofilm biomass was drastically reduced when treated with 1 and 10 μM of **42** compared to the untreated PA14 control. Function of PqsR is involved in regulation of HQNO-mediated autolysis and eDNA release, which has been reported to be important for antibiotic tolerance of biofilm-inheriting bacteria. Hence, Rahme and co-workers investigated the effect of their compound **42** on the ability to improve antibiofilm effects of two clinically relevant drugs. When growing biofilms for 48 h in presence or absence of M64 (**42**), followed by treatment of 10 μg/mL of meropenem or tobramycin for 24 h, the activity of the otherwise ineffective antibiotics could be restored. Especially in the case of meropenem, which did not have any effects at all on biofilm viable cells, **42** lead to remarkable results. In 2018, Kitao et al. solved the crystal structure for PqsR ligand binding domain in complex with M64 (**42**) with a resolution of 2.65 Å (Figure 19), unravelling the exact interactions of the compound with the protein [79].

Indicated key interactions are π-stacking of Y258 with the phenoxy moiety in the tail region and a hydrogen bond formed between the Q194 side chain and the carboxamide in the linker area. Furthermore the benzimidazole core shows hydrophobic contacts with isoleucins 149 and 236. More hydrophobic interactions were observed in the tail region, in particular with leucins 189 and 208 as well as Y258. Mutations at these specific residues indicated that the π–π interactions of Y258 are crucial for M64's full inhibition with respect to pyocyanin production, which was only weakly inhibited in an Y258M *P. aeruginosa* mutant strain. The importance of the phenoxy substitutent was further supported by a congener of M64 that lacks this motif and therefore is unable to be involved in π-stacking resulting in a nine-fold increased IC_{50} value compared to M64. Even though there is no specific interaction observed for the nitro function it is crucial for the activity and thus believed to form an instable H-bond with T265. The Rahme group already demonstrated in a former ITC assay that M64 is directly bound in the PqsR LBD [77]. However, they were also suggesting inverse agonistic effect of M64 based on mutation experiments [79]. Moreover an in vivo cross-linking assay of full-length PqsR and a corresponding I68F mutant was carried out leading to the suggestion that upon binding of M64 the protein stability might be increased. Based on these results it was proposed that M64 induces a change in conformation of the PqsR-DNA binding domain, whereas the LBD is not affected extensively.

Aryloxyacetindoles

Spero Therapeutics further optimized M64 (**42**), firstly by changing the phenoxyphenylamide into a carbonyl-linked

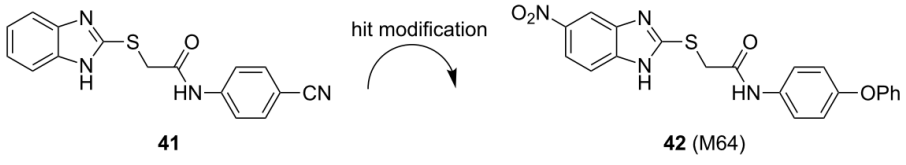

41 **42** (M64)

Figure 18: Initial hit **21** and optimized compound **42** (M64).

Beilstein J. Org. Chem. **2018,** *14,* 2627–2645.

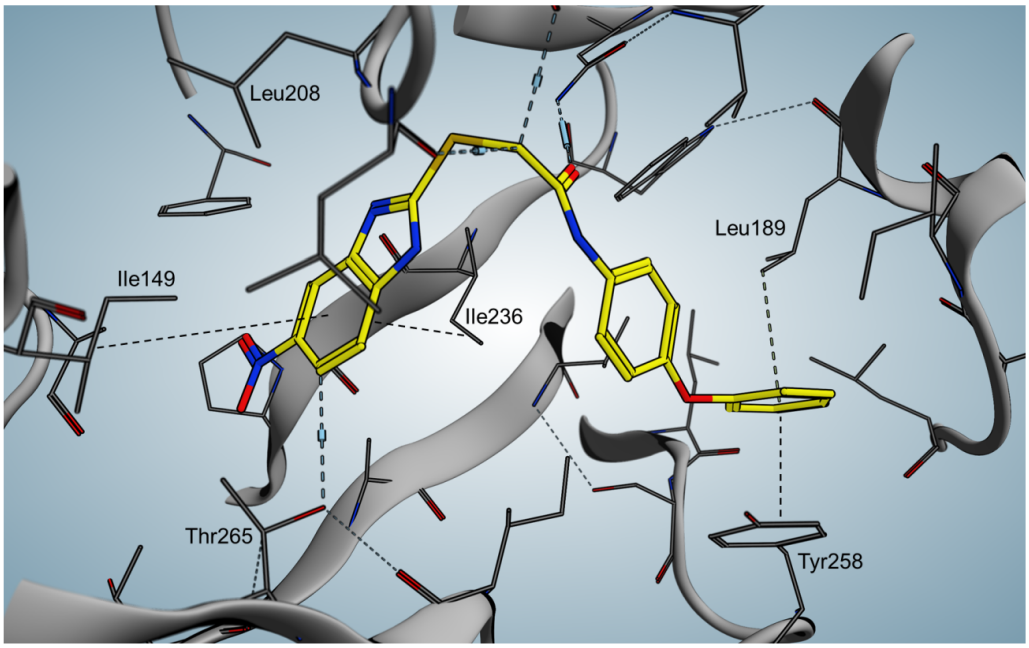

Figure 19: Co-crystal structure of M64 (**42**) with $PqsR^{LBD}$.

indole containing a hetarylether (**43**) [80]. Afterwards they varied the linkage of the benzimidazole moiety (compound not shown) [80]. In a follow-up patent they generated PqsR inhibitor **45** as a front-runner compound [81], in which the benzimidazole headgroup was replaced by a substituted naphthalene bearing a carboxamide, in analogy to a fragment **44** of Zender et al. [82] and similar to the carboxamide-decorated nitro-quinoline scaffold described by Lu et al. (Figure 20) [73].

Compound **45** was highly potent in inhibiting pyocyanin production (stated IC_{50} in a range of 50–250 nM) and was furthermore able to suppress PQS and HHQ production (50 nM < IC_{50} < 250 nM). In a murine thigh infection model using PA14, target engagement was demonstrated in vivo measuring PQS and HHQ levels from the corresponding tissues after treatment. Compound **45** was able to reduce PQS and HHQ levels to 50% and 40%, respectively, 12 hours post-infection. Up to now no further optimization or development of these compounds has been reported.

Fragment-based design

In 2012 Klein et al. obtained the benzamides **46** and **47**, as well as the hydroxamic acid **48** as hits within an SPR screening, which were further evaluated in ITC experiments in order to have a clearer view on the thermodynamic parameters (Figure 21). The antagonists displayed activity in a low double-digit µM range, but had only a marginal impact on the production of the virulence factor pyocyanin [83].

Further SPR screenings afforded hits **49**–**51** with EC_{50} between 7.5–17.8 µM. When compared to the benzamide class, compound **49** shows no significant increase in affinity to the target receptor but is able to inhibit pycocyanin formation by 46 ± 9% at a concentration of 250 µM, and is capable of reducing the AQ's HHQ and HQNO up to 43 ± 3% at the same concentration [82]. With these fragments in hand further growing and subsequent linking or merging may open new avenues for the generation of new drug-like PqsR inverse agonists.

Dual target QS inhibitors

PqsBC/PqsR

In an initial target assessment, Maura et al. found that compound **52** showed an ambiguous profile. This raised the question if this compound class could target additional targets of the PQS-system besides PqsR [68]. Experiments with a PqsR isogenic mutant strain revealed that **52** inhibits HHQ and PQS production, while raising 2-AA levels, pointing at PqsBC as a second target, which was corroborated via SPR studies. When exchanging the chlorine to bromine **53** a high PqsR activity was obtained while the affinity to PqsBC decreased (Figure 22).

The iodine-substituted derivative **54** showed both, a high PqsR, as well as a high PqsBC activity. Exchanging the electron-withdrawing nitro functionality with an electron-donating methyl group turned the PqsR antagonist **53** into a very potent PqsBC inhibitor while losing activity on the initial target PqsR. In addition to these mechanistic findings, it was also shown that the

Beilstein J. Org. Chem. **2018,** *14,* 2627–2645.

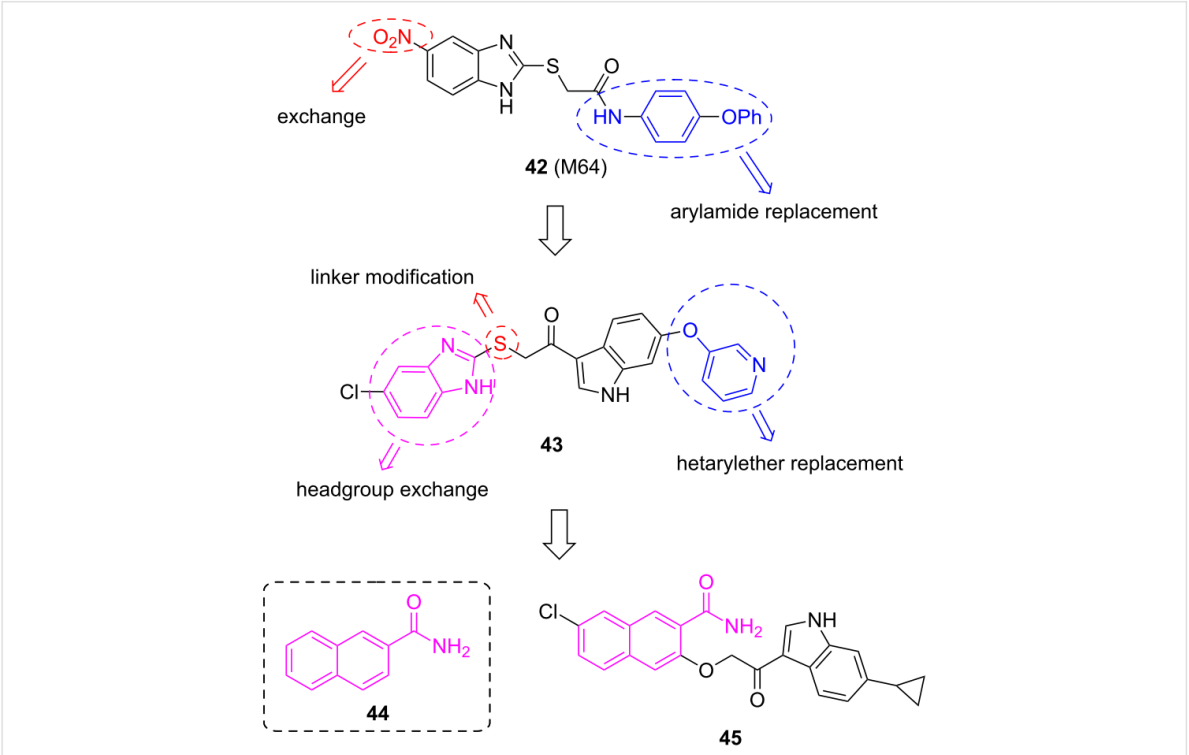

Figure 20: M64 (**42**) as the starting point for further optimization leading to **43**, which was further modified and merged with the fragment **44** to give compound **45**.

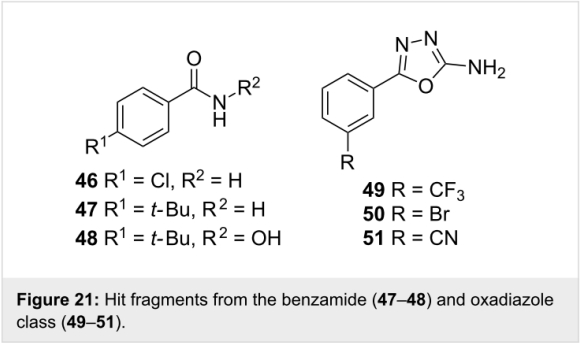

Figure 21: Hit fragments from the benzamide (**47**–**48**) and oxadiazole class (**49**–**51**).

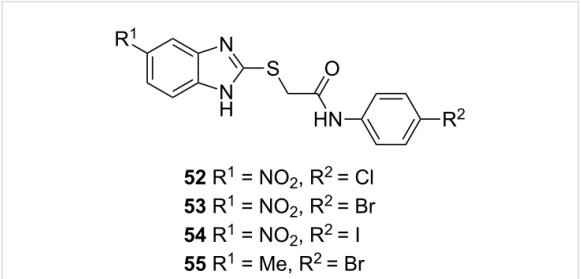

Figure 22: Structures of dual inhibitors **52**–**55**.

dual inhibitors are capable of rescuing human lung epithelial cells and macrophages at a concentration of 50 µM in cell-based infection models. Also antibiotic activity of meropenem (dose: 10 µg/mL) in presence of 10 µM of dual inhibitors could be partially reinstalled.

PqsD/PqsR

Thomann et al. showed that combining a PqsD and a PqsR activity synergistically affects pyocyanin production. Based on these results combining fragments from a PqsR and a PqsD inhibitor belonging to a sulfonyl-pyrimidine class, compound **56** was generated and its ability to reduce pyocyanin evaluated (Figure 23) [84]. While exhibiting IC_{50} values of 15 µM on PqsR and 21 µM on PqsD, the compound was able to inhibit the pyocyanin production with an IC_{50} of 86 µM. Moreover **56** also proved to be efficient in blocking pyoverdine production, another important *P.aeruginosa* virulence factor. When applied at a concentration of 500 µM less than 10% of pyoverdine production was remaining. At 100 µM the pyoverdine amount was cut to a half. Since also the levels of extracellular DNA could be reduced to a minimum with their dual inhibitor, the group investigated the effect of adding **56** to ciprofloxacin. The combination of this QSI together with the antibiotic significantly increased antibiofilm activity at the used concentrations

Beilstein J. Org. Chem. **2018,** *14,* 2627–2645.

([CIPX] = 1 μM, [56] = 50 μM). The compound also proved to be active in a *Galleria melonella* survival assay being capable of ensuring survival up to more than 50% after 4.5 d post-infection at a dosage of 1.25 nmol compared to untreated PA14-infected larvae.

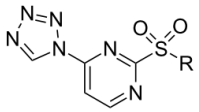

56 R = Me
57 R = *n*-Hex
58 R = 3,4-di-Cl-Ph

Figure 23: Sulfonyl pyrimidines **56**–**58** acting as dual PqsD/PqsR inhibitors.

Following the dual inhibitor concept, the class of sulfonyl-pyrimidines further afforded compounds **57** and **58** with promising activity. While PqsR activity slightly decreased (50 μM and 24 ± 5 μM, respectively) **57** exhibited an IC_{50} of 1.7 μM and **58** displayed sub-micromolar activity of 0.4 ± 0.1 μM. The effects on biofilm formation and eDNA release were evaluated at a concentration of 100 μM. Even if **57** was less potent on both PqsR and PqsD compared to **58**, it turned out to be more efficient in inhibiting biofilm production. When assessed on their ability to reduce extracellular DNA all three compounds were equally potent. Nevertheless compound **58** only showed a weak effect on the inhibition of pyocyanin (14% inhibition at 100 μM) [85].

Conclusion

In the past decade, the pqs QS system of *P. aeruginosa* has attracted increasing interest by academic researchers. This is certainly due to its prominent involvement in virulence regulation of this important Gram-negative pathogen. Among the various pathoblocker strategies, targeting a master regulator of pathogenicity traits appears to have huge translational potential. Hitting an array of virulence mechanisms at once instead of addressing just singular factor holds great promise for future discovery and development of pqs-targeting QSI. Compared to the other QS systems present in *P. aeruginosa* the pqs system is lacking some of the liabilities associated with the las and the rhl systems. The former AHL-dependent regulatory circuit has been described to be the first QS system to get lost upon chronification of *P. aeruginosa* infections [86]. However, chronic lung infections are one of the major indications with a very high medical need. In the case of addressing the rhl system, a non-unidirectional virulence modulatory effect is observed. Agonists of RhlR reduce pyocyanin, but induce rhamnolipid production, while antagonists have the inverted effect [87]. This raises some concerns about the applicability of RhlR as an effective 'stand-alone' pathoblocker target. A combination of rhl- and pqs-targeting QSI, however, seemed to provide promising and clear-cut antivirulence effects [88]. Finally, the potential of iqs-targeting approaches remains to be investigated as more insight in the function of this rather recently discovered regulator is needed. The pqs system is active in chronically infected cystic fibrosis patients and, according to the current knowledge, blockade of this master regulator delivers an unambiguous antivirulence effect.

In terms of published research, the most studied molecular targets within the pqs system are the signal molecule synthase PqsD and the receptor PqsR (MvfR), while in the latter case projects are currently in a clearly more advanced stage. When comparing the reported antivirulence effects of PqsD- and PqsR-targeting QSI, evidence is growing that hitting the transcriptional regulator results in more pronounced pathoblocking effects than addressing the biosynthetic enzyme cascade. However, a synergistic effect for dual-target inhibitors hitting PqsR and PqsD or PqsBC simultaneously has been described [68,84]. Additionally, the authors believe that attempts to effectively target PqsE are still worthwhile pursuing, given its prominent involvement in pqs virulence regulation. However, this would require elucidating the still unknown mechanism behind its regulatory function.

In order to translate the promising hit and lead compounds described above into the clinic, continuous discovery and development efforts are required. Especially the lead optimization stage is strongly dependent on integrated medicinal chemistry and biological profiling teams. In addition to potency considerations, drug-like properties aiming at favorable pharmacokinetics move into the focus [89]. Due to the complex nature of virulence phenotype assays as well as ADME/T testing cascades assembling the required teams, expertise, and resources might be a challenge especially for academic groups. Hence, often proclaimed drug discovery timelines for target-to-candidate projects of about 6 years or less [90] are quite unrealistic in this field. This actually underpins the urgency for current anti-infective discovery efforts to enable refilling the pipeline in due time before available treatment options run out. However, we believe the translational perspective for such pathoblockers is quite promising. Specifically, it has been shown that PqsR-targeting QSI are able to increase the susceptibility of *P. aeruginosa* biofilms against antibiotics [78]. Hence, adjunctive treatment approaches where a conventional backbone antibiotic therapy is potentiated by pathoblocking agents appears quite attractive. In analogy to current antiviral and anticancer strategies, more personalized pathogen-specific drug combinations should be pursued also in the bacterial infections

field. As a consequence, more advanced diagnostic tools have to be devised to enable fast and reliable analysis of the pathogen and its resistance profile. We are curious what future research will uncover in this important, yet underexploited, drug discovery field and believe exploring such strategies further will be a worthwhile endeavour.

Acknowledgements

We are grateful to Rolf W. Hartmann for his generous and persistent support and guiding expertise.

ORCID® iDs

Martin Empting - https://orcid.org/0000-0002-0503-5830

References

1. Price, L.; Gozdzielewska, L.; Young, M.; Smith, F.; MacDonald, J.; McParland, J.; Williams, L.; Langdridge, D.; Davis, M.; Flowers, P. *J. Antimicrob. Chemother.* **2018,** *73,* 1464–1478. doi:10.1093/jac/dky076
2. Ventola, L. C. *Pharm. Ther.* **2015,** *40,* 277–283.
3. Coates, A. R. M.; Halls, G.; Hu, Y. *Br. J. Pharmacol.* **2011,** *163,* 184–194. doi:10.1111/j.1476-5381.2011.01250.x
4. WHO. An analysis of the antibacterial clinical development pipeline, including tuberculosis. http://www.who.int/medicines/areas/rational_use/antibacterial_agents_clinical_development/en/ (accessed July 30, 2018).
5. Wagner, S.; Sommer, R.; Hinsberger, S.; Lu, C.; Hartmann, R. W.; Empting, M.; Titz, A. *J. Med. Chem.* **2016,** *59,* 5929–5969. doi:10.1021/acs.jmedchem.5b01698
6. Li, X.-H.; Lee, J.-H. *J. Microbiol. (Seoul, Repub. Korea)* **2017,** *55,* 753–766. doi:10.1007/s12275-017-7274-x
7. Żelechowska, P.; Agier, J.; Kozłowska, E.; Brzezińska-Błaszczyk, E. *Przegl. Lek.* **2016,** *73,* 334–339.
8. Mühlen, S.; Dersch, P. Anti-virulence Strategies to Target Bacterial Infections. In *How to Overcome the Antibiotic Crisis. Current Topics in Microbiology and Immunology;* Stadler, M.; Dersch, P., Eds.; Springer: Cham, 2015; Vol. 398, pp 147–183. doi:10.1007/82_2015_490
9. Dickey, S. W.; Cheung, G. Y. C.; Otto, M. *Nat. Rev. Drug Discovery* **2017,** *16,* 457–471. doi:10.1038/nrd.2017.23
10. Kufel, W. D.; Devanathan, A. S.; Marx, A. H.; Weber, D. J.; Daniels, L. M. *Pharmacotherapy* **2017,** *37,* 1298–1308. doi:10.1002/phar.1990
11. Soukarieh, F.; Williams, P.; Stocks, M. J.; Camara, M. *J. Med. Chem.* **2018,** in press. doi:10.1021/acs.jmedchem.8b00540
12. WHO. Global priority list of antibiotic-resistant bacteria to guide research, discovery, and development of new antibiotics. http://www.who.int/medicines/publications/global-priority-list-antibiotic-resistant-bacteria/en/ (accessed July 30, 2018).
13. Schweizer, H. P. *GMR, Genet. Mol. Res.* **2003,** *2,* 48–62.
14. Strateva, T.; Yordanov, D. *J. Med. Microbiol.* **2009,** *58,* 1133–1148. doi:10.1099/jmm.0.009142-0
15. Breidenstein, E. B. M.; de la Fuente-Núñez, C.; Hancock, R. E. W. *Trends Microbiol.* **2011,** *19,* 419–426. doi:10.1016/j.tim.2011.04.005
16. Golemi-Kotra, D. Pseudomonas Infections. *xPharm: The Comprehensive Pharmacology Reference;* Elsevier, 2008; pp 1–8.
17. Bodey, G. P.; Bolivar, R.; Fainstein, V.; Jadeja, L. *Rev. Infect. Dis.* **1983,** *5,* 279–313. doi:10.1093/clinids/5.2.279
18. da Silva Filho, L. V. R. F.; de Agujar Ferreira, F.; Reis, F. J. C.; de Britto, M. C. A.; Levy, C. E.; Clark, O.; Ribeiro, J. D. *J. Bras. Pneumol.* **2013,** *39,* 495–512. doi:10.1590/S1806-37132013000400015
19. Crull, M. R.; Ramos, K. J.; Caldwell, E.; Mayer-Hamblett, N.; Aitken, M. L.; Goss, C. H. *BMC Pulm. Med.* **2016,** *16,* 176. doi:10.1186/s12890-016-0333-y
20. Sordé, R.; Pahissa, A.; Rello, J. *Infect. Drug Resist.* **2011,** *4,* 31–41. doi:10.2147/IDR.S16263
21. Barr, H. L.; Halliday, N.; Barrett, D. A.; Williams, P.; Forrester, D. L.; Peckham, D.; Williams, K.; Smyth, A. R.; Honeybourne, D.; Whitehouse, J. L.; Nash, E. F.; Dewar, J.; Clayton, A.; Knox, A. J.; Cámara, M.; Fogarty, A. W. *J. Cystic Fibrosis* **2017,** *16,* 230–238. doi:10.1016/j.jcf.2016.10.005
22. Lee, J.; Zhang, L. *Protein Cell* **2015,** *6,* 26–41. doi:10.1007/s13238-014-0100-x
23. Li, S.; Chen, S.; Fan, J.; Cao, Z.; Ouyang, W.; Tong, N.; Hu, X.; Hu, J.; Li, P.; Feng, Z.; Huang, X.; Li, Y.; Xie, M.; He, R.; Jian, J.; Wu, B.; Xu, C.; Wu, W.; Guo, J.; Lin, J.; Sun, P. *Eur. J. Med. Chem.* **2018,** *145,* 64–73. doi:10.1016/j.ejmech.2017.12.076
24. Dubern, J.-F.; Diggle, S. P. *Mol. BioSyst.* **2008,** *4,* 882–888. doi:10.1039/b803796p
25. Coleman, J. P.; Hudson, L. L.; McKnight, S. L.; Farrow, J. M., III; Calfee, M. W.; Lindsey, C. A.; Pesci, E. C. *J. Bacteriol.* **2008,** *190,* 1247–1255. doi:10.1128/JB.01140-07
26. Zhang, Y.-M.; Frank, M. W.; Zhu, K.; Mayasundari, A.; Rock, C. O. *J. Biol. Chem.* **2008,** *283,* 28788–28794. doi:10.1074/jbc.M804555200
27. Dulcey, C. E.; Dekimpe, V.; Fauvelle, D.-A.; Milot, S.; Groleau, M.-C.; Doucet, N.; Rahme, L. G.; Lépine, F.; Déziel, E. *Chem. Biol.* **2013,** *20,* 1481–1491. doi:10.1016/j.chembiol.2013.09.021
28. Hutter, M. C.; Brengel, C.; Negri, M.; Henn, C.; Zimmer, C.; Hartmann, R. W.; Empting, M.; Steinbach, A. *J. Mol. Model.* **2014,** *20,* 2255. doi:10.1007/s00894-014-2255-z
29. Drees, S. L.; Fetzner, S. *Chem. Biol.* **2015,** *22,* 611–618. doi:10.1016/j.chembiol.2015.04.012
30. Witzgall, F.; Depke, T.; Hoffmann, M.; Empting, M.; Brönstrup, M.; Müller, R.; Blankenfeldt, W. *ChemBioChem* **2018,** *19,* 1531–1544. doi:10.1002/cbic.201800153
31. Drees, S. L.; Li, C.; Prasetya, F.; Saleem, M.; Dreveny, I.; Williams, P.; Hennecke, U.; Emsley, J.; Fetzner, S. *J. Biol. Chem.* **2016,** *291,* 6610–6624. doi:10.1074/jbc.M115.708453
32. Schertzer, J. W.; Brown, S. A.; Whiteley, M. *Mol. Microbiol.* **2010,** *77,* 1527–1538. doi:10.1111/j.1365-2958.2010.07303.x
33. Rampioni, G.; Falcone, M.; Heeb, S.; Frangipani, E.; Fletcher, M. P.; Dubern, J.-F.; Visca, P.; Leoni, L.; Cámara, M.; Williams, P. *PLoS Pathog.* **2016,** *12,* e1006029. doi:10.1371/journal.ppat.1006029
34. Lin, J.; Cheng, J.; Wang, Y.; Shen, X. *Front. Cell. Infect. Microbiol.* **2018,** *8,* No. 230. doi:10.3389/fcimb.2018.00230
35. Maura, D.; Hazan, R.; Kitao, T.; Ballok, A. E.; Rahme, L. G. *Sci. Rep.* **2016,** *6,* No. 34083. doi:10.1038/srep34083
36. Legendre, C.; Reen, F. J.; Mooij, M. J.; McGlacken, G. P.; Adams, C.; O'Gara, F. *Infect. Immun.* **2012,** *80,* 3985–3992. doi:10.1128/IAI.00554-12
37. Kim, K.; Kim, Y. U.; Koh, B. H.; Hwang, S. S.; Kim, S.-H.; Lépine, F.; Cho, Y.-H.; Lee, G. R. *Immunology* **2010,** *129,* 578–588. doi:10.1111/j.1365-2567.2009.03160.x
38. Hazan, R.; Que, Y. A.; Maura, D.; Strobel, B.; Majcherczyk, P. A.; Hopper, L. R.; Wilbur, D. J.; Hreha, T. N.; Barquera, B.; Rahme, L. G. *Curr. Biol.* **2016,** *26,* 195–206. doi:10.1016/j.cub.2015.11.056

39. Gruber, J. D.; Chen, W.; Parnham, S.; Beauchesne, K.; Moeller, P.; Flume, P. A.; Zhang, Y.-M. *PeerJ* **2016,** *4,* e1495. doi:10.7717/peerj.1495
40. Que, Y.-A.; Hazan, R.; Strobel, B.; Maura, D.; He, J.; Kesarwani, M.; Panopoulos, P.; Tsurumi, A.; Giddey, M.; Wilhelmy, J.; Mindrinos, M. N.; Rahme, L. G. *PLoS One* **2013,** *8,* e80140. doi:10.1371/journal.pone.0080140
41. Hall, S.; McDermott, C.; Anoopkumar-Dukie, S.; McFarland, A. J.; Forbes, A.; Perkins, A. V.; Davey, A. K.; Chess-Williams, R.; Kiefel, M. J.; Arora, D.; Grant, G. D. *Toxins* **2016,** *8,* No. 236. doi:10.3390/toxins8080236
42. Allen, L.; Dockrell, D. H.; Pattery, T.; Lee, D. G.; Cornelis, P.; Hellewell, P. G.; Whyte, M. K. B. *J. Immunol.* **2005,** *174,* 3643–3649. doi:10.4049/jimmunol.174.6.3643
43. Rada, B.; Jendrysik, M. A.; Pang, L.; Hayes, C. P.; Yoo, D.-G.; Park, J. J.; Moskowitz, S. M.; Malech, H. L.; Leto, T. L. *PLoS One* **2013,** *8,* e54205. doi:10.1371/journal.pone.0054205
44. Arai, H. *Front. Microbiol.* **2011,** *2,* No. 103. doi:10.3389/fmicb.2011.00103
45. Lépine, F.; Dekimpe, V.; Lesic, B.; Milot, S.; Lesimple, A.; Mamer, O. A.; Rahme, L. G.; Déziel, E. *Biol. Chem.* **2007,** *388,* 839–845. doi:10.1515/BC.2007.100
46. Witzgall, F.; Ewert, W.; Blankenfeldt, W. *ChemBioChem* **2017,** *18,* 2045–2055. doi:10.1002/cbic.201700374
47. Lesic, B.; Lépine, F.; Déziel, E.; Zhang, J.; Zhang, Q.; Padfield, K.; Castonguay, M.-H.; Milot, S.; Stachel, S.; Tzika, A. A.; Tompkins, R. G.; Rahme, L. G. *PLoS Pathog.* **2007,** *3,* 1229–1239. doi:10.1371/journal.ppat.0030126
48. Ji, C.; Sharma, I.; Pratihar, D.; Hudson, L. L.; Maura, D.; Guney, T.; Rahme, L. G.; Pesci, E. C.; Coleman, J. P.; Tan, D. S. *ACS Chem. Biol.* **2016,** *11,* 3061–3067. doi:10.1021/acschembio.6b00575
49. Bera, A. K.; Atanasova, V.; Robinson, H.; Eisenstein, E.; Coleman, J. P.; Pesci, E. C.; Parsons, J. F. *Biochemistry* **2009,** *48,* 8644–8655. doi:10.1021/bi9009055
50. Pistorius, D.; Ullrich, A.; Lucas, S.; Hartmann, R. W.; Kazmaier, U.; Müller, R. *ChemBioChem* **2011,** *12,* 850–853. doi:10.1002/cbic.201100014
51. Weidel, E.; de Jong, J. C.; Brengel, C.; Storz, M. P.; Braunshausen, A.; Negri, M.; Plaza, A.; Steinbach, A.; Müller, R.; Hartmann, R. W. *J. Med. Chem.* **2013,** *56,* 6146–6155. doi:10.1021/jm4006302
52. Hinsberger, S.; de Jong, J. C.; Groh, M.; Haupenthal, J.; Hartmann, R. W. *Eur. J. Med. Chem.* **2014,** *76,* 343–351. doi:10.1016/j.ejmech.2014.02.014
53. Hinsberger, S.; Hüsecken, K.; Groh, M.; Negri, M.; Haupenthal, J.; Hartmann, R. W. *J. Med. Chem.* **2013,** *56,* 8332–8338. doi:10.1021/jm400485e
54. Storz, M. P.; Maurer, C. K.; Zimmer, C.; Wagner, N.; Brengel, C.; de Jong, J. C.; Lucas, S.; Müsken, M.; Häussler, S.; Steinbach, A.; Hartmann, R. W. *J. Am. Chem. Soc.* **2012,** *134,* 16143–16146. doi:10.1021/ja3072397
55. Storz, M. P.; Brengel, C.; Weidel, E.; Hoffmann, M.; Hollemeyer, K.; Steinbach, A.; Müller, R.; Empting, M.; Hartmann, R. W. *ACS Chem. Biol.* **2013,** *8,* 2794–2801. doi:10.1021/cb400530d
56. Storz, M. P.; Allegretta, G.; Kirsch, B.; Empting, M.; Hartmann, R. W. *Org. Biomol. Chem.* **2014,** *12,* 6094–6104. doi:10.1039/c4ob00707g
57. Sahner, J. H.; Brengel, C.; Storz, M. P.; Groh, M.; Plaza, A.; Müller, R.; Hartmann, R. W. *J. Med. Chem.* **2013,** *56,* 8656–8664. doi:10.1021/jm401102e
58. Sahner, J. H.; Empting, M.; Kamal, A.; Weidel, E.; Groh, M.; Börger, C.; Hartmann, R. W. *Eur. J. Med. Chem.* **2015,** *96,* 14–21. doi:10.1016/j.ejmech.2015.04.007
59. Allegretta, G.; Weidel, E.; Empting, M.; Hartmann, R. W. *Eur. J. Med. Chem.* **2015,** *90,* 351–359. doi:10.1016/j.ejmech.2014.11.055
60. Weidel, E.; Negri, M.; Empting, M.; Hinsberger, S.; Hartmann, R. W. *Future Med. Chem.* **2014,** *6,* 2057–2072. doi:10.4155/fmc.14.142
61. Thomann, A.; Zapp, J.; Hutter, M.; Empting, M.; Hartmann, R. W. *Org. Biomol. Chem.* **2015,** *13,* 10620–10630. doi:10.1039/c5ob01006c
62. Prothiwa, M.; Szamosvári, D.; Glasmacher, S.; Böttcher, T. *Beilstein J. Org. Chem.* **2016,** *12,* 2784–2792. doi:10.3762/bjoc.12.277
63. Sangshetti, J. N.; Khan, F. A. K.; Patil, R. H.; Marathe, S. D.; Gade, W. N.; Shinde, D. B. *Bioorg. Med. Chem. Lett.* **2015,** *25,* 874–880. doi:10.1016/j.bmcl.2014.12.063
64. Farrow, J. M., III; Sund, Z. M.; Ellison, M. L.; Wade, D. S.; Coleman, J. P.; Pesci, E. C. *J. Bacteriol.* **2008,** *190,* 7043–7051. doi:10.1128/JB.00753-08
65. Rampioni, G.; Pustelny, C.; Fletcher, M. P.; Wright, V. J.; Bruce, M.; Rumbaugh, K. P.; Heeb, S.; Cámara, M.; Williams, P. *Environ. Microbiol.* **2010,** *12,* 1659–1673. doi:10.1111/j.1462-2920.2010.02214.x
66. Zender, M.; Witzgall, F.; Drees, S. L.; Weidel, E.; Maurer, C. K.; Fetzner, S.; Blankenfeldt, W.; Empting, M.; Hartmann, R. W. *ACS Chem. Biol.* **2016,** *11,* 1755–1763. doi:10.1021/acschembio.6b00156
67. Kesarwani, M.; Hazan, R.; He, J.; Que, Y.; Apidianakis, Y.; Lesic, B.; Xiao, G.; Dekimpe, V.; Milot, S.; Deziel, E.; Lépine, F.; Rahme, L. G. *PLoS Pathog.* **2011,** *7,* e1002192. doi:10.1371/journal.ppat.1002192
68. Maura, D.; Drees, S. L.; Bandyopadhaya, A.; Kitao, T.; Negri, M.; Starkey, M.; Lesic, B.; Milot, S.; Déziel, E.; Zahler, R.; Pucci, M.; Felici, A.; Fetzner, S.; Lépine, F.; Rahme, L. G. *ACS Chem. Biol.* **2017,** *12,* 1435–1443. doi:10.1021/acschembio.6b01139
69. Allegretta, G.; Maurer, C. K.; Eberhard, J.; Maura, D.; Hartmann, R. W.; Rahme, L.; Empting, M. *Front. Microbiol.* **2017,** *8,* No. 924. doi:10.3389/fmicb.2017.00924
70. Rahme, L.; Lepine, F.; Starkey, M.; Lesic-Arsic, B. Antibiotic tolerance inhibitors. WO Patent WO2012116010A3, Oct 26, 2012.
71. Kamal, A. A. M.; Petrera, L.; Eberhard, J.; Hartmann, R. W. *Org. Biomol. Chem.* **2017,** *15,* 4620–4630. doi:10.1039/c7ob00263g
72. Lu, C.; Kirsch, B.; Zimmer, C.; de Jong, J. C.; Henn, C.; Maurer, C. K.; Müsken, M.; Häussler, S.; Steinbach, A.; Hartmann, R. W. *Chem. Biol.* **2012,** *19,* 381–390. doi:10.1016/j.chembiol.2012.01.015
73. Lu, C.; Maurer, C. K.; Kirsch, B.; Steinbach, A.; Hartmann, R. W. *Angew. Chem., Int. Ed.* **2014,** *53,* 1109–1112. doi:10.1002/anie.201307547
74. Lu, C.; Kirsch, B.; Maurer, C. K.; de Jong, J. C.; Braunshausen, A.; Steinbach, A.; Hartmann, R. W. *Eur. J. Med. Chem.* **2014,** *79,* 173–183. doi:10.1016/j.ejmech.2014.04.016
75. Shanahan, R.; Reen, F. J.; Cano, R.; O'Gara, F.; McGlacken, G. P. *Org. Biomol. Chem.* **2017,** *15,* 306–310. doi:10.1039/c6ob01930g
76. Ilangovan, A.; Fletcher, M.; Rampioni, G.; Pustelny, C.; Rumbaugh, K.; Heeb, S.; Cámara, M.; Truman, A.; Chhabra, S. R.; Emsley, J.; Williams, P. *PLoS Pathog.* **2013,** *9,* e1003508. doi:10.1371/journal.ppat.1003508
77. Starkey, M.; Lepine, F.; Maura, D.; Bandyopadhaya, A.; Lesic, B.; He, J.; Kitao, T.; Righi, V.; Milot, S.; Tzika, A.; Rahme, L. *PLoS Pathog.* **2014,** *10,* e1004321. doi:10.1371/journal.ppat.1004321
78. Maura, D.; Rahme, L. G. *Antimicrob. Agents Chemother.* **2017,** *61,* e01362-17. doi:10.1128/AAC.01362-17

79. Kitao, T.; Lepine, F.; Babloudi, S.; Walte, F.; Steinbacher, S.; Maskos, K.; Blaesse, M.; Negri, M.; Pucci, M.; Zahler, B.; Felici, A.; Rahme, L. G. *mBio* **2018,** *9,* e02158-17. doi:10.1128/mBio.02158-17
80. Zahler, R.; Cui, D.; Zhou, D. Carbonyl linked bicyclic heteroaryl N-benzimidazoles and analogs as antibiotic tolerance inhibitors. WO Patent WO2016040764A1, March 17, 2016.
81. Zahler, R. Aryloxyacetylindoles and analogs as antibiotic tolerance inhibitors. WO Patent WO2016112088A1, July 14, 2016.
82. Zender, M.; Klein, T.; Henn, C.; Kirsch, B.; Maurer, C. K.; Kail, D.; Ritter, C.; Dolezal, O.; Steinbach, A.; Hartmann, R. W. *J. Med. Chem.* **2013,** *56,* 6761–6774. doi:10.1021/jm400830r
83. Klein, T.; Henn, C.; de Jong, J. C.; Zimmer, C.; Kirsch, B.; Maurer, C. K.; Pistorius, D.; Müller, R.; Steinbach, A.; Hartmann, R. W. *ACS Chem. Biol.* **2012,** *7,* 1496–1501. doi:10.1021/cb300208g
84. Thomann, A.; de Mello Martins, A. G. G.; Brengel, C.; Empting, M.; Hartmann, R. W. *ACS Chem. Biol.* **2016,** *11,* 1279–1286. doi:10.1021/acschembio.6b00117
85. Thomann, A.; Brengel, C.; Börger, C.; Kail, D.; Steinbach, A.; Empting, M.; Hartmann, R. W. *ChemMedChem* **2016,** *11,* 2522–2533. doi:10.1002/cmdc.201600419
86. Bjarnsholt, T.; Jensen, P. Ø.; Jakobsen, T. H.; Phipps, R.; Nielsen, A. K.; Rybtke, M. T.; Tolker-Nielsen, T.; Givskov, M.; Høiby, N.; Ciofu, O. *PLoS One* **2010,** *5,* e10115. doi:10.1371/journal.pone.0010115
87. Welsh, M. A.; Eibergen, N. R.; Moore, J. D.; Blackwell, H. E. *J. Am. Chem. Soc.* **2015,** *137,* 1510–1519. doi:10.1021/ja5110798
88. Welsh, M. A.; Blackwell, H. E. *Cell Chem. Biol.* **2016,** *23,* 361–369. doi:10.1016/j.chembiol.2016.01.006
89. Kerns, E. H.; Di, L. *Drug-like properties. Concepts, structure design and methods: from ADME to toxicity optimization;* Academic Press: Amsterdam, London, 2008.
90. Maqbool, F.; Abid, A.; Ahmed, I. *Int. J. Pharm.* **2017,** *13,* 773–784. doi:10.3923/ijp.2017.773.784

License and Terms

2. Aim and Scope

The WHO rated carbapenem-resistant PA in priority class 1: critical for research and development of new antibiotics. Since common treatments are associated with several drawbacks when it comes to side-effects or even ineffectiveness, the need for novel strategies for treating bacterial infections is incontrovertible. An attractive approach to selectively tackle pathogenic bacteria and leave the human microbiome unharmed, is the so-called “Pathoblocker” approach. Not only is this strategy promising for safety reasons but rather also aims at lower selection pressure among the bacteria. This could ultimately lead to lower rates of resistance. Targeting bacterial virulence factors and “disarming” the pathogen could help the immune system to eradicate the infection on its own or with the help of a co-administered antibiotic.

In the department of drug design and optimization such pathoblockers inhibiting the PQS system have been synthesized and evaluated.[82,83] First experiments in *G. melonella* and *C. elegans* showed promising results, enhancing survival rates upon treatment with a QSI.[84] Moreover, it was demonstrated that dual QSIs were not only able to reduce important virulence factors such as pyocyanin and pyoverdine but also reducing biofilm formation and with that, restoring antibiotic efficacy.[85]

Lately, a fragment-based screening lead to the identification and optimization of an early hit which resulted in a new class of potent PqsR inverse agonists, capable of reducing pyocyanin *in vitro*.[86] The discovery of this novel motif marks the beginning of a medicinal chemistry campaign aiming at the exploration of chemical space, multi-parameter optimization and ultimately lead generation. The objectives of this thesis were embedded within this project and are as follows:

1. Establishment of a reliable and divergent synthesis in order to explore the chemical space around optimized hit compounds.
2. Synthesis and SAR investigations of novel QSI and generation of lead compounds.
3. Multiparamter optimization of lead compounds with respect to activity and pharmacokinetic properties.

3. Results and Discussion

3.1. Lead Generation 1

3.1.1. Design and synthesis of PqsR inverse agonists

The Hartmann group recently reported a potent PqsR inverse agonist **1A**, equipped with an aminopyridine in the *head* part of the molecule (Figure 3.1.1).[86] Moreover, it is equipped with a propyl linker attached to an aromatic moiety. In another series of compounds, the aminopyridine moiety proved to play a crucial role in activity on the target compared to pyocyanin inhibition. In terms of on-target activity compound **1C** was more active than the corresponding analogue **1B**. However, when it comes to the ability of reducing pyocyanin production, compound **1B** benefitted from the amino-function (Figure 3.1.1). Therefore, it was of great interest to further investigate the influence of this motif. Additionally, the possibility of identifying a possible growth vector was given in this class but has not been explored yet. Due to the synthetically non-trivial substitution pattern, the first aim was to investigate the role of the amino function present in the pyridine headgroup.

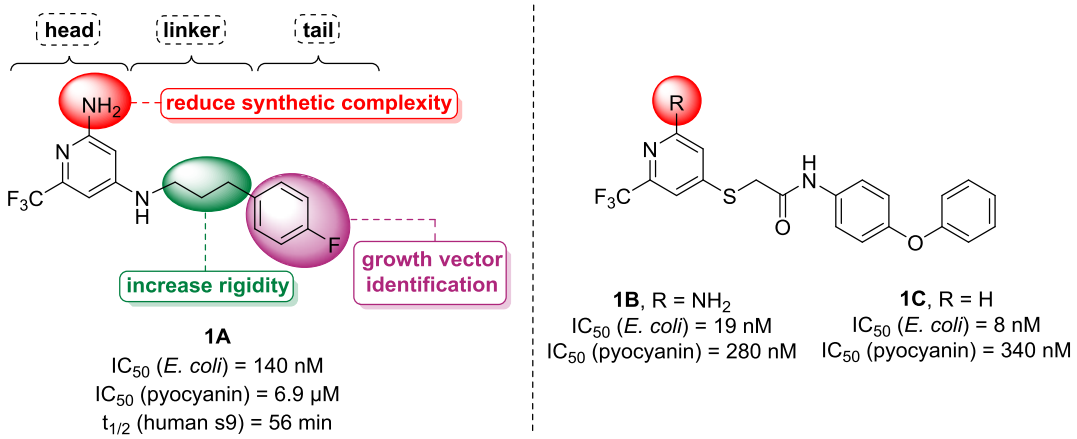

***Figure 3.1.1: 1A** as starting point, comparison of **1B** and **1C** with respect to the amino function in the head.*

Structural modifications in the linker chain are also of high interest as well as the investigation of the *tail* region. With **1A** as the starting point for optimization, the analogous compound **1.1**, lacking the amino function in the head should be synthesized (Scheme 3.1.1). First attempts to generate **1.1** using the initial route by Zender *et al.*, in which S_NAr and *Buchwald-Hartwig*-type chemistry was used, did not yield the desired compound (Scheme 3.1.1, route A). Moreover, this approach was not promising regarding modification in the *tail* phenyl moiety, since different starting materials for *tail* modification were not commercially available and needed to be synthesized from scratch over several steps. Since time played a crucial role in this project, the chemical accessibility and feasibility had to be considered for compound selection and synthesis planning.

Scheme 3.1.1: *Retrosynthetic analysis of* ***1.1****.*

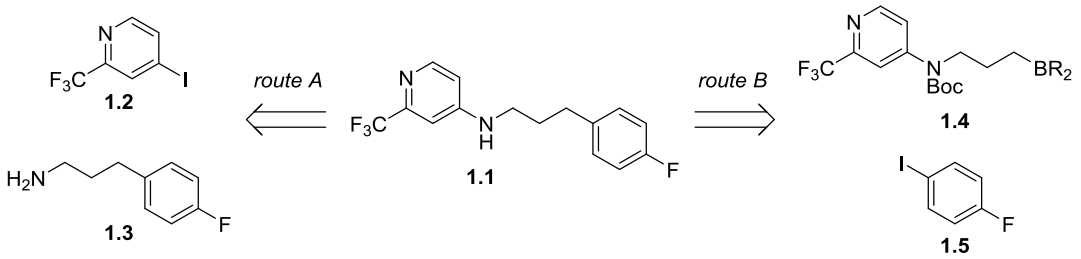

In order to accelerate exploration of chemical space, a different disconnection strategy was chosen (Scheme 3.1.1, route B). This required synthesis of the allyl carbamate precursor **1.9** (Scheme 3.1.2). A route starting from commercially available aminopyridine **1.6** did not succeed. Under various conditions only small amounts of the desired mono-allylated product were obtained, whereas the main product was the double allylated species. The initial strategy to equip aminopyridine **1.7** with a single Boc-protecting group only led to mixtures of mono- and di-protected compounds **1.7** and **1.8** when DMAP was used as a catalyst. Without the catalyst, no reaction occurred at all. This was overcome by using a two-step sequence. Starting material **1.6** was *di*-Boc-protected with DIPEA, DMAP and Boc_2O in DCM followed by selective mono-deprotection in a mixture of DCM/TFA (1:9).[87] Allylation of the carbamate with NaH (60 wt%) in DMF and allyl bromide led to the desired intermediate **1.9** in an excellent yield of 96% (Figure 3.1.2). Attempts to directly introduce the allylamine in **1.2** *via* S_NAr or *Buchwald*-type chemistry did not yield the desired product.

Scheme 3.1.2: *Synthesis of the* ***1A*** *analogue* ***1.14*** *via a protection-deprotection-allylation sequence, followed by Heck coupling, deprotection and hydrogenation.*[a]

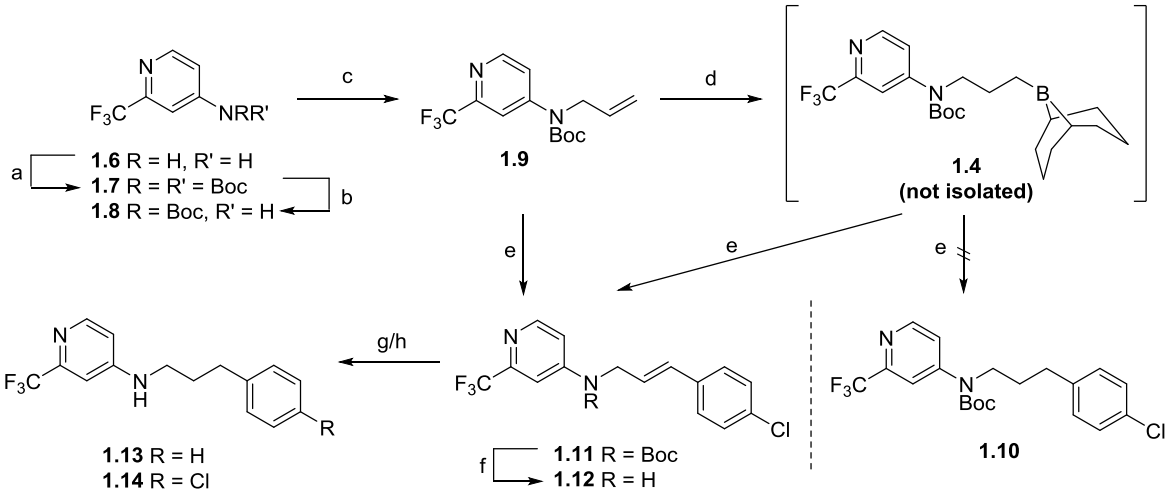

[a]***Reagents and conditions****: a: DIPEA, DMAP, Boc_2O, DCM, 18 h, rt; b: DCM/TFA 9:1, 16 h, rt, > 98% (2 steps); c: NaH (60 wt%), DMF, 0 °C, 1 h, then allyl bromide, 3 h, rt, 96%; d: 9-BBN, THF, rt, 30 min; e: 1 M NaOH, $PdCl_2$(dppf), 1-chloro-4-iodobenzene, THF, 18 h, 70 °C, 69% (from* ***1.9****), 67%(from* ***1.4****); f: DCM/TFA 1:1, 24 h, rt, > 98%; g: Pd black, H_2, MeOH, 2 h, rt, > 98%; h: Pd black, H_2, MeOH, 10 min, 0 °C, > 98%.*

For the introduction of the *tail* moiety, a *Suzuki-Miyaura* reaction was chosen.[88] Compound **1.4** would provide a versatile building block for combinatorial chemistry were different aryl iodides or bromides could be used. Hydroboration was carried out with 9-BBN in THF and TLC and LC-MS analysis indicated full consumption of the starting material (Scheme 3.1.2). The compound was not isolated but directly used in the next step. Since 1-chloro-4-iodobenzene was available, and the chlorine substituent was a desired derivative, this aryl iodide was chosen for the model study. However, when subjected to the coupling conditions with 1 M NaOH and $PdCl_2$(dppf), only compound **1.11** was obtained. This can be rationalized by simple β-hydride elimination from intermediate **1.15**, which is formed after transmetalation in the catalytic cycle, leading to allylic precursor **1.9**. The allyl carbamate can then react in a *Heck* reaction with the aryliodide (Scheme 3.1.3). It is known, that β-hydride elimination in sp^3–sp^2 couplings are often faster than the desired reductive elimination.[88] In order to prove the hypothesis that the *Heck* reaction actually takes place, precursor **1.9** was subjected to the exact same coupling conditions and indeed yielded **1.11**.

Scheme 3.1.3: *β-hydride elimination in intermediate **1.14** leads to formation of Heck coupling product **1.10**.*[a]

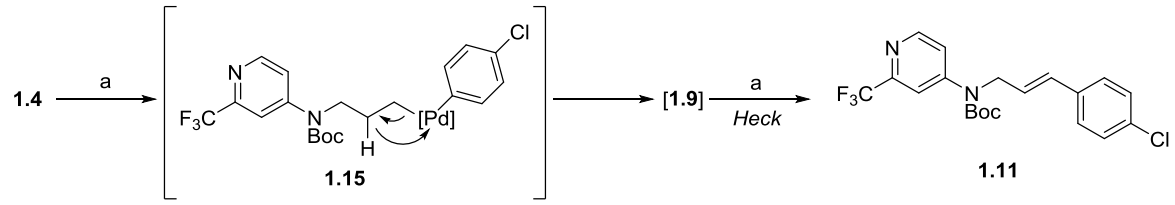

[a]***Reagents and conditions:*** *a: 1-chloro-4-iodobenzene, 1 M NaOH, $PdCl_2$(dppf), THF, 18 h, 70 °C, 67%.*

The Boc-protecting group in **1.11** was removed first with DCM/TFA (1:1), since **1.12** represents an interesting analogue of **1A** bearing a more rigid linker. Hydrogenation of the double bond with Pd black in MeOH under an H_2 atmosphere at room temperature also led to dehalogenation, resulting in compound **1.13** (Scheme 3.1.2.). The desired product **1.14** was obtained in excellent yield when the reaction was carried out at 0 °C. The established protocol was further used to synthesize compounds **1.18**, a pyridine analogue of **1.12**, and **1.19**, in order to explore a possible growth vector (Scheme 3.1.4). Applying the aforementioned reaction conditions from Scheme 3.1.2, compounds **1.16** and **1.17** were only isolated in small quantities. Optimization of the reaction conditions slightly improved the yields and generated sufficient amounts for biological evaluation. Phenoxy-substituted **1.16** was generated by using a tetrafluoro borate diazonium salt with NaOAc and Pd_2dba_3 in PhCN.[89] The corresponding chloro-pyridyl derivative **1.17** was synthesized by using the corresponding aryl iodide, 1 M NaOH and $PdCl_2$(dppf) in THF.[88] Subsequent Boc-cleavage with DCM/TFA (1:1) gave **1.18** and **1.19** in excellent yields.

Scheme 3.1.4: *Synthesis of derivatives **1.18** and **1.19**.*

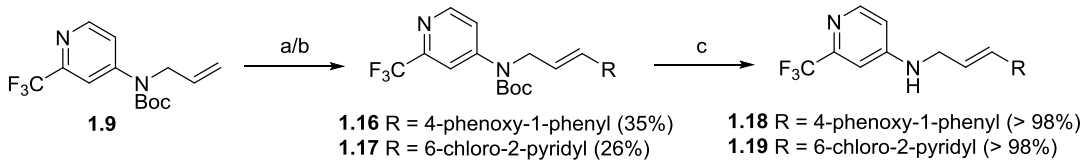

[a]Reagents and conditions: *a: 4-phenoxybenzenediazonium tetrafluoro borate, NaOAc, Pd_2dba_3, PhCN, 2 h, rt, 35% (**1.15**); b: 2-chloro-5-iodopyridine, $PdCl_2(dppf)$ 1 M NaOH, 24 h, 70 °C, 26% (**1.16**); c: DCM/TFA 1:1, 24 h, rt.*

At the same time, a route towards more rigid alkyne derivatives was established. Therefore building blocks **1.20a – 1.23a** were synthesized by simple alkylation of the corresponding iodophenols (Scheme 3.1.5). Starting material **1.8** was subjected to propargylation using NaH (60 wt%) and propargyl bromide (Scheme 3.1.6). It proved to be crucial for the reaction process to add the latter at room temperature. Addition of the electrophile at lower temperatures led to mixtures of the desired product and the corresponding allene (not shown). Attempts to propargylate free aminopyridine **1.6** only delivered mixtures of mono- and di-propargylated products, in favor of latter. Also *Buchwald*-type chemistry and S_NAr-type reactions failed.

Scheme 3.1.5: *Building block synthesis via phenol alkylation.[a]*

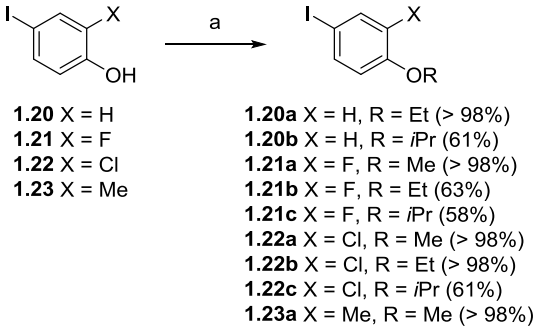

[a]Reagents and conditions: *K_2CO_3, MeI/EtI/iPrBr, DMF, 80 °C, 16 h.*

Even though the free nitrogen in building block **1.25** might interfere with the catalyst in the following *Sonogashira* couplings, Boc-deprotection was carried out first, since compounds with an electron-donating substituent in the *tail* region did undergo water addition to the triple bond under various acidic cleavage conditions. Several commercially available and synthesized aryl iodides were then applied in the following *Sonogashira* couplings, leading to compounds **1.26 – 1.46** (Scheme 3.1.6).

Scheme 3.1.6: *Synthesis of building block* ***1.25*** *and subsequent Sonogashira couplings yielding* ***1.26–1.46****.*[a]

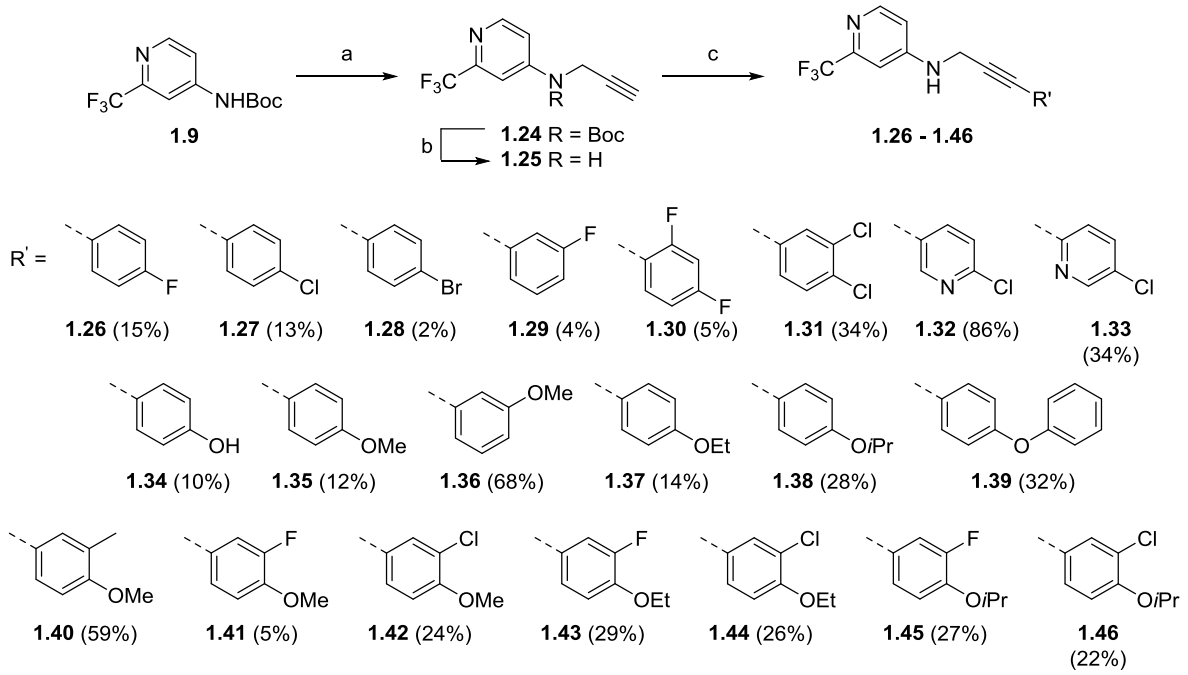

[a]***Reagents and conditions:*** *a: NaH (60 wt%), DMF, 0 °C, 1 h, then propargyl bromide, 3 h, rt, 96%; b: DCM/TFA 1:1, 6 h, rt, > 98%; c: aryliodide, Pd(PPh$_3$)$_4$, CuI, DIPEA, 18 h, 80 °C.*

Selected derivatives were subsequently hydrogenated and yielded the corresponding fully saturated analogues **1.47 – 1.49**, including **1.1**, the desired **1A** analogue (Scheme 3.1.7).

Scheme 3.1.7: *Synthesis of saturated linker analogues* ***1.1, 1.47 – 1.49*** *via hydrogenation.*

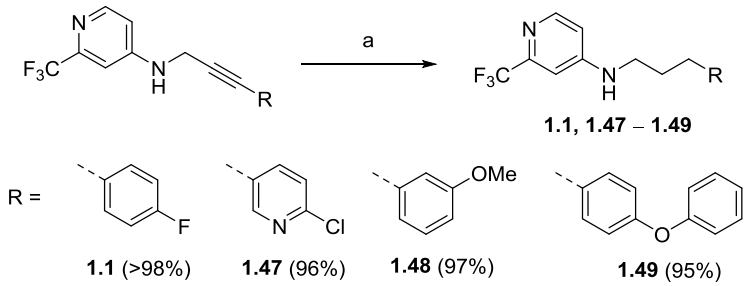

[a]***Reagents and conditions:*** *a: Pd/C, H$_2$, MeOH, 18 h, rt.*

Additionally, compound **1.32** was subjected to a (*Z*)-selective hydrogenation with Pd/C In EtOH under an atmosphere of H_2 for 10 minutes to afford **1.50** (Scheme 3.1.8).

Scheme 3.1.8: *Synthesis of (Z)-alkene* ***1.50****.*

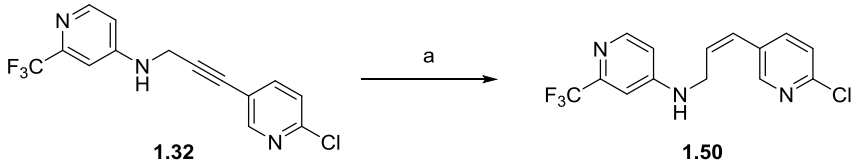

[a]***Reagents and conditions:*** *Pd/C, H$_2$, EtOH, 10 min, rt, > 98%.*

3.1.2. Biological Evaluation

3.1.2.1. *E. coli*-based reporter gene assay

The synthesized compounds were then evaluated in a heterologous reporter gene assay in *Escherichia coli* to investigate their on-target activity.[86] With this assay, the pharmacological profile of the tested compounds could also be evaluated. They could either act as agonists, antagonists, inverse agonists or partial agonists (Figure 3.1.2).[90] All reporter gene assay results were conducted by Simone Amann, Dennis Jener, Tabea Schramm or Selina Wolter.

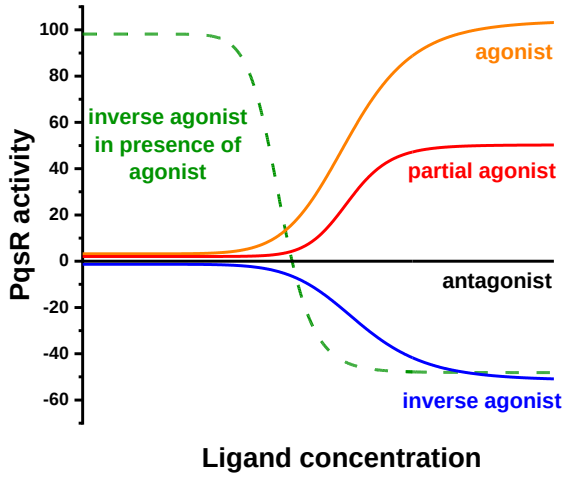

Figure 3.1.2: *Schematic representation of pharmacological profiles: agonist (organge), partial agonist (red), antagonist (black), inverse agonist (blue) and inverse agonist in presence of agonist (green).*

The innate receptor PqsR has a basal activity and typical antagonists are not able to suppress PqsR activity beyond this point, ultimately resulting in low impact in down-stream regulated processes like pyocyanin production for example.[90] It is important not only to antagonize PqsR, but also to revert its activity below the basal level. In this scenario, which is achieved by inverse agonists, an effective interruption of down-stream processes like the aforementioned pyocyanin production is achieved. This assay therefore serves as a tool for the preselection of potent compounds, which are then tested in a pyocyanin inhibition assay. First, spot-tests at a concentration of 1 µM were conducted and for those compounds showing promising activity, IC_{50} values were determined. The results for compounds **1.26** – **1.46** are summarized in Table 3.1.1, the activities of compounds **1.1**, **1.12**, **1.13**, **1.17**, **1.18**, **1.19**, **1.47 – 1.50** are depicted in Table 3.1.2.

Table 3.1.1: *Biological evaluation of compounds* ***1.26–1.46*** *based on E. coli reporter gene assay.*

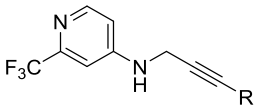

entry	cpd	R	IC_{50} [nM]	entry	cpd	R	IC_{50} [nM]
1	**1.26**	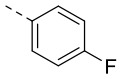	141	12	**1.37**	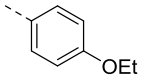	170
2	**1.27**	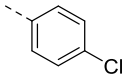	281	13	**1.38**	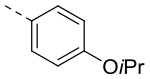	n.d.
3	**1.28**	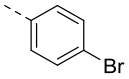	115% effect @1μM	14	**1.39**	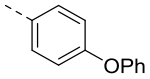	20
4	**1.29**	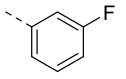	222	15	**1.40**	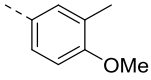	289
5	**1.30**	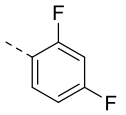	70% effect @1μM	16	**1.41**	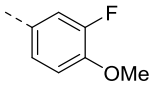	n.d.
6	**1.31**	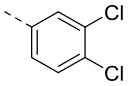	35% effect @1μM	17	**1.42**	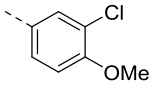	29% effect @1μM
7	**1.32**	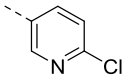	33% effect @1μM	18	**1.43**	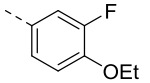	n.d.
8	**1.33**	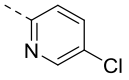	53% effect @1μM	19	**1.44**	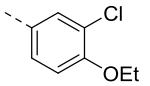	150
9	**1.34**	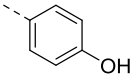	82% effect @1μM	20	**1.45**	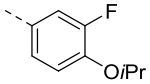	80
10	**1.35**	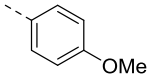	8% effect @1μM	21	**1.46**	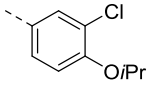	129
11	**1.36**	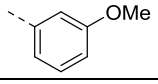	58% effect @1μM				

Table 3.1.2: *Biological evaluation of compounds* ***1.1, 1.12, 1.13, 1.17–1.19, 1.47–1.50*** *based on E. coli reporter gene assay*

entry	compound	structure	IC_{50} [nM]
1	**1.12**	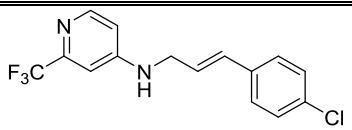	479
2	**1.13**	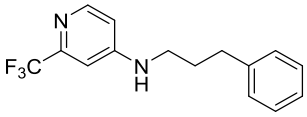	52% effect @1µM
3	**1.14**	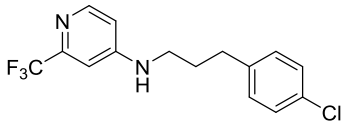	149
4	**1.18**	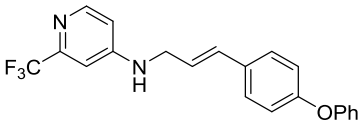	464
5	**1.19**	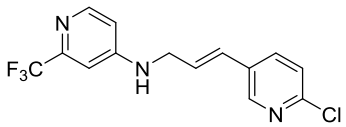	81% effect @1µM
6	**1.1**	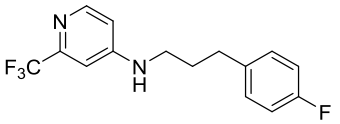	251
7	**1.47**	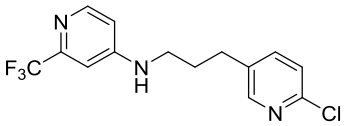	n.d. (insoluble)
8	**1.48**	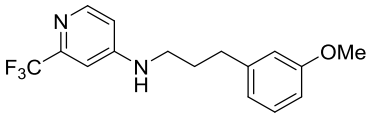	59% effect @1µM
9	**1.49**	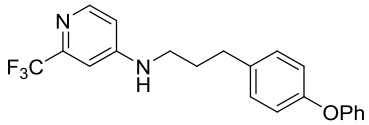	-41%effect@1µM
10	**1.50**	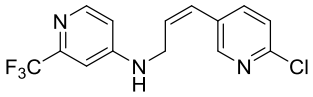	45%effect@10µM

3.1.2.2. Pyocyanin inhibition assay

As mentioned before, in addition to the *E. coli*-based reporter gene assay, the compounds with the most promising on-target activity were further evaluated on their ability to inhibit pyocyanin production in *P. aeruginosa* PA14. It is worth mentioning that a decrease in activity in this antivirulence assay is expected, since the *E. coli* DH5α strain employed in the reporter gene assay is known to possess a more permeable cell wall than *P. aeruginosa*.[86] The fully functional barrier of the Gram-negative cell wall present in PA14 reduces intracellular accumulation of the tested compounds. All pyocyanin inhibition assay results were generated by Simone Amann and Tabea Schramm. The results are summarized in Table 3.1.3.

Table 3.1.3: *Biological evaluation of selected compounds for their ability to inhibit pyocyanin production.*

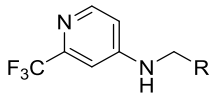

entry	cpd.	R	IC_{50} [µM]	entry	cpd.	R	IC_{50} [µM]
1	**1.26**	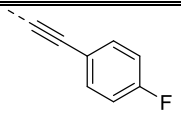	3.47	10	**1.44**	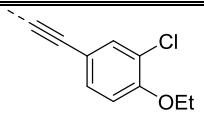	0.39
2	**1.27**	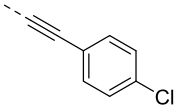	13.5	11	**1.45**	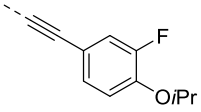	0.44
3	**1.37**	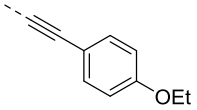	0.46	12	**1.46**	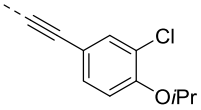	0.56
4	**1.38**	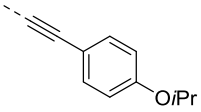	0.65	13	**1.1**	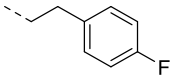	7.54
5	**1.39**	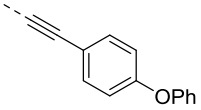	0.49	14	**1.14**	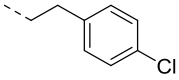	1.05
6	**1.40**	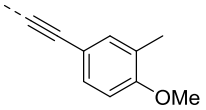	5% inhibition @0.2µM	15	**1.49**	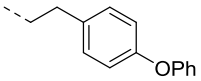	0% inhibition @0.2µM
7	**1.41**	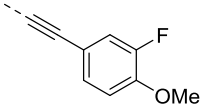	3.17	16	**1.12**	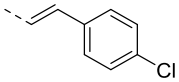	93% inhibition @10µM
8	**1.42**	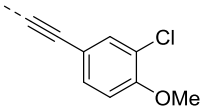	4% inhibition @0.2µM	17	**1.18**	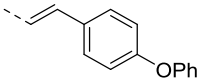	3.83
9	**1.39**	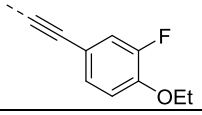	0.28				

3.1.3. Structure-Activity-Relationship

3.1.3.1. SAR based on reporter gene assay

Rigidifying the linker moiety from alkyl to alkyne was accepted. This result can be rationally explained by entropy considerations. Having less degrees of rotational freedom lower the entropy penalty. When comparing **1.26** to **1A**, the activity remains the same, even though **1.26** is lacking the amino function in the head. Exchanging the fluorine substituent with a chlorine atom led to a drop in activity, while increasing size with a bromine atom in this position abolished activity. Moving the fluorine atom from 4- to 3-position was accepted but slightly decreased the activity. Di-halogenated moieties as in **1.30** and **1.31** were not accepted, as well as exchange of chlorophenyl to chloropyridyl residues (compounds **1.32** and **1.33**). When installing a free hydroxyl group in 4-position, activity was again drastically decreased, whereas the methoxy analogue **1.35** showed improved activity compared to **1.34**. Moving

the methoxy substituent to the 3-position in this case was not tolerated and led to a drop in activity. Increasing the size of the 4-alkoxy substituent drastically boosted activity as can be seen in compound **1.37**. Compound **1.39** with its large phenoxy tail even showed an IC_{50} value in the low double digit nanomolar range (IC_{50} = 20 nM). This indicates that a substituent creating an angle in the 4-position is more effective than a simple bulky substituent. When it comes to di-substitution with 4-alkoxy moieties, introduction of an additional substituent in 3-position proved to be beneficial in some cases. For the 4-methoxy derivatives, an electron-donating methyl substituent gave the best results (compound **1.40**), while adding a chlorine (compound **1.44**) decreased activity in comparison to its parent compound **1.35**. Contrary to this, the second halogen substituent in **1.44** – **1.46** increased the activity with compound **1.45** being a very strong inverse agonist (IC_{50} = 80 nM).

Satisfyingly, the initial structural modification, omitting the amino group in the head, was accepted even though activity of compound **1.1** was decreased in comparison with **1A**. Compound **1.14** already indicates a difference in the alkyne and alkyl scaffold since installation of the larger chlorine atom in 4-position was not beneficial in derivatives with an alkyne linkage. In the case of **1.14**, activity was increased compared to **1.13**. Direct comparison of **1.14** and **1.27** with the corresponding (*E*)-alkene **1.12** shows that the alkene linker is least active. This also holds true for the phenoxy and chloropyridyl analogues **1.18** and **1.19**, being less potent than their alkyne and alkyl congeners **1.28**, **1.32** and **1.39** respectively. The (*Z*)-alkene derivative **1.50** was not active at all. In the alkane-linker series of compounds, the 4-phenoxy substituent also proved to be most efficient (compound **1.49**) as already mentioned for the alkyne class.

3.1.3.2. SAR based on pyocyanin inhibition

As already discussed in chapter 2.2.2., a decrease in activity was expected when moving from heterologous *E. coli* to *P. aeruginosa*. The **1A** analogue without the amino function in the head (compound **1.1**) was comparably active, while the corresponding alkyne analogue **1.26** was almost two times more active (IC_{50} = 3.47 µM). Compound **1.14** which was equipotent with **1.26** considering on-target activity, is an almost 3-fold better inhibitor of pyocyanin production. This hints at possible permeation issues. Moreover, efflux can play a crucial role in *P. aeruginosa*. Even more drastically, this effect is present in the alkoxy-linked derivatives. While **1.37** is slightly less active in the reporter gene assay than **1.26**, its IC_{50} value for pyocyanin inhibition is in the sub-micromolar range (IC_{50} = 0.46 µM). Moreover, compound **1.45** which is two-times more active on the target compared to **1.37** shows a similar pyocyanin inhibitory effect. The 4-phenoxy substituted compound **1.35** which was the most active inverse agonist, is also almost as potent as **1.37**. Pyocyanin production was best inhibited by

compound **1.43** (IC_{50} = 0.28 µM), the 3-fluoro derivative of **1.37**. The alkene derivatives **1.12** and **1.18** were less potent than their alkyne/alkane-linked analogues.

3.1.4. Cocrystal structure of 1.26 in complex with PqsR

Dr. Andrea Scrima from the working group of Prof. Dr. Wulf Blankenfeldt at HZI was able to solve the crystal structure of **1.26** in complex with $PqsR^{91-319}$ at a resolution of 2.3 Å. As can be seen from Figure 3.1.3, the proton attached to the secondary nitrogen interacts with Thr265 *via* a hydrogen bond (NH as donor) and therefore plays a crucial role. Putative interactions involve Ile263 and Tyr258. A possible π-π interaction with the latter might explain the increased activity of **1.39**. By now, no cocrystallate was obtained to confirm this but there is evidence from other QSI classes.

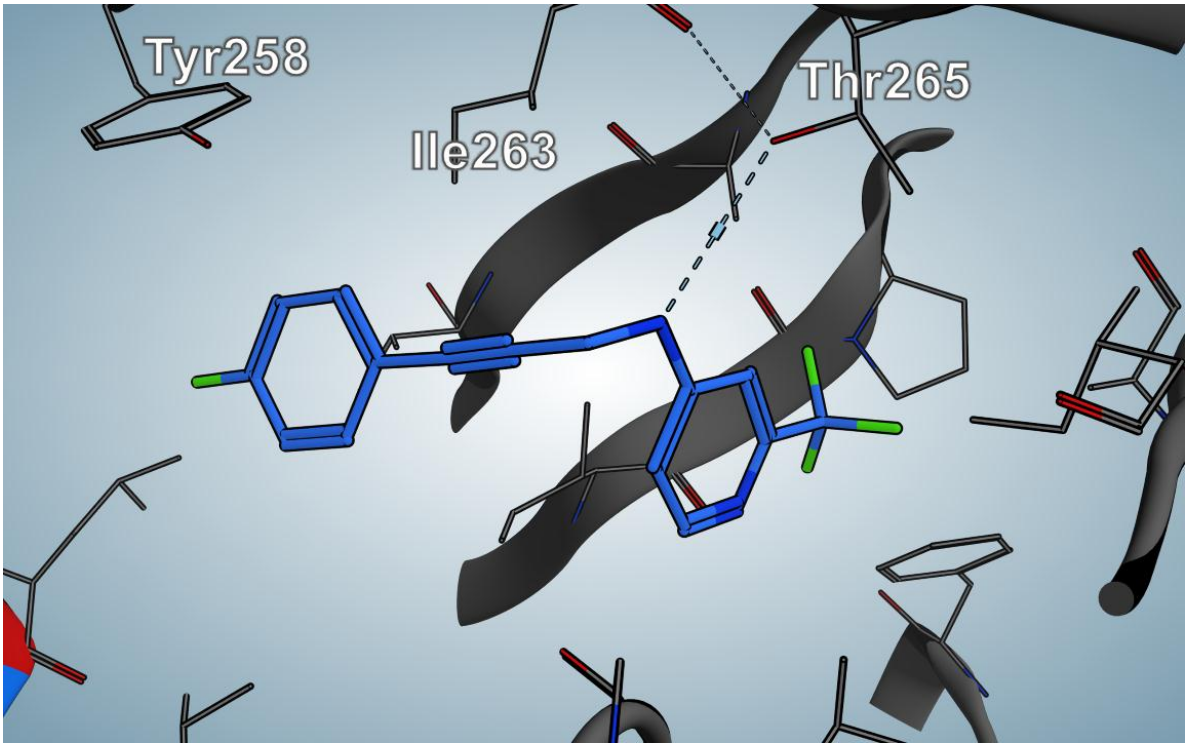

Figure 3.1.3: *Cocrystal structure of compound **1.26** in complex with $PqsR^{91-319}$ at a resolution of 2.3 Å. Main interaction residues are labeled. Color code: blue: C, dark blue: N, green: F, red: O.*

3.1.5. DMPK profiling

The most promising compounds based on activity, as well as some tool compounds were further evaluated in order gain insights into their DMPK profile (Table 3.1.4). First the alkyl and alkyne derivatives **1.26** and **1.1** were investigated on possible cytotoxicity using Hep G2 and HEK293 cells. Both satisfyingly exhibited LD_{50} values of above 50 µM for Hep G2 and compound **1.26** also showed no toxic effects towards HEK293. The alkyne derivatives might therefore be less toxic than their alkyl congeners. For Hep G2, compound **1.39** displayed little toxicity, whereas moderate results with an LD_{50} between 10 and 25 µM were determined for HEK293. All of the compounds were tested with respect

to metabolic stability in human S9 fractions. While alkane linked compound **1.1** ($t_{1/2}$ = 58 min) is superior to its alkyne congener **1.26** ($t_{1/2}$ = 11 min), metabolic stability is improved in the 4-phenoxy derivative **1.39** ($t_{1/2}$ = 120 min). Changing the phenoxy *tail* unit to alkyloxy substituents reduces metabolic stability dramatically in **1.43** ($t_{1/2}$ = 1 min) and **1.45** ($t_{1/2}$ = 1.1 min). This indicates that an alkyl *tail* might be a metabolic hotspot. By now, neither investigations on metabolite identification, nor the synthesis of fluorinated or deuterated alkyloxy motifs have been conducted. In terms of solubility, isopropyl substituted **1.45** (S_{kin} = 48.9 µM) is far more soluble than **1.39** (S_{kin} = 13.2 µM) with its large lipophilic phenyl residue. Even though the alkyne class offers optimization potential, the focus shifted to another class described in the next chapter.

Table 3.1.4: *DMPK data of selected compounds including solubility, half-life in human S9 fraction and cytotoxicity.*

entry	cpd	structure	S_{kin}	$t_{1/2}$ h S9	LD_{50} HepG2	LD_{50} HEK293
1	**1.1**	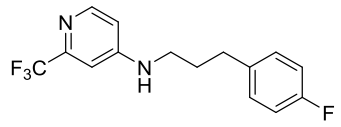	n.d.	58 min	~75 µM	25 – 50 µM
2	**1.26**	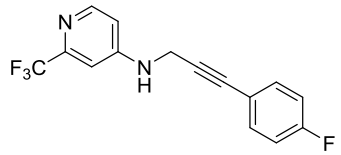	n.d.	11 min	>50 µM	>50 µM
3	**1.43**	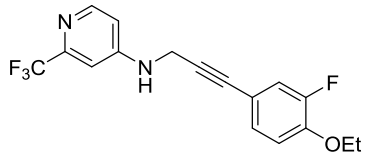	n.d.	1 min	n.d.	n.d.
4	**1.45**	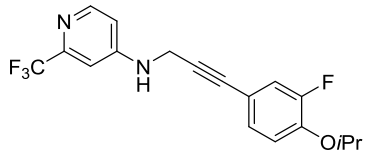	48.9 µM	1.1 min	n.d.	n.d.
5	**1.39**	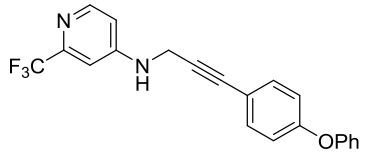	13.2 µM	120 min	>>25 µM	10 – 25 µM

3.2. Lead Generation II

3.2.1. Design and synthesis of triaolze-linked PqsR inverse agonists

With building block **1.25** in hand, the next obvious linker modification was the conversion of the alkyne into a 1,2,3-triazole *via* copper-catalyzed azide-alkyne cycloaddition (CuAAC). This "click-chemistry" enables fast and easy access to compound libraries.[73] Triazoles are known to be amide mimics, overcoming the inherent disadvantage of enzymatic hydrolysis which would result in potentially

undesired aniline metabolites.[91–97] A corresponding amide-linked analogue **3A** has been synthesized within the project before and showed promising on-target activity (Figure 3.2.1).[86] The impact of the amine group in the *head* of this compound class should also be evaluated, as well as the possibilities of growing in the *tail* region.

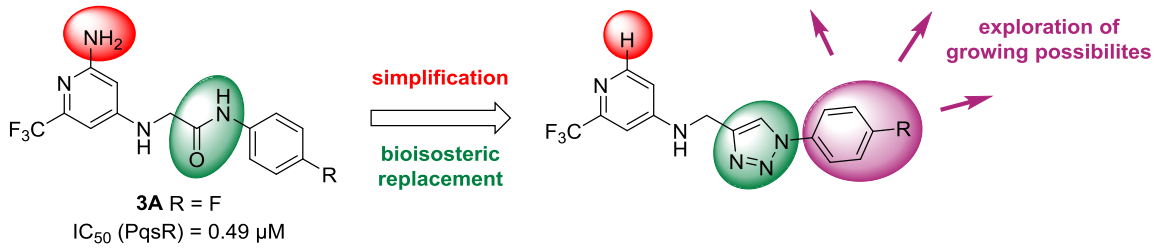

Figure 3.2.1: *Optimization strategies of* ***3A*** *via simplification, bioisosteric replacement and growing.*

In collaboration with PharmBioTec, a compound library was designed and specific derivatives were synthesized using an one-pot protocol. This made use of imidazole-1-sulfonyl azide hydrochloride to create the azide *in situ*, which then reacts with the alkyne and forms the desired five-membered desired heterocycle.[98] The drawback of this protocol were bad yields, as well as a limited scaffold for some anilines. Therefore, promising derivatives were resynthesized using a modified two-step protocol without isolation of the azide intermediate, described by Barral *et al.* (Scheme 3.2.1).[99] Moreover, other commercially available anilines have been used resulting in a total of 15 triazole-linked analogues.

Scheme 3.2.1: *Synthesis of 1,2,3- triazole compounds* ***3.14 – 3.27****.*[a]

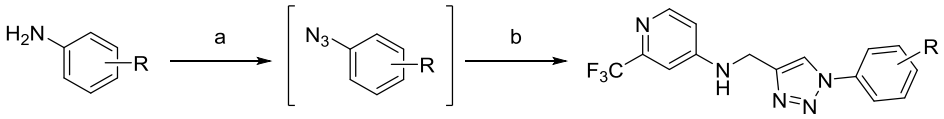

3.1a R = 2-F	**3.1b** R = 2-F	**3.16** R = 2-F (86%)
3.2a R = 3-F	**3.2b** R = 3-F	**3.17** R = 3-F (94%)
3.3a R = 4-F	**3.3b** R = 4-F	**3.18** R = 4-F (94%)
3.4a R = 2-Cl	**3.4b** R = 2-Cl	**3.19** R = 2-Cl (94%)
3.5a R = 3-Cl	**3.5b** R = 3-Cl	**3.20** R = 3-Cl (85%)
3.6a R = 4-Cl	**3.6b** R = 4-Cl	**3.21** R = 4-Cl (69%)
3.7a R = 4-Br	**3.7b** R = 4-Br	**3.22** R = 4-Br (94%)
3.8a R = 4-OH	**3.8b** R = 4-OH	**3.23** R = 4-OH (34%)
3.9a R = 4-OMe	**3.9b** R = 4-OMe	**3.24** R = 4-OMe (32%)
3.10a R = 4-O*i*Pr	**3.10b** R = 4-O*i*Pr	**3.25** R = 4-O*i*Pr (97%)
3.11a R = 4-OCF_3	**3.11b** R = 4-OCF_3	**3.26** R = 4-OCF_3 (88%)
3.12a R = 4-CF_3	**3.12b** R = 4-CF_3	**3.27** R = 4-CF_3 (83%)
3.13a R = 4-CN	**3.13b** R = 4-CN	**3.28** R = 4-CN (69%)
3.14a R = 4-OPh	**3.14b** R = 4-OPh	**3.29** R = 4-OPh (96%)
3.15a R = 4-NPh	**3.15b** R = 4-NPh	**3.30** R = 4-NPh (67%)

[a]***Reagents and conditions:*** *a: tBuONO, $TMSN_3$, MeCN, 0 °C, 1 – 3 h; b: $CuSO_4$·5 H_2O, Na ascorbate, DIPEA, N-(prop-2-yn-1-yl)-2-(trifluoromethyl)pyridin-4-amine (**1.25**), 1 – 24 h, 32 – 96%.*

Anilines **3.1a – 3.15a** were converted into the corresponding azides **3.1b – 3.15b** using the aforementioned protocol with *t*BuONO and $TMSN_3$ in MeCN. Subsequent addition of **1.25**, $CuSO_4$·5 H_2O, Na-ascorbate and DIPEA led to formation of the desired target compounds **3.16 – 3.30**

in moderate to good yields (Scheme 3.2.1). Moreover, commercially available disubstituted anilines **3.31a** – **3.34a** based on promising compounds of the alkyl class were used (Scheme 3.2.2). It is worth mentioning that yields in the CuAAC were improved when the crude reaction mixture was stirred with saturated EDTA solution prior to extraction.

Scheme 3.2.2: *Synthesis 1,2,3- triazole compounds* ***3.35 – 3.38****.*[a]

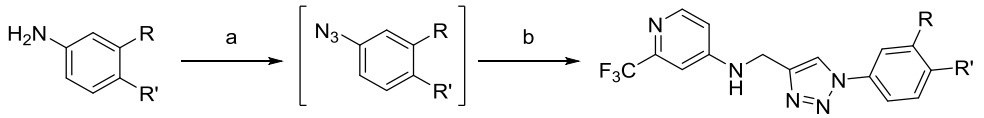

3.31a R = R' = Cl
3.32a R = F, R' = OMe
3.33a R = Cl, R' = OMe
3.34a R = Cl, R' = OCF_3

3.31b R = R' = Cl
3.32b R = F, R' = OMe
3.33b R = Cl, R' = OMe
3.34b R = Cl, R' = OCF_3

3.35 R = R' = Cl (60%)
3.36 R = F, R' = OMe (69%)
3.37 R = Cl, R' = OMe (73%)
3.38 R = Cl, R' = OCF_3 (70%)

[a]***Reagents and conditions:*** *a: tBuONO,* $TMSN_3$*, MeCN, 0 °C, 1 – 3 h; b:* $CuSO_4 \cdot 5\ H_2O$*, Na ascorbate, DIPEA, N-(prop-2-yn-1-yl)-2-(trifluoromethyl)pyridin-4-amine (****1.25****), 1 – 24 h, 60-73%.*

In order to further investigate growth possibilities in the *tail* region, different compounds bearing an alkoxy moiety were synthesized (Scheme 3.2.3).

Scheme 3.2.3: *Synthesis of aniline precursors* ***3.40b – 3.45b*** *and subsequent CuAAC towards target compounds* ***3.46 – 3.51****.*[a]

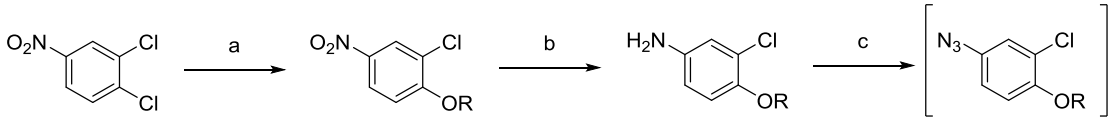

3.39

3.40a R = *i*Pr (78%)
3.41a R = cyclopropyl (68%)
3.42a R = cyclobutyl (43%)
3.43a R = 3-oxetanyl (64%)
3.44a R = 3-tetrahydrofuryl (53%)
3.45a R = Ph (> 98%)

3.40b R = *i*Pr (95%)
3.41b R = cyclopropyl (94%)
3.42b R = cyclobutyl (87%)
3.43b R = 3-oxetanyl (86%)
3.44b R = 3-tetrahydrofuryl (>98%)
3.45b R = Ph (97%)

3.40c R = *i*Pr
3.41c R = cyclopropyl
3.42c R = cyclobutyl
3.43c R = 3-oxetanyl
3.44c R = 3-tetrahydrofuryl
3.45c R = Ph

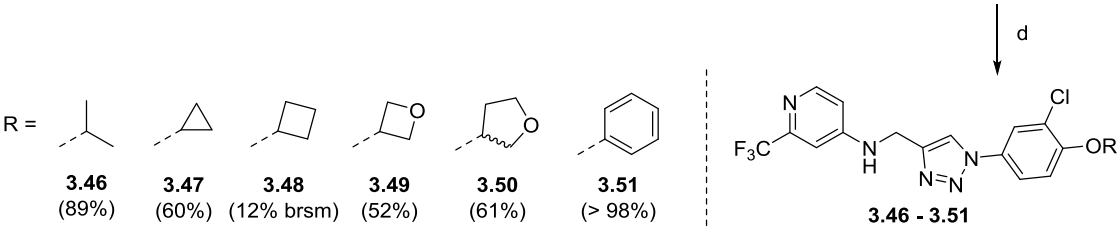

3.46 (89%) **3.47** (60%) **3.48** (12% brsm) **3.49** (52%) **3.50** (61%) **3.51** (> 98%)

3.46 - 3.51

[a]***Reagents and conditions:*** *a: ROH,* Cs_2CO_3*, 16 h, 80 °C (for* ***3.40a – 3.42a*** *and* ***3.45a****) or ROH, NaH (60 wt%), DMF, 16 h, 80 °C, 43 – 98%; b: Pt/C,* H_2*, toluene, 8 h, 86 – 98%; c: tBuONO,* $TMSN_3$*, MeCN, 0 °C, 1 – 3 h; d:* $CuSO_4 \cdot 5\ H_2O$*, Na ascorbate, DIPEA, N-(prop-2-yn-1-yl)-2-(trifluoromethyl)pyridin-4-amine (****1.25****), 1 – 24 h, 12 – 98%.*

The corresponding azides were prepared from commercially available 1,2-dichloro-4-nitroaniline **3.39** via S_NAr reaction with various alcohols, followed by hydrogenation. It is worth mentioning, that for derivatives **3.43a** and **3.44a**, NaH (60 wt%) in DMF was used as a base in order to achieve the S_NAr reaction with **3.39**.

3.2.2. Biological evaluation

The synthesized compounds were first tested for their on-target activity and further evaluated for pyocyanin production inhibition. The results are summarized in Table 3.2.1 for the mono-substituted derivatives and in Table 3.2.2 for the di-substituted ones. Fortunately, replacement of the amide in **3A** was accepted and for its triazole analogue **3.18** (IC_{50} = 196 nM) activity even improved almost three-fold in comparison to the parent compound. As expected, the 2-position is not suitable for the introduction of a substituent, whereas substituents in 3-position are accepted (compounds **3.17** and **3.20**). Moreover, increasing the size of the substituent from fluorine to chlorine gave a boost in on-target activity. The introduction of a bulky bromine in 4-position surprisingly led to active compound **3.22** (IC_{50} = 97 nM). These results are in contrast to the activities of the alkyne derivatives and resembles the observations made for the alkane compounds. This could be explained by the higher flexibility of the alkane analogues, which are more likely to adopt an active conformation similar to the 1,2,3-triazoles compounds, while the alkyne compounds might not be able to achieve this due to their rigidity. Notably, the linker-length and the geometry is different in the alkyne class. Introduction of a free hydroxyl group also did not lead to a potent compound in this class, while adding a methoxy substituent in **3.24** led to good activity (IC_{50} = 81 nM). With the possibility of metabolic instability in mind, trifluoromethoxy analogue **3.26** was synthesized and led to a drastic increase in activity (IC_{50} = 30 nM). The boost in on-target activity might have several reasons. First, steric reasons and lipophilicity, second, conformation and third stereoelectronic reasons. Compound **3.26** with a clogD (7.4) = 3.88, is much more lipophilic than its congener **3.24** (clogD (7.4) = 2.52). On the one hand, the trifluoromethoxy group is forced out of the ring plane of the phenyl moiety due to its size, being sterically more demanding. On the other hand stereoelectronic effects of this electron-withdrawing substituent might also be quite important.[100] Omitting the oxygen atom and directly attaching the trifluoromethyl group to the phenyl ring in compound **3.27** was accepted but led to a drop in activity (IC_{50} = 129 nM). Introduction of an electron-withdrawing nitrile substituent in the 4-position (**3.28**) further decreased the on-target activity. The most beneficial modification was the introduction of the 4-phenoxy moiety in compound **3.29**. This substituent already gave a boost in the alkyl-linked compounds and proved to be the most active compound in the triazole class with a low double-digit nanomolar IC_{50} (11 nM). The nitrogen linked congener **3.30** also exhibited high on-target activity but was slightly less active (IC_{50} = 31 nM).

Table 3.2.1: *Biological evaluation of mono-substituted compounds* ***3.16 – 3.30*** *in E. coli and P. aeruginosa.*

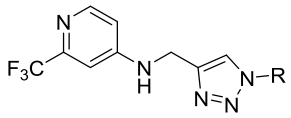

entry	cpd	R	IC_{50} PqsR	IC_{50} Pyocyanin
1	**3.16**	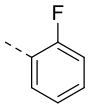	23% effect@10µM	>10 µM
2	**3.17**	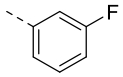	-16% effect@10µM	~5 µM
3	**3.18**	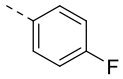	196 nM	~5 µM
4	**3.19**	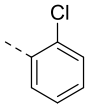	42% effect@10µM	n.d.
5	**3.20**	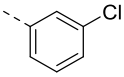	123 nM	2.5-5 µM
6	**3.21**	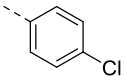	79 nM	8120 nM
7	**3.22**	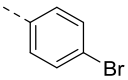	97 nM	n.d.
8	**3.23**	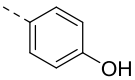	5% effect@10µM	n.d.
9	**3.24**	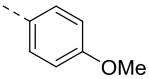	81 nM	2.5 µM
10	**3.25**	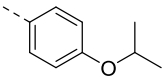	31 nM	447 nM
11	**3.26**	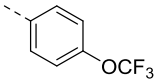	30 nM	1179 nM
12	**3.27**	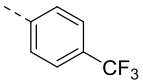	129 nM	2.5-5 µM
13	**3.28**	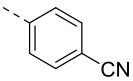	655 nM	>10 µM
14	**3.29**	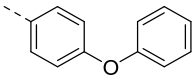	11 nM	199 nM
15	**3.30**	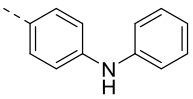	31 nM	1058 nM

Table 3.2.2: *Biological evaluation of di-substituted compounds* ***3.35 – 3.51*** *in E. coli and P. aeruginosa.*

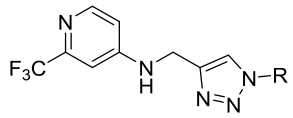

entry	cpd	R	IC_{50} PqsR	IC_{50} Pyocyanin
1	**3.35**	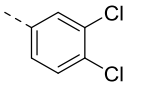	24 nM	354 nM
2	**3.36**	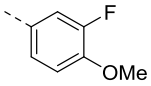	33 nM	2737 nM
3	**3.37**	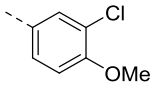	8 nM	350 nM
4	**3.38**	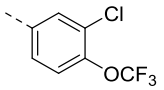	15 nM	438 nM
5	**3.46**	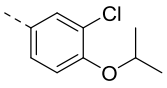	10 nM	237 nM
6	**3.47**	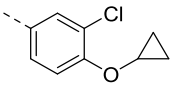	10 nM	409 nM
7	**3.48**	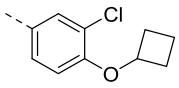	3 nM	220 nM
8	**3.49**	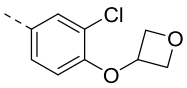	25 nM	2031 nM
9	**3.50**	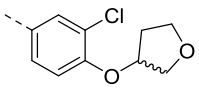	4 nM	316 nM
10	**3.51**	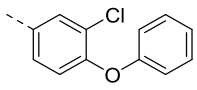	12 nM	181 nM

Again, contrary to the results obtained from the alkyne class, di-chloro-substituted **3.35** was well accepted exhibiting high on-target potency (IC_{50} = 24 nM). When considering the halogen substituent in position 3, chlorine is superior to fluorine as can be seen when comparing **3.36** with **3.37**. Possible reasons for this might be the increased size of the substituent and also its increased lipophilicity. Also, the trifluoromethoxy motif in **3.38** is well accepted with a chlorine substituent, even though activity is slightly decreased. Introduction of a more bulky isopropoxy group in **3.46** had no impact on PqsR activity, as well as the rigid cyclopropyl-bearing **3.47**. A more distinct impact was seen in compounds **3.48** and **3.50**, both equipped with larger alkoxy substituents. They showed activity in the low

single-digit nanomolar range (IC_{50} = 3 nM for **3.48** and IC_{50} = 4 nM for **3.50**). Upon introduction of an additional oxygen in the cyclobutyl ring, the activity of **3.49** is drastically decreased in comparison to its parent compound **3.48** (IC_{50} = 25 nM compared to IC_{50} = 3 nM). Combining the chlorine substituent with the phenoxy motif had no impact on the activity (compounds **3.29** and **3.51**).

For the pyocyanin inhibition assay, in general lower activities were observed for the reasons already discussed. Compounds **3.17** – **3.21** displayed poor activity in the range of 2.5 – 5 µM. It was surprising that compound **3.21**, possessing the best on-target activity of this set of compounds (IC_{50} = 79 nM), was less active than most of these derivatives (IC_{50} = 8.12 µM). While **3.24** exhibited similar activity in the *E. coli* reporter gene assay as compound **3.21**, its ability to reduce pyocyanin production was significantly higher (IC_{50} = 2.5 µM). As expected trifluoromethoxy-containing **3.26** showed good activity in the low micomolar range (IC_{50} = 1.18 µM). While the almost equipotent aniline-substituted **3.30** also displayed a similar effect on pyocyanin inhibition (IC_{50} = 1.06 µM) as **3.26**, its oxygen-linked congener **3.29** surprisingly showed an IC_{50} in the nanomolar range (IC_{50} = 199 nM). Although di-chloro compound **3.35** exhibits PqsR activity comparable to **3.30**, its ability to reduce pyocyanin activity is dramatically increased (IC_{50} = 354 nM). This, again, might be explained by the more difficult to penetrate bacterial cell-wall of *P. aeruginosa* and the efflux problem. More drastically, this is present when comparing fluoro- and chloro-methoxy derivatives **3.36** and **3.37**. While both possess good to excellent on-target activity, only **3.37** is highly potent in pyocyanin production inhibition (IC_{50} = 350 nM). The observed inter-assay variations are again reflected when comparing different alkoxy motifs in **3.47** – **3.50**. While cyclopropoxy compound **3.47** is equipotent to its isopropoxy analogue **3.46**, it is two-times less active as a pyocyanin production inhibitor (IC_{50} = 409 nM compared to IC_{50} = 237 nM). While **3.48** bearing a cyclobutyl moiety was the most active compound on the target, its pyocyanin activity is in the range of **3.29** and **3.46** (IC_{50} = 220 nM). The drop in activity for the corresponding oxetane derivative **3.49** is also resembled in *P. aeruginosa* (IC_{50} = 2.03 µM). The impact of the chlorine substituent in **3.51** did not affect potency when compared to its parent compound **3.29**, which is in contrast to **3.24** and **3.37**. Also, this observed non-linear SAR holds true for compounds **3.46** (compared to **3.25**) and **3.38** (compared to **3.26**). Non-linearity means, that combining beneficial motifs, e.g. the 3-chloro substituent (compound **3.37**) with another favorable moiety, e.g. the 4-phenoxy motif (compound **3.29**) does not result in additive effects, such as increased activity. This leads to the assumption that the substituent in 3-position is more relevant for alkoxy derivatives.

3.2.3. *In vitro* DMPK profiling

In order to select one or more possible lead compounds for *in vivo* studies, the most promising compounds were further evaluated. Parameters such as solubility, metabolic stability and cytotoxicity

were taken into consideration, as well as CYP interactions, hERG inhibition, AhR activation and other possible off-targets. The results for solubility, metabolic stability in mouse liver microsomes and cytotoxicity are given in Table 3.2.3. As already expected, compounds **3.29** and **3.51** bearing the 4-phenoxy showed solubility below 10 µM. The short chloro-methoxy analogue **3.37** showed the best solubility with 64 µM. Increasing lipophilicity with the change from methyl to trifluoromethyl, **3.36** proved to be less soluble. With the bigger alkoxy motifs, solubility was decreased in comparison to **3.37**, still being more soluble than the phenoxy derivatives.

Table 3.2.3: *DMPK data for selected compounds with respect to solubility, metabolic stability and cytotoxycity.*

entry	cpd	structure	S_{kin} [µM]	$t_{1/2}$ MLM [min]	Hep G2 LD_{50} [µM]	HEK293 LD_{50} [µM]
1	**3.29**	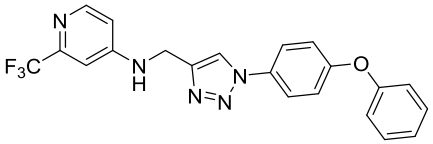	7.7	10	~25 µM	~25 µM
2	**3.37**	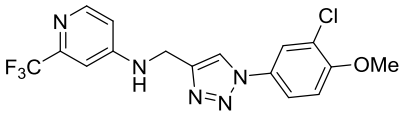	64.1	3	>75 µM	>50 µM
3	**3.36**	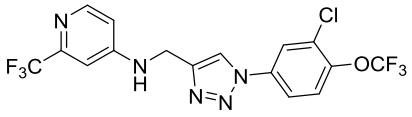	31.3	55	>25 µM	~25 µM
4	**3.46**	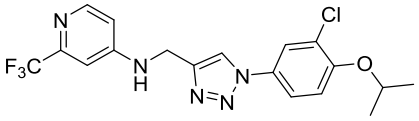	26.9	2	n.d.	n.d.
5	**3.47**	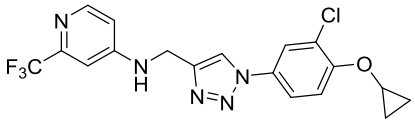	14.5	27	n.d.	n.d.
6	**3.48**	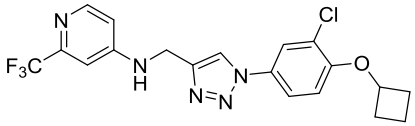	28	2	n.d.	n.d.
7	**3.49**	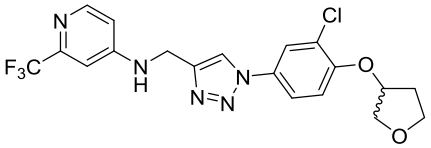	40.9	26	n.d.	n.d.
8	**3.51**	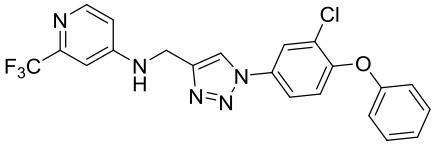	6.7	19	n.d.	n.d.

Exceptions are tetrahydrofuranyl derivative **3.49** with its additional oxygen atom, exhibiting good solubility of 40.9 µM and the cyclopropoxy compound **3.47** which is almost two-times less soluble than

its isopropoxy congener (S_{kin} = 14.5 µM). Regarding metabolic stability, those compounds with an alkoxy substituent in the *tail* region proved to be susceptible to degradation. This was already expected from the data for corresponding alkyne derivatives. Compound **3.47** with its cyclopropoxy motif was more stable ($t_{1/2}$ = 27 min), as well as the tetrahydrofuryloxy analogue **3.49**. For **3.47** this can be explained by the stronger C–H bonds compared to alkyl substituents.[101] Three compounds were then evaluated regarding possible cytotoxicity. The phenoxy-substituted **3.29** was chosen because of its high potency, **3.37** being the most soluble compound while exhibiting good activity and compound **3.36** due to its high stability and moderate solubility. Although **3.29** and **3.36** showed LD_{50} values of about 25 µM, **3.37** proved to be less toxic with LD_{50} values above 75 and 50 µM. Based on these results, compounds **3.29** and **3.37** were taken into further biological evaluation.

3.2.4. Secondary biological evaluation

The most advanced compounds **3.29** and **3.37** were further evaluated regarding their *in vitro* efficacy. Their potential to inhibit alkylquinolone (AQ) production of the signal molecules PQS and HHQ was determined, as well as the ability to inhibit eDNA production in biofilms. The results are depicted in Figure 3.2.2 and were generated by Simone Amann.

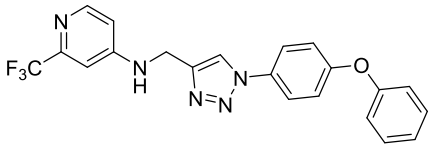

3.29
IC_{50} (HHQ) = 0.37 µM
IC_{50} (PQS) = 1.13 µM
IC_{50} (eDNA) = 0.22 µM

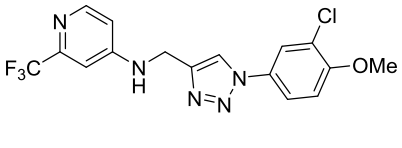

3.37
IC_{50} (HHQ) = 1.32 µM
IC_{50} (PQS) = 2.08 µM
IC_{50} (eDNA) = 1.60 µM

Figure 3.2.2: *AQ inhibition, eDNA inhibition and structure of **3.29** and **3.37**.*

Compound **3.29**, which already exhibited a higher efficacy in pyocyanin production inhibition, also proved to be superior to **3.37** in terms of AQ inhibition and eDNA inhibition. It is worth mentioning, that in this case a correlation between planktonic *P. aeruginosa* assays and these results are observed.

3.2.5. Safety pharmacology

Compounds **3.29** and **3.37** were further investigated with regard to safety pharmacology. Effects such as cytotoxicity, hERG inhibition, AhR activation and CYP inhibition were taken into consideration. The results for cytotoxicity were generated by Jeannine Jung, hERG inhibition, plasma protein binding (PPB) and AhR receptor induction and CYP inhibition assays were performed by *Cyprotex*. The latter are summarized in Table 3.2.5, the former in Table 3.2.4. When it comes to cytotoxicity compound **3.37** is superior to **3.29** (LD_{50} > 75 µM for HepG2 cells and LD_{50} > 50 µM for HEK293 cells), whereas **3.29** displays an LD_{50} of about 25 µM for both cell lines. Nevertheless, this is still in an acceptable range. Both compounds proved to be safe concerning hERG inhibition with an IC_{50} of above 25 µM. Plasma

protein binding for both compounds is above 99%. In terms of AhR receptor induction, **3.29** proved to be inferior to **3.37**, although still in acceptable range.

Table 3.2.4: *LD_{50} for HepG2 and HEK293, hERG inhibition, PPB and AhR receptor induction for compounds **3.29** and **3.37**.*

cpd	LD_{50} HepG2	LD_{50} HEK293	hERG inhibition [µM]	PPB	fold AhR receptor induction
3.29	~25 µM	~25 µM	>25 µM	>99%	17.6
3.37	>75 µM	>50 µM	>25 µM	>99%	25.9

In terms of CYP inhibition, **3.37** proved to be a stronger inhibitor of CYP2C19, an enzyme which is important for drug metabolism. Compound **3.29** inhibits CYP3A4 and CYP2C9 at a lower IC_{50} than **3.37**, nevertheless, still in an acceptable range.

Table 3.2.5: *Inhibition of CYP3A4, CYP2D6, CYP1A, CYP2C9 and CYP2C19 for compounds **3.29** and **3.37**.*

cpd	CYP3A4	CYP2D6	CYP1A	CYP2C9	CYP2C19
3.29	15 µM	>25 µM	>25 µM	16.4 µM	20.3 µM
3.37	>25 µM	>25 µM	22.1 µM	>25 µM	3.55 µM

A panel of 44 CEREP off-targets was screened by *Eurofins* (Table 3.2.6). It is worth mentioning, that the reported values are from binding assays. Therefore, no effects on a pharmacological level can be determined. They just give a hint on possible off-targets, which need to be evaluated further in functional assays. The results for those showing inhibition above 50% at a concentration of 10 µM are summarized in Table 3.2.6. The biggest drawback of **3.37** is the inhibition of β2 receptor, which can ultimately lead to cardiovascular stress or bronchospasm.[102] Both compounds show inhibition of several serotonin receptors of the 5-HT_2 family. Moreover, compound **3.29** shows pronounced inhibition of antidepressant targets dopamine and norepinephrine transporters. Compound **3.37** hits the androgen receptor (AR), which is involved in signal transduction of steroid or thyroid hormones, thus representing a severe off-target which could lead to inhibited spermatogenesis.[103] Both compounds inhibit the adrenoceptor α_{1A}, which plays a role in the cardiovascular system. Inhibition might lead to undesirable side effects such as orthostatic hypotension or headache due to vasodilation.[104] The L-type calcium channel dihydropyridine receptor (DHPR) is inhibited by **3.29**. Blockage of DHPR is the mechanism of action of dihydropyridines such as nitrendipine, which are used to treat hypertension. Neurotoxins such as batrachotoxin or veratridine bind to the site 2 sodium

channel and modulate it in a way, that the channel stays open.[105] Moreover, local anesthetics bind there, e.g. lidocaine, which blocks the channel and keeps it closed. Nevertheless, binding of **3.29** to this channel does not imply safety issues, since all these screening are solely based on binding, yet no effect is measured. A pronounced example for binding is the aforementioned hERG channel. Even though **3.29** shows inhibition of 76% at a concentration of 10 µM, **3.29** did not show hERG inhibition in a functional assay with an IC_{50} above 25 µM (see Table 3.2.4). Taken all the above mentioned results in account, **3.29** proved to be the most promising compound and therefore was taken into deeper profiling in *in vivo* studies.

Table 3.2.6: *Selected possible CEREP off-targets of* ***3.29*** *and* ***3.37****.*

entry	off-target	**3.29** (%inhibition @10 µM)	**3.37** (%inhibition @10 µM)
1	β_2 receptor	18.03	85.30
2	5-HT_{2B}	55.25	73.79
3	5-HT_{2A}	65.15	22.02
4	AR	-10.10	57.04
5	α_{1A} receptor	40.59	55.42
6	Dopamine transporter	97.25	28.91
7	Norepinephrine transporter	82.52	8.58
8	Ca^{2+} channel (L, dihydropyridine site)	78.29	30.36
9	Na^{+} channel (site 2)	54.62	-27.90
10	hERG channel	75.62	20.45

3.2.6. *In vivo* PK and target engagement

Before starting murine *in vivo* experiments, the maximum tolerated dose of compound **3.29** was evaluated in a dose escalation experiment, performed at the contract research organization *Aurigon*. Even at doses up to 60 mg/kg (i.v.) the compound was well-tolerated. This study was accompanied by a toxicokinetic analysis performed by Katharina Rox (HZI). A reasonable systemic exposure 30 minutes after administration was observed (around 3500 ng/mL plasma for 30 mg/kg dose), while a fast clearance was detected already after 4 h. Due to these results, pharmacokinetic parameters could not be calculated for this setup. So far, this study however demonstrated, that high doses of **3.29** should not lead to safety concerns.

An important next PK experiment was the evaluation after pulmonary application. To this end, the pharmacokinetic parameters after intratracheal instillation were investigated. Compound **3.29**

(0.5 mg/kg) was instilled intratracheally *via* intubation using a tyloxapol-based service formulation (10% EtOH, 1% tyloxapol, 5% glycerol in PBS).[106] Then the bronchoalveolar lavage fluid (BALF), epithelial lining fluid (ELF), plasma and lung concentrations of the compound were determined. It showed good retention in all compartments, especially the BALF. The results are summarized in Table 3.2.7.

Table 3.2.7: *PK parameter of* ***3.29*** *in plasma, lung, BALF and ELF after pulmonary application.*

	plasma	**lung**	**BALF**	**ELF**
$t_{1/2}$ [h]	0.86 ± 0.4	1.08 ± 0.5	0.72 ± 0.2	0.55 ± 0.3
T_{max} [h]	0.5 ± 0.0	0.50 ± 0.0	0.50 ± 0.0	1.67 ± 2.0
C_{max} [ng/ml]	62.58 ± 45.7	9856.67 ± 4623.1	3770.00 ± 2662.9	1286.91 ± 298.7
$AUC_{0\text{-}t}$ [ng/ml·h]	55.75 ± 21.3	7357.00 ± 2369.4	4844.88 ± 2185.2	3095.83 ± 330.2
MRT [h]	1.20 ± 0.1	1.27 ± 0.4	1.57 ± 0.1	1.61 ± 1.1
V_z/F_{obs} [l/kg]	10.46 ± 1.2	-	-	-
Cl/F_{obs} [ml/min/kg]	157.13 ± 55.5	-	-	-

For *in vivo* target engagement studies, which were conducted by Teresa Röhrig (HIPS) and Christian Herr (UKS), mice were infected with *P. aeruginosa* NH57388A, a clinical isolate, with an inoculum of $5 \cdot 10^7$ CFU/lung *via* the intratracheal (i.t.) route. At this time point also compound **3.29** (dose = 5 mg/kg) or vehicle (control) were co-administered using a methyl-cellulose-based suspension as vehicle (Figure 3.2.4 A). Pathoblocker **3.29** (5 mg/kg) was reapplied along with vehicle (control) 24 and 48 h post-infection. After 72 h, lungs were harvested, homogenized and extracted. The quantification of the signal molecules HHQ, PQS and HQNO were chosen as a readout. The proximal biomarkers of the bacterial target were found to be reduced significantly by > 95% (Figure 3.2.4 B). Surprisingly, CFU count was reduced two-fold, which was not expected, as the *in vitro* pharmacology of a pathoblocker target did not show bactericidal or bacteriostatic effects. A plausible explanation for this finding might be the impact of the host immune system on bacterial clearance, as well as reduced activity of other virulence factors towards host immune system evasion, such as biofilm formation. Further experiments to investigate this hypothesis are still ongoing.

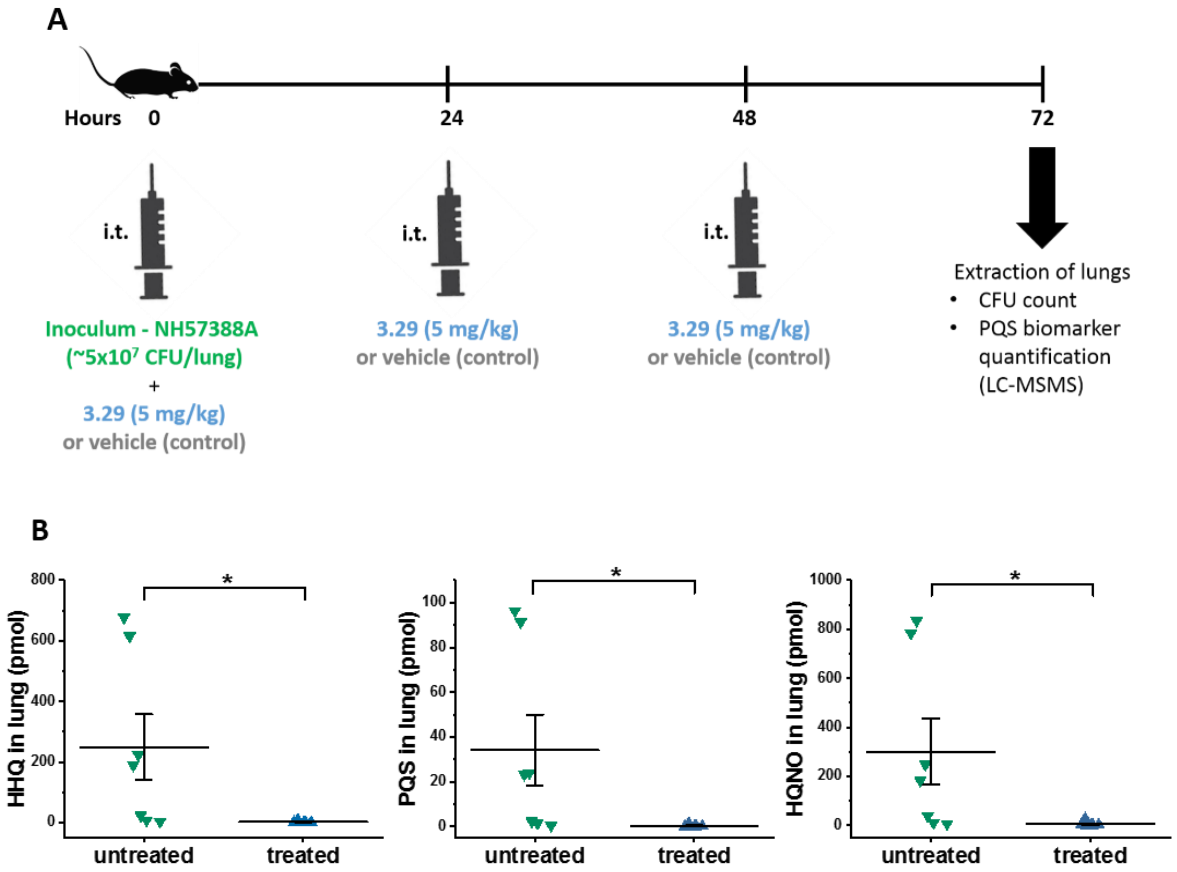

Figure 3.2.4: *A: Layout of the lung infection model for in vivo target engagement studies; B: Absolute levels of PQS-related biomarkers HHQ (left), PQS (middle) and HQNO (right) in infected lungs 72 h after infection in the treated and untreated groups.*

3.2.7. Cocrystal structure of 3.29 in complex with PqsR

Furthermore, Dr. Stefan Schmelz from the team of Prof. Dr. Wulff Blankenfeldt (HZI) was able to cocrystallize compound **3.29** in complex with $PqsR^{91-319}$ at a resolution of 2.15 Å. Main interactions involve a π-H interaction of the triazole ring with Ile263 and bridged crystal water between Ile236 and the pyridine nitrogen atom (Figure 3.2.5). In addition, the proton of the amino group acts as a hydrogen bond donor to the hydroxyl side chain of Thr265. As already proposed in chapter 3.1.4 a π-H interaction between Tyr258 and the phenyl ring of the 4-phenoxy motif is observed.

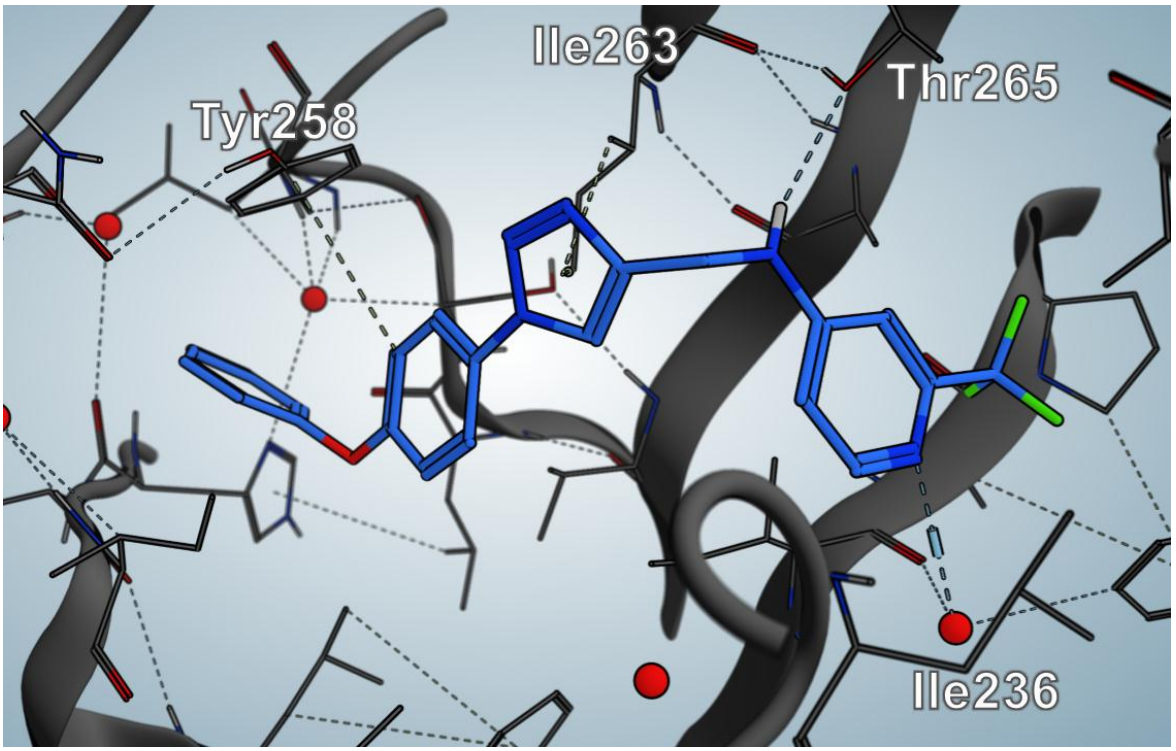

Figure 3.1.4: *Cocrystal structure of* ***3.29*** *in complex with PqsR$^{91-319}$ at 2.15 Å. Crystal water is displayed as a red ball. Color code: blue: C, dark blue: N, green: F, red: O, light grey: H.*

3.3. Lead optimization

3.3.1. *Head* modification I

3.3.1.1. Retrosynthetic analysis

The successful *in vivo* target engagement studies encouraged the optimization towards a possible preclinical candidate. Synthesis of **4.1**, bearing the previously described amino function in the *head* was of great interest. Not only should the introduction of this motif reduce lipophilicity and increase solubility, but also contributions to activity are possible. The retrosynthetic analysis is depicted in Scheme 3.3.1. Functional group interconversion of **4.1** reveals **4.2**, equipped with a chlorine atom for possible S_NAr or *Buchwald-Hartwig* reactions. In order to avoid side reactions of the propargyl unit in transition-metal catalyzed transformations, the amination was chosen as a late-stage modification. Furthermore, compound **4.2** should also be evaluated as a possible inverse agonist. Formation of the triazole should easily be realized *via* already established CuAAC, unraveling building block **4.3**. Since the corresponding free amino pyridine which could be converted to **4.4** was not commercially available when first planning the synthetic route towards **4.1** it also had to be synthesized. The aminopyridine building block **4.4** should be obtained from precursor **4.5** after reduction of the nitro functionality and the *N*-oxide. **4.5** should be generated *via* regioselective nitration of *N*-oxide **4.6**, which could be prepared from commercially available starting material **4.7**.[107,108]

Scheme 3.3.1: *Initial retrosynthetic analysis of* ***4.1****.*

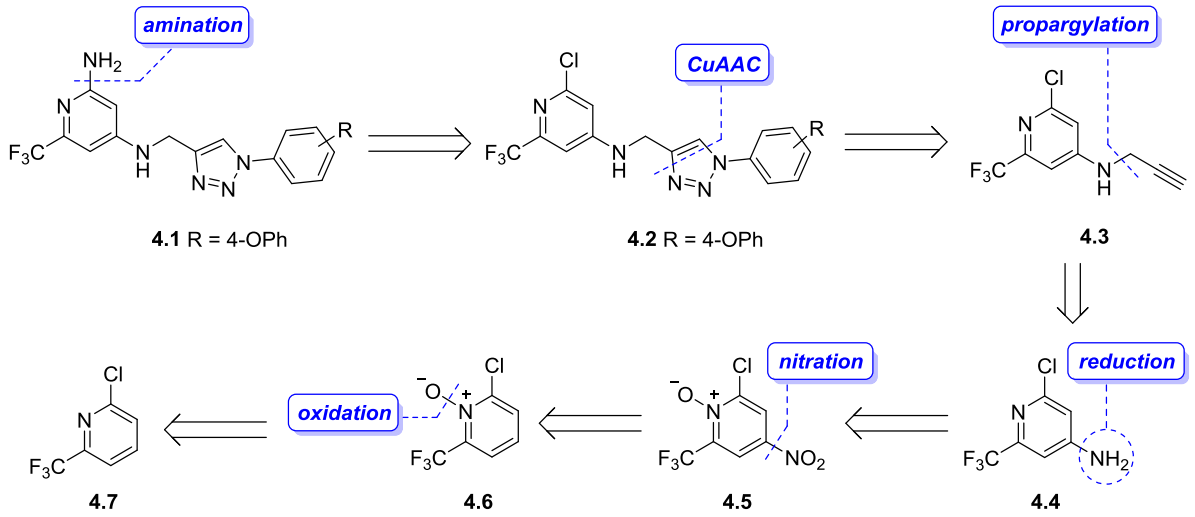

3.3.1.2. Synthesis of Building Block 4.3

Since the initially planned synthetic route towards **4.3** did not yield the desired building block, because several protocols using mCPBA or UHP trying to convert **4.7** into **4.6** failed, a different approach based on a *Curtius*-type reaction was investigated. Retrosynthetic analysis of the newly planned route is described in Scheme 3.3.2. Building block **4.3** should be obtained by propargylation of Boc-protected amine **4.8**, which could be synthesized from carboxylic acid **4.9** *via* a *Curtius*-type reaction. The corresponding precursor **4.10** could be synthesized by regioselective iodination of aforementioned commercially available 2-chloro-6-(trifluoromethyl)pyridine **4.7**.

Scheme 3.3.2: *Second retrosynthetic analysis of building block* ***4.3****.*

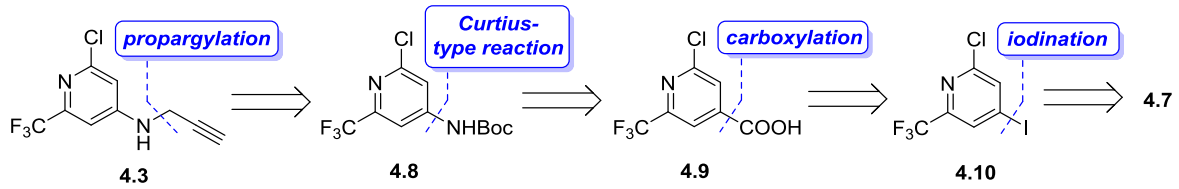

For the regioselective iodination of **4.7**, a protocol based on results by Cottet *et al.* was used.[109] Deprotonation with LDA in THF was carried out at –100 °C in order to yield the desired kinetic product **4.11** (Scheme 3.3.3). Increasing the temperature to –80 °C, followed by addition of an iodine solution in THF proved to be very difficult, since no cryostat was available. This rendered keeping a constant temperature difficult, which should be high enough for successful iodination of the lithiated species, but also low enough to prevent the latter from undergoing proton shuffling. Therefore only a 2:1 mixture of **4.12** and ***iso*-4.12** was obtained, yet in satisfying yield of 70%. Moreover, the regioisomers could not be separated *via* column chromatography. First attempts to directly introduce the carboxylic acid from lithiated species **4.11** were not successful and only led to proto-delithiation. Nevertheless,

the mixture was further used in the next step for carboxylation. The use of LiMg(*n*Bu)$_3$ as a transmetalation agent proved to be crucial.[109] When *i*PrMgCl, *i*PrMgCl·LiCl or TMPMgCl·LiCl were used, yields were significantly lower.

Scheme 3.3.3: *Synthesis of Boc-protected propargylation precursor* ***4.15*** *from* ***4.7****.*[a]

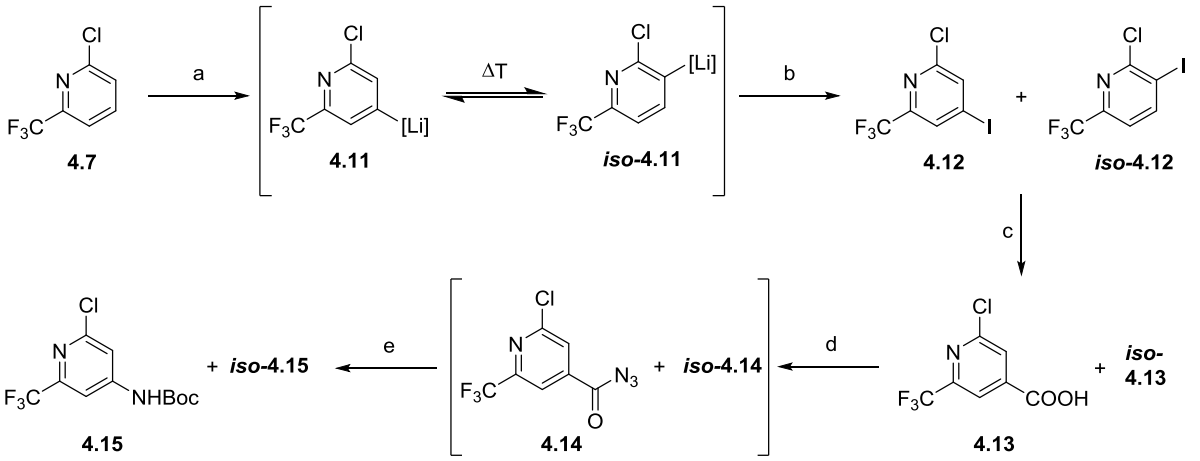

[a]***Reagents and conditions:*** *a: LDA, THF, –100 °C, 2.5 h; b: I_2, THF, –80 °C, 2 h, 70% (2:1); c: LiMg(nBu)$_3$, THF, 0 °C, then CO_2 (g) 30 min; d: DPPA, NEt_3, toluene, 100 °C, 20 h; e: KOtBu, 0 °C, 30 min, 25% (2 steps).*

Gaseous CO_2 and dry ice were used as electrophiles in the carboxylation reaction, both with comparable yields of the desired intermediate **4.13** and ***iso*-4.13** respectively. Subsequent conversion of carboxylic acids **4.13** and ***iso*-4.13** into the corresponding azides (**4.14** and ***iso*-4.14**), which underwent *Curtius* rearrangement, ultimately gave rise to Boc-protected aminopyridines **4.15** and ***iso*-4.15**. The desired propargylation precursor **4.15** was then obtained after purification *via* column chromatography. Using the established propargylation, deprotection and CuAAC sequence, amination precursor **4.2** was prepared in excellent yield (Scheme 3.3.4).

Scheme 3.3.4: *Completion of the synthesis towards amination precursor* ***4.2****.*[a]

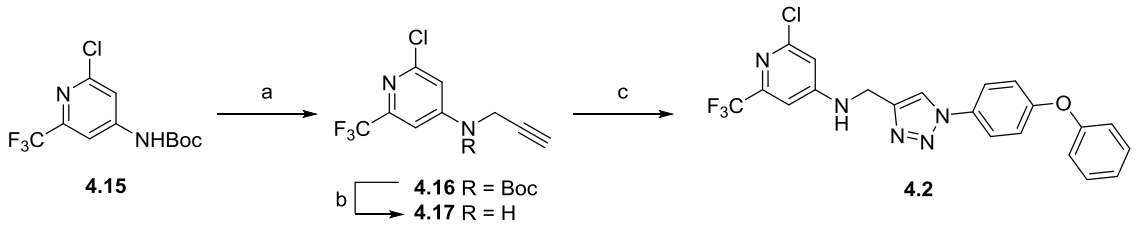

[a]***Reagents and conditions:*** *a: NaH (60 wt%), DMF, 0 °C, 1 h, then propargyl bromide, 5 h, rt, 97%; b: DCM/TFA 1:1, 6 h, rt, > 98%; c: tBuONO, $TMSN_3$, 4-phenoxyaniline, MeCN, 0 °C, 1 h, then* ***4.17****, $CuSO_4$·5 H_2O, Na ascorbate, DIPEA, rt, 16 h, 93%.*

3.3.1.3. Amination studies of 4.2

The initial strategy to prepare the desired target compound **4.1** was to install the amino function in an S_NAr reaction. Several conditions were tested and are summarized in Table 3.3.1.

Table 3.3.1: *Conditions for the amination attempts of **4.2** into **4.1**.5.0 eq. of nucleophile were used in a 0.1 M solution of solvent.*

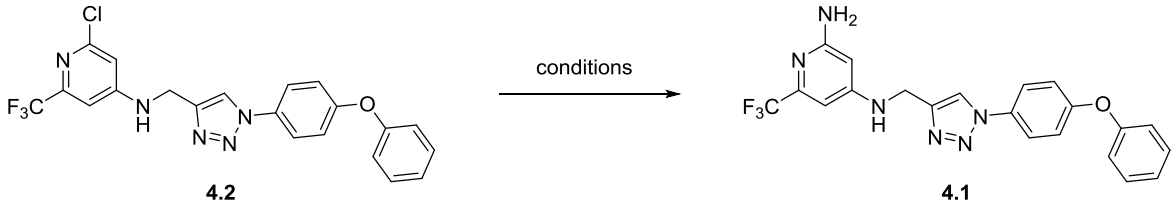

4.2 **4.1**

entry	nucleophile	additives	solvent	T	t
1	NH_4OH	-	DMSO	100 °C	21 h
2	NH_4OH	-	1,4-dioxane	100 °C	21 h
3	NH_4OH	-	NMP	100 °C	21 h
4	NH_4OH	Cu_2O, 1,10-phenanthroline	DMSO	100 °C	21 h
5	NH_4OH	Cu_2O, 1,10-phenanthroline	1,4-dioxane	100 °C	21 h
6	NH_4OH	Cu_2O, 1,10-phenanthroline	NMP	100 °C	21 h
7*	NH_4OH	Cu_2O, 1,10-phenanthroline	DMSO	100 °C	21 h
8*	NH_4OH	Cu_2O, 1,10-phenanthroline	1,4-dioxane	100 °C	21 h
9*	NH_4OH	Cu_2O, 1,10-phenanthroline	NMP	100 °C	21 h
10	NH_3 (7 M in MeOH)	Cu_2O, 1,10-phenanthroline	1,4-dioxane	100 °C	21 h
11	NHMDS (1 M in THF)	-	DMF	80 °C	21 h
12	HMDS	NEt_3	DMF	80 °C	21 h
13	NaN_3	-	DMF	80 °C	8 h

* = microwave-assisted

Since no conversion was observed at all for any of the reaction conditions, the strategy was changed towards a transition metal-catalyzed protocol, making use of a *Buchwald-Hartwig* coupling. The conversion of aryl chlorides into primary anilines has been vastly described in literature.[63] In order to reduce complexity of parameter optimization for the reaction conditions, the initial screening was based on NH_3 (0.5 M in 1,4-dioxane) as a nucleophile and the NaO*t*Bu (2.0 M in 1,4-dioxane) as base. As a palladium source, the "KitAlysis High-Throughput Palladium Precatalyst Cross-Coupling Reaction Screening Kit" from Sigma Aldrich was used. The advantage of utilizing such a precatalyst kit is that many of the included palladium sources are well-established and studied, therefore offering a promising starting point. They are bench-stable, easily activated under mildly basic conditions and lead

to fewer undesired byproducts, such as the formation of di- or tri-arylated species.[110,111] The screening reactions were carried out on a 10 µmol scale, using 10 mol% of precatalyst, 2.0 equivalents of nucleophile and 2.2 equivalents of base. After stirring in a pre-heated bath at 80 °C for 24 h, the reaction mixtures were quenched with HOAc in MeCN and analyzed *via* LCMS. The results are summarized in Table 3.3.2.

Table 3.3.2: *Catalyst screening for transformation of* ***4.2*** *into* ***4.20****. 5.0 eq. of NH_3 (0.5 M in 1,4-dioxane) were used, 2.2 eq. of base and 10 mol% of precatalyst. Molarity was 0.1 M in 1,4-dioxane. Reactions were run at 80 °C for 24 h.*

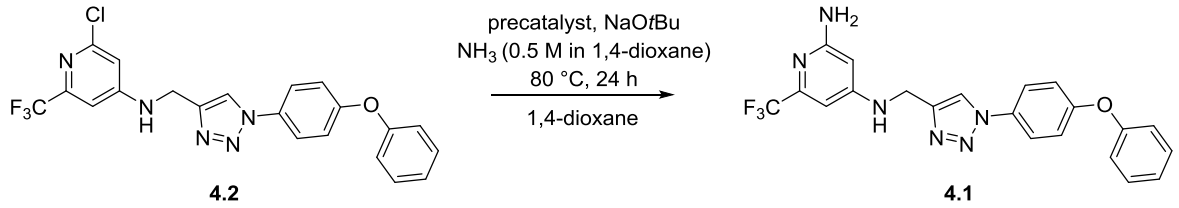

entry	precatalyst	conversion	entry	precatalyst	conversion
1	AdBrettPhos Pd G3	0%	**13**	Me_4*t*BuXPhos Pd G3	0%
2	APhos Pd G3	0%	**14**	MorDalPhos Pd G3	0%
3	*rac*-BINAP Pd G3	0%	**15**	P(Cy_3) Pd G3	0%
4	BrettPhos Pd G4	0%	**16**	P(*t*Bu_3) Pd G2	X
5	cataCXium A Pd G3	0%	**17**	Pd-PEPPSI™-IPent cat	0%
6	CPhos	X	**18**	RuPhos Pd G4	0%
7	CyJohnPhos Pd G3	0%	**19**	SPhos Pd G4	0%*
8	DavePhos Pd G3	0%	**20**	*t*BuBrettPhos Pd G3	100%**
9	DPPF Pd G3	0%	**21**	*t*BuXPhos Pd G3	100%**
10	JackiePhos Pd G3	X	**22**	XantPhos Pd G3	0%
11	JosiPhos SL-J009-1 Pd G3	X	**23**	XPhos Pd G4	0%
12	meCgPPh Pd G3	0%	**24**	$PdCl_2(PPh_3)_4$	0%

X = decomposition, complex mixture; * = only oxidized ligand detected, ** = formation of **4.18**

While most of the precatalysts showed no reaction, some led to decomposition of the starting material and complex mixtures (entries 6, 10, 11 and 16). Only entries 20 and 21 showed clear conversion, but exclusively to **4.19**, an undesired byproduct. Formation of **4.19** could be explained by coupling of the *tert*-butoxide anion and subsequent cleavage of the resulting *tert*-butyl ether **4.18** upon acidic workup (Scheme 3.3.5).

Scheme 3.3.5: *Explanation for the formation of* ***4.19****.*[a]

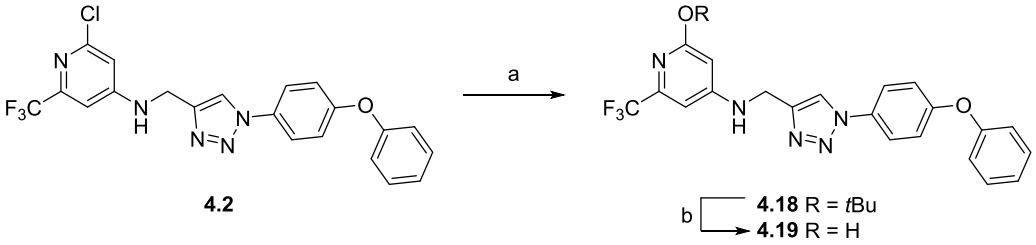

[a]***Reagents and conditions:*** *a: tBuBrettPhos Pd G3 or tBuXPhos Pd G3, NaOtBu, NH_3 (0.5 M in 1,4-dioxane), 1,4-dioxane 80 °C, 24 h; b: HOAc, MeCN.*

The screening was then repeated under the same conditions, but this time with benzophenone imine (BPI), an ammonia surrogate, as the nucleophile. The reagent is known for its utilization in *Buchwald-Hartwig* couplings.[112–115] One advantage of this substitute is the inability to form per-arylated byproducts, since the *N*-aryl imine serves as a protecting group. Reaction of **4.2** under the aforementioned conditions from Table 3.3.2 did not lead to any conversion to the desired target compound at all.

Therefore other conditions with BPI as the nucleophile were evaluated. Moreover, other ammonia surrogates, such as benzylamine, *tert*-butyl amine, HMDS, NHMDS, LHMDS and $BocNH_2$ were applied. The results are summarized in Table 3.3.3. The combination of Pd_2dba_3 with CataCXium A as ligand and Cs_2CO_3 as base in toluene at elevated temperature proved to be successful in synthesizing the *N*-arylated benzophenone imine **4.20** (Figure 3.3.1). When benzylamine was used, these conditions did not yield the desired product, only dehalogenated starting material was obtained.

The attempt of copper-catalyzed coupling with DMEDA only led to addition of the latter. However, the combination of $[Pd(cinnamyl)Cl]_2$ and BippyPhos, as well as *t*BuXPhos Pd G3 as a precatalyst with NaO*t*Bu in 1,4-dioxane led to formation of **4.21** in moderate yields.[116] The combination of $[Pd(cinnamyl)Cl]_2$ and BippyPhos also worked well when *tert*-butyl amine was utilized as a nucleophile (**4.22** Figure 3.3.1). Nevertheless, the compound could not be purified *via* automated flash chromatography or preperative HPLC. For HMDS, NHMDS, LHMDS and $BocNH_2$ only Pd_2dba_3 and CataCXium A were tested which did not yield the desired target compounds, rather dehalogenated starting material. For $CbzNH_2$, these conditions also only yielded dehalogenated starting material, as well as for a protocol applying $Pd(OAc)_2$ with dppf and K_3PO_4 in 1,4-dioxane.[117]

Table 3.3.3: *Conditions for transition metal-catalyzed C–N couplings. 4.0 eq. of nucleophile, 10 mol% of catalyst and ligand were used. 4.0 eq. of base were used. Molarity was 0.1 M in the given solvent. Reactions were run for 24 h.*

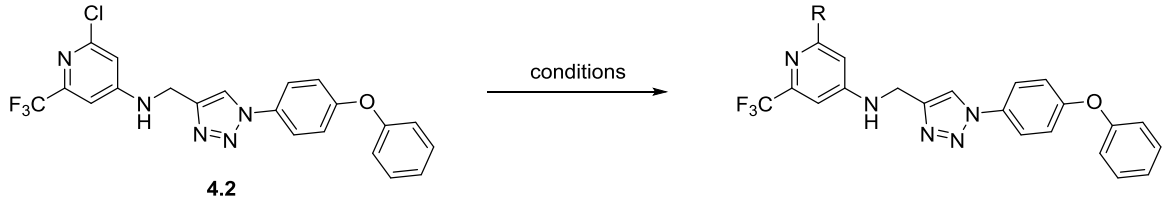

entry	nucleophile	catalyst	ligand	base	solvent	T	yield
1	BPI	Pd_2dba_3	CataCXium A	Cs_2CO_3	toluene	120 °C	68%
2	BPI	$[Pd(cinnamyl)Cl]_2$	BippyPhos	NaO*t*Bu	1,4-dioxane	80 °C	X
3	NH_2Bn	Pd_2dba_3	CataCXium A	Cs_2CO_3	toluene	80 °C	X
4	NH_2Bn	$[Pd(cinnamyl)Cl]_2$	BippyPhos	NaO*t*Bu	1,4-dioxane	80 °C	35%
5	NH_2Bn	*t*BuXPhos Pd G3	-	NaO*t*Bu	1,4-dioxane	80 °C	60%
6	NH_2Bn	CuI	DMEDA	K_3PO_4	1,4-dioxane	80 °C	X
7	NH_2Bn	Cu_2O	1,10-phenanthroline	DIPEA	DMSO	80 °C	X
8	NH_2*t*Bu	$[Pd(cinnamyl)Cl]_2$	BippyPhos	NaO*t*Bu	1,4-dioxane	80 °C	70%*
9	HMDS	Pd_2dba_3	CataCXium A	Cs_2CO_3	toluene	120 °C	X
10	NHMDS	Pd_2dba_3	CataCXium A	-	toluene	120 °C	X
11	KHMDS	Pd_2dba_3	CataCXium A	-	toluene	120 °C	X
12	$BocNH_2$	Pd_2dba_3	CataCXium A	Cs_2CO_3	toluene	80 °C	X
13	$CbzNH_2$	Pd_2dba_3	CataCXium A	Cs_2CO_3	toluene	80 °C	X
14	$CbzNH_2$	$Pd(OAc)_2$	dppf	K_3PO_4	1,4-dioxane	80 °C	X

X = no conversion to desired product was detected, * = conversion

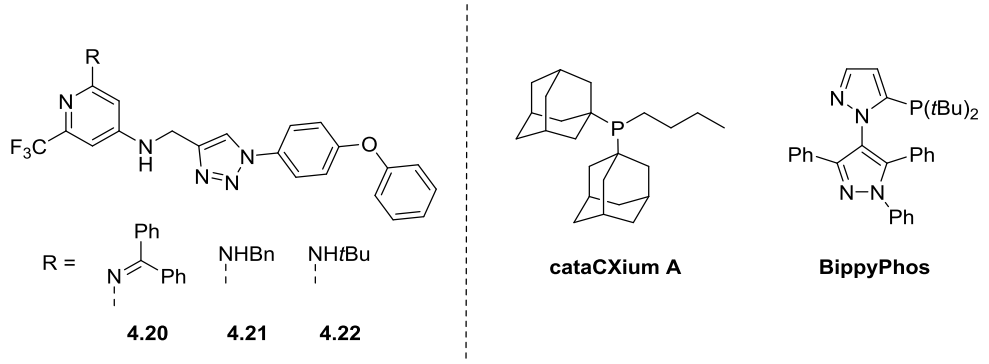

Figure 3.3.1: *Structures oft he obtained compounds from Table 3.3.5 (left) and structures of the ligands cataCXium A and BippyPhos (right).*

When trying to liberate the free primary amine from **4.20** under acidic conditions, no desired product was detectable. Even at elevated temperatures (100 °C) and long reaction times (> 7 d) only decomposition took place. Benzyl-protected **4.21** was subjected to several hydrogenation conditions, unfortunately also being stable under all conditions tested. Therefore, $BocNH_2$ as an alternative ammonia surrogate was chosen again, since it proved to be successful for the *Buchwald-Hartwig* coupling with a substrate from another class of project compounds. The conditions tested are summarized below (Table 3.3.4).

Table 3.3.4: *Reaction conditions optimization for Buchwald-Hartwig coupling with $BocNH_2$. Reactions were run for 24 h on a scale of 50 µmol with 10 mol% catalyst and ligand, 2.0 eq. of $BocNH_2$ and 2.2 eq. of base, in a 0.1 M solution of solvent.*

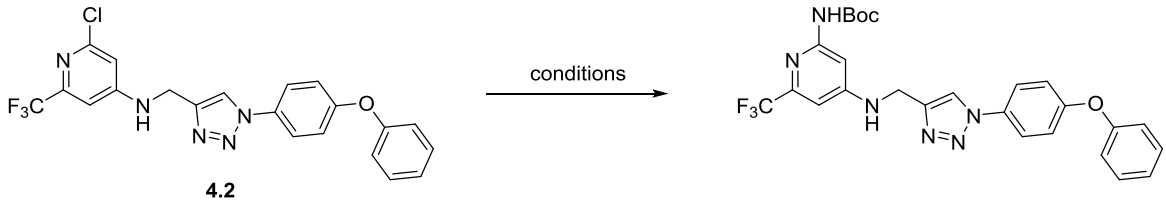

entry	catalyst	ligand	base	solvent	T	conversion*
1	$[Pd(cinnamyl)Cl]_2$	BippyPhos	NaO*t*Bu	1,4-dioxane	90 °C	0%
2	*t*BuXPhos Pd G3	-	Cs_2CO_3	toluene	100 °C	0%
3	*t*BuXPhos Pd G3	-	NaO*t*Bu	toluene	100 °C	0%
4	*t*BuXPhos Pd G3	-	NaO*t*Bu	1,4-dioxane	90 °C	0%
5	Pd-175	-	Cs_2CO_3	1,4-dioxane	80 °C	92%

* = determined *via* LCMS

The established conditions with $[Pd(cinnamyl)Cl]_2$ and BippyPhos, which worked well for NH_2*t*Bu and NH_2Bn, did not result in any conversion in this case. Also, the use of commonly-used precatalyst *t*BuXPhos Pd G3 with adjusted conditions did not show conversion to the desired target compound. Applying another precatalyst, Pd-175, which is basically the commercial name for

[*t*BuBrettPhosPd(allyl)]OTf from Johnson Matthey, led to almost full conversion with Cs_2CO_3 as the base in 1,4-dioxane. The reaction was then repeated on a larger scale and after automated flash chromatography with EtOAc and cyclohexane, the free amine was obtained (Scheme 3.3.6).

Scheme 3.3.6: *Synthesis of **4.1** from **4.2** using optimized reaction conditions.*[a]

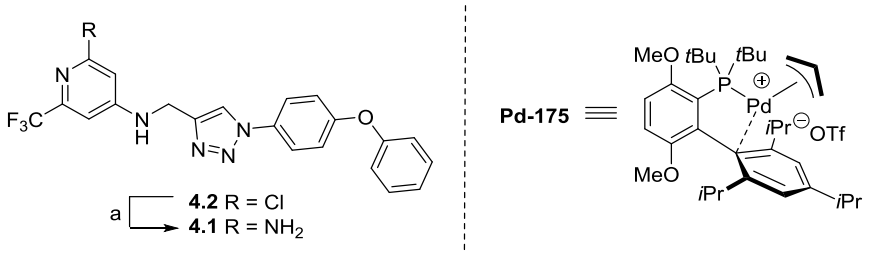

[a]***Reagents and conditions:*** *$BocNH_2$, Pd-175, Cs_2CO_3, 1,4-dioxane, 28 h, 90 °C, 39%.*

The catalyst used in this reaction is barely described in literature and was initially synthesized by DeAngelis *et al.* in order to investigate μ-allylpalladium complexes as air-stable and highly-reactive precatalysts.[118–120] It proved to be superior in challenging C–N cross coupling reactions.

3.3.1.4. Biological evaluation

The desired amino derivative **4.1**, as well as the chlorine-containing precursor **4.2** and the byproduct **4.19** were tested directly in the *P. aeruginosa* pyocyanin inhibition assay. The results are shown in Figure 3.3.7. The introduction of chlorine was well-accepted and had no impact on the activity of **4.2**, whereas the primary amine in this position (compound **4.1**) led to a significant drop in activity resulting in an IC_{50} of 322 nM. Activity was completely abolished in **4.19**, which might be explained by equilibrating to pyridone ***iso*-4.19**.

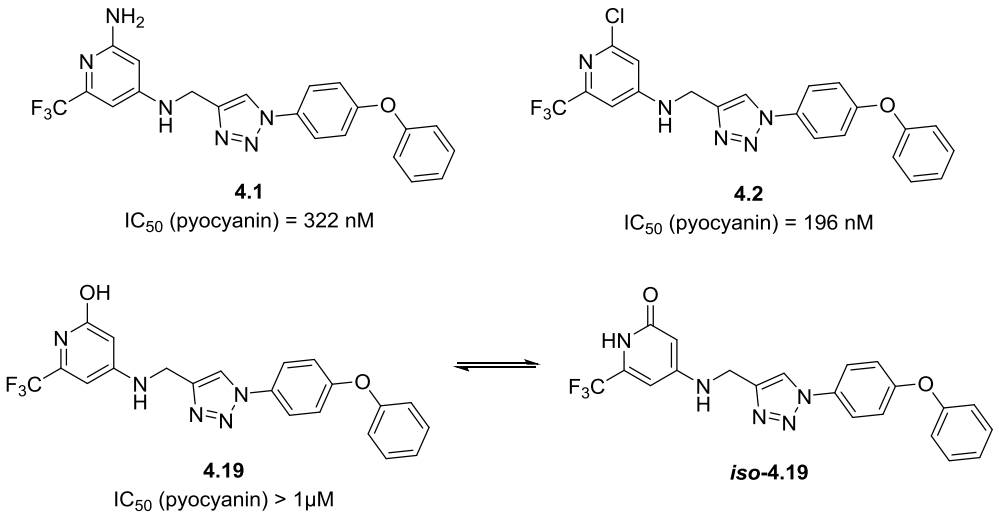

Figure 3.3.7: *Derivatives **4.1, 4.2** and **4.19** with its tautomer **iso-4.19** with corresponding IC_{50} values for pyocyanin inhibition.*

By now, no results for the initial on-target activity in the *E. coli* reporter gene assay are available. Nevertheless, these values are not important endpoints and thus play a minor role in this optimization.

3.3.2. *Tail* Modification

In order to further explore the possibilities of the given growth vector present in **3.29** (see chapter 3.2.2), the 4-phenoxy moiety should be modified. The main goal was not only to improve activity but also increase solubility and eventually metabolic stability.

3.3.2.1. Fluorophenoxy Derivatives

The introduction of fluorine in pharmacologically relevant molecules is of great importance in medicinal chemistry and has been vastly discussed and investigated in the past.[100,121–127] Potency and selectivity can be increased as well as permeability. Moreover, metabolic stability can be improved significantly. In order to investigate the possible benefits of fluorination, the corresponding aniline precursors **5.1b** and **5.2b** should be synthesized (Scheme 3.3.7). The 4-fluorophenoxy derivative was omitted, since this substitution pattern was already installed in a comparable class of compounds and proved to be inefficient. The effects of 2- and 3-fluorinated phenoxy analogues remained unclear. The synthetic procedure, which was already established for alkoxy substituents in chapter 3.2.1 was applied. Starting with commercially available 1-chloro-4-nitrobenzene (**5.1**), S_NAr reaction with the corresponding fluorophenols resulted in formation of **5.1a** and **5.2a**, which were then reduced by hydrogenation with Pd/C. Subsequent conversion of **5.1b** and **5.2b** into azides **5.1c** and **5.2c**, followed by CuAAC with alkyne **1.25** delivered the desired target compounds **5.3** and **5.4** in excellent yields (Scheme 3.3.7).

Scheme 3.3.7: *Synthesis of fluorinated analogues **5.3** and **5.4**.*[a]

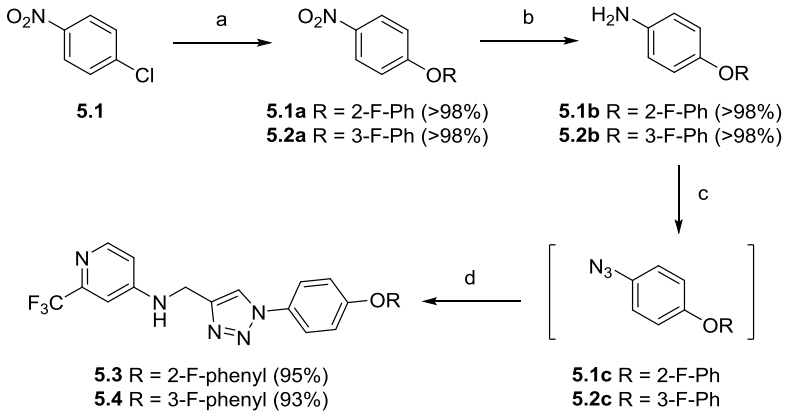

[a]Reagents and conditions: *a: K_2CO_3, fluorophenol, DMF, 80 °C, 15 h, > 98%; b: Pd/C, H_2, EtOH, rt, 8 h, > 98%; c: tBuONO, $TMSN_3$, MeCN, rt, 3.5 h; d: $CuSO_4 \cdot 5\ H_2O$, Na ascorbate, DIPEA, N-(prop-2-yn-1-yl)-2-(trifluoromethyl)pyridin-4-amine (**1.25**), rt, 13 h, 93–95%.*

The compounds were then evaluated for biological activity, solubility and metabolic stability in mouse liver microsomes. The results are summarized in Table 3.3.4, compound **3.29** is included as a reference. Installation of a fluorine substituent in 2-position (**5.3**) gave a significant boost in both on-target activity and pyocyanin inhibition. Satisfyingly, also solubility was increased drastically. When migrating the

fluorine to 3-position (**5.4**), activity in pyocyanin inhibition was slightly decreased, but solubility also benefitted from the additional substituent and was in the same range as for **5.3**. Interestingly, for **5.4** the metabolic stability was comparable to **3.29**, while **5.3** proved to be almost five times more stable. Thus, **5.3** is suitable as a frontrunner compound for further optimization.

Table 3.3.4: *Biological evaluation and DMPK profiling for compounds **5.3** and **5.4**.*

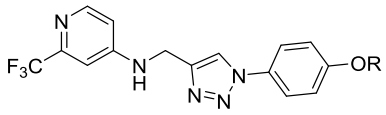

entry	cpd	R	IC_{50} (PqsR)	IC_{50} (pyocyanin)	S_{kin}	$t_{1/2}$ MLM
1	**3.29***		11 nM	199 nM	7.7 µM	10 min
2	**5.3**	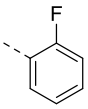	5 nM	81 nM	29.6 µM	49 min
3	**5.4**	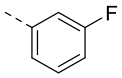	n.d.	214 nM	29.4 µM	15 min

* = reference; n.d. = not determined

Dr. Stefan Schmelz (HZI) obtained a cocrystal structure of **5.3** in complex with $PqsR^{91-319}$ (Figure 3.3.8).

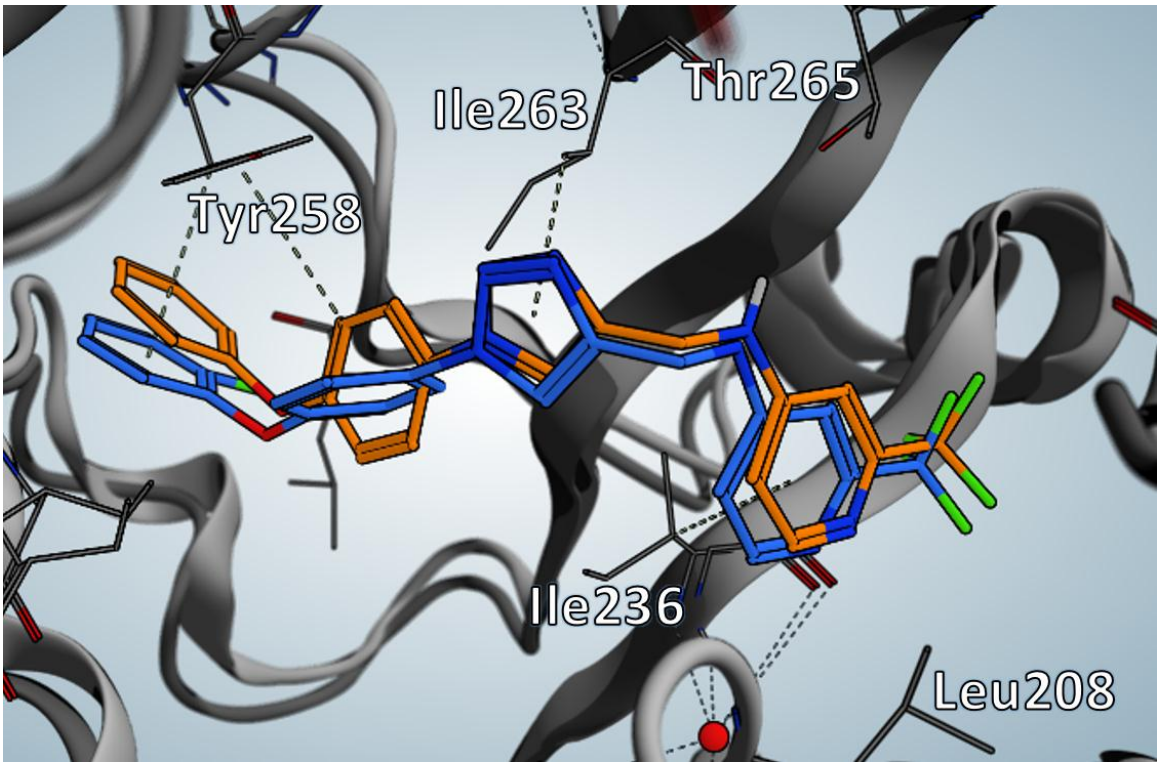

Figure 3.3.8: *Overlay of cocrystal structures of **3.29** (orange) and **5.3** (blue) with $PqsR^{91-319}$. Dark grey ribbon refers to **5.3**, light grey to **3.29**. Color code: dark blue: N, green: F, red: O, grey: H.*

In Figure 3.3.8 an overlay with the structure of **3.29** is depicted. It is clear, that the phenyl ring directly attached to the triazole nitrogen is twisted approximately 90°. This conformational change leads to a CH-π interaction of the fluorinated phenyl motif with the benzylic proton of Tyr258, in contrast to **3.29**, which shows CH-π interaction of the Tyr258 arene with the CH of the phenyl moiety. Moreover, an additional CH-π interaction of the pyridine headgroup with Ile236 can be found for **5.3**.

3.3.2.2. Pyridine Derivatives

Since the introduction of fluorine in 2-position proved to be beneficial in terms of activity, as well as solubility, the introduction of a nitrogen in the fluorophenyl moiety was promising with respect to reduced lipophilicity and, thus, might further increase solubility. Due to limited commercial availability starting material and challenging syntheses of precursors only one derivative was synthesized (Scheme 3.3.8). Commercially available 2-fluoropyridin-3-ol was subjected to S_NAr with 1-fluoro-4-nitrobenzene (**5.5**) with K_2CO_3 in DMF yielding biarylether **5.6a**, which was then reduced *via* hydrogenation with Pd/C under an atmosphere of H_2 in DCM resulting in aniline derivative **5.6b** in excellent yields for both steps.

Scheme 3.3.8: *Synthesis of fluorinated pyridine analogue **5.7**.*[a]

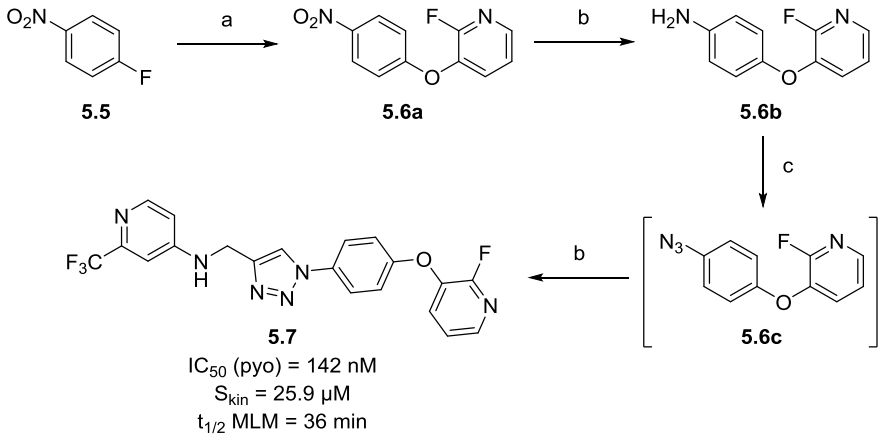

[a]***Reagents and conditions:*** *a: 2-fluoropyridin-3-ol, K_2CO_3, DMF, 80 °C, 18 h, > 98%; b: Pd/C, H_2, DCM, 20 h, rt, 97%; c: tBuONO, $TMSN_3$, MeCN, rt, 3 h; d: $CuSO_4$·5 H_2O, Na ascorbate, DIPEA, N-(prop-2-yn-1-yl)-2-(trifluoromethyl)pyridin-4-amine (**1.25**), rt, 13 h, 52%.*

Then, the established CuAAC protocol was applied, converting **5.6b** into the corresponding azide **5.6c** with *t*BuONO and $TMSN_3$ in MeCN, to which alkyne **1.25**, $CuSO_4$·5 H_2O, Na ascorbate and DIPEA were added. The desired target compound **5.7** was then isolated in moderate yield of 52%. The compound was then tested for its ability to inhibit pyocyanin production in a spot-test. Unfortunately, it showed only 35% inhibition at a concentration of 0.2 µM, which marks a dramatically drop in activity. Moreover, the initial plan to increase solubility also did not succeed, since **5.7** was less soluble than the parent compound **5.3**. Metabolic stability was improved compared to **3.29** and **5.2** but still was inferior to **5.3**.

In order to further investigate the impact of the nitrogen atom, the corresponding defluorinated compound **5.9** was synthesized from commercially available 4-(pyridin-3-yloxy)aniline **5.8a**. Azidation and subsequent CuAAC were carried out under the established conditions (Scheme 3.3.9).

Scheme 3.3.9: *Synthesis of pyridine analogue* ***5.9****.*[a]

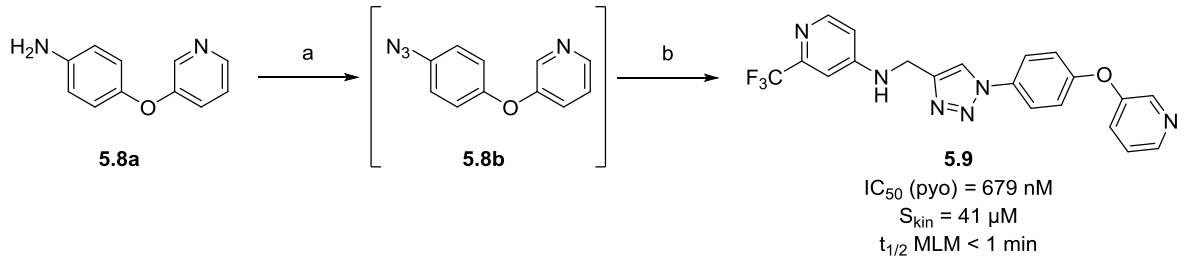

[a]***Reagents and conditions:*** *a: tBuONO, $TMSN_3$, MeCN, rt, 3 h; b: $CuSO_4 \cdot 5\ H_2O$, Na ascorbate, DIPEA, N-(prop-2-yn-1-yl)-2-(trifluoromethyl)pyridin-4-amine (**1.25**), rt, 19 h, 56%.*

Since a non-additive SAR has been observed so far in this class when it comes to *tail* modification (chapter 3.2), the role of the nitrogen atom itself remained unclear. When **5.9** was tested for pyocyanin inhibition, activity was decreased, showing an IC_{50} of 679 nM. This very likely explains the drop in activity observed for **5.7**. Nevertheless, solubility was increased to 41 µM, whereas metabolic stability in mouse liver microsomes was drastically decreased to less than 1 minute.

3.3.2.3. Indazole Analogues

As already described in Chapter 2.3.1, **3.30**, the *N*-linked **3.29**-analogue showed reasonable on-target activity but when it comes to its efficacy in pyocyanin inhibition the IC_{50} drops significantly. To further investigate the possibility of keeping the nitrogen as a linking atom, a rigidification approach was pursued (Scheme 3.3.10).

Scheme 3.3.10: *Design rationale for compound* ***5.10****.*

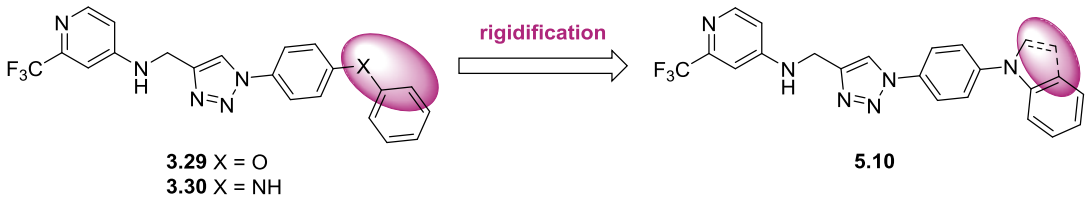

The indole moiety was introduced *via* an *Ullmann*-type coupling with the previously synthesized 4-bromine derivative **3.22**. Here, a protocol using CuI, K_2CO_3 and L-proline in DMSO was applied.[128] Even though the reaction took three days to reach full conversion, the desired target compound **5.10** was isolated with a good yield of 82% (Scheme 3.3.11).

Scheme 3.3.11: *Synthesis of compound* ***5.10****.*[a]

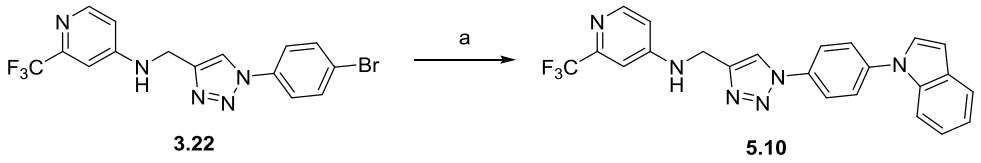

[a]***Reagents and conditions:*** *a: indole, K_2CO_3, CuI, L-proline, DMSO, 80 °C, 3 d, 82%.*

In order to investigate the influence of additional nitrogen atoms in the *tail* region, compounds **5.16 – 5.19** were synthesized (Scheme 3.3.12). Unfortunately, the aforementioned synthetic procedure did not yield the desired target compounds. Therefore, the approach was switched to the more promising sequence of S_NAr reaction, hydrogenation, azidation and CuAAC. Starting from commercially available 1-chloro-4-nitrobenzene **5.11** the corresponding derivatives **5.16 – 5.19** were obtained**.**[129]

Scheme 3.3.12: *Synthesis of different heteroaryl derived compounds* ***5.16 – 5.19****.*[a]

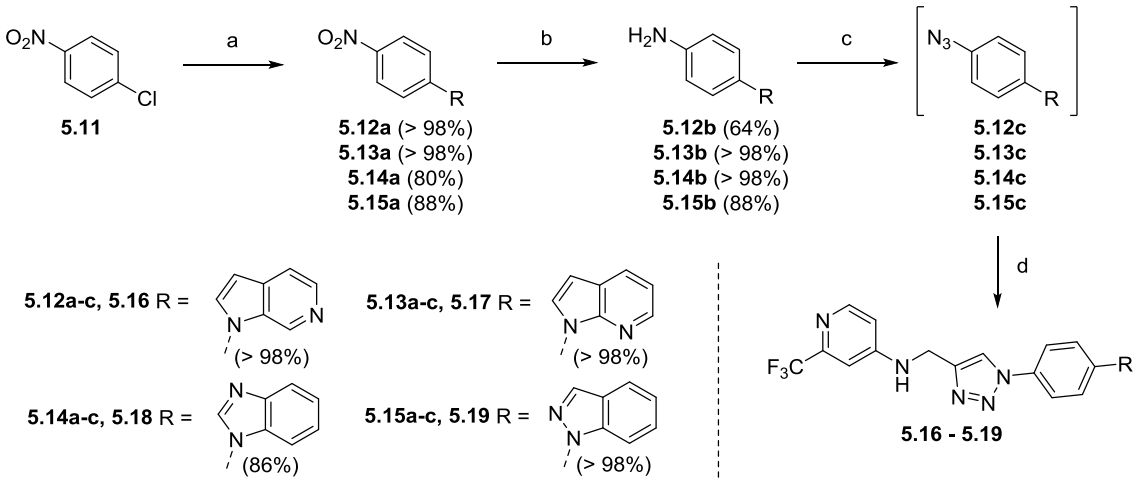

[a]***Reagents and conditions:*** *a: Cs_2CO_3, corresponding heterocycle, DMF, 80 °C; b: Pt/C, H_2, MeOH, rt; c: tBuONO, $TMSN_3$, MeCN, rt; d: $CuSO_4 \cdot 5\ H_2O$, Na ascorbate, DIPEA, N-(prop-2-yn-1-yl)-2-(trifluoromethyl)pyridin-4-amine (**1.25**), rt.*

The compounds were then evaluated for their efficacy, solubility and metabolic stability (Table 3.3.6). Initial rigidification towards indole-substituted compound **5.10** did not have a significant effect on activity. When installing a second nitrogen atom, on-target activity is drastically increased in compounds **5.16**, **5.17** and **5.19** (IC_{50} = 4 – 9 nM), whereas benzimidazole introduction resulted in a two-fold decrease in activity (IC_{50} = 61 nM). Once again, changing from *E. coli* to *P. aeruginosa*, inter-assay variations regarding qualitative SAR outcomes were observed. By now, no investigations on possible influx or efflux problems were conducted.

Table 3.3.6: *Biological evaluation and DMPK profiling of compounds* ***5.10*** *and* ***5.16 – 5.19****.*

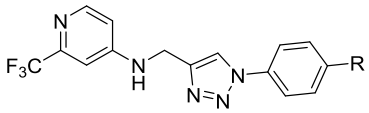

entry	cpd	R	IC_{50} (PqsR)	IC_{50} (pyocyanin)	S_{kin}	$t_{1/2}$ MLM
1	**3.29***	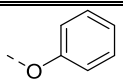	11 nM	199 nM	7.7 µM	10 min
2	**3.30***	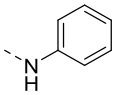	31 nM	1058 nM	n.d.	n.d.
3	**5.10**	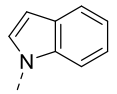	41 nM	1161 nM	32 µM	58 min
4	**5.16**	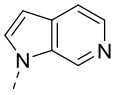	9 nM	993 nM	43.9 µM	19 min
5	**5.17**	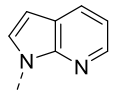	8 nM	1899 nM	32.4 µM	10 min
6	**5.18**	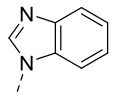	61 nM	2384 nM	35.1 µM	43 min
7	**5.19**	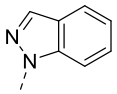	4 nM	277 nM	26 µM	31 min

* = reference

While on-target activities in the single-digit nanomolar range were detected for the whole series of compounds, only indazole-derived analogue **5.19** proved to significantly inhibit pyocyanin production with an IC_{50} of 277 nM. Moreover, this compound showed improved solubility in comparison to parent compound **3.29**, even though it is the least soluble derivative within this series. Despite being less active, compounds **5.16** – **5.18** exhibit good solubility. Additionally, metabolic stability could be improved up to six-fold (compound **5.10**). However, 7-azaindole analogue **5.17** was only as stable as initial lead compound **3.29**. Adding a nitrogen atom into the phenyl part of the indole moiety seems to be more detrimental for metabolic susceptibility than addition in the five-membered ring (all compared to compound **5.10**).

In order to further increase the solubility of **5.19**, an additional nitrogen atom should be introduced in positions 5 and 6 respectively (Scheme 3.3.13). These positions were chosen upon the pyocyanin results of compounds **5.16** and **5.17**, with **5.16** being more active. The initial planned synthesis based on the approach in accordance with Scheme 3.3.12 failed in the last step. No optimization of the CuAAC was performed, since in the meantime coupling with bromine precursor **3.22** was optimized.

Utilization of DMEDA as a ligand and K_3PO_4 as the base delivered the desired target compounds **5.20** and **5.21**.

Scheme 3.3.13: *Synthesis of indazole derivatives **5.20** and **5.21**.*[a]

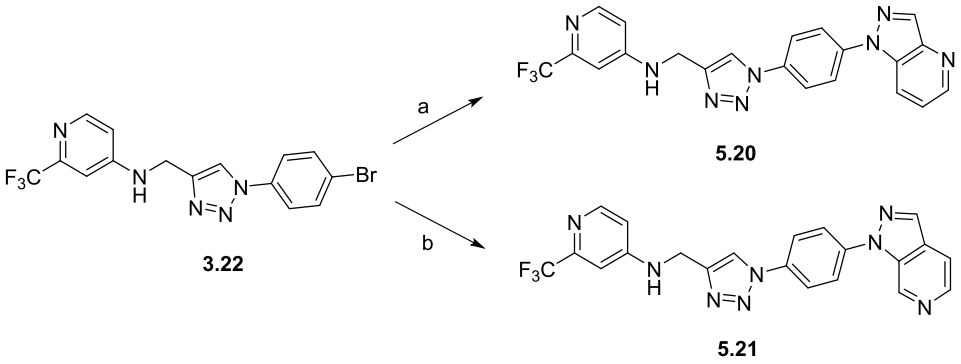

Reagents and conditions: *a: 1H-pyrazolo[4,3-b]pyridine, K_3PO_4, DMEDA, CuI, 25 h, 80 °C, 37%; b: 1H-pyrazolo[3,4-c]pyridine K_3PO_4, DMEDA, CuI, 25 h, 80 °C, 33%.*

Moreover, the addition of fluorine atoms in the *tail* region should be investigated (Scheme 3.3.14). Using the coupling conditions from Scheme 3.3.13 did not yield the desired analogues. Also the initial conditions from Scheme 3.3.12 failed, due to problems in the hydrogenation step or the formation of the corresponding azide. Also, trials with the precatalysts *t*BuXPhos Pd G3 and Me_3(OMe)*t*BuXPhos Pd G3 with NaO*t*Bu in 1,4-dioxane were not successful. However, Pd-175 once again proved to be beneficial, giving access to the desired derivatives in moderate yields ranging from 36 – 60% (Scheme 3.3.15).

Scheme 3.3.14: *Design rationale for fluorinated indazole compounds.*

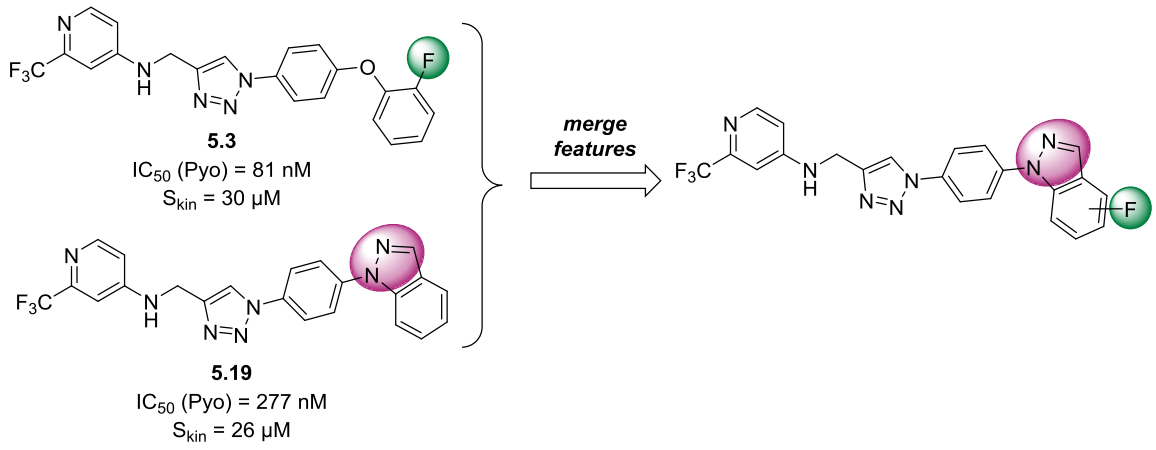

It is worth mentioning, that temperature is crucial for chemoselectivity. When the reaction mixture was not pre-heated or the temperature exceeded 80 °C, mixtures of the corresponding isomeric *N*-arylated and the desired product were observed. Similar findings were reported by Anderson *et al*, yet with slightly different conditions.[130]

Scheme 3.3.15: *Synthesis of fluorinated analogues* ***5.22 – 5.25****.*[a]

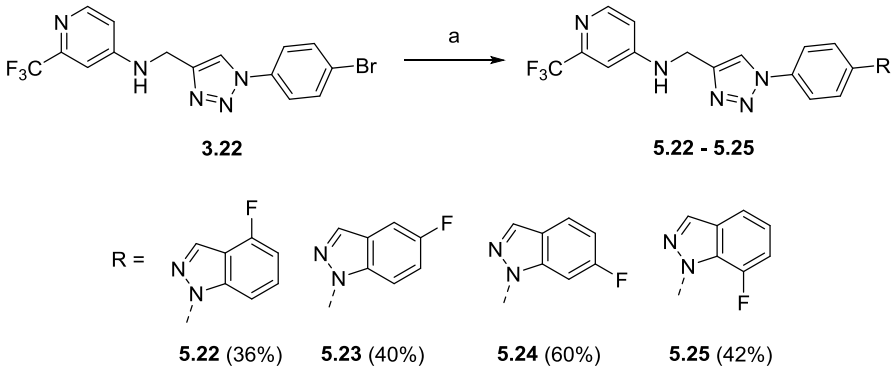

[a]***Reagents and conditions:*** *a: corresponding fluoro-1H-indazole, Cs_2CO_3, Pd-175, 1,4-dioxane, 24 h, 80 °C.*

The synthesized derivatives were then subjected to the established testing cascade. Results are summarized in Table 3.3.7.

Table 3.3.7: *Biological evaluation and DMPK profiling of compounds* ***5.20 – 5.25****.*

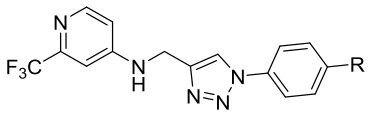

entry	cpd	R	IC_{50} (PqsR)	IC_{50} (pyocyanin)	S_{kin}	$t_{1/2}$ MLM
1	**5.19***	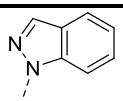	4 nM	277 nM	26 µM	31 min
2	**5.20**	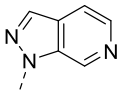	n.d.	609 nM	67.5 µM	31 min
3	**5.21**	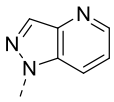	n.d.	695 nM	44.6 µM	55 min
4	**5.22**	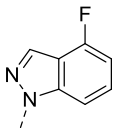	n.d.	1.7 µM	52.6 µM	n.d.
5	**5.23**	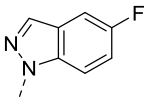	n.d.	1.47 µM	40.0 µM	n.d.
6	**5.24**	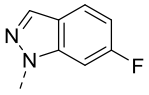	n.d.	637 nM	50.8 µM	n.d.
7	**5.25**	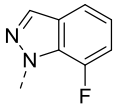	n.d.	405 nM	53.0 µM	n.d.

* = reference; n.d. = not determined

Addition of a third nitrogen in the tail region was not beneficial for activity, but increased solubility and in case of **5.21** also metabolic stability. Installing a fluorine in the indazole motif led to decreased activity, if the substituent was in 6- or 7-position, while 4- and 5-fluorinated analogues were significantly less active. Based on the results obtained beforehand (**5.3** *versus* **5.4**), compound **5.25** was expected to be more active which is reflected in its increased pyocyanin inhibition when compared to **5.24**. Overall, the addition of a fluorine to the indazole motif resulted in less active but more soluble compounds.

3.3.2.4. Aniline Derivatives

The introduction of a fluorine substituent in **4.35** proved to be very beneficial for activity and solubility. Therefore, another optimization step was to include this motif also in aniline derivative **3.30**, which showed good on-target activity, but lacked pronounced pyocyanin efficacy (Scheme 3.3.15).

Scheme 3.3.15: *Design rationale for compound* ***5.26***

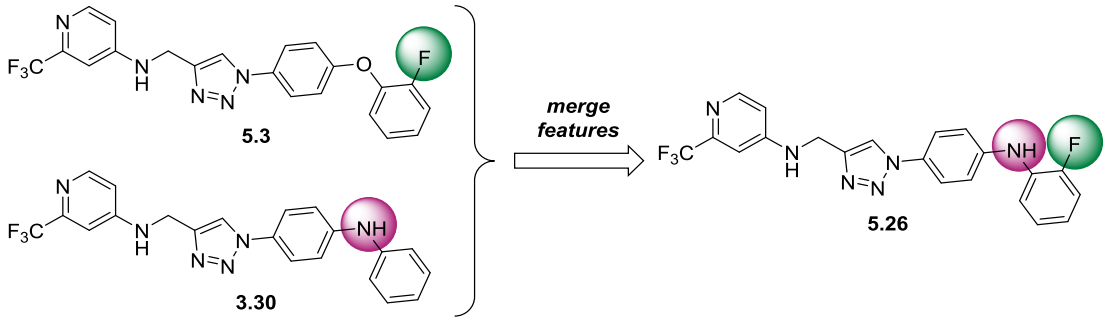

The desired target compound **5.26** was synthesized using bromine-containing precursor **3.22** in a *Buchwald-Hartwig* reaction with 2-fluoroaniline. The coupling was realized with $[Pd(cinnamyl)Cl]_2$, BippyPhos and NaO*t*Bu in 1,4-dioxane (Scheme 3.3.16).

Scheme 3.3.16: *Synthesis of compound* ***5.26*** *and ist biological evaluation, as well as DMPF profiling.*[a]

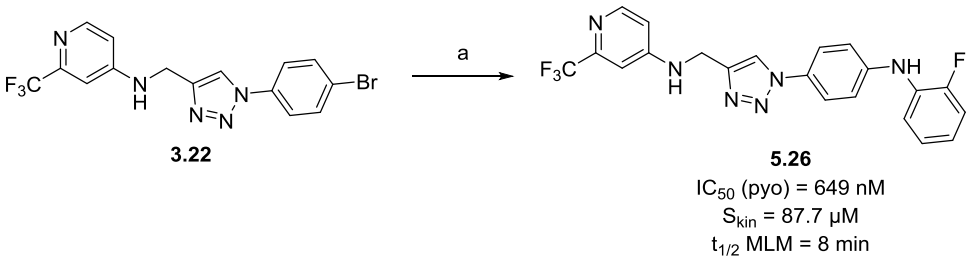

[a]***Reagents and conditions:*** *2-fluoroaniline, $[Pd(cinnamyl)Cl]_2$, BippyPhos, NaOtBu, 1,4-dioxane, 80 °C, 27 h, 44%.*

In order to investigate the impact of the anilines attachment, 3-substituted derivatives **5.27** was synthesized (Scheme 3.3.17). Since the reaction conditions used for analogue **5.26** seemed promising, the desired target compound should be accessible from aryl bromide **5.28**. This precursor can easily

be prepared starting from building block **1.25** and commercially available 3-bromoaniline **5.29**, by using the established diazotation-CuAAC sequence.

Scheme 3.3.17: *Design rationale and retrosynthetic analysis of compound **5.27**.*

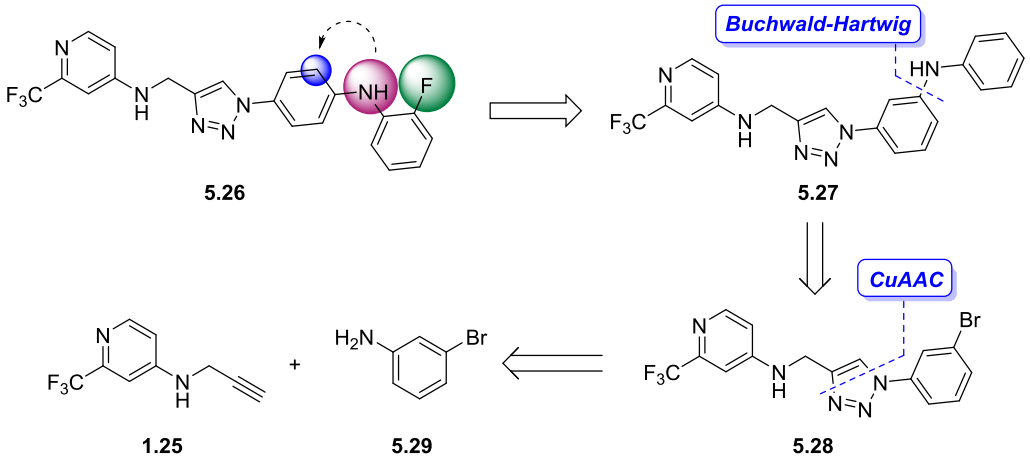

Synthesis of the precursor **5.28** was straightforward and delivered the desired compound in excellent yield of 97%. The subsequent *Buchwald-Hartwig* coupling also worked well with the conditions already established and 3-substituted aniline **5.27** was obtained.

Scheme 3.3.18: *Synthesis of precursor **5.28** and target compounds **5.27** and **5.30 – 5.34**.*[a]

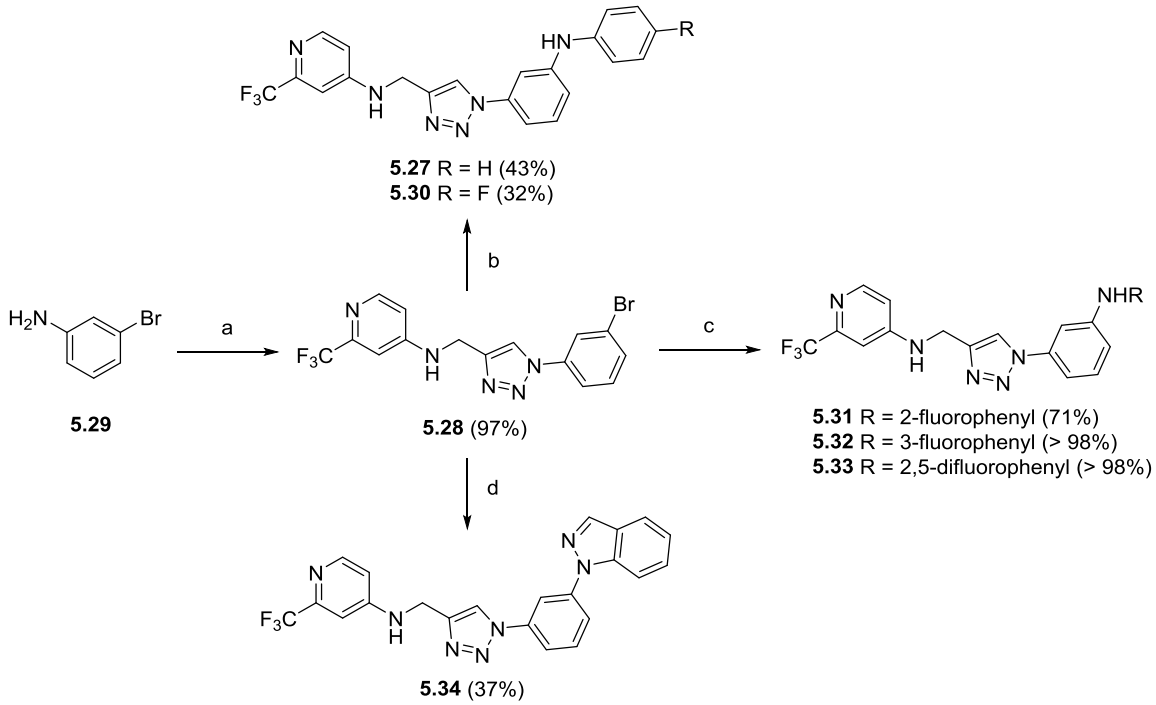

[a]***Reagents and conditions:*** *a: tBuONO, $TMSN_3$, MeCN, rt, 1 h, then $CuSO_4 \cdot 5\ H_2O$, Na ascorbate, DIPEA, N-(prop-2-yn-1-yl)-2-(trifluoromethyl)pyridin-4-amine (**1.25**), rt, 3 h; b: corresponding aniline, $[Pd(cinnamyl)Cl]_2$, BippyPhos, NaOtBu, 1,4-dioxane, 80 °C, 18 h; c: corresponding aniline, Pd-175, Cs_2CO_3, 1,4-dioxane, 90 °C, 24 h. d: 1H-indazole, K_3PO_4, CuI, DMEDA, 1,4-dioxane, 80 °C, 21 h.*

Since the introduction of a fluorine in the *tail* moiety proved to be very beneficial, as already discussed before, aiming for various fluoroaniline motifs seemed promising. With bromine **5.28** in hand, the corresponding fluoroanilines were subjected to *Buchwald-Hartwig* couplings under the previously described conditions. Unfortunately, only the installation of 4-fluoroaniline in compound **5.30** was successful, whereas 2- and 3-fluoroanilines did not undergo the desired C–N coupling. While application of *t*BuXPhos Pd G3 as a precatalyst did not show any conversion, full conversion was obtained when Pd-175 was used. Changing the base to Cs_2CO_3 delivered the desired target compounds **5.31** and **5.32** in good to excellent yields (Scheme 3.3.18). Moreover, a 2,5-difluorinated motif in compound **5.33** could be installed, also in excellent yield. Additionally, indazole derivative **5.34** was synthesized in order to gain further insights into the role of the substitution patterns. Using the already established protocol with CuI, DMEDA and K_3PO_4 in 1,4-dioxane yielded compound **5.34** (Scheme 3.3.18). From a comparable compound class of this project it was obvious, that shifting the phenoxy moiety to the 3-position completely abolished activity. Therefore this modification was not considered.

3.3.2.5. Biological Evaluation and DMPK Profiling

The synthesized compounds were tested for their pyocyanin inhibition, solubility and metabolic stability in mouse liver microsomes. The results are summarized in Table 3.3.8. Introduction of the fluorine resulting in compound **5.26** boosted activity, while also showing good solubility. Nevertheless, metabolic stability is relatively low. When moving the aniline motif to 3-position, highly potent compound **5.27** was obtained (IC_{50} = 156 nM). Despite, being less soluble than the initial project lead **3.29** it was still in a good range (S_{kin} = 44.6 µM). Moreover, this compound showed very good metabolic stability of up to 55 minutes. When a fluorine substituent is introduced in 2-position of the aniline tail (compound **5.31**), potency is further increased, yet at the expense of solubility and metabolic stability. Especially the latter dropped drastically down to 9 minutes. When the fluorine substituent is moved to 3-position in compound **5.32**, activity decreases in comparison to **5.31**, whereas solubility and metabolic stability are slightly increased. Yet, **5.32** still proved to be a highly potent compound. Also installation of the halogen in 4-position (compound **5.30**) resulted in decreased activitiy, while solubility was in the range of **5.27**. In case of monofluorinated derivatives compound **5.30** proved to be the most stable one. The 2,5-di-fluorinated analogue **5.33** exhibited very good potency with also good DMPK properties. As for the activity, the fluorination pattern gave the same results as in the oxygen linked derivatives. A fluorination in 2-position gave the best result, followed by 3-position and 4-position being the least favorable. Even though, compounds **5.31** and **5.32** demonstrate powerful optimized compounds, a possible drawback of these aniline derivatives could be the release of toxic metabolites upon metabolic cleavage. By now, no such studies were performed.

Table 3.3.8: *Structure, biological evaluation and DMPK profiling of compounds* ***5.26, 5.27*** *and* ***5.30 – 5.34****.*

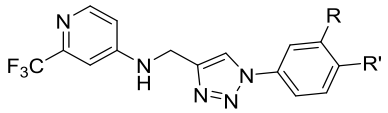

entry	cpd	R	R'	IC_{50} (PqsR) [nM]	IC_{50} (pyocyanin) [nM]	S_{kin} [µM]	$t_{1/2}$ MLM [min]
1	**3.29***	H	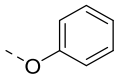	11	199	7.7	10
2	**3.30***	H	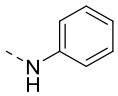	31	1058	n.d.	n.d.
3	**5.26**	H	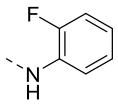	n.d.	649	87.7	8
4	**5.27**	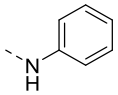	H	n.d.	156	44.6	55
5	**5.30**	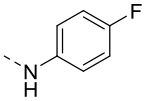	H	n.d.	176	40	19
6	**5.31**	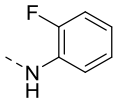	H	n.d.	68	17.4	9
7	**5.32**	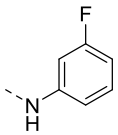	H	n.d.	99	21.9	16
8	**5.33**	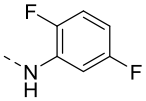	H	n.d.	89	21	14
9	**5.34**	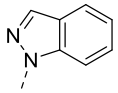	H	n.d.	277	14.3	7

n.d. = not determined

3.3.3. *Head* Modification II

3.3.3.1. Chlorine-containing Headgroup

With the chlorine-containing building block **4.17** in hand, it was obvious to further investigate the impact of this additional substituent with other *tail* modifications. Therefore, derivatives which showed good overall potency, good potency in *E. coli* but not in *P. aeruginosa*, and those with favorable DMPK properties were combined with the chlorine motif in the head. With the corresponding aniline derivatives in hand, the established diazotation/CuAAC protocol was used and yielded compounds **5.35** – **5.41** (Scheme 3.3.19).

Scheme 3.3.19: *Synthesis of compounds* ***5.35 – 5.41****.*[a]

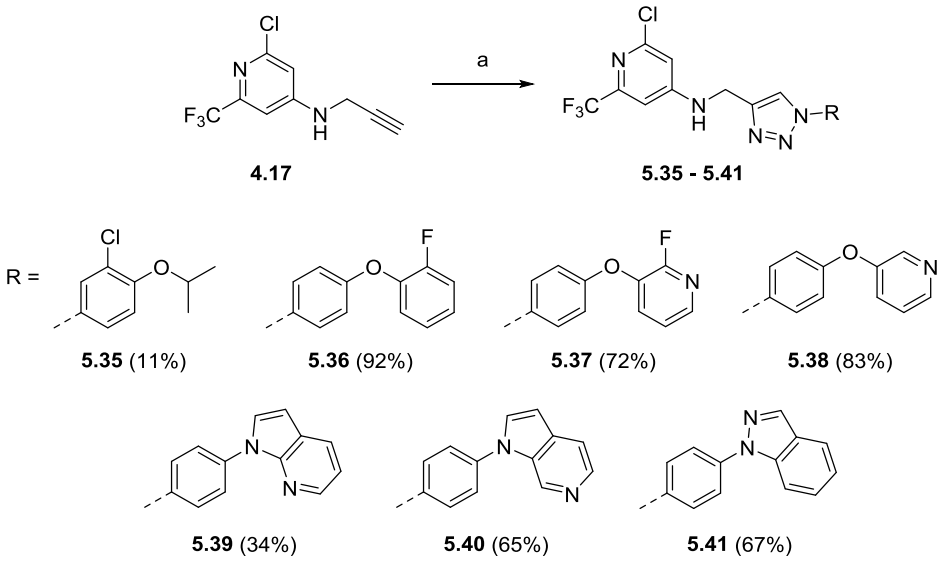

[a]***Reagents and conditions:*** *corresponding azides, $CuSO_4 \cdot 5\ H_2O$, Na ascorbate, DIPEA, rt.*

Since the corresponding anilines were not available for aza-indazole and fluoro-indazole, as well as an aniline-derivative, these moieties should be introduced *via Buchwald-Hartwig* chemistry. Therefore, bromine-containing precursors **5.42** and **5.43** were synthesized from **4.17** (Scheme 3.3.20). For the indazole analogues, *t*BuXPhos Pd G3 with NaO*t*Bu in 1,4-dioxane proved to be feasible for the coupling of both, the fluorine- and the aza-derivative **5.44** and **5.45**. It is worth mentioning, that an impurity of N2-arylated isomer (not shown, 2% by ^{1}H-NMR) were generated under these conditions. This was also proven by a cocrystal structure of **5.44** and its impurity in complex with PqsR (see Figure 3.3.9 and Figure 3.3.10). For **5.46**, first attempts with Pd-175 and Cs_2CO_3 only delivered bis-coupled products or no reaction, when the temperature was decreased. Also, working under higher dilution did not yield the desired compounds in satisfying amounts. With $[Pd(cinnamyl)Cl]_2$ and BippyPhos, only dechlorinated starting material was observed. The same conditions where applied for 2,5-di-fluoro aniline, leading only to bisarylated product. Also in this case the change of the reaction temperature

did not have the desired impact. The synthesis was accomplished using Pd-175 and Cs_2CO_3 under the exact same conditions. Even though 20% of the bisarylated product where isolated, the desired target compound **5.46** was the main product and could be isolated with a yield of 54%.

Scheme 3.3.20: *Synthesis of precursors **5.42** and **5.43** with subsequent transformation to compounds **5.44 – 5.46.***

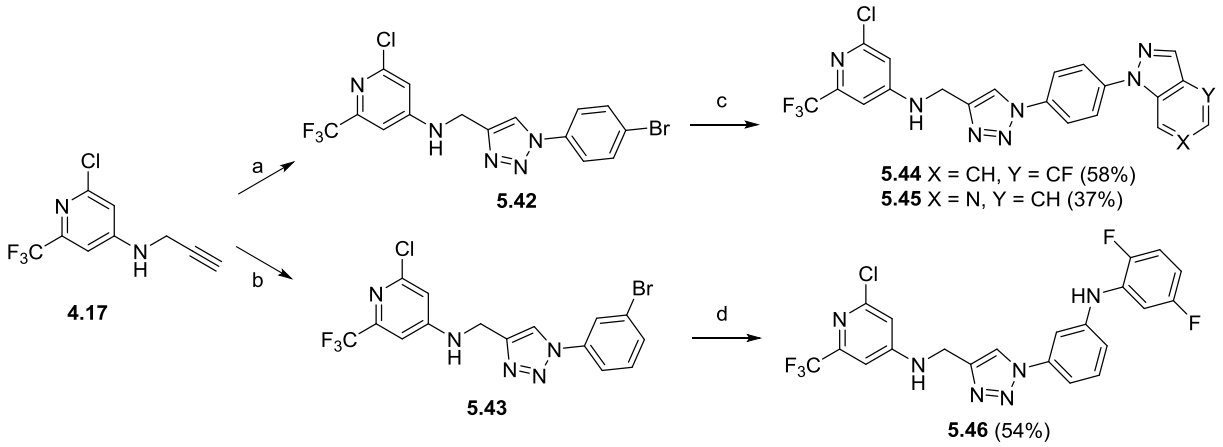

[a]Reagents and conditions: *a: 4-bromoaniline, tBuONO, $TMSN_3$, MeCN, rt, 1 h, then **4.17**, $CuSO_4 \cdot 5\ H_2O$, Na ascorbate, DIPEA, rt, 3 h, 97%; b: 3-bromoaniline, tBuONO, $TMSN_3$, MeCN, rt, 1 h, then **4.17**, $CuSO_4 \cdot 5\ H_2O$, Na ascorbate, DIPEA, rt, 3 h, 94%; c: 4-F-1H-indazole or 1H-pyrazolo[4,3-*b*]pyridine, NaOtBu, tBuXPhos Pd G3, toluene, 100 °C, 18 h; d: 2,5-difluoroaniline, Cs_2CO_3, Pd-175, 1,4-dioxane, 80 °C, 3 h, 54%.*

The chlorine analogues were then subjected to the testing cascade and the results are summarized in Table 3.3.9. The values in brackets are the references lacking the chloro headgroup. Once again, a non-additive SAR is observed. While for some compounds the introduction of chlorine in the head did not affect activity at all (compounds **5.36**, **5.44** and **5.37**), others showed decreased pyocyanin inhibition (**5.41** and **5.46**). Nevertheless, in some cases this modification even significantly boosted potency (**5.35** and **5.45**). Especially compound **5.45** displayed an almost four-fold increased ability to inhibit pyocyanin production. This finding might be further supported by the fact that enhanced lipophilicity might lead to a better effect in *P. aeruginosa*.[131,132] As expected, solubility was decreased upon introduction of a chlorine atom, except for compound **5.46**, showing slightly improved solubility. All of the above mentioned compounds were then subjected to the amination conditions with Pd-175 and Cs_2CO_3 in 1,4-dioxane. Unfortunately, for none of these, formation of the desired product was observed.

Table 3.3.9: *Structure, biological evaluation and DMPK profiling of* ***5.36 – 5.41*** *and* ***5.44 – 5.46****.*

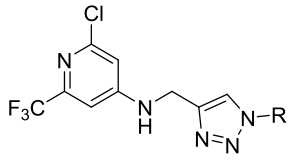

entry	cpd	R	IC_{50} (pyocyanin)*	S_{kin}*	$t_{1/2}$ MLM*
1	**5.35**	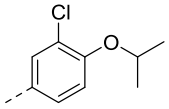	107 (237) nM	15.8 (26.9) µM	30 (2) min
2	**5.36**	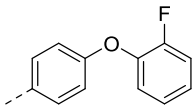	85 (81) nM	22 (29.6) µM	n.d. (9) min
3	**5.37**	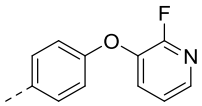	134 (142) nM	8.5 (25.9) µM	73 (36) min
4	**5.38**	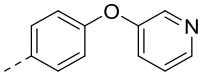	184 (679) nM	22.7 (41) µM	59 (<1) min
5	**5.39**	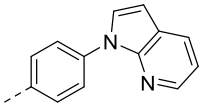	725 (1899) nM	20.9 (32.4) µM	n.d. (10) min
6	**5.40**	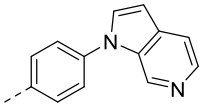	839 (993) nM	21.1 (43.9) µM	n.d. (19) min
7	**5.41**	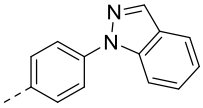	447 (277) nM	8 µM (26 µM)	40 (31) min
8	**5.44**	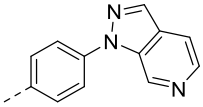	25% (22%)**	21.1 (67.5) µM	32 (31) min
9	**5.45**	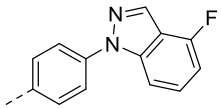	462 nM (1.7 µM)	20.7 (52.6) µM	93 (n.d.) min
10	**5.46**	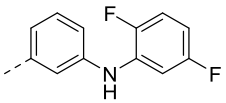	162 (89) nM	25.5 (21) µM	24 (14) min

* values in brackets refer to parent compounds without chlorine in the headgroup; n.d. = not determined; ** = %effect at 0.2 µM

As mentioned before, for compounds **5.45** and its N2-arylated isomer ***iso*-5.45** Dr. Stefan Schmelz obtained cocrystal structures in complex with $PqsR^{91-319}$. The structures are depicted in Figures 3.3.9 (**5.45**) and 3.3.10 (***iso*-5.45**). It is woth mentioning, that the results presented here are preliminary. The two compounds show common and different interactions with the protein. In contrast to the PqsR inverse agonists lacking a chlorine atom in the *head*, compound **5.45** does not interact with a crystal water molecule *via* its pyridine nitrogen atom (Figure 3.3.9). Instead, a π-H interaction with Leu208 and an H-O interaction with the backbone oxygen atom of Leu207 is observed. Moreover, the trifluoromethyl group interacts with backbone Pro238. Main interactions of the *tail* moiety involve an F-H interaction with the sidechain of His184, a π-H interaction with Leu189 and N-H interaction with Val170.

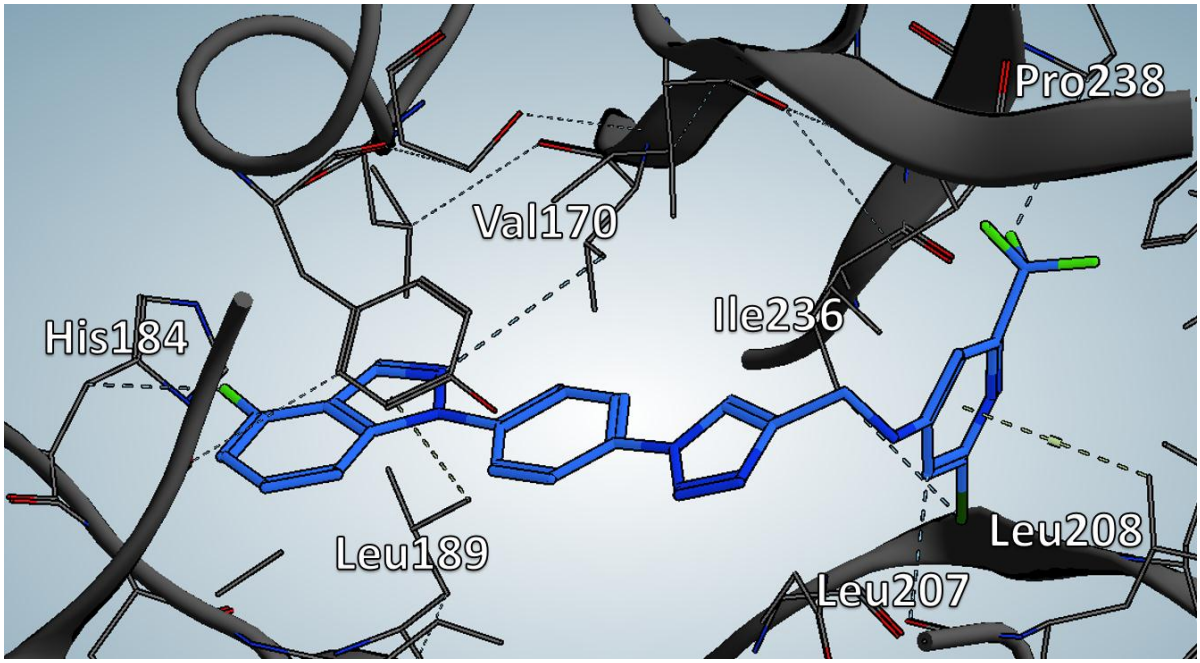

Figure 3.3.9: *Cocrystal structure of compound **5.45** in complex with $PqsR^{91-319}$ at a resolution of 2.8 Å. Main interaction residues are labeled. Color code: blue: C, dark blue: N, green: F, dark green: Cl.*

Compound ***iso*-5.45** also shows the aforementioned interactions with Leu207 and Leu208. Additionally, an NH-O interaction with the bacbone oxygen atom of Leu207 is observed. In contrast to **5.45**, the trifluoromethyl substituent of ***iso*-5.45** interacts with Thr265 and Ala168. Also, the *tail* region does not show a π-H interaction with the already mentioned Leu189 rather a π-H interaction with Tyr258. Similar to **5.45** the nitrogen atom of the indazole moiety interacts with Val170. The interaction of the fluorine atom with His184 is not observed.

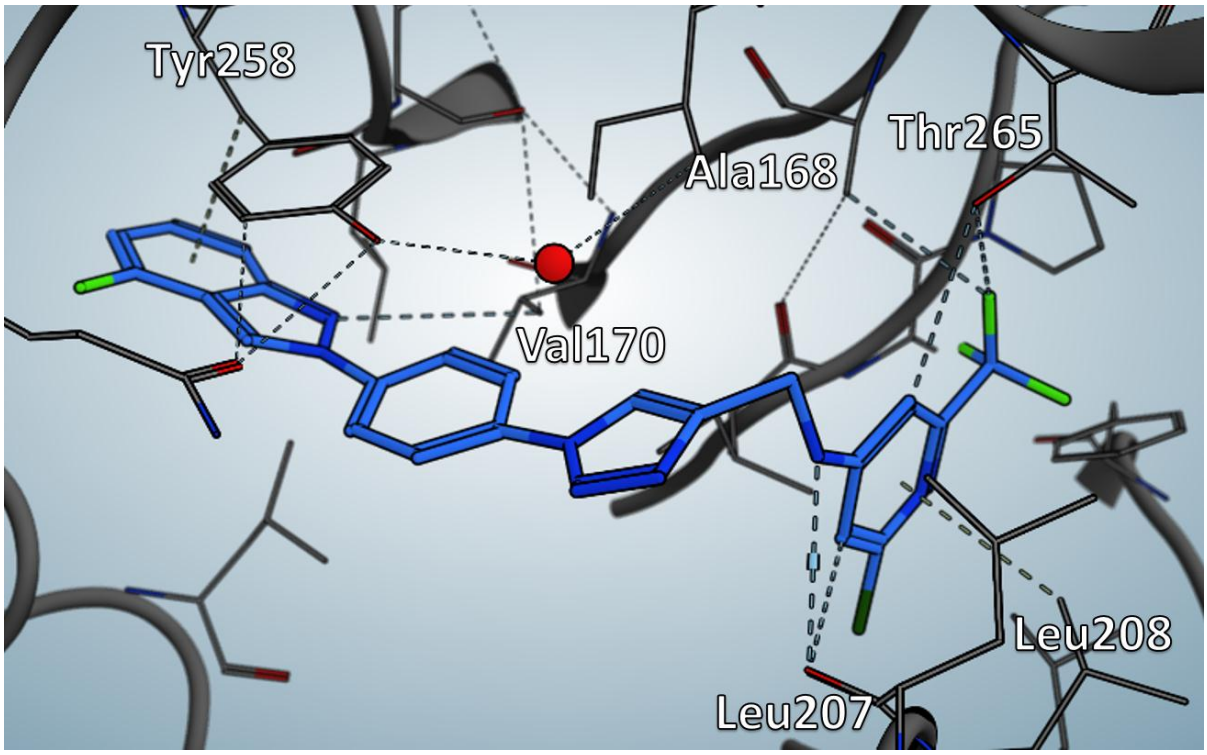

Figure 3.3.10: *Cocrystal structure of compound* ***iso-5.45*** *in complex with PqsR$^{91-319}$ at a resolution of 2.8 Å. Main interaction residues are labeled. Color code: blue: C, dark blue: N, green: F, dark green: Cl.*

3.3.3.2. Pyrimidine Modification

Another modification, which was planned in order to increase solubility, was the introduction of a second nitrogen to the *head*. It is known that the amino-pyrimidine moiety in **5A** is accepted and even boosts activity on the target (Figure 3.3.11). Pyocyanin inhibition is however decreased for **5A**.

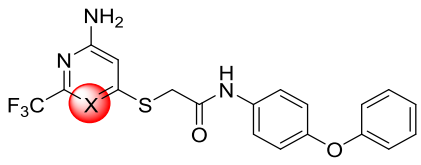

1B, R = CH
IC_{50} (*E. coli*) = 19 nM
IC_{50} (pyocyanin) = 280 nM
12.5 µM < S_{kin} < 25 µM

5A, R = N
IC_{50} (*E. coli*) = 7 nM
IC_{50} (pyocyanin) = 380 nM
25 µM < S_{kin} < 50 µM

Figure 3.3.11: *Structure and biological evaluation of compounds* ***1B*** *and* ***5A****.*

For the synthesis of **5.49**, commercially available 4,6-dichloro-2-(trifluoromethyl)pyrimidine **5.47** was treated with propargylamine and Cs_2CO_3 in DMF, affording the desired alkyne precursor **5.48** in 58% yield (Scheme 3.3.21). Only small amounts of di-amination product were observed (<5%). Subsequent CuAAC with 1-azido-4-phenoxybenzene gave the desired target compound **5.49**. The chlorine atom was removed to give pyrimidine analogue **5.50** in excellent yields after hydrogenation.

Scheme 3.3.21: *Synthesis of compounds **5.49** and **5.50**.*

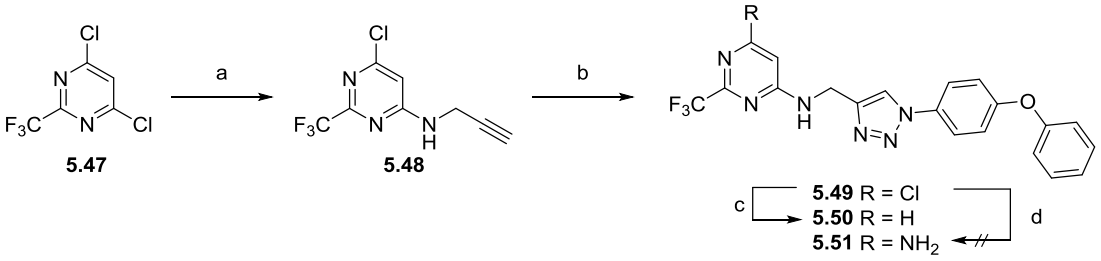

[a]Reagents and conditions: *a: propargylamine, Cs_2CO_3, DMF, microwave, 75 °C, 1 h, 58%; b: 1-azido-4-phenoxybenzene, $CuSO_4 \cdot 5\ H_2O$, Na ascorbate, DIPEA, tBuOH/H_2O, rt, 24 h, 81%; c: Pd black, H_2, MeOH, rt, 2 d, 96%; d: various conditions, see Table 3.3.10.*

Attempts to convert the chlorine into the corresponding amine **5.51** were not successful. The tested conditions are summarized in Table 3.3.10.

Table 3.3.10: *Attempted amination conditions of **5.49**. 5.0 eq. of nucleophile, 2.2 eq. of base and 10 mol% of catalyst/20 mol% of ligand were used. Molarity was 0.1 M in the given solvent.*

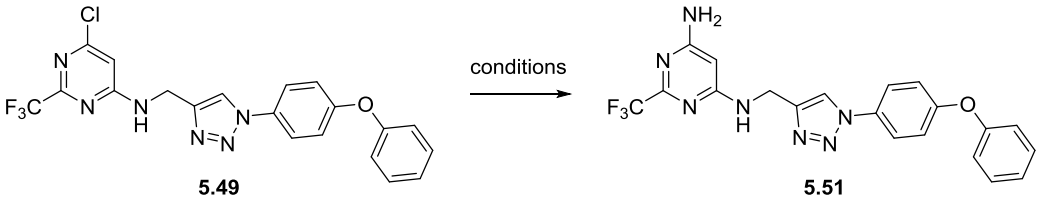

entry	nucleophile	catalyst/ligand	base	solvent	T	t
1	$BocNH_2$	Pd-175	Cs_2CO_3	1,4-dioxane	80 °C	21 h
2	NH_4OH	Cu_2O/1,10-phenanthroline	-	DMSO	100 °C	18 h
3	NH_4OH	CuI/DMEDA	K_3PO_4	1,4-dioxane	80 °C	21 h
4	NH_3 (7 M in MeOH)	Cu_2O/1,10-phenanthroline	-	1,4-dioxane	100 °C	21 h

The two derivatives **5.49** and **5.50** were then tested in the *E. coli*-based reporter gene assay. While **5.49** showed an IC_{50} of 174 nM, activity was abolished for **5.50** (>> 1 µM) (Figure 3.3.12). Therefore, none of these compounds were further tested for their ability to inhibit pyocyanin production. Nevertheless, the chloro-pyrimidine analogue was evaluated regarding solubility and metabolic stability and showing an increase in both parameters.

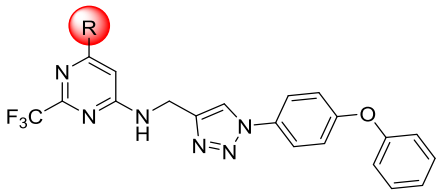

5.49 R = Cl
IC_{50} (*E. coli*) = 174 nM
S_{Kin} = 29.4 µM
$t_{1/2}$ MLM = 35 min

5.50 R = H
IC_{50} (*E. coli*) >> 1 µM
S_{Kin} = n.d.
$t_{1/2}$ MLM = n.d.

Figure 3.3.12: *Biological evaluation and DMPK profiling of compounds **5.49** and **5.50**.*

The obtained results did not render compound **5.51** a highly prioritized compound, due to the relatively low on-target activity in comparison to advanced lead compounds.

3.3.3.3. Heteropentacycle-containing Headgroup

The established chlorine motif was further used in other project-related compounds and was exploited as a growth vector by Dr. Ahmed Saad Abdelsamie. The introduction of a pyrazole, imidazole and a 1,2,4-triazole proved to be very beneficial in terms of activity and DMPK properties. The properties of these compounds are summarized in Table 3.3.11.

Table 3.3.11: *Structure, activity and DMPK profiling of compounds **5B – 5F**.*

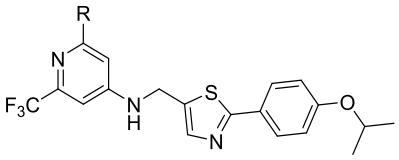

entry	cpd	R	IC_{50} (pyocyanin)	S_{Kin}	$t_{1/2}$ MLM
1	**5B**	H	118 nM	17.8 µM	29 min
2	**5C**	Cl	82 nM	34.9 µM	15 min
3	**5D**		52 nM	23.3 µM	56 min
4	**5E**		47 nM	24.3 µM	52 min
5	**5F**		75 nM	51.8 µM	79 min

Compared to parent compound **5B**, all derivatives showed improved activity. Especially the imidazolyl analogue **5E** exhibited excellent pyocyanin inhibition with an IC_{50} of 47 nM, followed by the pyrazole

5D. The triazole **5F**, although not being the most potent congener of this series, was superior in terms of solubility and metabolic stability.

Based on these results, corresponding derivatives with the triazole linkage were synthesized (Scheme 3.3.22). The 4-phenoxy derivatives were the first to be prepared, since large amounts of precursor **4.2** were available. Compound **5.52**, initially established by *PharmBioTec*, was resynthesized with different conditions. When the corresponding pyrazole-boronic acid pinacol ester was combined with $Pd(PPh_3)_4$ and Na_2CO_3 in a water/dioxane mixture compound **5.52** was obtained in low yields. Since larger amounts of **5.52** were needed for PK experiments, the route was first optimized. For the *Suzuki-Miyaura* reaction, Pd_2dba_3, cataCXium A in toluene, with Cs_2CO_3 as a base, proved to be beneficial, delivering the desired target compound **5.52** in a high yield of 85%. These conditions were also utilized for the coupling with imidazole and 1*H*-1,2,4-triazole. While the reaction worked with imidazole leading to compound **5.53**, for the desired triazole analogue, no conversion was observed. Simple microwave-aided S_NAr with Cs_2CO_3 in 1,4-dioxane then delivered compound **5.54**. Moreover, fluorine-containing compound **5.36** was converted into the corresponding pyrazole analogue using the established conditions (4-(4,4,5,5-tetramethyl-1,3,2-dioxaborolan-2-yl)-1*H*-pyrazole, Pd_2dba_3, cataCXium A and Cs_2CO_3 in toluene).

Scheme 3.3.22: *Synthesis of* ***5.52 – 5.55****.*[a]

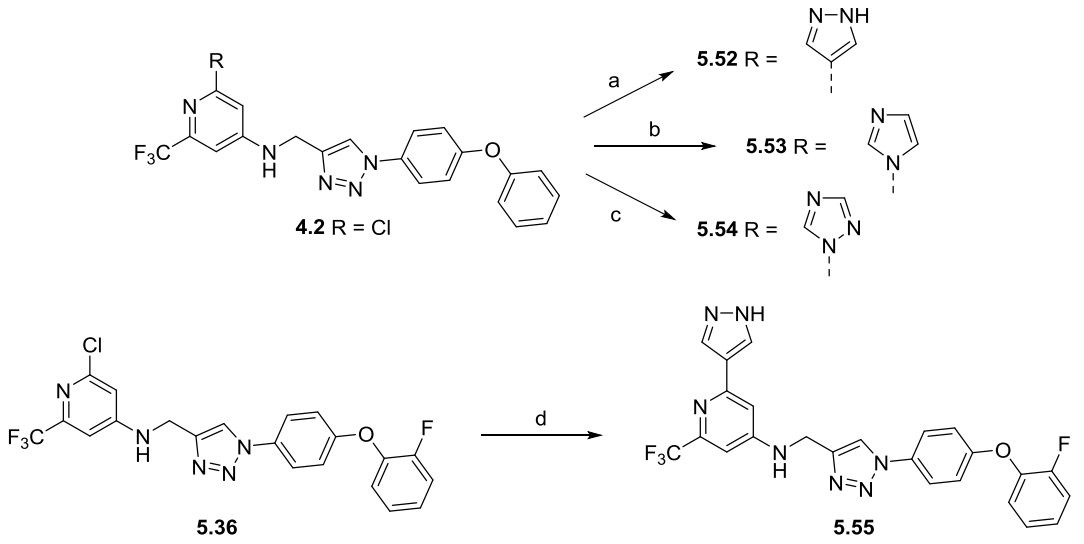

[a]***Reagents and conditions:*** *a: 4-(4,4,5,5-tetramethyl-1,3,2-dioxaborolan-2-yl)-1H-pyrazole, Pd_2dba_3, cataCXium A, Cs_2CO_3, toluene, 2 h, 100 °C, microwave, 84%; b: imidazole, Pd_2dba_3, cataCXium A, Cs_2CO_3, toluene, 2 h, 100 °C, microwave, 23%; c: 1H-1,2,4-triazole, Cs_2CO_3, 1,4-dioxane, 2 h, 100 °C, microwave, 35%; d: 4-(4,4,5,5-tetramethyl-1,3,2-dioxaborolan-2-yl)-1H-pyrazole, Pd_2dba_3, cataCXium A, Cs_2CO_3, toluene, 2 h, 100 °C, microwave, 63%.*

In order to further investigate the impact of the new modifications in the corresponding isopropoxy derivatives, precursor **5.56** was prepared from building block **4.17** *via* CuAAC with 1-azido-4-isopropoxybenzene (Scheme 3.3.23). The latter was prepared *in situ* by diazotation of the

corresponding aniline. Subsequent *Suzuki-Miyaura* reaction gave the corresponding pyrazole analogue **5.57** in an excellent yield of 92%. The same conditions were employed in order to convert the chlorine into an imidazole moiety but failed to construct **5.58**. Aforementioned S_NAr conditions with imidazole and Cs_2CO_3 in 1,4-dioxane did not yield the desired target compound. Since imidazolyl and pyrazolyl derivatives **5D** and **5E** from the thiazole-class did not differ much in their properties, it was decided to not further optimize the reaction conditions. For the triazole congener, the S_NAr reaction worked very well and delivered compound **5.59**.

Scheme 3.3.23: *Synthesis of derivatives **5.56 – 5.58**.*[a]

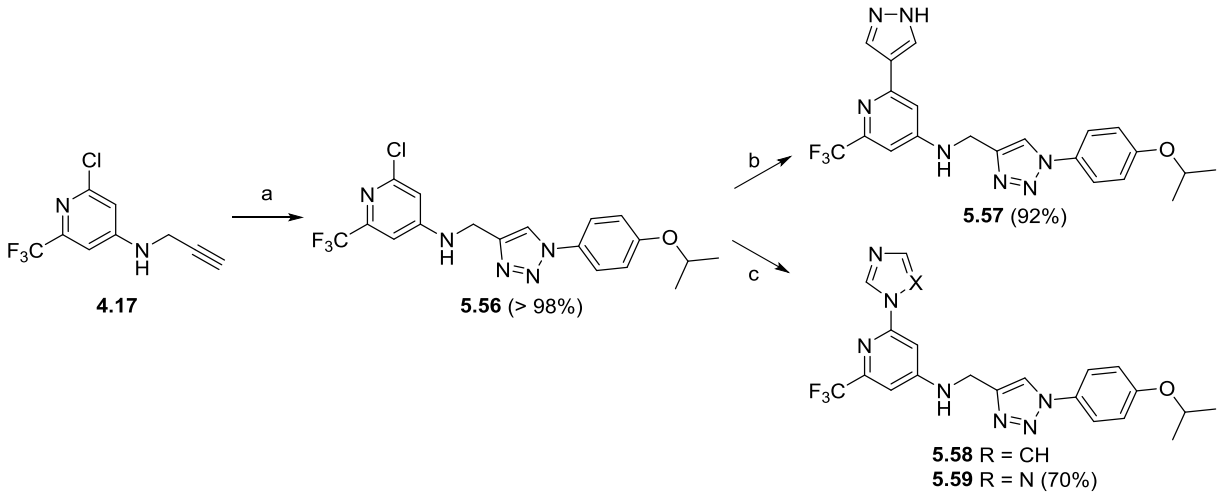

[a]***Reagents and conditions:*** *a: tBuONO, $TMSN_3$, 4-isopropoxyaniline, MeCN, 0 °C, 1 h, then **1.21**, $CuSO_4 \cdot 5\ H_2O$, Na ascorbate, DIPEA, rt, 16 h, > 98%; b: 4-(4,4,5,5-tetramethyl-1,3,2-dioxaborolan-2-yl)-1H-pyrazole, Pd_2dba_3, CataCXium A, Cs_2CO_3, toluene, 2 h, 100 °C, microwave; c: 1H-1,2,4-triazole, Cs_2CO_3, 1,4-dioxane, microwave.*

The new derivatives, as well as the precursor **5.56** were then subjected to the testing cascade of pyocyanin inhibition, solubility and metabolic stability. The results are summarized in Table 3.3.12. Here again, a clearly non-additive and highly non-linear SAR was observed. While for the phenoxy analogue **4.2**, the additional chlorine in the *head* had no impact on activity, the corresponding isopropoxy derivative **5.56** displayed a drastical increase in its abilitiy to inhibit pyocyanin production (IC_{50} = 111 nM), making it four times more potent than its parent compound **3.25** (IC_{50} = 447 nM). Also, the metabolic stability was improved almost seven-fold. However, solubility dropped to 23.4 µM. With its pyrazole moiety in the *head*, phenoxy compound **5.52** showed improved ability to inhibit pyocyanin production, whereas the isopropoxy congener **5.57** had decreased activity (IC_{50} = 246 nM) in comparison to the chloro analogue **5.56**. In both cases metabolic stability was increased compared to the parent compounds **3.29** and **3.25**. For the phenoxy derivative **5.52**, an increase in solubility (S_{kin} = 48.6 µM) was observed, whereas **5.57** proved to be less soluble (S_{kin} = 36.9 µM). Combining the pyrazole moiety with the 2-fluoro-substituted phenoxy tail in compound **5.55** lead to a decreased activity (IC_{50} = 134 nM) compared to the parent compound **5.36** (IC_{50} = 85 nM), being equipotent with

5.52. Also, solubility is decreased more than two-fold when comparing **5.55** (S_{kin} = 21.0 µM) to **5.52** lacking the fluorine. Beneficially, metabolic stability is increased in **5.55** up to 33 minutes.

Table 3.3.12: *Structure, activity and DMPK profiling of compounds **5.52** – **5.59**.*

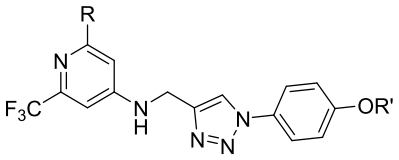

entry	cpd	R	R'	IC_{50} (pyocyanin)	S_{Kin}	$t_{1/2}$ MLM
1	**3.29***	H	Ph	199 nM	7.7	10
2	**4.2***	Cl	Ph	196 nM	n.d.	n.d.
3	**5.52**		Ph	136 nM	48.6 µM	26 min
4	**5.53**		Ph	293 nM	26.9 µM	14 min
5	**5.54**		Ph	182 nM	26.3 µM	76 min
6	**5.55**		2-F-Ph	134 nM	21.0 µM	33 min
7	**3.25***	H	*i*Pr	447 nM	101.2 µM	4 min
8	**5.56**	Cl	*i*Pr	111 nM	23.4 µM	27 min
9	**5.57**		*i*Pr	246 nM	36.9 µM	20 min
10	**5.59**		*i*Pr	309 nM	23.7 µM	71 min

* = reference, n.d. = not determined

While in the thiazole-class, the analogue **5F**, bearing the triazole in the head, displayed the best solubility and metabolic stability, in this set of compounds it proved to be only beneficial in terms of stability. The solubility was decreased in congeners **5.54** and **5.59**. The imidazole modification, being the most potent one in analogue **5E**, did not give the anticipated benefit for compound **5.53** but rather

decreased activity (IC_{50} = 293 nM). Reasons for these non-linearities in SAR and structure-property relationship (SPR) might be the high flexibility of PqsR in the region where the *tail* part of the molecules bind to PqsR. Furthermore, non-linearity relies on the concept that the substituents do not affect each other. In this case, the chlorine atom and the alkoxy or phenoxy moiety are next to each other.

Scheme 3.3.24: *Synthesis attempts to introduce heterocyclic moieties in the head group.*[a]

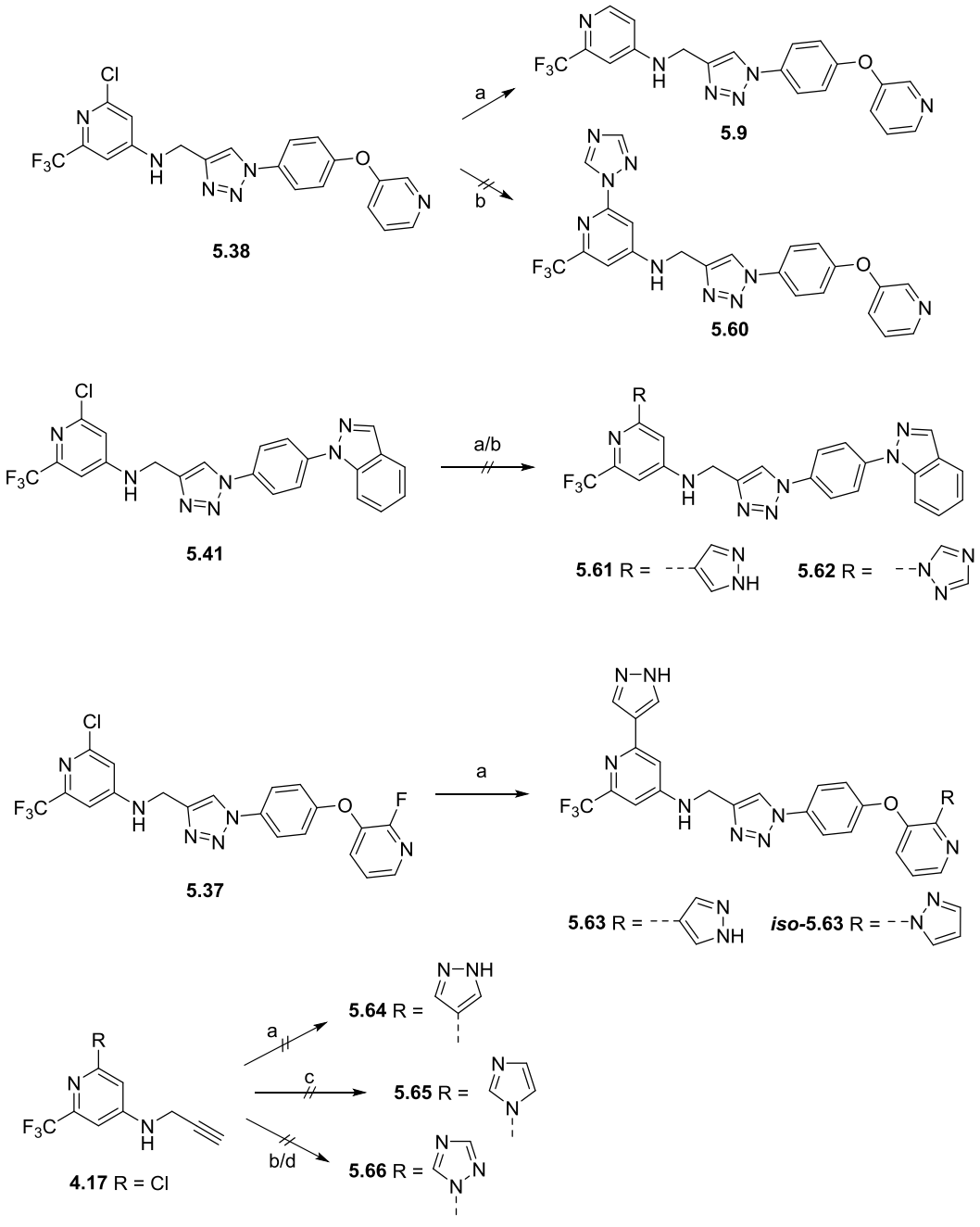

[a]***Reagents and conditions:*** *a: 4-(4,4,5,5-tetramethyl-1,3,2-dioxaborolan-2-yl)-1H-pyrazole, Pd_2dba_3, CataCXium A, Cs_2CO_3, toluene, 2 h, 100 °C, microwave; b: 1H-1,2,4-triazole, Cs_2CO_3, 1,4-dioxane, microwave; c: imidazole Cs_2CO_3, 1,4-dioxane, microwave; d: 1H-1,2,4-triazole, Pd_2dba_3, CataCXium A, Cs_2CO_3, toluene, 2 h, 100 °C, microwave.*

Since the introduction of the pyrazole moiety proved to be beneficial in terms of all of the above mentioned properties, attempts to incorporate this motif into selected derivatives were conducted. Treatment of **5.38** with pyrazole-boronic acid pinacol ester, Pd_2dba_3, cataCXium A and Cs_2CO_3 in toluene only resulted in dehalogenation of the starting material. Attempts to incorporate the triazole moiety under S_NAr conditions did not show any conversion to desired target compound **5.60**. For the indazole derivative **5.41**, neither S_NAr reaction, nor *Suzuki-Miyaura* coupling led to the desired target compounds **5.61** or **5.62**. For the latter, only dehalogenated starting material was observed again (Scheme 3.3.24). Surprisingly, treatment of **5.37** under these conditions led to bis-coupled product **5.63** or ***iso*-5.63** and other non-identified byproducts, resulting either from a rare *Suzuki-Miyaura* reaction with fluorine, or more likely S_NAr reaction of the pyrazole-boronic acid pincaol ester followed by ester cleavage. Nevertheless, further optimization of reaction conditions was not attempted. Attempts to introduce heteropentacycles starting from alkyne building block **4.17** under the aforementioned conditions to the corresponding precursors **5.64** – **5.66** were also not successful (Scheme 3.3.24).

As already mentioned in the beginning of this section, larger amounts of **5.52** were needed for PK experiments, which were conducted at Saretius. The results are summarized below in Table 3.3.13 and **5.52** proved to be less favorable in terms of these parameter.

Table 3.3.13: *PK data for **5.52** in plasma, lung and BALF.*

	plasma	**lung**	**BALF**
$t_{1/2}$ [h]	0.48 ± 0.0	0.74 ± 0.0	0.50
T_{max} [h]	0.50 ± 0.0	1.00 ± 0.9	0.50 ± 0.0
C_{max} [ng/ml]	15.61 ± 2.4	173.05 ± 161.4	265.70 ± 135.9
$AUC_{0\text{-}t}$ [ng/ml·h]	9.99 ± 2.9	119.16 ± 80.4	206.07 ± 12.6
MRT [h]	0.84 ± 0.0	1.22 ± 0.2	0.83
V_z/F_{obs} [l/kg]	1682.34 ± 599.9	-	-
Cl/F_{obs} [ml/min/kg]	39900.48 ± 11294.0	-	-

3.3.4. *Core* Modification

By now, only modifications in the *tail* region and the *head* were investigated. In order to gain further structural insights, the triazole linker should be modified and different secondary substituents should be introduced (Figure 3.3.13).

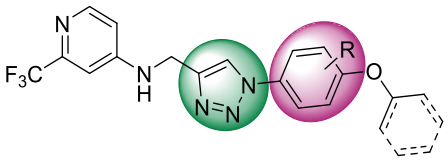

Figure 3.3.13: *Possible variations in the core motif.*

When thinking of a triazole replacement without high synthetic efforts, the isoxazole can easily be introduced *via* click reaction with nitriloxide **5.68**, which can be generated *in situ* from **5.69**. This can be obtained from oxime **5.70**, which is accessible from commercially available aldehyde **5.71**.

Scheme 3.3.25: *Retrosynthetic analysis of* ***5.67****.*

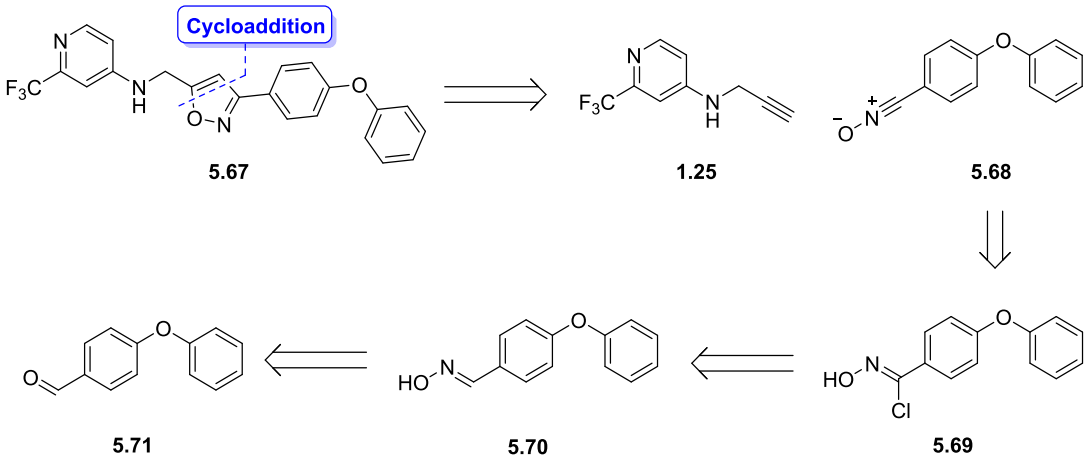

With the alkyne building block already in hand, only the nitriloxide precursor **5.68** had to be synthesized (Scheme 3.3.26). Starting from 4-phenoxybenzaldehyde **5.71**, treatment with hydroxylamine hydrochloride and Na_2CO_3 in a MeOH/H_2O mixture gave oxime **5.70**, which was then submitted to chlorination with NCS in DCM.

Scheme 3.3.26: *Synthesis of* ***5.67*** *and its biological evaluation, as well as DMPK profiling.*[a]

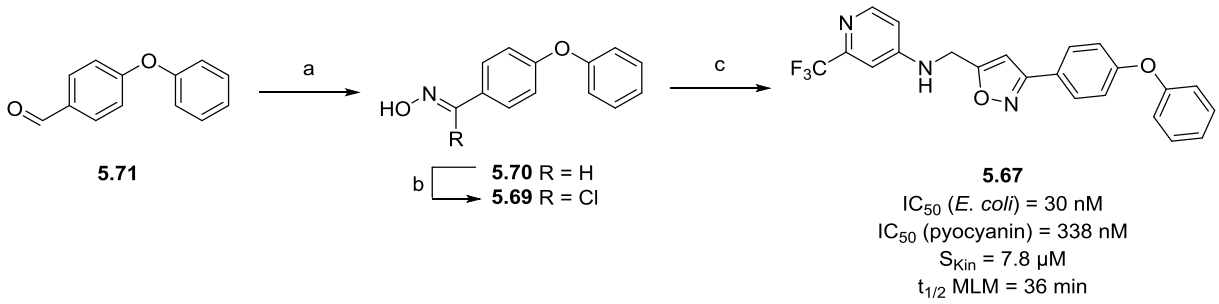

[a]***Reagents and conditions:*** *a: $NH_2OH{\cdot}HCl$, Na_2CO_3, MeOH/H_2O (1:3), rt, 3 h, 59%; b: NCS, DCM, 6 h; c: $CuSO_4{\cdot}5\ H_2O$, Na ascorbate, Na_2CO_3, tBuOH/H_2O (1:1), rt, 16 h, 2% (over 2 steps).*

Subsequent nitriloxide formation from **5.69** with NEt_3 followed by cycloaddition with $CuSO_4 \cdot 5\ H_2O$, Na ascorbate and Na_2CO_3 in *t*BuOH/H_2O led to target compound **5.67** in 2% overall yield over three steps.[133] The low yield can be explained by low conversion in the coupling step and problems within the purification process. The compound still showed good activity, which was lower than the activity of the triazole parent compound. Nevertheless, metabolic stability was improved, while solubility was not affected. Due to the low solubility, no attempts to synthesize the corresponding derivative with a chlorine in the head were done.

Exchanging the triazole in **5G** to a 1,3,4-oxadiazole in **5H** proved to be beneficial in a set of compounds prepared by Ahmed Kamal in this project (Figure 3.3.14). Since it was known, that in *N*-linked derivatives instead of *S*-linked congeners were generally more potent it was obvious to synthesize the corresponding derivative **5.72**, already equipped with the 4-phenoxy *tail*.

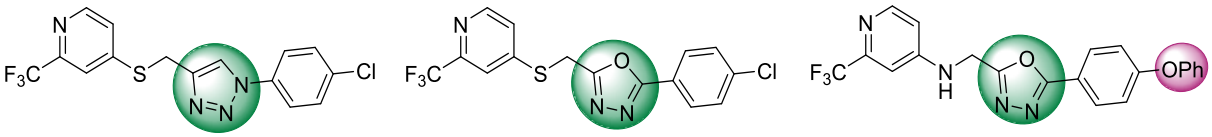

5G, IC_{50} (PqsR) = 666 nM | **5H**, IC_{50} (PqsR) = 515 nM | **5.72**

Figure 3.3.14: *Design rationale for* ***5.72****.*

Retrosynthetic analysis of **5.72** is based on an *N*-alkylation approach and reveals Boc-protected aminopyridine **1.8** and bromide **5.73** (Scheme 3.3.27).

Scheme 3.3.27: *Retrosynthetic analysis of* ***5.72****.*

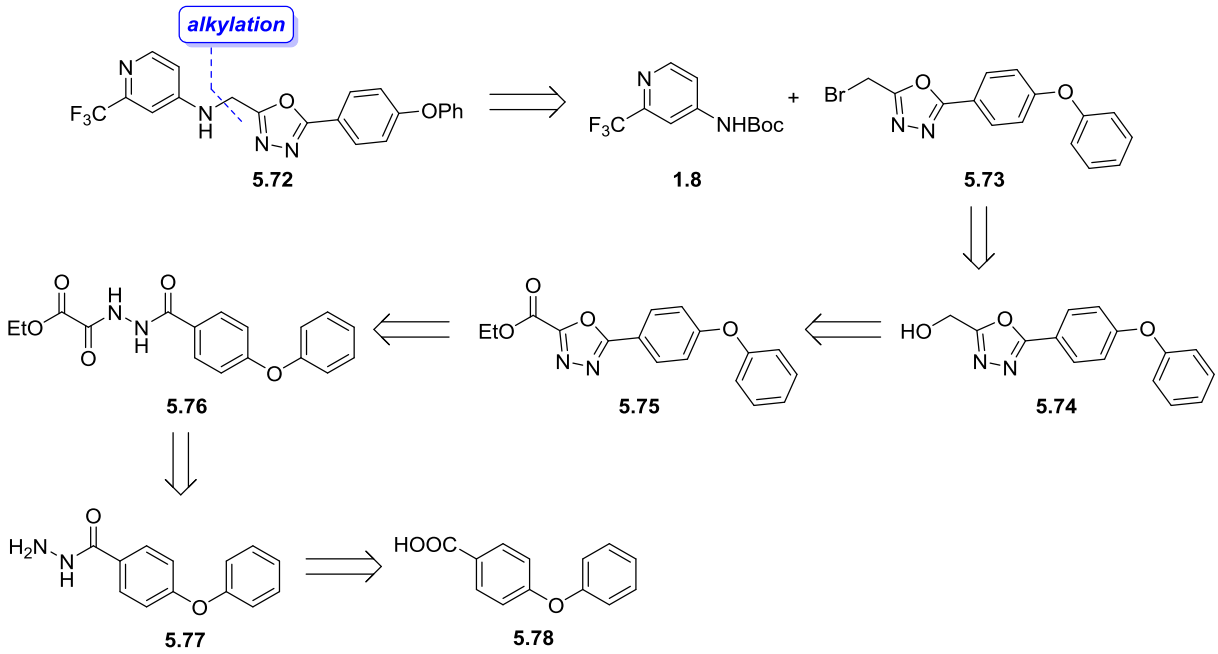

5.72 | **1.8** | **5.73** | **5.74** | **5.75** | **5.76** | **5.77** | **5.78**

This can be obtained from alcohol **5.74** which itself should be generated by reduction of ester **5.75**.

The oxadiazole formation should be accomplished by ring closure of corresponding ethyl 2-oxo-2-(2-(4-phenoxybenzoyl)hydrazinyl)acetate **5.76**, which can be prepared from hydrazide **5.77**, revealing commercially available 4-phenoxybenzoic acid **5.78** as starting material.

Activation of 4-phenoxybenzoic acid **5.78** with CDI in THF, followed by addition of $N_2H_4 \cdot H_2O$ gave the corresponding hydrazide **5.77** in quantitative yield (Scheme 3.3.28).[134] Subsequent treatment with ethyl 2-chloro-2-oxoacetate in DCM with DIPEA and DMAP resulted in desired cyclization precursor **5.76**. The formation of the 1,3,4-oxadiazole was realized *via* a protocol using TsCl and NEt_3 in DCM.[135] Subsequent reduction of the corresponding ester with $NaBH_4$ in THF gave **5.74** in 43% yield over two steps. Conversion of the alcohol to the bromide was carried out with PBr_3 in Et_2O and yielded **5.73** in quantitative yield. The coupling was then performed under the established conditions with NaH (60 wt%) in DMF and subsequent deprotection of **5.79** yielded the desired target compound **5.72**. It is worth mentioning, that in the alkylation step it was crucial to add deprotonated building block **1.8** to a stirred solution of **5.73**. Otherwise yields were lower and partial decomposition was observed.

Scheme 3.3.28: *Synthesis, biological evaluation and DMPK profiling of* ***5.72****.*[a]

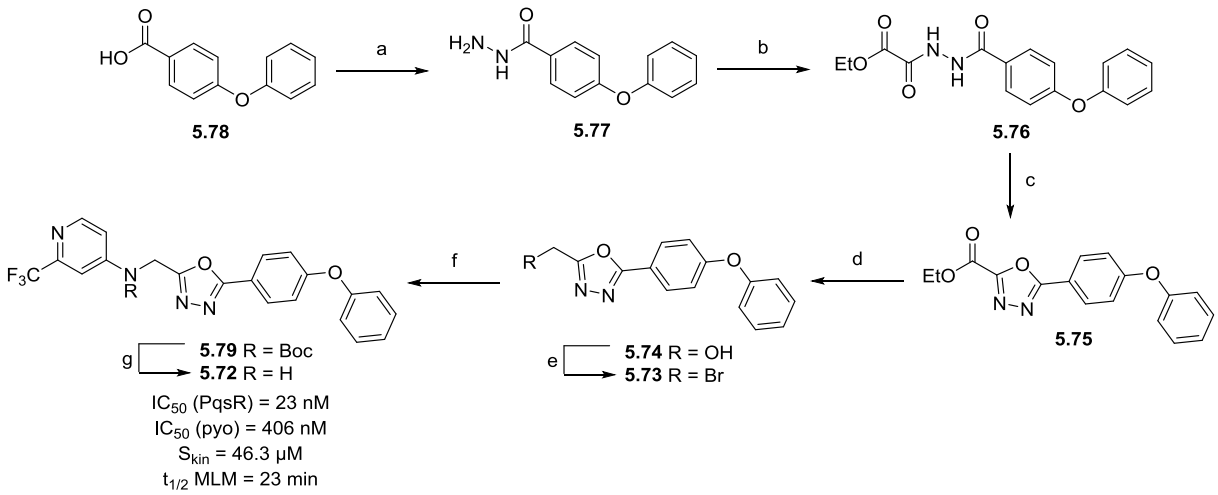

[a]***Reagents and conditions:*** *a: CDI, $N_2H_4 \cdot H_2O$, THF, rt, 3 h, > 98%; b: 2-chloro-2-oxoacetate, DIPEA, DCM 0 °C → rt, 5 h, 83%; c: NEt_3, TsCl, 0 °C → rt, 13 h, 71%; d: $NaBH_4$, THF, MeOH, 0 °C → rt, 3 h, 61%; e: PBr_3, DCM 0 °C → rt, 3 h, 98%; f:* ***1.8****, NaH (60 wt%), DMF, 0 °C → rt, 2 h, 51%; g: TFA/DCM (1:9), rt, 18 h, 87%.*

Even though, for **5.72** activity is decreased almost two-fold, both in *E. coli* and *P. aeruginosa*, solubility is significantly increased compared to its parent compound **3.29** (S_{kin} = 7.7 µM). Also, **5.72** proves to be more stable in mouse liver microsomes in comparison to **3.29** ($t_{1/2}$ = 10 min) (Scheme 3.3.28).

With respect to the *tail* region, a 3-chloro4-isopropoxy derivative was planned to be synthesized in order to investigate the combination with the oxadiazole core motif. The alkylation precursor was synthesized from commercially available methyl 3-chloro-4-hydroxybenzoate **5.80** (Scheme 3.3.29).

First, the isopropoxy group was introduced *via* microwave-aided nucleophilic substitution with isopropyl bromide in acetone, followed by conversion into the corresponding hydrazide **5.82** with $N_2H_4 \cdot H_2O$ in EtOH. Formation of oxadiazole **5.83** was achieved in an excellent yield of 94% by applying a protocol from Kumar *et al*. using ethyl 2-chloro-2-oxoacetate, NEt_3 and TsCl in DCM.[135]

Scheme 3.3.29: *Synthesis of alkylation precursor **5.84** and attempt to synthesize **5.85**.*

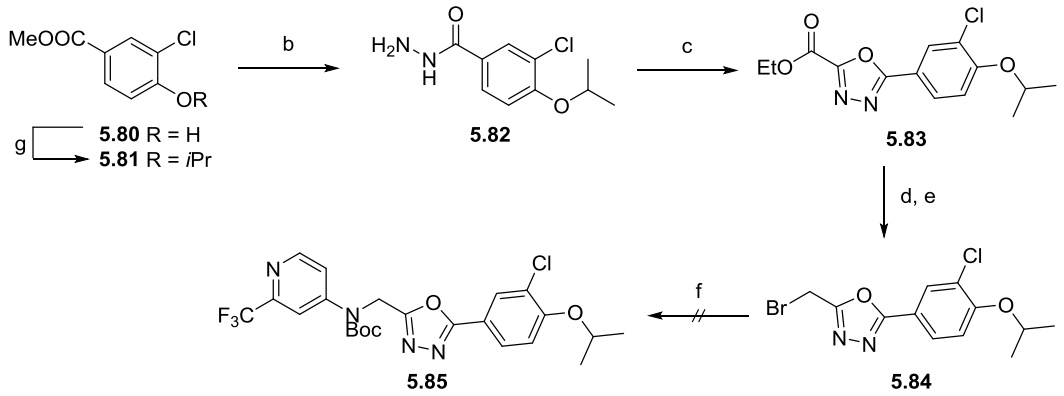

[a]Reagents and conditions: *a: isopropyl bromide, Cs_2CO_3, 50 °C, 3 h, microwave, 82%; b: $N_2H_4 \cdot H_2O$, EtOH, 80 °C, 5 h, 87%; c: ethyl 2-chloro-2-oxoacetate, NEt_3, DCM, 0 °C → rt, 15 h, then NEt_3, TsCl, 0 °C → rt, 4 h, 94%; d: $NaBH_4$, MeOH, 0 °C → rt, 24 h; e: PBr_3, DCM, 0 °C → rt, 3 h, 94% (2 steps); f: tert-butyl (2-(trifluoromethyl)pyridin-4-yl)carbamate **1.8**, NaH (60 wt%), DMF, 0 °C → rt, 1 – 3 h.*

Next, ester **5.83** was reduced with $NaBH_4$ in MeOH and the obtained alcohol was directly used in the bromination step with PBr_3. The alkylation precursor **5.84** was isolated in excellent yield of 94% over two steps and was also used without further purification in the next step, since purification *via* flash chromatography led to decomposition. It is also worth mentioning, that **5.84** proved to be instable in $CDCl_3$, DMSO-d_6, MeOD and acetone-d_6 over time (< 1 h). This might also be a plausible reason why the initially planned S_N reaction with building block **1.8** was not successful. When using the same alkylation protocol from Scheme 3.3.28, only decomposition was observed. Different addition methods were also evaluated, e.g. deprotonation of **1.8** followed by addition of **5.84** in DMF. Also, test reactions with THF instead of DMF were carried out. However, none of the conditions gave the desired compound **5.85**. Attempts to convert the alcohol into a toslyate with TsCl and NEt_3 in DCM led to decomposition of the starting material. Due to the lower priority of this compound, no further experiments were conducted.

In order to explore a possible growth vector in the triazole linker, the methyl substituted analogue **5.87** was synthesized (Scheme 3.3.30). First, propargylated carbamate **1.24** was alkylated using LDA in THF and MeI, leading to **5.86**. This compound was then subjected to thermic cycloaddition with 1-azido-4-phenoxybenzene in *t*BuOH/H_2O at 80 °C. Under these conditions, the Boc-protecting group was also

cleaved off, delivering desired target compound **5.87** directly. It is worth mentioning, that only one isomer was formed during this reaction.

Scheme 3.3.30: *Synthesis of compound* ***5.87****.*[a]

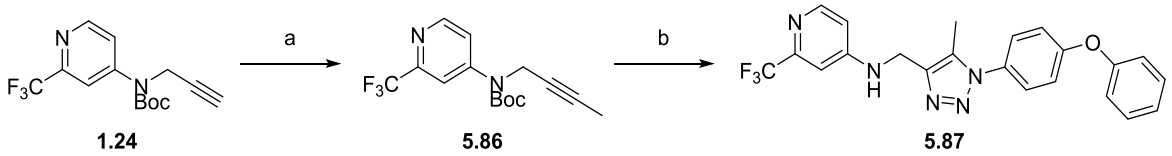

[a]***Reagents and conditions:*** *a: LDA, THF, –78 °C, 1 h, then MeI, rt, 18 h, 83%; b: 1-azido-4-phenoxybenzene, MeCN, 80 °c, 3 d, 10%.*

The compound was then tested in *P. aeruginosa*, showing only 48% effect in inhibiting pyocyanin production at 1 µM. Therefore, no steps towards growing in this direction were undertaken.

Regarding further investigations of the substituents in the phenyl moiety, derivatives **5.94** and **5.95** were synthesized (Scheme 3.3.31). The nitrile substituent was chosen to boost solubility, while the fluorine atom in 2-position should give more information about possible combinations. Commercially available phenols **5.88** and **5.89** were converted into the corresponding azides **5.90** and **5.91** *via* diazotation before installing the isopropoxy moiety to avoid *N*-alkylation. Subsequent CuAAC yielded alkylation precursors **5.92** and **5.93**.

Scheme 3.3.31: *Synthesis of compounds* ***5.94*** *and* ***5.95****.*[a]

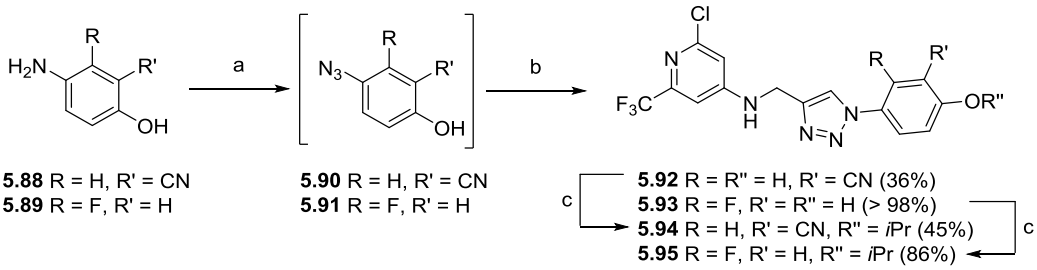

[a]***Reagents and conditions:*** *a: tBuONO, $TMSN_3$, MeCN, rt; b: Na-ascorbate, $CuSO_4 \cdot 5\ H_2O$, DIPEA, MeCN, rt; c: iPrBr, Cs_2CO_3, acetone, 60 °C, 2 d.*

The chlorine motif in the head was chosen, since it previously showed to increase potency in alkoxy derivatives. Alkylation with isopropylbromide and Cs_2CO_3 in acetone gave the desired target compounds **5.94** and **5.95**. The new derivatives were then again evaluated on their ability to reduce pyocyanin inhibition, solubility and metabolic stability. Results are summarized in Table 3.3.14.

Table 3.3.14: *Biological evaluation and DMPK profiling of* ***5.94*** *and* ***5.95****.*

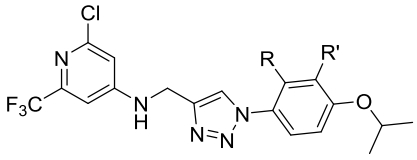

entry	cpd	R	R'	IC_{50} (pyocyanin)	S_{kin}	$t_{1/2}$ MLM
1	**5.56***	H	H	111 nM	23.4 µM	27 min
2	**5.94**	H	CN	216 nM	17.8 µM	21 min
3	**5.95**	F	H	185 nM	21.6 µM	1 min

* = reference

Introduction of the nitrile group did not lead to the expected benefits in solubility. In contrast, it decreased it as well as the metabolic stability. Adding a fluorine in 2-position was accepted in terms of activity and also solubility was not affected drastically. Metabolic stability however dropped to 1 minute. Therefore no other derivatives were synthesized.

3.4. Computer-aided Drug Design

3.4.1. Nitrile Headgroup

Based on the cocrystal structure of **3.29**, a promising modification was the replacement of the pyridine nitrogen with a nitrile substituent. This could replace the crystal water molecule (green circle in Figure 3.4.1) located nearby Ile236, which interacts with the pyridine nitrogen. If the water molecule is not tightly bound to PqsR, this modification might lead to increased affinity of the the putative PqsR inverse agonist.

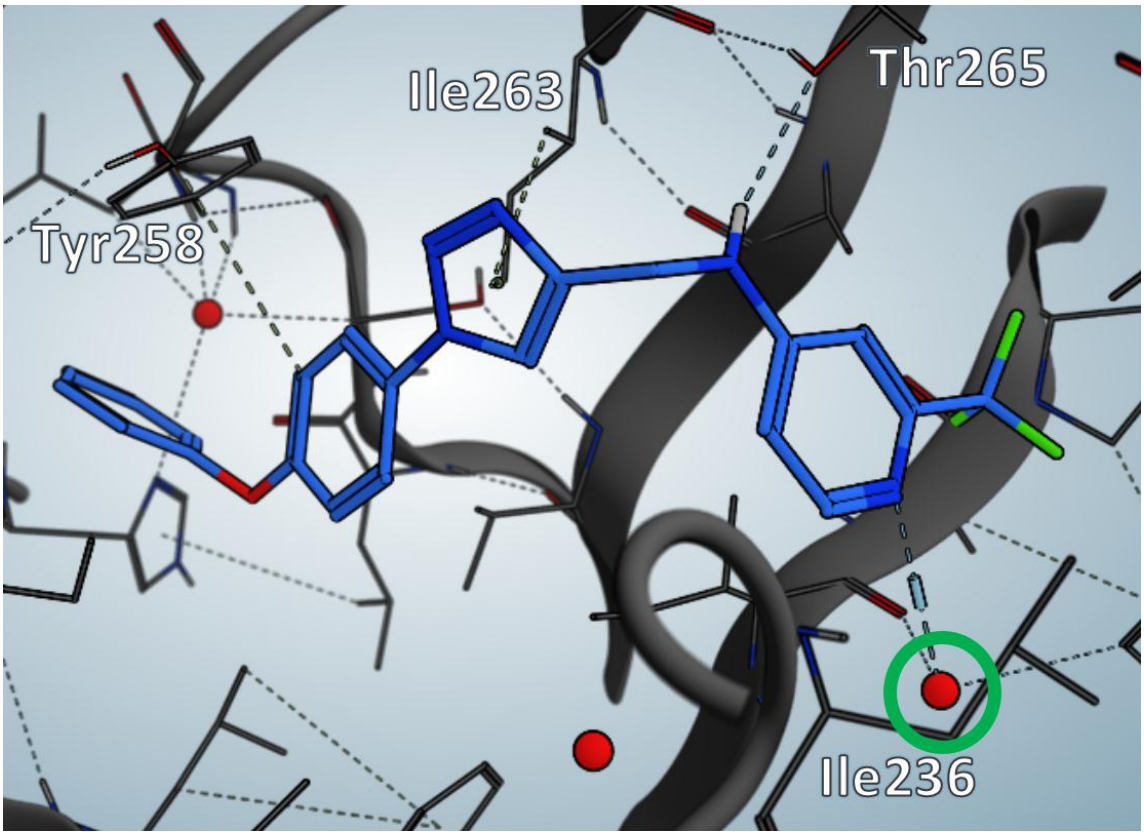

Figure 3.4.1: *Cocrystal structure of* ***3.29*** *in complex with PqsR$^{91-319}$ at 2.15 Å. Color code: blue: C, dark blue: N, red: O, green: F, grey: H, crystal water is displayed as a red ball.*

Commercially available aniline derivative **6.1** was treated with Boc_2O and DMAP in THF, which afforded compound **6.2**. Subsequent propargylation yielded alkyne **6.3** in an excellent yield of 96%. The desired target compound **6.5** was obtained by Boc-deprotection, followed by CuAAC with 1-azido-4-phenoxybenzene (Scheme 3.4.1).

Scheme 3.4.1.: *Synthesis of nitrile headgroup analogue* ***6.5****.*

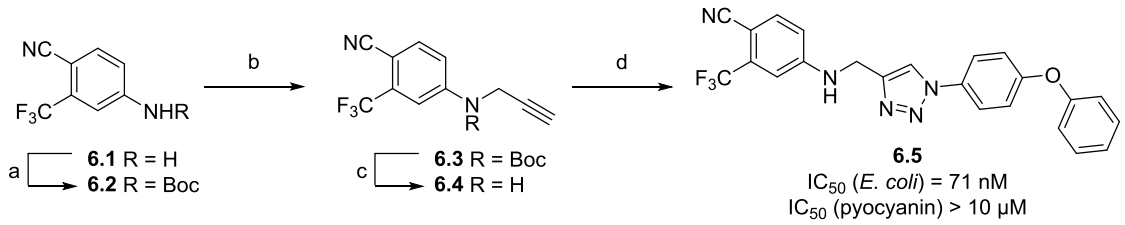

Reagents and conditions: *a: Boc_2O, DMAP, THF, 15 h, rt, 69%; b: NaH (60 wt%), DMF, 10 min, 0 °C, then propargyl bromide, rt, 3 h, 96%; c: TFA, DCM, 16 h, rt, 96%; d: 1-azido-4-phenoxybenzene, DIPEA, Na ascorbate, $CuSO_4 \cdot 5\ H_2O$, H_2O/tBuOH (1:1), 18 h, 40 °C, 28%.*

The compound was then tested for its biological activity. On-target activity was drastically decreased in comparison to the parent compound and pyocyanin activity was completely abolished. A reason for this might be a tightly bound water molecule, which then does not give the expected entropic benefit

upon replacement in the pocket. Moreover, delayed penetration or efflux might explain the abolished pyocyanin activity.

3.4.3. Merged Headgroup I

Based on the crystal structures of hit compound **6A** and fragment **6B**, *in silico* fragment merging made compound **6C** an interesting target compound (Figure 3.4.2).[86]

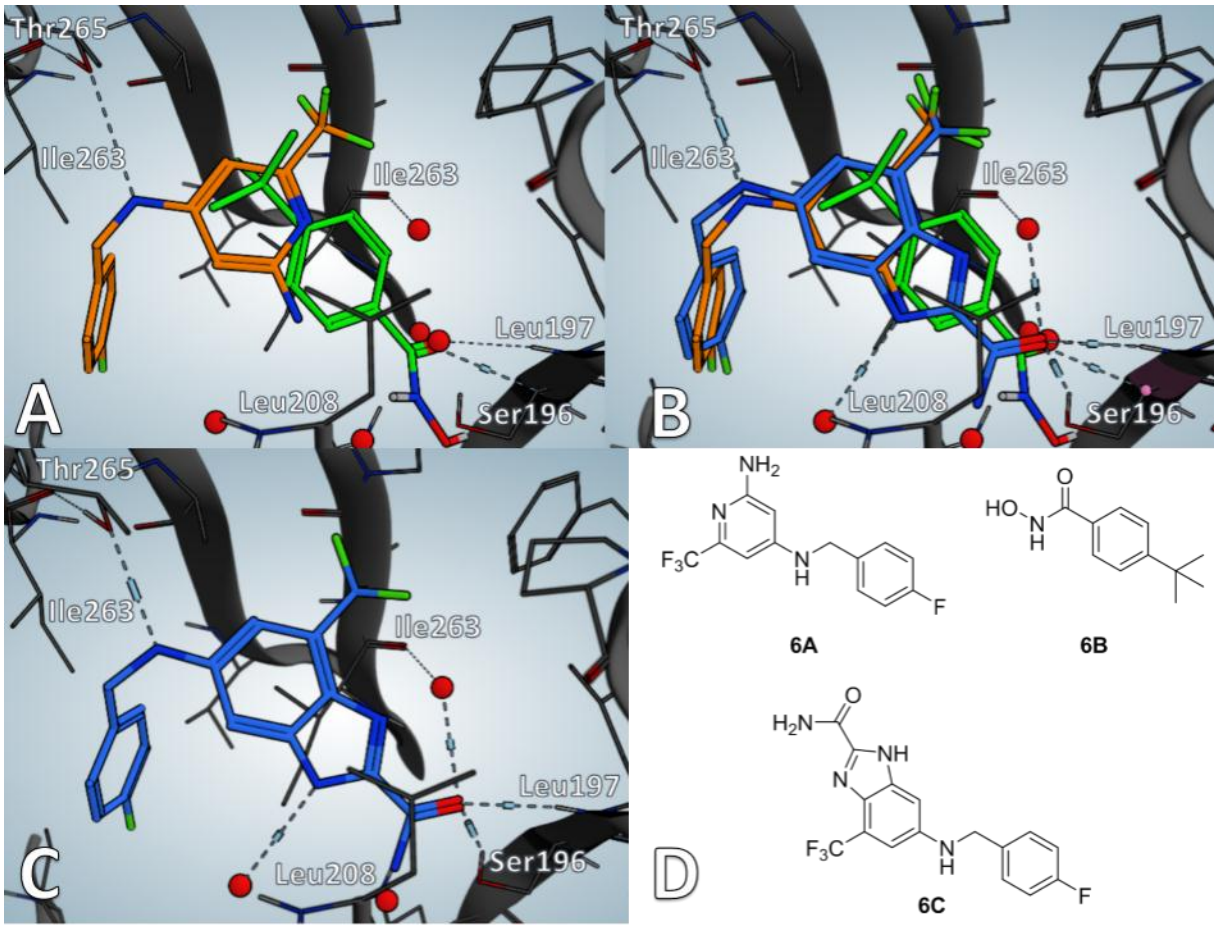

Figure 3.4.2: *A: Compound **6A** (orange) and fragment **6B** (green) in complex with PqsR. B: Overlay of **6A** (orange), **6B** (green) and hypothetical compound **6C** (blue) C: Hypothetical compound **6C** (blue) alone.*

In Scheme 3.4.2, two different retrosynthetic approaches of compounds such as **6C** are shown. Starting with route A, based on a *Buchwald*-type or S_NAr approach, arylbromine **6.7** is a building block which has already been described by Miller *et al.* and can be synthesized by hydrolysis of trichloromethyl benzimidazole **6.8**.[136] This can be easily prepared form commercially available **6.9**. Route B, which follows an alkylation approach, gives amino precursor **6.10**. Ring-opening leads to cyclization precursor **6.11** which should be prepared from aniline derivative **6.12** *via* acylation. The aniline should be accessible by S_NAr reaction with commercially available **6.13.**

Scheme 3.4.2: *Retrosynthetic analysis of compound* ***6C****.*

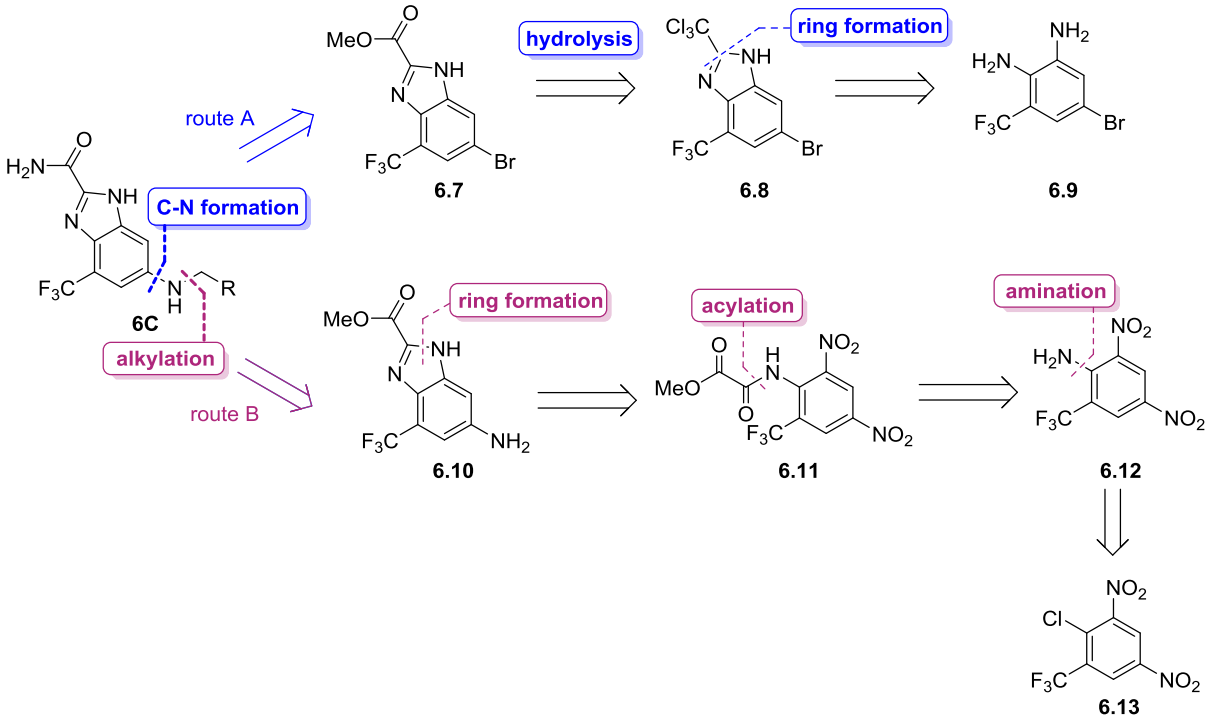

Due to the previously described synthesis of building block **6.7**, route A was pursued first (Scheme 3.4.3). Treatment of commercially available 5-bromo-3-(trifluoromethyl)benzene-1,2-diamine **6.9**, with methyl 2,2,2-trichloroacetimidate in AcOH afforded intermediate **6.8** in quantitative yield. Subsequent hydrolysis gave the corresponding methyl ester **6.7**. The free nitrogen was then Boc-protected in order to prevent interaction with catalysts (Scheme 3.4.3).

Scheme 3.4.3: *Synthesis of building block* ***6.14****.*[a]

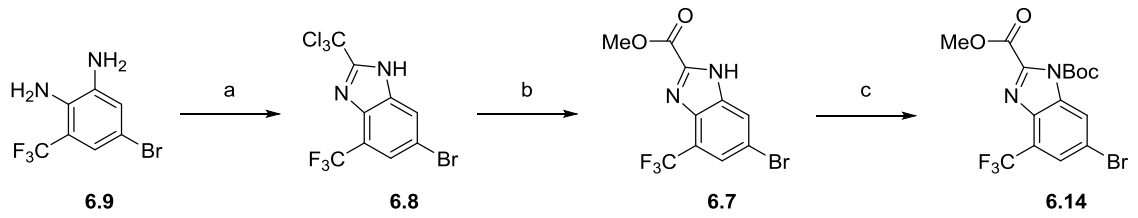

[a]***Reagents and conditions****: a: 2,2,2-trichloroacetimidate, AcOH, rt, 2 h, > 98%; b: MeOH, Na_2CO_3, 28 h, 98%; c: Boc_2O, NEt_3, DMAP, DCM, rt, 21 h, > 98%.*

Aryl bromide **6.14** was then subjected to Pd-catalyzed coupling under various conditions. First, 4-fluoro-benzylamine was used as a nucleophile since compound **6A** proved to be active.[86] The evaluated reaction conditions are summarized in Table 3.4.1.

Table 3.4.1: *Buchwald-Hartwig optimization studies towards* ***6.15****. The reactions were carried out in a 0.1 M solution and were run for 24 h. 3.3 eq. of nucleophile, 2.2 eq. of base and 10 mol% of ligand and 5 mol% of catalyst were used.*

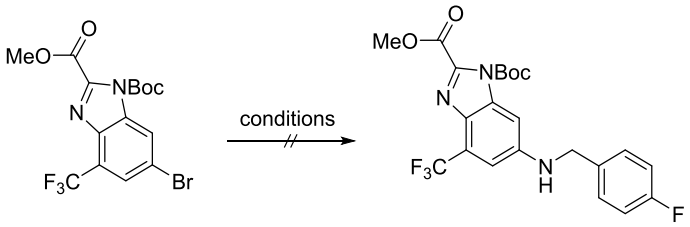

6.14 **6.15**

entry	catalyst	ligand	base	solvent	T
1	Pd_2dba_3	DavePhos	Cs_2CO_3	1,4-dioxane	65 °C
2	Pd_2dba_3	XantPhos	Cs_2CO_3	1,4-dioxane	65 °C
3	Pd_2dba_3	BINAP	Cs_2CO_3	1,4-dioxane	65 °C
4	$Pd(OAc)_2$	BINAP	Cs_2CO_3	1,4-dioxane	65 °C
5	$Pd(OAc)_2$	BINAP	KO*t*Bu	1,4-dioxane/toluene	65 °C
6	$Pd(OAc)_2$	XantPhos	Cs_2CO_3	1,4-dioxane	80 °C
7	$Pd(OAc)_2$	PCy_3	Cs_2CO_3	1,4-dioxane	80 °C
8	CX 31	-	Cs_2CO_3	1,4-dioxane	80 °C
9	$Pd(OAc)_2$	BINAP	Cs_2CO_3	1,4-dioxane	80 °C

None of these conditions led to any formation of the desired target compound. Therefore, other nucleophiles were investigated. The conditions are summarized in Table 3.4.2. The nucleophiles used were propargylamine, Boc-protected propargylamine, $BocNH_2$ and $CbzNH_2$. The first represents a very challenging attempt, since it is known that primary amines easily undergo β-hydride elimination.[64]

Table 3.4.2: *Buchwald-Hartwig coupling conditions. 2.2 eq. of either propargylamine, Boc protected propargylamine, $BocNH_2$ or $CbzNH_2$ were used, 2.2 eq. of base, 5 mol% of catalyst and 10 mol% of ligand. Reactions were run for 24 h.*

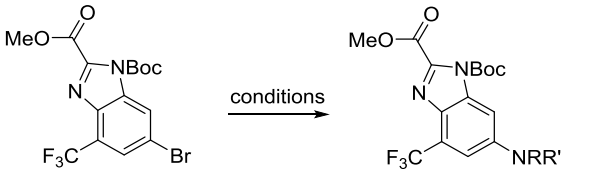

6.14

6.16 R = propargyl, R' = H
6.17 R = propargyl, R' = Boc
6.18 R = H, R' = Boc
6.19 R = H, R' = Cbz

entry	catalyst	ligand	base	solvent	T
1	$[Pd(cinnamyl)Cl]_2$	BippyPhos	Cs_2CO_3	1,4-dioxane	80 °C
2	$[Pd(cinnamyl)Cl]_2$	BippyPhos	NaO*t*Bu	1,4-dioxane	80 °C
3	Pd_2dba_3	CataCXium A	Cs_2CO_3	toluene	80 °C
4	$Pd(PPh_3)_4$	XantPhos	Cs_2CO_3	dioxane	80 °C
5	*t*BuXPhos Pd G3	-	NaO*t*Bu	1,4-dioxane	80 °C
6	Me_3(OMe)*t*BuXPhos Pd G3	-	NaO*t*Bu	1,4-dioxane	80 °C
7	$Pd(OAc)_2$	PCy_3	Cs_2CO_3	1,4-dioxane	80 °C
8	Pd_2dba_3	PCy_3	Cs_2CO_3	toluene	80 °C
9	Pd_2dba_3	DavePhos	Cs_2CO_3	1,4-dioxane	100 °C

Even though the S_NAr reaction of **6.13** with NH_4OH or NH_3 in 1,4-dioxane seemed to be straight forward, the introduction of the amine function proved to be rather difficult. Reaction conditions required optimization and are summarized in Table 3.4.3. When NH_3 (0.5 M in 1,4-dioxane) was used with or without Cs_2CO_3 (entries 1, 2), no conversion at all was observed. With CuI and DMEDA as catalytic system (entry 3) only addition of the ligand occurred. Changing to the non-nuclophilic TMEDA (entry 4) as a ligand did not result in any formation of the product. Also treatment with Cu_2O and 1,10-phenanthroline did not yield the desired target compound. Applying Pd-catalyzed coupling methods, which were successful for the installation of a primary amine within this thesis were tested (entries 6 – 8), but also did not result in the formation of desired aniline **6.12**. Only when NH_4OH with Cu_2O and 1,10-phenanthroline was used in DMSO, **6.12** was isolated with an excellent yield of 93%.

Table 3.4.3: *Reaction condition screening for conversion of **6.13** into **6.12**. Reactions were run for 21 h in a 0.2 M solution. In case of entries 1-8, 4.4 eq. of nucleophile, 10 mol% of ligand, 5 mol% of catalyst or 10 mol% of precatalyst were used. In case of entry 9, 40 mol% of ligand, 20 mol% of catalyst were used and the reaction was carried out in a 0.1 M solution of DMSO/NH_4OH (1:1).*

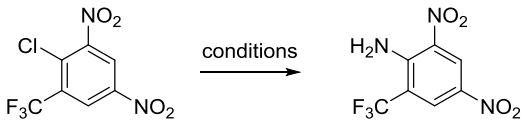

6.13 **6.12**

entry	nucleophile	catalyst	ligand	base	solvent	T	yield
1	NH_3*	-	-	-	1,4-dioxane	100 °C	X
2	NH_3*	-	-	Cs_2CO_3	1,4-dioxane	100 °C	X
3	NH_3*	CuI	DMEDA	K_3PO_4	1,4-dioxane	100 °C	X
4	NH_3*	CuI	TMEDA	K_3PO_4	1,4-dioxane	100 °C	X
5	NH_3*	Cu_2O	1,10-phenanthroline	K_3PO_4	1,4-dioxane	100 °C	X
6	$BocNH_2$	*t*BuXPhos Pd G3	-	NaO*t*Bu	1,4-dioxane	80 °C	X
7	$BocNH_2$	Pd-175	-	Cs_2CO_3	1,4-dioxane	80 °C	X
8	*t*$BuNH_2$	Pd-175	-	Cs_2CO_3	1,4-dioxane	50 °C	X
9	NH_4OH	Cu_2O	1,10-phenanthroline	-	DMSO	80 °C	93%

* = 0.5 M in 1,4-dioxane, X = no conversion to target mass

Subsequent acylation of **6.12** with methyl 2-chloro-2-oxoacetate with DMAP and DIPEA in DCM afforded desired cyclization precursor **6.11** in quantitative yield (Scheme 3.4.4). The nitro group was reduced with Pd/C and H_2 in EtOH and condensation of the *in situ* generated amine with the carboxamide resulted in formation of building block **6.10**. Selective alkylation of the aniline nitrogen is very challenging and mixtures were expected. Nevertheless, various conditions using K_2CO_3 as a base in DMF at different temperatures failed to only propargylate the desired aniline nitrogen. Also changing the solvent from DMF to THF did not give the desired target compound.

Scheme 3.4.4: *Synthesis of **6.10** and attempted propargylation.*[a]

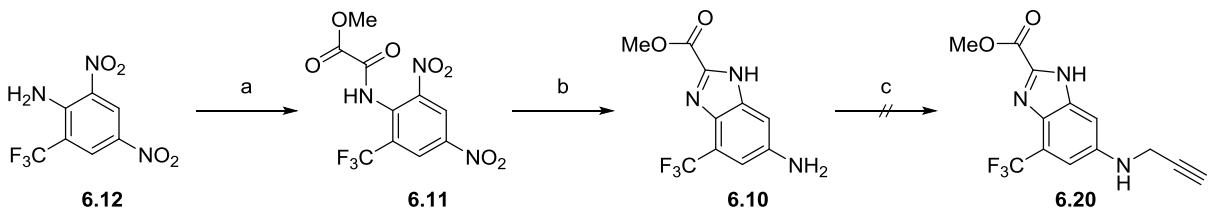

6.12 **6.11** **6.10** **6.20**

[a]***Reagents and conditions:*** *a: methyl 2-chloro-2-oxoacetate, DMAP, DIPEA, 0 °C → rt, 30 min, > 98%; b: Pd/C, H_2, EtOH, rt, 5 h, 68%; c: K_2CO_3, propargyl bromide, DMF or THF, 16 h, rt or 50 °C.*

Another possible option was the introduction of an aryl moiety *via* reductive amination. In a comparable class of project compounds, the pyrimidine core proved to be a potent variation of the triazole core. Since the corresponding aldehyde **6D** was available in large amounts, several attempts with this aldehyde were carried out (Scheme 3.4.5).

Scheme 3.4.5: *Attempts for reductive amination of* ***6.10****.*

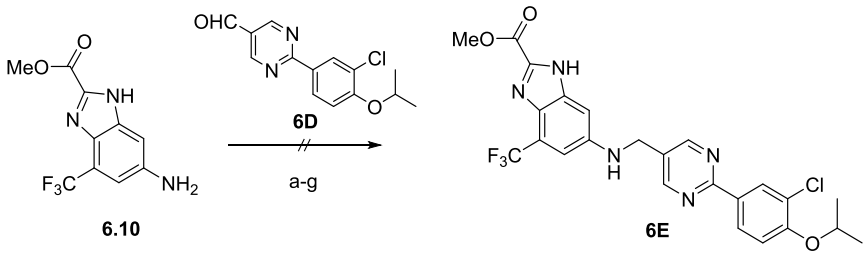

[a]Reagents and conditions: a: Ti(OiPr)$_4$, NaBH(OAc)$_3$, HOAc, DCM, 0 °C → rt; b: 1.) PhMe, 100 °C; 2.) NaBH$_4$, EtOH; c: 1.) EtOH, 80 °C; 2.) NaBH$_4$, MeOH, rt; d: 1.) EtOH, 4 Å MS, 80 °C; 2.) NaBH$_4$, MeOH, rt; e: 1.) EtOH, 4 Å MS, 80 °C; 2.) NaBH$_4$, MeOH, 0 °C; f: 1.) EtOH, 4 Å MS, 80 °C; 2.) NaBH(OAc)$_3$, MeOH, 0 °C; g: 1.) EtOH, 4 Å MS, 80 °C; 2.) NaBH(OAc)$_3$, MeOH, rt.

When the protocol with Ti(O*i*Pr)$_4$ and NaBH(OAc)$_3$ with HOAc in DCM was used, which was applied by Sygnature Discoveries in course of this project, only decomposition occurred. Trying to first generate the imine in toluene and reduce it *in situ* also led to decomposition, also when changing from toluene to EtOH. Using 4 Å mol sieves in EtOH at 80 °C, full conversion of the starting material was observed (TLC). Nevertheless, when the reduction with NaBH$_4$ in MeOH was carried out at room temperature, only the corresponding primary alcohol derived from **6D** was isolated and no product formation was detected (LC-MS). Carrying out the reduction step at 0 °C had no effect and only upon warming to room temperature again the alcohol derived from **6D** was detected (LC-MS). Attepmts with the milder NaBH(OAc)$_3$ in MeOH neither led to conversion to the desired target compound **6E**, nor the alcohol derived from **6D**. No optimization towards this step were undertaken by now.

3.4.4. Merged Headgroup II

Moreover, merging of the known PqsR inverse agonist **M64** and **3.29** gave hypothetical compound **6.23** with a sophisticated imidazopyridine (Figure 3.4.2). By now, no synthesis for this unprecedented trifluoromethyl-substituted imidazopyridine, bearing a carboxamide motif in 2-position of the imidazole ring, is known in literature. Therefore, the desired target compounds represents a very unique, synthetically challenging structure. The retrosynthetic analysis is depicted in Scheme 3.4.6.

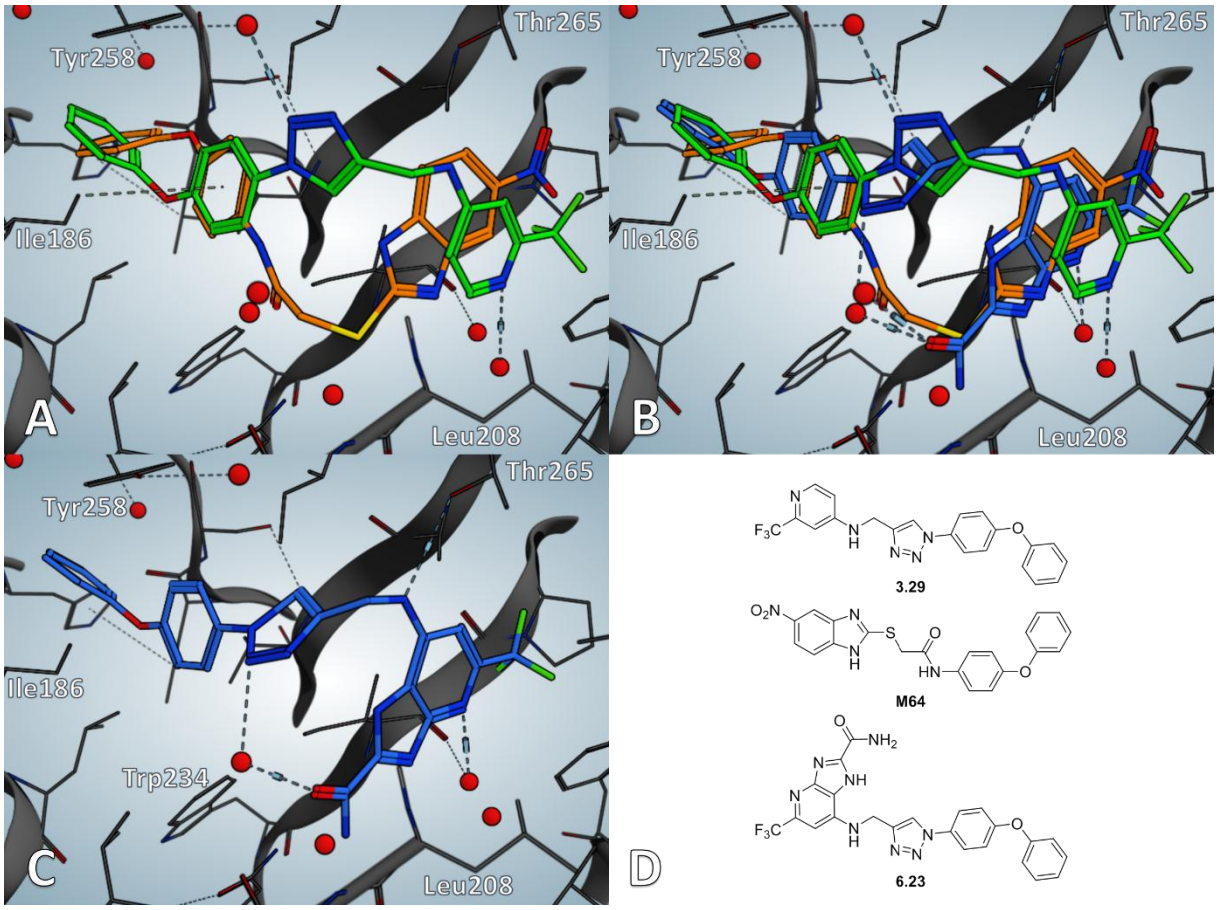

Figure 3.4.2: *A: cocrystal structures of* ***M64*** *(orange) and* ***3.29*** *(green) in complex with PqsR; B: cocrystal structures of* ***M64*** *(orange) and* ***3.29*** *(green) in complex with PqsR with putative molecule* ***6.23****; C: putative molecule* ***6.23*** *alone with protein; D: structures of* ***M64, 3.29*** *and* ***6.23****.*

The initial retrosynthesis was based on the cyclisation approach from Chapter 3.4.3, revealing diamino-pyridine **6.24**. This compound should be synthesized *via* amination and subsequent reduction from **6.25**. Functional group interconversion reveals hydroxy-pyridine **6.26**, which should be synthesized by CuAAC from precursor **6.27**. Disconnection of the propargylamine unit leads to compound **6.28**, which is already described in literature and can be synthesized from commercially available building blocks **6.29** and **6.30**.[137]

Scheme 3.4.6: *Retrosynthetic analysis of* ***6.23****.*

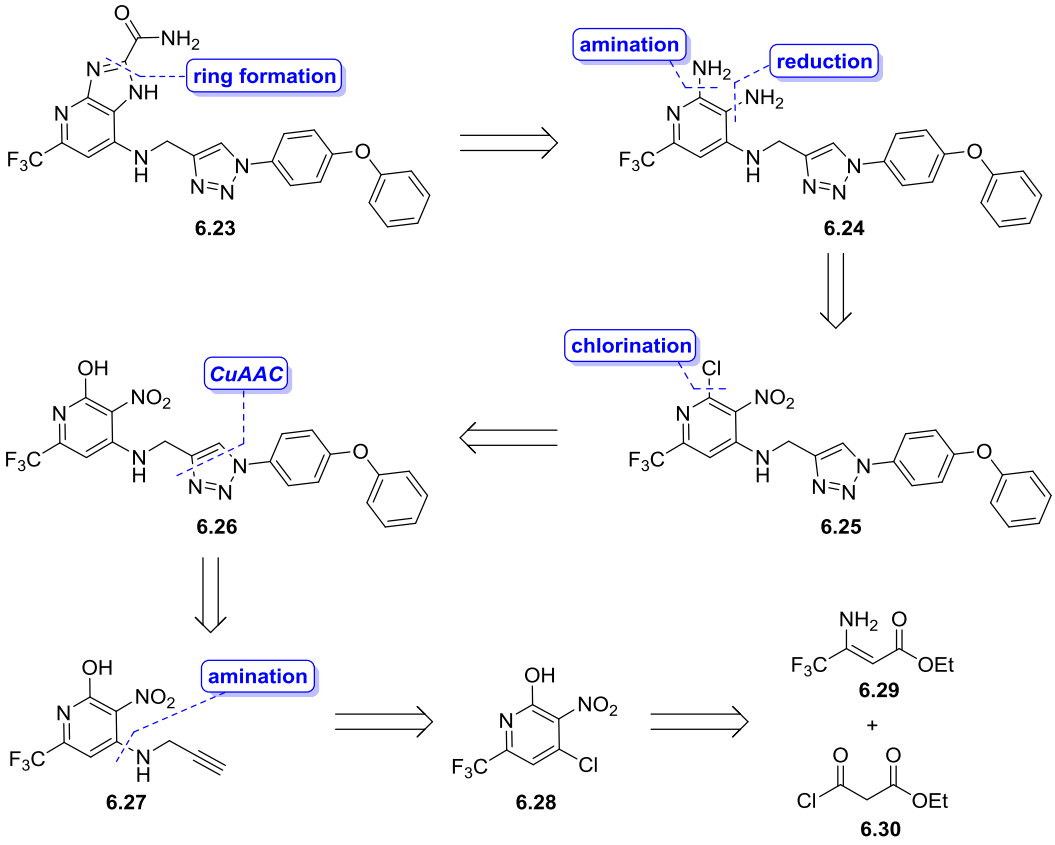

Based on a route by Adam *et al.*, the reaction conditions were slightly adjusted.[137] Pyridine-catalyzed acylation of ethyl (*E*/*Z*)-3-amino-4,4,4-trifluorobut-2-enoate **6.29** with ethyl 3-chloro-3-oxopropanoate **6.30** led to intermediate **6.31**, which was cyclized under basic conditions with KO*t*Bu in EtOH to **6.32** (Scheme 3.4.7). Subsequent decarboxylation afforded dihydroxy-pyridine **6.33** in 55% yield over three steps. Optimized nitration conditions with HNO_3 (70%) in concentrated H_2SO_4 gave **6.34** in quantitative yield. Ph_2POCl_2 cleanly reacted with the 4-hydroxy group and building block **6.28** was isolated in excellent yield of 89%. The following amination to generate compound **6.27** worked best using 2.2 equivalents of propargylamine and 1.1 equivalent of DIPEA, affording **6.27**. Excess of propargylamine (3 – 10 equivalents) or increased amounts of DIPEA (1.1 – 5.5 equivalents) resulted in poorer yields. It is worth mentioning that formation of the triazole followed by chlorination gave better results, than first converting the hydroxyl-function into the corresponding chloride and then subjecting this intermediate to CuAAC. For the CuAAC, yields were quite low and the solvent was changed to a *t*BuOH/H_2O mixture ultimately leading to intermediate **6.26** in 64% yield. The reason for this might be the pyridone-hydroxypyridine tautomerism, making the pyridone tautomer more favorable in water. Chlorination with Ph_2POCl_2 and subsequent microwave-aided amination of **6.35** with NH_4OH and Cu_2O/1,10-phenanthroline as catalytic system in 1,4-dioxane gave **6.36** in 72% over two steps. The following reduction of the nitro group required some optimization. Adam *et al.* used Fe/HOAc in the

first place, which only gave various acylated byproducts. Even though Pt/C and H_2 in THF gave excellent conversion to the desired target compound **6.24**, the compound could not be isolated in sufficient amounts.

Scheme 3.4.7: *Synthesis of precursor **6.36** and hydrogenation attempt to **6.24**.*

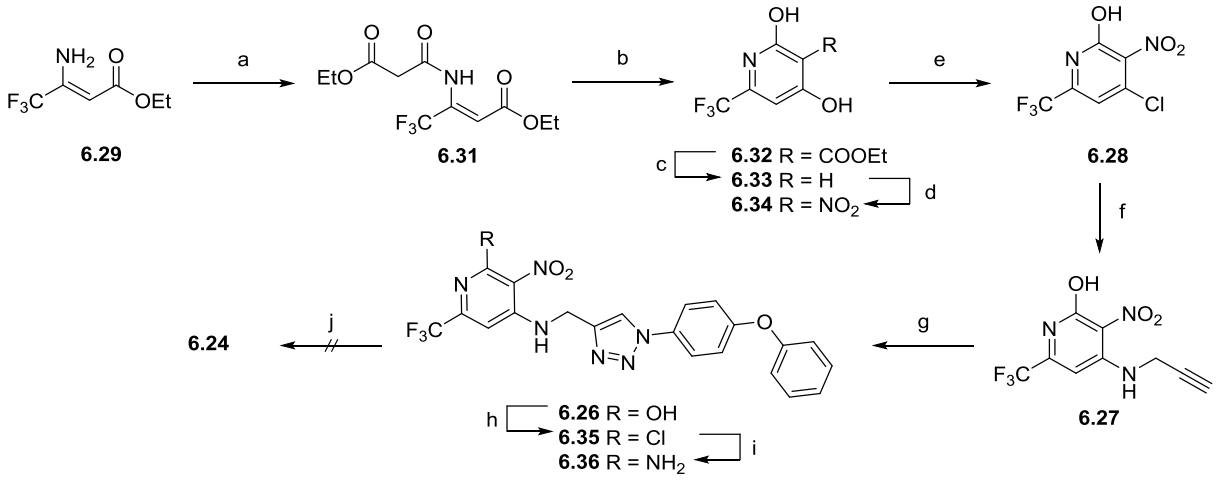

[a]Reagents and conditions: *a: ethyl 3-chloro-3-oxopropanoate, pyridine, DCM, 0 °C then rt, 18 h; b: KOtBu, EtOH, 80 °C, 18 h; c: 6 M HCl, 100 °C, 23 h, 55% (3 steps); d: $H_2SO_{4\,conc.}$, HNO_3 (70%), 16 h, > 98%; e: $PhPOCl_2$, 100 °C, 5 h, 89%; f: propargylamine, DIPEA THF, rt, 18 h, 48%; g: 1-azido-4-phenoxybenzene, $CuSO_4 \cdot 5\,H_2O$, Na ascorbate, DIPEA, $tBuOH/H_2O$, rt, 21 h 64%; h: $PhPOCl_2$, 80 °C, 5 h; i: Cu_2O, NH_4OH, 1,10-phenanthroline, dioxane, microwave 72% (2 steps); j: Fe/HOAc, EtOH, rt/80 °C, 8 – 24 h or Pt/C, H_2, THF, rt, 24 h.*

No investigation upon this issue was done since cyclization conditions from Scheme 3.4.4 seemed more promising. Starting with precursor **6.36**, DMAP-catalyzed acylation of the primary amino function with ethyl 3-chloro-3-oxopropanoate and DIPEA in DCM gave cyclization precursor **6.39** in good yield of 80% (Scheme 3.4.8). Crucial for selective mono acylation was the slow addition of acylchloride **6.37** as a solution in DCM at 0 °C. Subsequent treatment with Pd/C in MeOH gave no conversion at all to the desired target compound **6.40**, nor the cyclization precursor **6.39**. Only when formic acid was added, conversion to cyclized **6.40** was observed after seven days, yet only below 5%. By now, no optimization towards the cyclization was step was performed.

Scheme 3.4.8: *Attempted synthesis of* ***6.41*** *via cyclization precursor* ***6.39****.*[a]

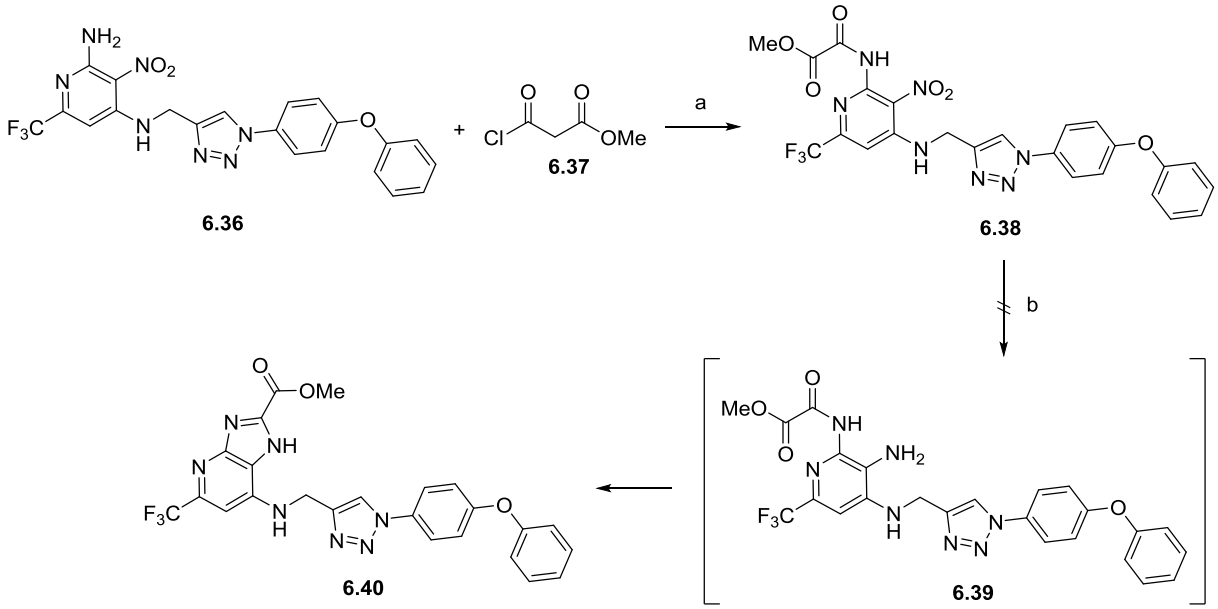

[a]***Reagents and conditions:*** *a: DIPEA, DMAP, DCM, 0 °C → rt, 3 h, 80%; b: Pd/C, HCOOH, rt, 7 d.*

4. Conclusion

The first aim of this thesis was the establishment of a reliable synthetic route towards PqsR inverse agonists within lead generation, based on previously described compound **1A**.[86] Due to synthetic complexity, at first only compounds lacking the amino function in the pyridine head were generated. The corresponding precursor was synthesized in excellent yield and moreover, precursor **1.25** was prepared. These two precursor facilitated a highly divergent synthetic route towards different classes of PqsR inverse agonists for the generation of a lead compound (Scheme 4.1).

Scheme 4.1: *Divergent lead generation starting from commercially available* ***1.5****.*

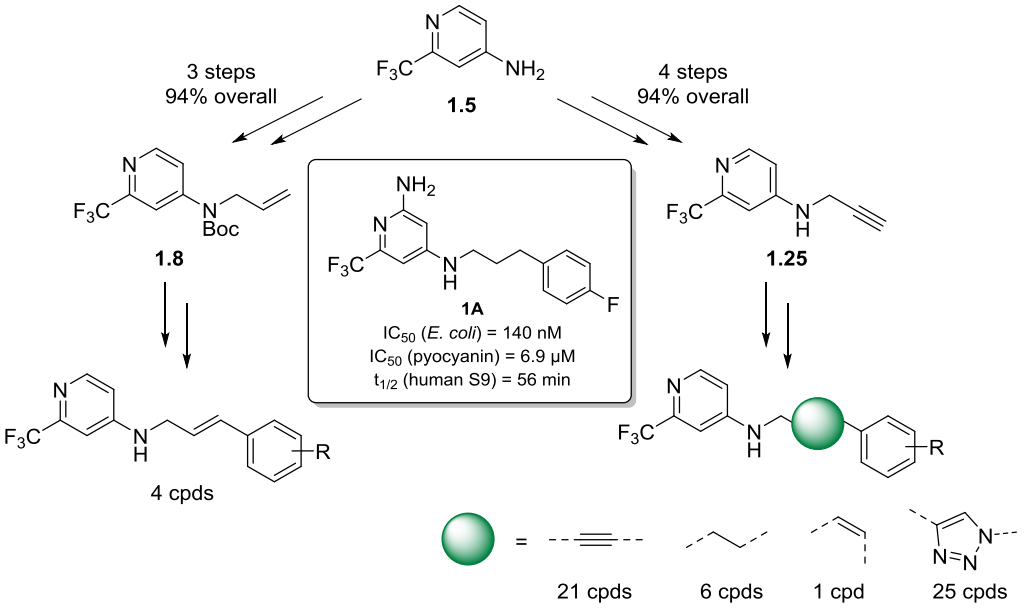

In each class, several sets of compounds were synthesized for SAR studies and evaluated for their biological activities regarding on-target activity in an *E. coli*-based reporter gene assay and their ability to inhibit pyocyanin production in *P. aeruginosa*, as well as DMPK parameters for selected compounds. Based on these parameters, **3.29** and **3.37** were further evaluated as promising lead compounds with respect to advanced biological profiling and safety pharmacology. Compound **3.29** proved to be superior in terms of activity and also exhibited a safer pharmacological profile. Moreover, **3.29** showed suitable *in vivo* PK and was also well-tolerated in mice. Therefore, it was chosen as the lead compound and was evaluated in *in vivo* target engagement studies in a murine lung infection model. **3.29** showed excellent reduction of proximal biomarkers HHQ, PQS and HQNO (Figure 4.1).

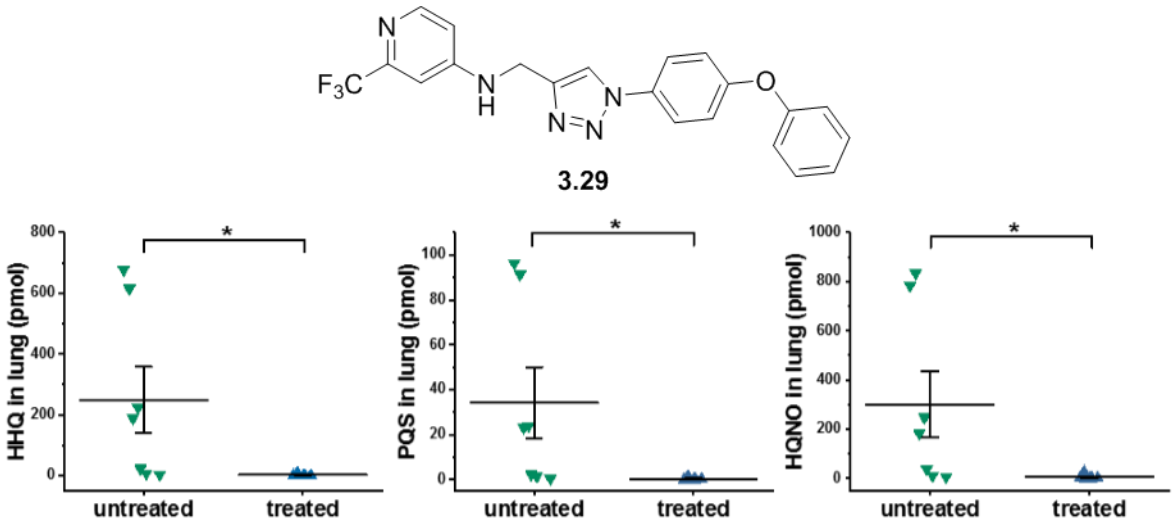

Figure 4.1: *Structure of **3.29**, HHQ, PQS and HQNO levels of treated and untreated mice.*

After **3.29** showed successful *in vivo* target engagement, synthetically challenging analogue **4.1** was prepared in order to investigate the role of the amino function in the headgroup. The precursor **4.3** was synthesized in six steps with an overall yield of 17%. Subsequent CuAAC led to compound **4.2**, which served as a precursor for *Buchwald-Hartwig* amination. After a long optimization campaign, derivative **4.1** was obtained using Pd-175 (Scheme 4.2).[118] Due to the lower activity of **4.1**, compounds bearing the amino motif in the head were not further prioritized.

Scheme 4.2: *Synthesis of **4.1**.*

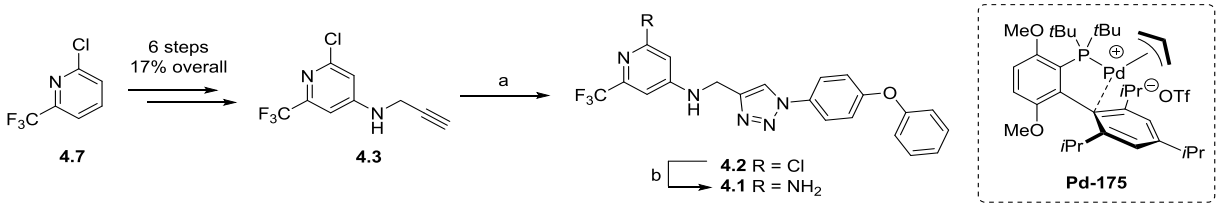

[a]***Reagents and conditions:*** *a: tBuONO, $TMSN_3$, 4-phenoxyaniline, MeCN, 0 °C, 1 h, then **4.17**, $CuSO_4 \cdot 5\ H_2O$, Na ascorbate, DIPEA, rt, 16 h, 93%; b: $BocNH_2$, Pd-175, Cs_2CO_3, 1,4-dioxane, 28 h, 90 °C, 39%.*

In order to further optimize lead compound **3.29**, several modifications in the *tail* region were accomplished. A total of 21 derivatives were synthesized in this lead optimization step. The most beneficial modification was the introduction of a 2-fluoro substituent in the 4-phenoxy motif (compound **5.3**) which drastically increased, solubility and metabolic stability (Figure 4.2).

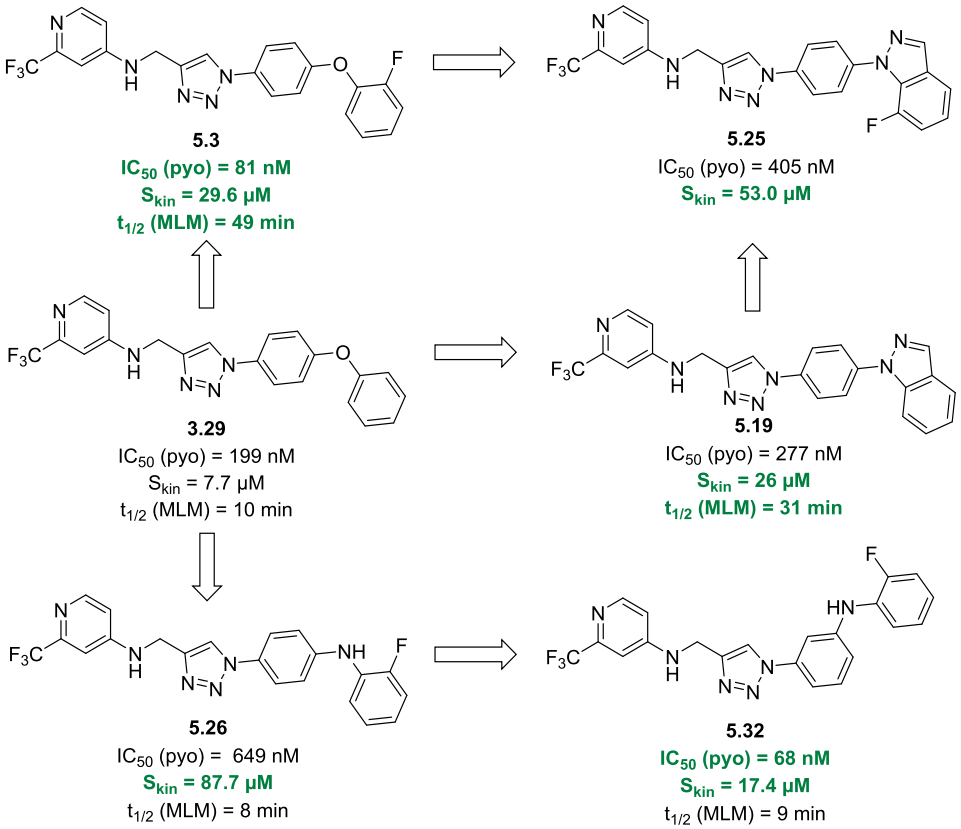

Figure 4.2: *Tail modifications of* ***3.29****. Improved parameters are highlighted in green.*

Also, the introduction of various *N*-heterocyclic moieties in the tail region were evaluated and the indazole-analogue **5.19** proved to be a promising modification. Nevertheless, installing the beneficial fluorine motif from **5.3** in **5.19**, did not lead to improved activity or solubility of compound **5.25**. Combination of the fluorine motif with a nitrogen-bridged tail group gave compound **5.26** with drastically improved solubility and improved activity compared to its parent compound. Changing the attachment of the fluoro-aniline moiety resulted in a potent and well soluble compound (**5.32**).

In the next optimization step, the head group was modified with various *N*-heterocycles and also their precursors were evaluated. A highly non-additive SAR was observed, since derivatives with a short 3-chloro-4-isopropoxy tail motif benefitted from the additional chlorine atom in the pyridine head.

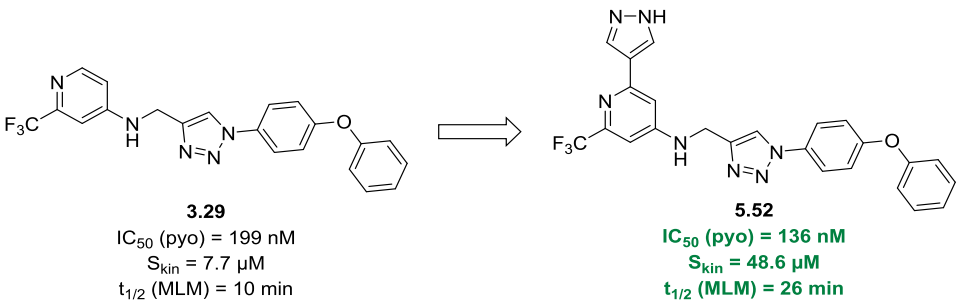

Figure 4.3: *Head modification of* ***3.29*** *resulting in optimized lead* ***5.52****. Improved parameter are highlighted in green.*

Nevertheless, this modification had little impact on the acitivity of compounds with a larger moiety, such as 4-phenoxy. However, the installation of a pyrazole led to improved activity, solubility and metabolic stability in compound **5.52** (Figure 4.3).

Additionally, computer-aided drug design based on co-crystal structures of known inverse agonists or fragments in complex with PqsR resulted in challenging hypothetical compounds. During the course of this thesis, several synthetic routes were designed and evaluated (Scheme 4.3). Even though, the desired target compounds could not be synthesized, the synthetic efforts provide an informative basis for further optimization, since advanced precursors have been synthesized on scalable and reliable routes.

Scheme 4.3: *Synthesis of building blocks **6.10** as a precursor for **6A** and **6.39** as a precursor for **6.23**.*

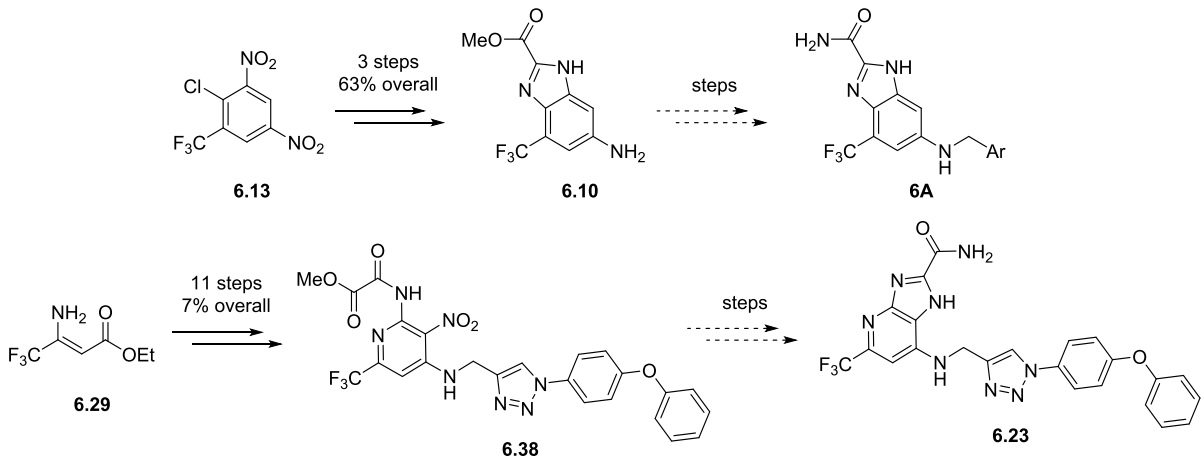

In total, more than 100 target compounds were synthesized, enabling deep SAR and SPR insights. Due to the high-flexibility of the ligand binding domain of PqsR, confirmed by co-crystal structures of several inverse agonists in complex with PqsR, a non-additive SAR was observed. A lead compound was generated, which showed *in vivo* efficacy in a murine lung infection model. Based on this compound, a lead optimization campaign resulted in multiparameter-optimized lead structures with improved activity in terms of pyocyanin inhibition, solubility and metabolic stability. Ultimately, some of the herein described compounds contribute to three patents.[138–140]

Even though, significant improvements were achieved in the triazole class, at the end of the medicinal chemistry campaign another class proved to be more suitable. These “Class E” compounds exhibited better activity, a more beneficial PK profile and less CEREP off-targets. Nevertheless, the triazole compounds remain an important follow-up class.

5. Outlook

Considering lead optimization, combinations of promising fluoro-aniline motifs with *N*-heterocyclic headgroups (**8A** – **8C**), such as pyrazole containing trifluoromethyl pyridines still need to be evaluated (Figure 5.1 A). In addition to this, adding a second fluorine in the core structure could increase activity as has been demonstrated for isopropoxy derivative **5.95** (chapter 5.3). Moreover, the beneficial properties of the oxadiazole linker regarding solubility and metabolic stability could be exploited by installing a different *tail* group, or adding further substituents in the *head* (Figure 5.1 B).

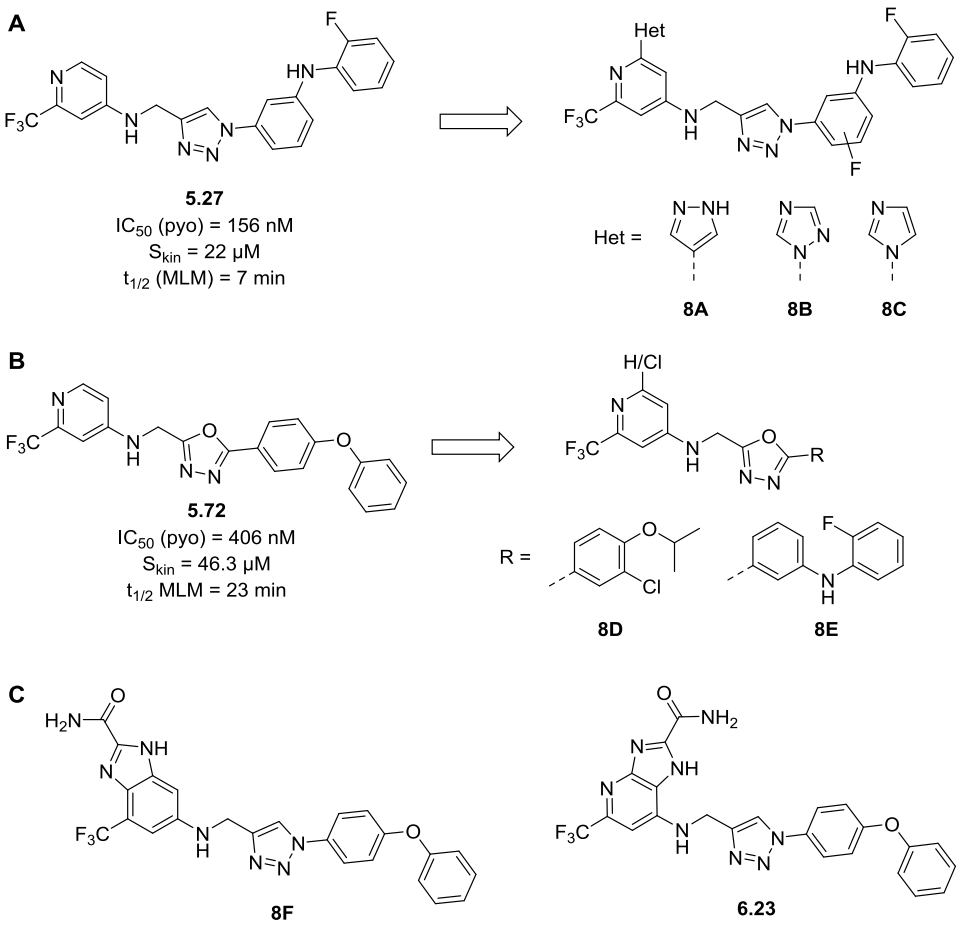

Figure 5.1: *A: possible modifications of **5.27**; B: possible modifications of **5.72**; C: in silico-designed compounds **8F** and **6.23**.*

The *in silico* designed compounds **8F** and **6.23** should be synthesized upon optimization of the herein established route towards their precursor. Depending on their activity, combinations of favorable tail modifications should be synthesized and evaluated.

To this end, compounds of the aforementioned "Class E" have been nominated as preclinical candidate which should be co-administered with a standard-of-care antibiotic, such as tobramycin. A possible formulation could consist of squalene-based nanocarriers, which is also suitable for co-administration of the standard-of-care antibiotic tobramycin.[141] Moreover, the co-administration of a PqsR inverse

agonist with another antibiotic of the aminoglycosides, such as gentamycin is conceivable. In addition to this, also novel therapeutics could be combined with a pathoblocker, such as the outer membrane protein targeting antibiotic (OMPTA) POL7306 from Polyphor which is in preclinical trials at the moment.[142] Another possible and attractive combination would be the co-administration of a PqsR inverse agonist with another pathoblocker, such as compounds targeting LasB or LecB.[143–145]

Even though, compounds of "Class E" have preclinical candidate status, preclinical development poses a tough challenge. The successful preclinical candidate has to be synthesized in large quantities in GMP quality and moreover development of a suitable formulation might be a further obstacle to tackle. Moreover, further toxicology studies are needed to prove the preclinical candidate safe. In addition, *in vivo* efficacy of "Class E" compounds needs to be verified, as well as a preclinical proof of concept. Taken all together, the journey towards a new compound to enter clinical trials is far from over and requires more time and deeper profiling.

6. Experimental Section

6.1. General Information

Solvents and chemicals were used from *Zentrales Chemikalienlager der Universität des Saarlandes* or specified vendors (*Carbolution, Acros Organics, Sigma Aldrich, Fluorochem, TCI, abcr, Alfa Aesar, VWR).*

For **thin-layer chromatography**, *Merck* Silica 60 F_{254} plates were used. Visualization was accomplished with UV-light (λ = 254 nm) and $KMnO_4$.

For **automated flash chromatography**, either a *Teledyne ISCO CombiFlash Rf+ 150* or a *Teledyne ISCO CombiFlash NEXTGEN 300+* equipped with *RediSepRf* silica columns were used.

NMR spectra were recorded on either a *Bruker* 300 MHz or a *Bruker UltraShield Plus* 500 MHz device. Chemical shifts (δ) were given in parts per million (ppm) and referenced against the residual solvent peak. Coupling constants (*J*) were given in Hertz (Hz). Multiplicities were described using the abbreviations s (singlet), bs (broad singlet), d (doublet), dd (doublet of a doublet), ddd (doublet of a doublet of a doublet), t (triplet), dt (doublet of a triplet), q (quartet), hept (heptet) and m (multiplet).

Liquid chromatography-mass spectrometry (LC-MS) spectra were measured on a Thermo Scientific DIONEX UltiMate3000 consisting of a diode array detector, column compartment, autosampler and pump.

High resolution mass (HRMS) was determined by LC-MS/MS using Thermo Scientific Q Exactive Focus Orbitrap LC-MS/MS system.

Microwave-assisted syntheses were carried out in a *CEM Discover Explorer Hybrid 12* microwave synthesis system.

For **pictures of cocrystal structures** MOE2019.0102 was used.

6.2. Syntheses

General Procedure 1: Phenol alkylation

To a suspension of the phenol derivative (1.0 eq.) and K_2CO_3 (3.0 eq.) in DMF (1 mL/mmol) was added the corresponding alkylation agent (1.0 eq.). The reaction mixture was stirred at the temperature as stated until full conversion (TLC). After cooling to r.t. the reaction mixture was quenched with saturated NH_4Cl solution and extracted with EtOAc. The combined organic layers were washed with saturated LiCl solution and dried over Na_2SO_4, filtrated and evaporated under reduced pressure. The crude product was used without further purification.

General Procedure 2: *Sonogashira* coupling

To a solution of *N*-(prop-2-yn-1-yl)-2-(trifluoromethyl)pyridin-4-amine **1.25** (1.0 eq.) in dry DMF (5 mL/mmol) was added DIPEA (2.1 eq.) and the corresponding aryl iodide (1.0 eq.). The reaction mixture was purged with argon three times and $Pd(PPh_3)_4$ (5 mol%) and CuI (5 mol%). After stirring for 18 h at 80 °C, the reaction mixture was quenched with saturated NH_4Cl solution and extracted with EtOAc. The combined organic layers were washed with saturated LiCl solution and dried over Na_2SO_4, filtrated and evaporated under reduced pressure. The crude product was purified *via* automated flash chromatography.

General Procedure 3: Hydrogenation

The corresponding alkyne (1.0 eq.) was dissolved in methanol (5 mL/mmol). The solution was purged with argon for 10 minutes and the hydrogenation catalyst (5 mol%) was added. The reaction mixture was purged with argon for 10 minutes and H_2 was bubbled through the solution for 10 minutes. The reaction mixture was stirred at room temperature under an atmosphere of H_2 for 18 h. After full conversion (LCMS) the mixture was filtered over silica gel and the solvent was evaporated under reduced pressure. The crude product was purified *via* automated flash chromatography.

General Procedure 4: Diazotation/CuAAC

To a solution of the corresponding aniline (0.100 mmol) in MeCN (10 mL/mmol) was added *tert*-butyl nitrite (0.110 mmol, 12.6 mg, 14.5 µL) at 0 °C. After stirring for 5 minutes trimethylsilylazide (0.110 mmol, 13.3 mg, 15.2 µL) was slowly added. The mixture was stirred for 2 h and *N*-(prop-2-yn-1-yl)-2-(trifluoromethyl)pyridine-4-amine **1.25** (0.120 mmol, 24.0 mg) was added at r.t. in one portion. After addition of DIPEA (0.120 mmol, 15.5 mg, 20.9 µL), the reaction mixture was purged with argon and $CuSO_4 \cdot 5\ H_2O$ (2.5 mg, 10 mol%) and Na-ascorbate (3.9 mg, 20 mol%) were added. The mixture was again purged with argon and stirred at room temperature. After LCMS analysis indicated full conversion, saturated NH_4Cl solution was added to the reaction mixture and stirred for 5 minutes. Then EtOAc and saturated EDTA solution were added and the mixture was stirred for 15 minutes until the aqueous phase showed a clear blue color. The phases were separated and the aqueous phase was extracted with EtOAc three times. The combined organic layers were dried over $MgSO_4$, filtered and concentrated *in vacuo*. The crude product was purified *via* automated flash chromatography.

General Procedure 5: S_NAr using alcohols as nucleophiles

The corresponding alcohol (1.0 eq.) was dissolved in DMF (3 mL/mmol) and Cs_2CO_3 (3.0 eq.) was added in one portion. The reaction mixture was stirred at r.t. for 10 minutes and the corresponding nitrobenzene (1.0 eq.) was added in one portion. The reaction mixture was stirred at 80 °C for 16 h,

allowed to cool to r.t. and extracted three times with EtOAc. The combined organic layers were washed with saturated LiCl solution, dried over $MgSO_4$, and concentrated *in vacuo*. The crude product was used in the next step without further purification.

General Procedure 6: S_NAr using *N*–heterocycles as nucleophiles

The corresponding *N*–heterocycle (1.0 eq.) and 1-chloro-4-nitrobenzene (1.0 eq.) were dissolved in DMF (2 mL/mmol) and Cs_2CO_3 (3.0 eq.) was added. The mixture was stirred in a pre-heated oilbath at 80 °C until LCMS analysis showed full conversion. The mixture was allowed do cool to room temperature and H_2O was added. The mixture was stirred for 10 minutes and then extracted three times with EtOAc. The combined organic layers were washed with saturated LiCl solution, dried over Na_2SO_4, filtered and concentrated *in vacuo*. The crude product was used in the next step without further purification.

General Procedure 7: Reduction of nitrobenzenes

The corresponding nitro arene (1.0 eq.) was dissolved in MeOH (5 mL/mmol) and the solution was purged with argon for 10 minutes. Pt/C (5 mol%) was added and the reaction mixture was again purged with argon for 10 minutes. Subsequently H_2 was bubbled through the solution for 15 minutes and the reaction mixture was stirred under an H_2 atmosphere until the starting material was fully consumed (LCMS). The mixture was filtered over silica gel, washed with EtOAc and concentrated *in vacuo*. The crude product was used in the next step without further purification.

General Procedure 8: *Buchwald-Hartwig* coupling of fluoro-1*H*-indazoles

N-((1-(4-bromophenyl)-1*H*-1,2,3-triazol-4-yl)methyl)-2-(trifluoromethyl)pyridin-4-amine (1.0 eq.) and the corresponding fluoro-1*H*-indazole (1.0 eq.) were dissolved in 1,4-dioxane (10 mL/mmol). Then, Cs_2CO_3 (1.1 eq.) was added and the reaction mixture was purged with argon for 10 minutes. Pd-175 (5 mol%) was added and the solution was purged again with argon for 15 minutes. The reaction mixture was then stirred for 24 h in a pre-heated oil bath at 90 °C. After cooling to room temperature H_2O was added, followed by extraction with EtOAc. The combined organic layers were dried over Na_2SO_4 and the solvent was removed under reduced pressure. The crude product was purified *via* automated flash chromatography (PE/EtOAc).

Di-*tert*-butyl (2-(trifluoromethyl)pyridin-4-yl)carbamate 1.7

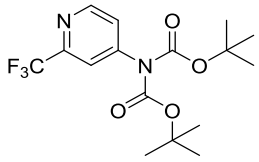

To a solution of 2-trifluoromethyl-4-aminopyridine (3.24 g, 20.0 mmol) in DCM (60 mL) were added Boc_2O (9.82 g, 45.0 mmol), DIPEA (7.66 mL, 44.0 mmol) and DMAP (806 mg, 6.60 mmol). The reaction mixture was stirred for 18 h at r.t. and saturated NH_4Cl solution was added followed by extraction with EtOAc. The combined organic layers were washed with Brine, dried over Na_2SO_4, filtrated and evaporated under reduced pressure. The crude product was obtained as white crystals (7.14 g, 19.7 mmol, > 98%) and used in the next step without further purification.

TLC: R_f = 0.68 (PE/EtOAc 9:1)

LC-MS: m/z: 363 $(M+H)^+$

^{1}H-NMR (300 MHz, $CDCl_3$): δ [ppm] = 8.72 (d, *J* = 5.4 Hz, 1 H), 7.52 (d, *J* = 1.7 Hz, 1 H), 7.31 (dd, *J* = 5.3 Hz, *J* = 1.8 Hz, 1 H), 1.47 (s, 18 H).

^{13}C-NMR (76 MHz, $CDCl_3$): δ [ppm] = 150.8, 150.3, 148.1, 124.2, 122.5, 119.0, 118.1, 84.53, 27.78.

***Tert*-butyl (2-(trifluoromethyl)pyridin-4-yl)carbamate 1.8**

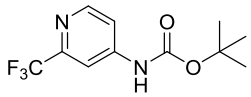

Di-tert-butyl (2-(trifluoromethyl)pyridin-4-yl)carbamate **1.7** (2.17 g, 6.00 mmol) was dissolved in DCM/TFA 9:1 (12 mL) and stirred for 16 h at r.t. until the starting material was fully consumed (TLC control). Saturated Na_2CO_3 solution was added followed by extraction with DCM. The combined organic layers were dried over Na_2SO_4 filtrated and concentrated *in vacuo*. The desired compound (1.55 g, 5.91 mmol, > 98%) was used without further purification.

TLC: R_f = 0.43 (PE/EtOAc 8:2)

LC-MS: m/z: 207 $(M-t\text{Bu}+H)^+$

^{1}H-NMR (300 MHz, $CDCl_3$): δ [ppm] = 8.53 (d, *J* = 5.6 Hz, 1 H), 7.78 (d, *J* = 2.0 Hz, 1 H), 7.44 (dd, *J* = 5.5 Hz, *J* = 2.1 Hz, 1 H), 6.92 (bs, 1 H), 1.53 (s, 9 H).

^{13}C-NMR (76 MHz, $CDCl_3$): δ [ppm] = 151.4, 150.8, 146.9, 133.2), 114.2, 109.3, 109.2, 82.48, 28.16.

***Tert*-butyl allyl(2-(trifluoromethyl)pyridin-4-yl)carbamate 1.9**

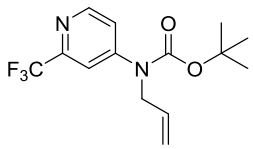

A solution of *tert*-butyl(2-(trifluoromethyl)pyridin-4-yl)carbamate **1.8** (1.49 g, 5.70 mmol) was cooled to 0 °C and NaH (60 wt%) (273 mg, 6.83 mmol) were added portionwise under vigorous stirring. After 1 h the reaction mixture was warmed to r.t. and allylbromide (0.62 mL, 7.40 mmol) was added dropwise and stirred for 3 h at r.t. Addition of saturated NH_4Cl solution and extraction with Et_2O followed by washing the combined organic layers with saturated LiCl solution yielded the crude product after drying over Na_2SO_4, filtration and concentration *in vacuo*, which was purified by automated flash chromatography (PE/EtOAc). The title compound (1.65 g, 5.47 mmol, 96%) was isolated as a white solid.

LC-MS: m/z: 247 $(M\text{-}t\text{Bu}+H)^+$

^{1}H-NMR (300 MHz, $CDCl_3$): δ [ppm] = 8.62 (d, *J* = 5.6, 1 H), 7.84 (d, *J* = 2.1 Hz, 1 H), 7.54 (dd, *J* = 5.5 Hz, *J* = 2.2 Hz, 1 H), 5.90 – 5.87 (m, 1 H), 5.28 – 5.25 (m, 1 H), 5.23 – 5.21 (m, 1 H), 5.03 (bs, 1 H), 4.58 – 4.57 (m, 2 H).

***Tert*-butyl (*E*)-(3-(4-chlorophenyl)allyl)(2-(trifluoromethyl)pyridin-4-yl)carbamate 1.11**

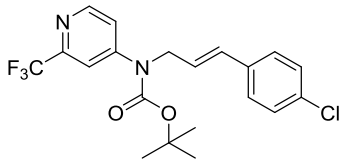

Tert-butyl allyl(2-(trifluoromethyl)pyridin-4-yl)carbamate **1.9** (52.9 mg, 0.175 mmol), and 1-chloro-4-iodobenzene (41.7 mg, 0.175 mmol) were dissolved in THF and 1 M NaOH (0.52 mL, 0.525 mmol) was added. The reaction mixture was purged with argon for 15 minutes and $PdCl_2$(dppf) (6.4 mg, 5 mol%) was added. The solution was purged with argon for 10 more minutes and then stirred for 18 h at 70 °C. The reaction mixture was allowed to cool to room temperature, 1 M HCl was added and extracted with EtOAc. The combined organic layers were dried over $MgSO_4$, filtered and the solvent was removed under reduced pressure. Automated flash chromatography (PE/EtOAc) afforded the title compound as a white solid (50.0 mg, 0.121 mmol, 69%).

LC-MS: m/z: 356 $(M\text{-}t\text{Bu}+H)^+$

^{1}H-NMR (300 MHz, $CDCl_3$): δ [ppm] = 8.60 (d, *J* = 5.5 Hz, 1 H), 7.81 (d, *J* = 2.1 Hz, 1 H), 7.44 (dd, *J* = 5.5 Hz, *J* = 2.1 Hz, 1 H), 7.32 – 7.28 (m, 4 H), 6.48 (dd, *J* = 16.0 Hz, *J* = 1.5 Hz, 1 H), 6.26 (dt, *J* = 16.0 Hz, *J* = 5.4 Hz, 1 H), 4.52 (dd, *J* = 5.4 Hz, *J* = 1.5 Hz, 1 H), 1.54 (s, 9 H).

(*E*)-*N*-(3-(4-chlorophenyl)allyl)-2-(trifluoromethyl)pyridin-4-amine 1.12

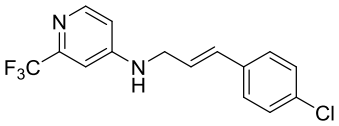

Tert-butyl (*E*)-(3-(4-chlorophenyl)allyl)(2-(trifluoromethyl)pyridin-4-yl)carbamate **1.11** (48.0 mg, 153 mmol) were dissolved in DCM (2 mL) and TFA (2 mL) was added. The reaction mixture was stirred for 24 h at r.t. and saturated $NaHCO_3$ solution was added carefully. The phases were separated and the aqueous phase was extracted twice with DCM. The combined organic layers were dried over Na_2SO_4 and the solvent was removed under reduced pressure. Automated flash chromatography (PE/EtOAc) afforded the title compound as a yellow solid (47.4 mg, 0.152 mmol, > 98%).

^{1}H-NMR (300 MHz, $CDCl_3$): δ [ppm] = 8.25 (d, *J* = 6.0 Hz, 1 H), 7.24-7.30 (m, 4 H), 6.94 (d, *J* = 2.3 Hz, 1 H), 6.66 (dd, *J* = 5.9 Hz, *J* = 2.3 Hz, 1 H), 6.55 (d, *J* = 15.9 Hz, 1 H), 6.19 (dt, *J* = 15.9 Hz, *J* = 5.6 Hz, 1 H), 5.94 (bs, 1 H, NH), 4.03 (d, *J* = 5.5 Hz, 2 H).

^{13}C-NMR (76 MHz, $CDCl_3$): δ [ppm] = 155.1, 148.2, 134.5, 133.7, 131.7, 128.8, 127.6, 124.4, 108.9, 44.77.

HRMS (ESI): $C_{15}H_{13}ClF_3N_2^+$ $(M+H)^+$ calculated: 313.07139 found: 313.07065

***N*-(3-phenylpropyl)-2-(trifluoromethyl)pyridin-4-amine 1.13**

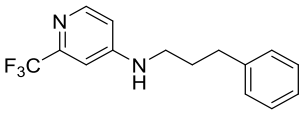

N-(3-(4-chlorophenyl)prop-2-yn-1-yl)-2-(trifluoromethyl)pyridin-4-amine **1.27** (10.2 mg, 0.033 mmol) was dissolved in MeOH (0.66 mL) and the reaction mixture was purged with argon. Then, Pd black (0.4 mg, 10 mol%) was added and the reaction mixture was purged again with argon. After stirring for 10 minutes, H_2 was bubbled through the solution and the mixture was stirred for 2 h under an atmosphere of H_2. The mixture was then filtered over SiO_2 and washed with EtOAc. The title compound was obtained as a colorless solid (9.1 mg, 0.033 mmol, > 98%).

^{1}H-NMR (300 MHz, $CDCl_3$): δ [ppm] = 8.26 (d, *J* = 5.7 Hz, 1 H), 7.35 – 7.29 (m, 2 H), 7.26 – 7.19 (m, 3 H), 6.74 (d, *J* = 2.4 Hz, 1 H), 6.48 (dd, *J* = 5.7 Hz, *J* = 2.4 Hz, 1 H), 4.40 (bs, 1 H), 3.23 (dd, *J* = 13.5 Hz, *J* = 6.9 Hz, 2 H), 2.75 (dd, *J* = 7.5 Hz, 2 H), 2.06 – 1.95 (m, 2 H).

^{13}C-NMR (75 MHz, $CDCl_3$): δ [ppm] = 154.1, 150.1, 148.9, 140.8, 128.8, 128.6, 128.3, 126.3, 123.6, 108.9, 104.2, 42.13, 33.11, 30.27, 29.69.

HRMS (ESI): $C_{15}H_{16}F_3N_2^+$ $(M+H)^+$ calculated: 281.12601 found: 281.12531

***N*-(3-(4-chlorophenyl)propyl)-2-(trifluoromethyl)pyridin-4-amine**

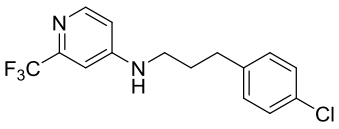

N-(3-(4-chlorophenyl)prop-2-yn-1-yl)-2-(trifluoromethyl)pyridin-4-amine **1.27** (10.3 mg, 0.033 mmol) was dissolved in MeOH (0.66 mL) and the reaction mixture was purged with argon. The mixture was cooled to 0 °C and Pd black (0.4 mg, 10 mol%) was added and the reaction mixture was purged again with argon. After stirring for 10 minutes, H_2 was bubbled through the solution and the mixture was stirred for 10 min under an atmosphere of H_2. The mixture was then purified *via* automated flash chromatography (PE/EtOAc). The title compound was obtained as a colorless solid (9.3 mg, 0.033 mmol, > 98%).

^{1}H-NMR (300 MHz, $CDCl_3$): δ [ppm] = 8.27 (d, *J* = 5.7 Hz, 1 H), 7.31 – 7.28 (m, 2 H), 7.14 – 7.11 (m, 2 H), 6.75 – 6.74 (m, 1 H), 6.50 – 6.48 (m, 1 H), 4.41 (bs, 1 H), 3.25 – 3.18 (m, 2 H), 2.74 – 2.69 (m, 2 H), 2.01 – 1.92 (m, 2 H).

^{13}C-NMR (75 MHz, $CDCl_3$): δ [ppm] = 154.5, 150.6, 149.1, 139.6, 132.5, 130.1, 129.2, 123.9, 120.4, 109.3, 104.7, 42.41, 32.84, 30.70.

HRMS (ESI): $C_{15}H_{15}ClF_3N_2^+$ $(M+H)^+$ calculated: 315.08704 found: 315.08674

***Tert*-butyl (*E*)-(3-(4-phenoxyphenyl)allyl)(2-(trifluoromethyl)pyridin-4-yl)carbamate 1.16**

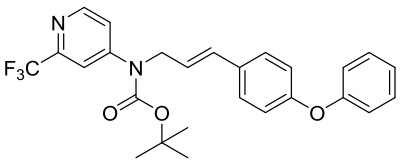

4-Phenoxyaniline (300 mg, 1.62 mmol) was dissolved in Et_2O (2 mL) and cooled to 0 °C. $HB_4{\cdot}H_2O$ (1.02 mL, 5.18 mmol) was then added slowly, followed by $NaNO_2$ (112 mg, 1.62 mmol) in H_2O (1 mL). The mixture was stirred for 1 h, filtered and washed with cold EtOH and Et_2O. The filter residue was dissolved in acetone and 4-phenoxybenzenediazonium tetrafluoro borate was precipitated and filtrated to yield a purple solid (250 mg, 0.880 mmol, 70%).

Tert-butyl allyl(2-(trifluoromethyl)pyridin-4-yl)carbamate **1.9** (91.0 mg, 0.300 mmol), NaOAc (61.0 mg, 0.750 mmol) and Pd_2dba_3 (9 mg, 4 mol%) were suspended in PhCN (1 mL). 4-phenoxybenzenediazonium tetrafluoro borate (71.0 mg, 0.250 mmol) was added the reaction mixture was stirred open-flask for 2 h at room temperature. The mixture was filtered and the solvent

was removed *in vacuo*. The crude product was purififed using automated flash chromatography (PE/EtOAc) and afforded the title compound as a brownish solid (41.1 mg, 0.088 mmol, 35%).

LC-MS: m/z: 414 $(M\text{-}t\text{Bu}+H)^+$

***Tert*-butyl (*E*)-(3-(6-chloropyridin-2-yl)allyl)(2-(trifluoromethyl)pyridin-4-yl)carbamate 1.17**

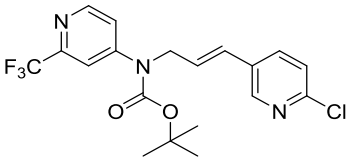

Tert-butyl allyl(2-(trifluoromethyl)pyridin-4-yl)carbamate **1.9** (52.9 mg, 0.175 mmol) and 1-chloro-4-iodobenzene (41.79mg, 0.175 mmol) were dissolved in THF and 1 M NaOH (0.52 mL, 0.525 mmol) was added. The reaction mixture was purged with argon for 15 minutes and $PdCl_2$(dppf) (6.4 mg, 5 mol%) was added. The solution was purged with argon for 10 more minutes and then stirred for 18 h at 70 °C. The reaction mixture was allowed to cool to room temperature, 1 M HCl was added and extracted with EtOAc. The combined organic layers were dried over $MgSO_4$, filtered and the solvent was removed under reduced pressure. Automated flash chromatography (PE/EtOAc) afforded the title compound as a colorless solid (18.8 mg, 0.046 mmol, 26%).

LC-MS: m/z: 357 $(M\text{-}t\text{Bu}+H)^+$

(*E*)-*N*-(3-(4-phenoxyphenyl)allyl)-2-(trifluoromethyl)pyridin-4-amine 1.18

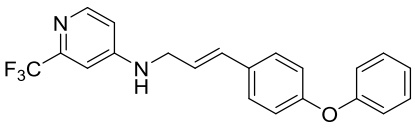

Tert-butyl (*E*)-(3-(4-phenoxyphenyl)allyl)(2-(trifluoromethyl)pyridin-4-yl)carbamate **1.16** (28.0 mg, 0.060 mmol) was dissolved in DCM (2 mL) and TFA (2 mL) was added. The reaction mixture was stirred at room temperature for 24 h. After slow addition of saturated Na_2CO_3 solution the reaction mixture was extracted with EtOAc and the combined organic layers were dried over $MgSO_4$. The crude product was purified *via* automated flash chromatography (PE/EtOAc) and afforded the title compound as a colorless solid (21.8 mg, 0.059 mmol, > 98%).

HRMS (ESI): $C_{21}H_{18}F_3N_2O^+$ $(M+H)^+$ calculated: 371.13657 found: 371.13593

(*E*)-*N*-(3-(6-chloropyridin-2-yl)allyl)-2-(trifluoromethyl)pyridin-4-amine 1.19

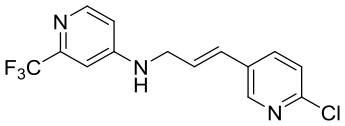

Tert-butyl (*E*)-(3-(6-chloropyridin-2-yl)allyl)(2-(trifluoromethyl)pyridin-4-yl)carbamate **1.17** (18.8 mg, 0.046 mmol) was dissolved in DCM (2 mL) and TFA (2 mL) was added. The reaction mixture was stirred at room temperature for 24 h. After slow addition of saturated Na_2CO_3 solution the reaction mixture was extracted with EtOAc and the combined organic layers were dried over $MgSO_4$. The crude product was purified *via* automated flash chromatography (PE/EtOAc) and afforded the title compound as a colorless solid (14.1 mg, 0.045 mmol, > 98%).

^{1}H-NMR (300 MHz, $CDCl_3$): δ [ppm] = 8.33 (d, *J* = 2.2 Hz, 1 H), 8.26 (d, *J* = 6.5 Hz, 1 H), 7.67 (dd, *J* = 8.3 Hz, *J* = 2.4 Hz), 7.31 (d, *J* = 8.4 Hz, 1 H), 7.13 (d, *J* = 1.8 Hz, 1 H), 6.82 (dd, *J* = 6.5 Hz, *J* = 1.8 Hz, 1 H), 5.68 (d, *J* = 15.9 Hz, 1 H), 6.29 (dt, *J* = 16.0 Hz, *J* = 5.4 Hz, 1 H), 4.15 (d, *J* = 5.0 Hz, 2 H).

^{13}C-NMR (76 MHz, $CDCl_3$): δ [ppm] = 157.1, 147.8, 130.4, 128.3, 125.9, 124.5, 124.3, 120.4, 101.4, 57.82.

HRMS (ESI): $C_{14}H_{12}ClF_3N_3^+$ $(M+H)^+$ calculated: 314.06664 found: 314.06604

1-Ethoxy-4-iodobenzene 1.20a

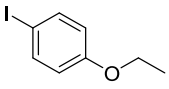

The compound was prepared according to **GP1**. 4-Iodophenol (550 mg, 2.50 mmol) and ethyl iodide (0.22 mL, 429 mg, 2.75 mmol) were used. The reaction was stirred at 70 °C. The crude product was obtained as a colorless oil (620 mg, 2.50 mmol, > 98%).

TLC: R_f = 0.75 (PE/EtOAc 8:2)

^{1}H-NMR (300 MHz, $CDCl_3$): δ [ppm] = 7.53 (d, *J* = 8.9 Hz, 2 H), 6.66 (d, *J* = 8.8 Hz, 2 H), 3.98 (q, *J* = 8.7 Hz, 2 H), 1.39 (t, *J* = 7.0 Hz, 3 H).

^{13}C-NMR (76 MHz, $CDCl_3$): δ [ppm] = 158.9, 138.3, 117.0, 82.57, 67.67, 14.82.

1-Iodo-4-isopropoxybenzene 1.20b

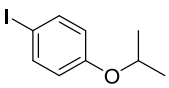

The compound was prepared according to **GP1**. 4-Iodophenol (550 mg, 2.50 mmol) and isopropyl bromide (0.24 mL, 310 mg, 2.50 mmol) were used. The reaction was stirred at 70 °C. The crude product was obtained as a colorless oil (397 mg, 1.51 mmol, 61%).

TLC: R_f = 0.77 (PE/EtOAc 8:2)

^{1}H-NMR (300 MHz, $CDCl_3$): δ [ppm] = 7.53 (d, *J* = 8.3 Hz, 2 H), 6.66 (d, *J* = 8.3 Hz, 2 H), 4.49 (sept, *J* = 6.1 Hz, 1 H), 1.33 (dd, *J* = 6.1 Hz, *J* = 0.7 Hz, 6 H).

^{13}C-NMR (76 MHz, $CDCl_3$): δ [ppm] = 157.9, 138.4, 118.4, 82.51, 70.25, 22.06.

2-Fluoro-4-iodo-1-methoxybenzene 1.21a

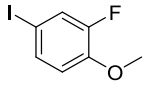

The compound was prepared according to **GP1**. 2-Fluoro-4-iodophenol (238 mg, 1.00 mmol) and methyl iodide (0.10 mL, 14.2 mg, 1.00 mmol) were used. The reaction was stirred at 40 °C. The crude product was obtained as a colorless oil (248 mg, 0.987 mmol, > 98%).

TLC: R_f = 0.74 (PE/EtOAc 8:2)

^{1}H-NMR (300 MHz, $CDCl_3$): δ [ppm] = 7.41 – 7.39 (m, 1 H), 7.36 (s, 1 H), 6.78 – 6.69 (m, 1 H), 3.87 (s, 1 H).

^{13}C-NMR (76 MHz, $CDCl_3$): δ [ppm] = 152.6, 148.2, 133.6, 125.3, 115.5, 81.14, 56.51.

1-Ethoxy-2-fluoro-4-iodobenzene 1.21b

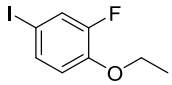

The compound was prepared according to **GP1**. 2-Fluoro-4-iodophenol (160 mg, 0.670 mmol) and ethyl iodide (0.05 mL, 105 mg, 0.670 mmol) were used. The reaction was stirred at 70 °C. The crude product was obtained as a red oil (111 mg, 0.420 mmol, 63%).

TLC: R_f = 0.74 (PE/EtOAc 8:2)

^{1}H-NMR (300 MHz, $CDCl_3$): δ [ppm] = 7.38 (dd, *J* = 8.3 Hz, *J* = 2.1 Hz, 1 H), 7.34 (dd, *J* = 2.1 Hz, 1.4 Hz, 1 H), 6.73-6.67 (m, 1 H), 4.08 (q, *J* = 3.0 Hz, 2 H), 1.44 (t, *J* = 2.0 Hz, 3 H).

^{13}C-NMR (76 MHz, $CDCl_3$): δ [ppm] = 153.5, 147.1, 133.2, 125.1, 116.4, 80.86, 64.94, 14.65.

2-Fluoro-4-iodo-1-isopropoxybenzene 1.21c

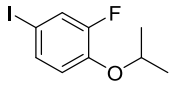

The compound was prepared according to **GP1**. 2-Fluoro-4-iodophenol (95.2 mg, 0.40 mmol) and isopropyl bromide (0.04 mL, 50.0 mg, 0.40 mmol) were used. The reaction was stirred at 60 °C. The crude product was obtained as a red oil (65.6 mg, 0.23 mmol, 58%).

TLC: R_f = 0.75 (PE/EtOAc 8:2)

^{1}H-NMR (300 MHz, $CDCl_3$): δ [ppm] = 7.40 – 7.35 (m, 1 H), 7.33 (dd, *J* = 2.0 Hz, *J* = 1.4 Hz, 1 H), 6.75 – 6.69 (m, 1 H), 4.50 (sept, *J* = 6.0 Hz, 1 H), 1.34 (d, *J* = 6.1 Hz).

^{13}C-NMR (76 MHz, $CDCl_3$): δ [ppm] = 154.9, 145.6, 132.8, 125.2, 118.9, 81.11, 72.16, 21.53.

2-Chloro-4-iodo-1-methoxybenzene 1.22a

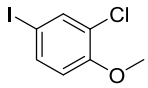

The compound was prepared according to **GP1**. 2-Chloro-4-iodophenol (127 mg, 0.500 mmol) and methyl iodide (0.05 mL, 7.1 mg, 0.500 mmol) were used. The reaction was stirred at 40 °C. The crude product was obtained as a colorless oil (133 mg, 0.497 mmol, > 98%).

TLC: R_f = 0.76 (PE/EtOAc 8:2)

^{1}H-NMR (300 MHz, $CDCl_3$): δ [ppm] = 7.67 (d, *J* = 2.1 Hz, 1 H), 7.52 (dd, *J* = 8.7 Hz, *J* = 2.2 Hz, 1 H), 6.68 (d, *J* = 8.8 Hz, 1 H), 3.89 (s, 3 H).

^{13}C-NMR (76 MHz, $CDCl_3$): δ [ppm] = 155.1, 138.2, 136.6, 123.8, 113.9, 81.92, 56.23.

2-Chloro-1-ethoxy-4-iodobenzene 1.22b

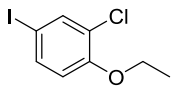

The compound was prepared according to **GP1**. 2-Chloro-4-iodophenol (100 mg, 0.400 mmol) and ethyl iodide (0.03 mL, 62.4 mg, 0.400 mmol) were used. The reaction was stirred at 70 °C. The crude product was obtained as a colorless oil (124 mg, 0.44 mmol, > 98%).

TLC: R_f = 0.76 (PE/EtOAc 8:2)

^{1}H-NMR (300 MHz, $CDCl_3$): δ [ppm] = 7.65 (d, *J* = 2.1 Hz, 1 H), 7.48 (dd, *J* = 8.7 Hz, *J* = 2.1 Hz, 1 H), 6.66 (d, *J* = 8.7 Hz, 1 H), 4.08 (q, *J* = 7.0 Hz, 2 H), 1.46 (t, *J* = 7.0 Hz, 3 H).

^{13}C-NMR (76 MHz, $CDCl_3$): δ [ppm] = 154.7, 138.4, 136.6, 124.4, 115.3, 81.85, 65.01, 14.74.

2-Chloro-4-iodo-1-isopropoxybenzene 1.22c

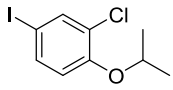

The compound was prepared according to **GP1**. 2-Chloro-4-iodophenol (70 mg, 0.28 mmo) and isopropyl bromide (0.03 mL, 34.4 mg, 0.28 mmol) were used. The reaction was stirred at 60 °C. The crude product was obtained as a yellow oil (51.2 mg, 0.17 mmol, 61%).

TLC: R_f = 0.75 (PE/EtOAc 8:2)

^{1}H-NMR (300 MHz, $CDCl_3$): δ [ppm] = 7.65 (d, *J* = 2.1 Hz, 1 H), 7.46 (dd, *J* = 8.6 Hz, *J* = 2.2 Hz, 1 H), 6.69 (d, *J* = 8.7 Hz, 1 H), 4.51 (sept, *J* = 6.1 Hz, 1 H), 1.36 (d, *J* = 6.1 Hz, 6 H).**^{13}C-NMR** (76 MHz, $CDCl_3$): δ [ppm] = 153.7, 138.4, 136.4, 125.5, 117.5, 82.00, 72.26, 21.90.

4-iodo-1-methoxy-2-methylbenzene 1.23a

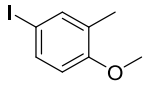

The compound was prepared according to **GP1**. 4-Iodo-1-methoxy-2-methylbenzene (117 mg, 0.500 mmol) and methyl iodide (0.05 mL, 7.1 mg, 0.500 mmol) were used. The reaction was stirred at 40 °C. The crude product was obtained as a colorless oil (124 mg, 0.498 mmol, > 98%).

TLC: R_f = 0.76 (PE/EtOAc 8:2)

^{1}H-NMR (300 MHz, $CDCl_3$): δ [ppm] = 7.45 – 7.43 (m, 2 H), 6.58 (d, *J* = 8.4 Hz, 1 H), 3.80 (s, 1 H), 2.17 (s, 3 H).

^{13}C-NMR (76 MHz, $CDCl_3$): δ [ppm] = 157.8, 139.2, 135.6, 129.6, 112.3, 82.61, 55.54, 16.03.

***Tert*-butyl prop-2-yn-1-yl(2-(trifluoromethyl)pyridin-4-yl)carbamate 1.24**

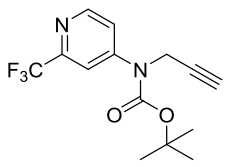

A solution of *tert*-butyl(2-(trifluoromethyl)pyridin-4-yl)carbamate **1.8** (1.49 g, 5.70 mmol) was cooled to 0 °C and NaH (60 wt%) (273 mg, 6.83 mmol) were added portionwise under vigorous stirring. After 1 h the reaction mixture was warmed to r.t. and propargylbromide (0.56 mL, 7.40 mmol) was added dropwise and stirred for 3 h at r.t. Addition of saturated NH_4Cl solution and extraction with Et_2O

followed by washing the combined organic layers with saturated LiCl solution yielded the crude product after drying over Na_2SO_4, filtration and concentration *in vacuo*, which was purified by automate column chromatography (PE/EtOAc). The title compound (1.64 g, 5.47 mmol, 96%) was isolated as a yellow solid.

TLC: R_f = 0.55 (PE/EtOAc 8:2)

LC-MS: m/z: 245 $(M\text{-}t\text{Bu} + H)^+$

^{1}H-NMR (300 MHz, $CDCl_3$): δ [ppm] = 8.63 (d, *J* = 5.5, 1 H), 7.85 (d, *J* = 2.0 Hz, 1 H), 7.55 (dd, *J* = 5.5 Hz, *J* = 2.1 Hz, 1 H), 4.48 (d, *J* = 2.3 Hz, 2 H), 2.25 (t, *J* = 2.4 Hz, 1 H).

^{13}C-NMR (75 MHz, $CDCl_3$): δ [ppm] = 151.8, 150.2, 150.1, 118.8, 114.5, 114.4, 114.3, 83.32, 78.04, 72.81, 38.01, 27.77.

***N*-(prop-2-yn-1-yl)-2-(trifluoromethyl)pyridin-4-amine 1.25**

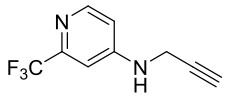

Tert-butyl prop-2-yn-1-yl(2-(trifluoromethyl)pyridin-4-yl)carbamate **1.24** (1.21 g, 4.03 mmol) was dissolved in DCM (1 mL) and TFA (1 mL) was added. After stirring at r.t. for 18 h the mixture was cooled to 0 °C and saturated Na_2CO_3 solution was added. The reaction mixture was extracted with DCM and the combined organic layers were washed with Brine, dried over Na_2SO_4, filtered and concentrated under reduced pressure. Automated flash chromatography (PE/EtOAc) yielded the title compound (820 mg, 4.03 mmol, > 98%) as a white solid.

TLC: R_f = 0.44 (PE/EtOAc 1:1)

LC-MS: m/z: 201 $(M+H)^+$

^{1}H-NMR (300 MHz, $CDCl_3$): δ [ppm] = 8.31 (d, *J* = 6.5 Hz, 1 H), 7.72 (bs, 1 H), 7.16 (d, *J* = 2.1 Hz, 1 H), 6.89 (dd, *J* = 6.5 Hz, *J* = 2.3 Hz, 1 H), 4.10 (d, *J* = 2.4 Hz, 2 H), 2.33 (t, *J* = 2.6 Hz, 1 H).

^{13}C-NMR (75 MHz, $CDCl_3$): δ [ppm] = 156.7, 145.2, 143.7, 119.33, 109.40, 106.50, 73.80, 73.63, 32.75.

***N*-(3-(4-fluorophenyl)prop-2-yn-1-yl)-2-(trifluoromethyl)pyridin-4-amine 1.26**

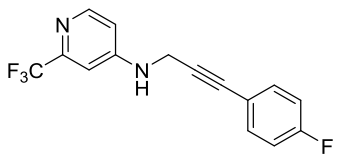

The compound was prepared according to **GP2**. *N*-(prop-2-yn-1-yl)-2-(trifluoromethyl)pyridin-4-amine **1.25** (40.0 mg, 0.200 mmol), 1-fluoro-4-iodobenzene (44.4 mg, 0.200 mmol), DIPEA (712 µL, 54 mg 0.420 mmol), $Pd(PPh_3)_4$ (11.4 mg, 5 mol%) and CuI (1.90 mg 5 mol%) were used. Automated flash chromatography (PE/EtOAc) afforded the title compound as a yellow solid (8.82 mg, 0.030 mmol, 15%).

^{1}H-NMR (300 MHz, $CDCl_3$): δ [ppm] = 8:36 (d, *J* = 5.6 Hz, 1 H), 7.41 – 7.36 (m, 2 H), 7.04 – 6.95 (m, 3 H), 6.71 – 6.68 (m, 1 H), 4.95 (bs, 1 H), 4.24 – 4.21 (m, 2 H).

^{13}C-NMR (75 MHz, $CDCl_3$): δ [ppm] = 164.4, 161.0, 153.3, 150.2, 149.1, 148.6, 133.7, 123.5, 119.9, 118.2, 115.8, 109.6, 105.0, 83.35, 33.26.

HRMS (ESI): $C_{15}H_{11}F_4N_2^+$ $(M+H)^+$ calculated: 295.08529 found: 295.08466

***N*-(3-(4-chlorophenyl)prop-2-yn-1-yl)-2-(trifluoromethyl)pyridin-4-amine 1.27**

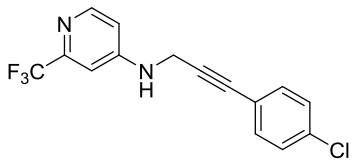

The compound was prepared according to **GP2**. *N*-(prop-2-yn-1-yl)-2-(trifluoromethyl)pyridin-4-amine **1.25** (40.0 mg, 0.200 mmol), 1-chloro-4-iodobenzene (47.6 mg, 0.200 mmol), DIPEA (712 µL, 54 mg 0.420 mmol), $Pd(PPh_3)_4$ (11.4 mg, 5 mol%) and CuI (1.90 mg 5 mol%) were used. Automated flash chromatography (PE/EtOAc) afforded the title compound as a white solid (8.06 mg, 0.026 mmol, 13%).

^{1}H-NMR (300 MHz, $CDCl_3$): δ [ppm] = 8.24 (d, *J* = 5.7 Hz, 1 H), 7.55 (t, *J* = 5.7 Hz, NH), 7.38 – 7.45 (m, 4 H), 7.04 (d, *J* = 2.2 Hz, 1 H), 6.83 (dd, *J* = 5.7 Hz, *J* = 2.2 Hz, 1 H), 4.30 (d, *J* = 5.7 Hz, 2 H).

^{13}C-NMR (75 MHz, $CDCl_3$): δ [ppm] = 153.9, 149.9, 133.4, 133.1, 128.9, 120.9, 87.31, 81.55, 31.87.

HRMS (ESI): $C_{15}H_{11}ClF_3N_2^+$ $(M+H)^+$ calculated: 311.05574 found: 311.05521

***N*-(3-(4-bromophenyl)prop-2-yn-1-yl)-2-(trifluoromethyl)pyridin-4-amine 1.28**

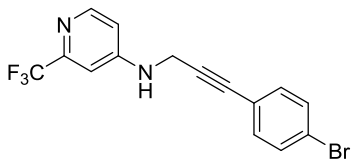

The compound was prepared according to **GP2**. *N*-(prop-2-yn-1-yl)-2-(trifluoromethyl)pyridin-4-amine **1.25** (40.0 mg, 0.200 mmol), 1-bromo-4-iodobenzene (56.4 mg, 0.200 mmol), DIPEA (712 µL, 54 mg 0.420 mmol), $Pd(PPh_3)_4$ (11.4 mg, 5 mol%) and CuI (1.90 mg 5 mol%) were used. Automated flash

chromatography (PE/EtOAc) afforded the title compound as a brown solid 1.42 (8.06 mg, 0.040 mmol, 2%).

^{1}H-NMR (300 MHz, $CDCl_3$): δ [ppm] = 8.37 (d, *J* = 5.6 Hz, 1 H), 7.44 (d, *J* = 8.2 Hz, 2 H), 7.24 – 7.26 (m, 2 H), 6.94 – 6.93 (m, 1 H), 6.69 (dd, *J* = 5.6 Hz, *J* = 1.8 Hz, 1 H), 4.73 (bs, 1 H), 4.22 (d, *J* = 5.8 Hz, 1 H).

^{13}C-NMR (75 MHz, $CDCl_3$): δ [ppm] = 152.9, 150.1, 143.1, 132.9, 131.4, 122.8, 120.8, 111.1, 109.4, 104.8, 84.50, 83.26, 29.44.

LCMS: m/z 356 $(M+H)^+$

***N*-(3-(3-fluorophenyl)prop-2-yn-1-yl)-2-(trifluoromethyl)pyridin-4-amine 1.29**

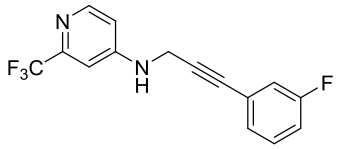

The compound was prepared according to **GP2**. *N*-(prop-2-yn-1-yl)-2-(trifluoromethyl)pyridin-4-amine **1.25** (40.0 mg, 0.200 mmol), 1-fluoro-3-iodobenzene (44.4 mg, 0.200 mmol), DIPEA (712 µL, 54 mg 0.420 mmol), $Pd(PPh_3)_4$ (11.4 mg, 5 mol%) and CuI (1.90 mg 5 mol%) were used. Automated flash chromatography (PE/EtOAc) afforded the title compound as a yellow solid (2.35 mg, 0.080 mmol, 4%).

^{1}H-NMR (300 MHz, $CDCl_3$): δ [ppm] = 8.38 (d, *J* = 5.6 Hz, 1 H), 7.29 – 7.28 (m, 2 H), 7.18 (d, *J* = 6.6 Hz, 1 H), 7.11 – 7.01 (m, 2 H), 6.95 (d, *J* = 2.2 Hz, 1 H), 6.71 (dd, *J* = 5.6 Hz, *J* = 2.3 Hz, 1 H), 4.76 (bs, 1 H), 4.25 (d, *J* = 5.8 Hz, 2 H).

^{13}C-NMR (75 MHz, $CDCl_3$): δ [ppm] = 165.6, 161.0, 153.4, 150.1, 149.2, 148.5, 128.9, 122.4, 119.9, 118.2, 115.8, 109.6, 105.1, 83.36, 33.27.

HRMS (ESI): $C_{15}H_{11}F_4N_2^+$ $(M+H)^+$ calculated: 295.08529 found: 295.08466

***N*-(3-(2,4-difluorophenyl)prop-2-yn-1-yl)-2-(trifluoromethyl)pyridin-4-amine 1.30**

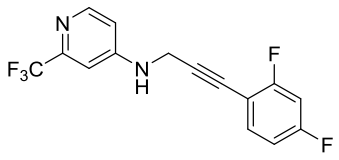

The compound was prepared according to **GP2**. *N*-(prop-2-yn-1-yl)-2-(trifluoromethyl)pyridin-4-amine **1.25** (40.0 mg, 0.200 mmol), 2,4-difluoro-1-iodobenzene (48.0 mg, 0.200 mmol), DIPEA (712 µL, 54 mg 0.420 mmol), $Pd(PPh_3)_4$ (11.4 mg, 5 mol%) and CuI (1.90 mg 5 mol%) were used. Automated flash chromatography (PE/EtOAc) afforded the title compound as a yellow solid (3.12 mg, 0.010 mmol, 5%).

^{1}H-NMR (300 MHz, $CDCl_3$): δ [ppm] = 8.38 (d, *J* = 5.8 Hz, 1 H), 7.09 – 7.06 (m, 1 H), 7.03 – 7.00 (m, 2 H), 6.96 (d, *J* = 2.3 Hz, 1 H), 6.71 (dd, *J* = 5.6 Hz, *J* = 2.3 Hz, 1 H), 4.93 (bs, 1 H), 4.28 (d, *J* = 5.8 Hz, 2 H).

^{13}C-NMR (75 MHz, $CDCl_3$): δ [ppm] = 160.4, 159.1, 157.8, 153.2, 150.3, 149.1, 123.1, 120.3, 119.5, 117.2, 111.8, 109.6, 105.1, 89.93, 33.31.

HRMS (ESI): $C_{15}H_{10}F_5N_2^+$ $(M+H)^+$ calculated: 313.07587 found: 313.07507

***N*-(3-(3,4-dichlorophenyl)prop-2-yn-1-yl)-2-(trifluoromethyl)pyridin-4-amine 1.31**

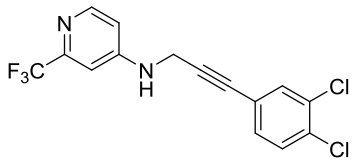

The compound was prepared according to **GP2**. *N*-(prop-2-yn-1-yl)-2-(trifluoromethyl)pyridin-4-amine **1.25** (40.0 mg, 0.200 mmol), 1,2-dichloro-4-iodobenzene (54.6 mg, 0.200 mmol), DIPEA (712 µL, 54 mg 0.420 mmol), $Pd(PPh_3)_4$ (11.4 mg, 5 mol%) and CuI (1.90 mg 5 mol%) were used. Automated flash chromatography (PE/EtOAc) afforded the title compound as a yellow solid (23.5 mg, 0.068 mmol, 34%).

^{1}H-NMR (300 MHz, $CDCl_3$): δ [ppm] = 8.36 (d, *J* = 5.6 Hz, 1 H), 7.47 (d, *J* = 1.9 Hz, 1 H), 7.37 (d, *J* = 8.3 Hz, 1 H), 7.20 (dd, *J* = 8.3 Hz, *J* = 2.0 Hz, 1 H), 6.93 (d, *J* = 2.3 Hz, 1 H), 6.69 (dd, *J* = 5.7 Hz, *J* = 2.4 Hz, 1 H), 4.86 (bs, 1 H), 4.23 (d, *J* = 5.9 Hz, 2 H).

^{13}C-NMR (75 MHz, $CDCl_3$): δ [ppm] = 153.2, 150.3, 133.3, 133.2, 132.6, 130.8, 130.4, 122.0, 109.5, 105.0, 85.7, 82.2, 33.2.

HRMS (ESI): $C_{15}H_{10}Cl_2F_3N_2^+$ $(M+H)^+$ calculated: 345.01677 found: 345.01620

***N*-(3-(6-chloropyridin-3-yl)prop-2-yn-1-yl)-2-(trifluoromethyl)pyridin-4-amine 1.32**

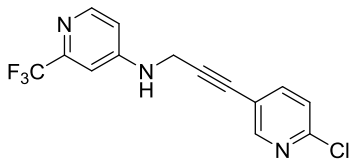

The compound was prepared according to **GP2**. *N*-(prop-2-yn-1-yl)-2-(trifluoromethyl)pyridin-4-amine **1.25** (40.0 mg, 0.200 mmol), 2-chloro-5-iodopyridine (47.9 mg, 0.200 mmol), DIPEA (712 µL, 54 mg 0.420 mmol), $Pd(PPh_3)_4$ (11.4 mg, 5 mol%) and CuI (1.90 mg 5 mol%) were used. Automated flash chromatography (PE/EtOAc) afforded the title compound as a yellow solid (53.6 mg, 0.172 mmol, 86%).

^{1}H-NMR (300 MHz, $CDCl_3$): Shift [ppm] = 8.41 (d, *J* = 2.2 Hz, 1 H), 8.38 (d, *J* = 5.7 Hz, 1 H), 7.63 (dd, *J* = 8.3 Hz, 2.3 Hz, 1 H), 7.29 (d, *J* = 8.3 Hz, 1 H), 6.95 (d, *J* = 2.3 Hz, 1 H), 6.71 (dd, *J* = 5.7 Hz, *J* = 2.4 Hz, 1 H), 4.90 (bs, 1 H), 4.27 (d, *J* = 5.9 Hz).

^{13}C-NMR (75 MHz, $CDCl_3$): Shift [ppm] = 153.2, 152.2, 151.0, 150.4, 141.1, 123.9, 118.2, 109.6, 105.0, 88.35, 79.99, 33.23.

HRMS (ESI): $C_{14}H_{10}ClF_3N_3^+$ $(M+H)^+$ calculated: 312.05099 found: 312.05038

***N*-(3-(5-chloropyridin-2-yl)prop-2-yn-1-yl)-2-(trifluoromethyl)pyridin-4-amine 1.33**

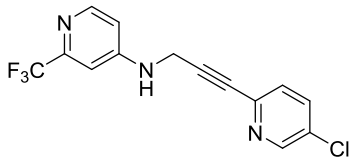

The compound was prepared according to **GP2**. *N*-(prop-2-yn-1-yl)-2-(trifluoromethyl)pyridin-4-amine **1.25** (40.0 mg, 0.200 mmol), 5-chloro-2-iodopyridine (47.9 mg, 0.200 mmol), DIPEA (712 µL, 54 mg 0.420 mmol), $Pd(PPh_3)_4$ (11.4 mg, 5 mol%) and CuI (1.90 mg 5 mol%) were used. Automated flash chromatography (PE/EtOAc) afforded the title compound as a yellow solid (21.2 mg, 0.068 mmol, 34%).

^{1}H-NMR (300 MHz, $CDCl_3$): δ [ppm] = 8.53 (d, *J* = 2.4 Hz, 1 H), 8.36 (d, *J* = 5.7 Hz, 1 H), 7.66 – 7.62 (m, 1 H), 7.34 (d, *J* = 8.3 Hz, 1 H), 6.93 (d, *J* = 2.2 Hz, 1 H), 6.69 (dd, *J* = 5.7 Hz, *J* = 2.1 Hz, 1 H), 4.96 (bs, 1 H), 4.27 (d, *J* = 5.8 Hz, 2 H).

^{13}C-NMR (75 MHz, $CDCl_3$): δ [ppm] = 153.3, 152.3, 151.1, 150.5, 141.2, 123.9, 118.2, 109.5, 105.1, 88.34, 76.89, 33.23.

HRMS (ESI): $C_{14}H_{10}ClF_3N_3^+$ $(M+H)^+$ calculated: 312.05099 found: 312.05035

4-(3-((2-(trifluoromethyl)pyridin-4-yl)amino)prop-1-yn-1-yl)phenol 1.34

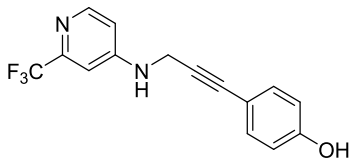

The compound was prepared according to **GP2**. *N*-(prop-2-yn-1-yl)-2-(trifluoromethyl)pyridin-4-amine **1.25** (40.0 mg, 0.200 mmol), 4-iodophenol (44.0 mg, 0.200 mmol), DIPEA (712 µL, 54 mg 0.420 mmol), $Pd(PPh_3)_4$ (11.4 mg, 5 mol%) and CuI (1.90 mg 5 mol%) were used. Automated flash chromatography (PE/EtOAc) afforded the title compound as a yellow solid (5.85 mg, 0.020 mmol, 10%).

^{1}H-NMR (300 MHz, $CDCl_3$): δ [ppm] = 8.42 (bs, OH), 8.33 (d, *J* = 5.7 Hz, 1 H), 7.26 – 7.22 (m, 2 H), 6.94 (d, *J* = 2.3 Hz, 1 H), 6.82 – 6.78 (m, 2 H), 6.69 (dd, *J* = 5.7 Hz, *J* = 2.3 Hz, 1 H), 5.11 (bs, NH), 4.20 (d, *J* = 7.2 Hz, 2 H).

^{13}C-NMR (75 MHz, $CDCl_3$): δ [ppm] = 157.6, 153.6, 150.0, 133.2, 123.5, 115.6, 113.1, 109.5, 105.0, 84.74, 81.82, 33.40.

HRMS (ESI): $C_{15}H_{12}F_3N_2O^+$ $(M+H)^+$ calculated: 293.08962 found: 293.08893

***N*-(3-(4-methoxyphenyl)prop-2-yn-1-yl)-2-(trifluoromethyl)pyridin-4-amine 1.35**

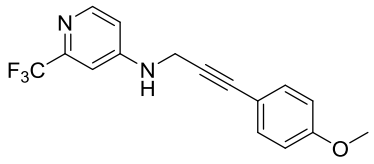

The compound was prepared according to **GP2**. *N*-(prop-2-yn-1-yl)-2-(trifluoromethyl)pyridin-4-amine **1.25** (40.0 mg, 0.200 mmol), 1-methoxy-4-iodobenzene (46.8 mg, 0.200 mmol), DIPEA (712 µL, 54 mg 0.420 mmol), $Pd(PPh_3)_4$ (11.4 mg, 5 mol%) and CuI (1.90 mg 5 mol%) were used. Automated flash chromatography (PE/EtOAc) afforded the title compound as a yellow solid (7.36 mg, 0.024 mmol, 12%).

^{1}H-NMR (300 MHz, $CDCl_3$): δ [ppm] = 8.33 (d, *J* = 5.8 Hz, 1 H), 7.26 – 7.22 (m, 2 H), 6.94 (d, *J* = 2.3 Hz, 1 H), 6.84 – 6.78 (m, 2 H), 6.69 (dd, *J* = 5.7 Hz, *J* = 2.3 Hz, 1 H), 5.11 (bs, NH), 4.20 (d, *J* = 7.2 Hz, 2 H).

^{13}C-NMR (75 MHz, $CDCl_3$): δ [ppm] = 162.3, 157.6, 153.6, 150.0, 133.2, 123.5, 114.3, 113.2, 109.4, 105.1, 84.76, 81.84, 57.40, 33.42.

HRMS (ESI): $C_{16}H_{14}F_3N_2O^+$ $(M+H)^+$ calculated: 307.10527 found: 307.10464

***N*-(3-(3-methoxyphenyl)prop-2-yn-1-yl)-2-(trifluoromethyl)pyridin-4-amine 1.36**

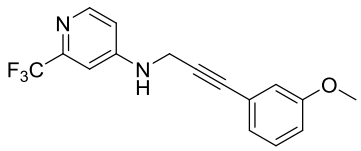

The compound was prepared according to **GP2**. *N*-(prop-2-yn-1-yl)-2-(trifluoromethyl)pyridin-4-amine **1.25** (40.0 mg, 0.200 mmol), 1-methoxy-3-iodobenzene (46.8 mg, 0.200 mmol), DIPEA (712 µL, 54 mg 0.420 mmol), $Pd(PPh_3)_4$ (11.4 mg, 5 mol%) and CuI (1.90 mg 5 mol%) were used. Automated flash chromatography (PE/EtOAc) afforded the title compound as a yellow solid (41.6 mg, 0.136 mmol, 68%).

^{1}H-NMR (300 MHz, $CDCl^{3}$): Shift [ppm] = 8.36 (d, *J* = 5.7 Hz, 1 H), 7.22 (t, *J* = 7.8 Hz, 1 H), 7.01 – 6.98 (m, 1 H), 6.95 (d, *J* = 2.3 Hz, 1 H), 6.93 – 6.87 (m, 2 H), 6.89 (dd, *J* = 5.7 Hz, *J* = 2.3 Hz, 1 H), 4.92 – 4.87 (m, 1 H), 4.23 (d, *J* = 5.7 Hz, 2 H), 3.82 (s, 3 H).

^{13}C-NMR (75 MHz, $CDCl^{3}$): Shift [ppm] = 162.1, 158.6, 151.0, 146.2, 130.1, 124.3, 121.2, 115.8, 115.3, 110.0, 108.9, 83.12, 82.79, 57.38, 33.45.

HRMS (ESI): $C_{16}H_{14}F_3N_2O^+$ $(M+H)^+$ calculated: 307.10527 found: 307.10480

***N*-(3-(4-ethoxyphenyl)prop-2-yn-1-yl)-2-(trifluoromethyl)pyridin-4-amine 1.37**

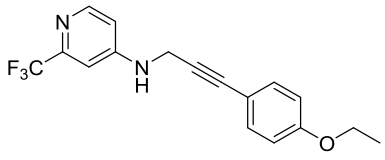

The compound was prepared according to **GP2**. *N*-(prop-2-yn-1-yl)-2-(trifluoromethyl)pyridin-4-amine **1.25** (40.0 mg, 0.200 mmol), 1-ethoxy-4-iodobenzene **1.20a** (49.6 mg, 0.200 mmol), DIPEA (712 µL, 54 mg 0.420 mmol), $Pd(PPh_3)_4$ (11.4 mg, 5 mol%) and CuI (1.90 mg 5 mol%) were used. Automated flash chromatography (PE/EtOAc) afforded the title compound as a yellow solid (8.97 mg, 0.028 mmol, 14%).

^{1}H-NMR (300 MHz, $CDCl_3$): δ [ppm] = 8.35 (d, *J* = 5.6 Hz, 1 H), 7.32 (d, *J* = 8.7 Hz, 2 H), 6.93 (d, *J* = 2.4 Hz, 1 H), 6.81 (d, *J* = 8.7 Hz, 2 H), 6.68 (dd, *J* = 5.6 Hz, *J* = 2.3 Hz, 1 H), 4.82 (bs, 1 H), 4.21 (d, *J* = 5.6 Hz, 2 H), 4.02 (q, *J* = 7.0 Hz, 2 H), 1.40 (t, *J* = 6.9, 3 H).

^{13}C-NMR (75 MHz, $CDCl_3$): δ [ppm] = 153.3, 150.2, 148.9, 148.6, 133.2, 120.6, 114.4, 113.8, 109.5, 105.0, 84.54, 82.05, 63.51, 33.44, 14.69.

HRMS (ESI): $C_{17}H_{16}F_3N_2O^+$ $(M+H)^+$ calculated: 321.12092 found: 321.12023

***N*-(3-(4-isopropoxyphenyl)prop-2-yn-1-yl)-2-(trifluoromethyl)pyridin-4-amine 1.38**

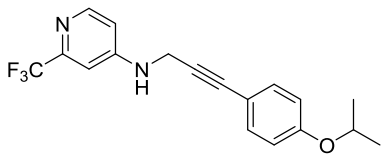

The compound was prepared according to **GP2**. *N*-(prop-2-yn-1-yl)-2-(trifluoromethyl)pyridin-4-amine **1.25** (40.0 mg, 0.200 mmol), 1-iodo-4-isopropoxybenzene **1.20b** (52.4 mg, 0.200 mmol), DIPEA (712 µL, 54 mg 0.420 mmol), $Pd(PPh_3)_4$ (11.4 mg, 5 mol%) and CuI (1.90 mg 5 mol%) were used. Automated flash chromatography (PE/EtOAc) afforded the title compound as a yellow solid (18.7 mg, 0.056 mmol, 28%).

^{1}H-NMR (500 MHz, $CDCl_3$): δ [ppm] = 8.36 (d, *J* = 5.7 Hz, 1 H), 7.33 – 7.31 (m, 2 H), 6.95 (d, *J* = 2.4 Hz, 1 H), 6.82 – 6.80 (m, 2 H), 6.70 (dd, *J* = 5.7 Hz, *J* = 2.4 Hz, 1 H), 4.81 (bs, 1 H), 4.55 (dq, *J* = 6.1 Hz, 1 H), 4.23 (d, *J* = 5.7 Hz, 2 H), 1.34 (d, *J* = 6.1 Hz, 6 H).

^{13}C-NMR (125 MHz, $CDCl_3$): δ [ppm] = 158.3, 153.4, 150.1, 133.2, 115.7, 113.7, 109.6, 105.0, 84.62, 81.91, 69.91, 33.47, 21.91.

HRMS (ESI): $C_{18}H_{18}F_3N_2O^+$ $(M+H)^+$ calculated: 335.13657 found: 335.13605

***N*-(3-(4-phenoxyphenyl)prop-2-yn-1-yl)-2-(trifluoromethyl)pyridin-4-amine 1.39**

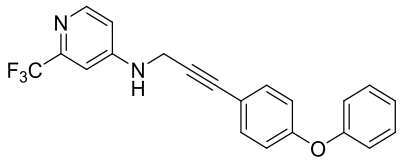

The compound was prepared according to **GP2**. *N*-(prop-2-yn-1-yl)-2-(trifluoromethyl)pyridin-4-amine **1.25** (40.0 mg, 0.200 mmol), 1-iodo-4-phenoxybenzene (59.2 mg, 0.200 mmol), DIPEA (712 µL, 54 mg 0.420 mmol), $Pd(PPh_3)_4$ (11.4 mg, 5 mol%) and CuI (1.90 mg, 5 mol%) were used. Automated flash chromatography (PE/EtOAc) afforded the title compound as a yellow solid (23.6 mg, 0.064 mmol, 32%).

^{1}H-NMR (300 MHz, $CDCl_3$): Shift [ppm] = 7.39 – 7.34 (m, 4 H), 7.15 – 7.14 (m, 1 H), 7.03 – 7.02 (m, 2 H), 6.96 – 6.95 (m, 1 H), 6.70 (dd, *J* = 5.6 Hz, *J* = 2.4 Hz, 1 H), 4.81 (bs, 1 H), 4.23 (d, *J* = 5.7 Hz, 2 H).

^{13}C-NMR (75 MHz, $CDCl_3$): Shift [ppm] = 158.0, 156.2, 153.3, 150.3, 149.1, 133.3, 129.9, 123.9, 119.5, 118.3, 116.5, 109.6, 105.0, 84.13, 82.88, 33.41.

HRMS (ESI): $C_{21}H_{16}F_3N_2O^+$ $(M+H)^+$ calculated: 369.12092 found: 369.12012

***N*-(3-(4-methoxy-3-methylphenyl)prop-2-yn-1-yl)-2-(trifluoromethyl)pyridin-4-amine 1.40**

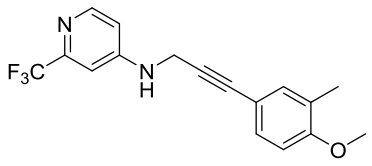

The compound was prepared according to **GP2**. *N*-(prop-2-yn-1-yl)-2-(trifluoromethyl)pyridin-4-amine **1.25** (40.0 mg, 0.200 mmol), 4-iodo-1-methoxy-2-methylbenzene **1.23a** (52.4 mg, 0.200 mmol), DIPEA (712 µL, 54 mg 0.420 mmol), $Pd(PPh_3)_4$ (11.4 mg, 5 mol%) and CuI (1.90 mg 5 mol%) were used. Automated flash chromatography (PE/EtOAc) afforded the title compound as a yellow solid (37.8 mg, 0.118 mmol, 59%).

^{1}H-NMR (300 MHz, $CDCl_3$): δ [ppm] = 8.35 (d, *J* = 5.8 Hz, 1 H), 7.24 – 7.21 (m, 1 H), 7.19 – 7.18 (m, 1 H), 6.94 (d, *J* = 2.3 Hz, 1 H), 6.74 (d, *J* = 8.4 Hz, 1 H), 6.68 (dd, *J* = 5.8 Hz, *J* = 2.3 Hz, 1 H), 4.90 (bs, NH), 4.21 (d, *J* = 5.8 Hz, 2 H), 3.83 (s, 3 H), 2.17 (s, 3 H).

^{13}C-NMR (75 MHz, $CDCl_3$): δ [ppm] = 157.7, 153.7, 150.1, 133.3, 123.5, 115.6, 113.1, 109.5, 105.0, 83.25, 80.73, 59.23, 33.38, 16.58.

HRMS (ESI): $C_{17}H_{16}F_3N_2O^+$ $(M+H)^+$ calculated: 321.12092 found: 321.12024

***N*-(3-(3-fluoro-4-methoxyphenyl)prop-2-yn-1-yl)-2-(trifluoromethyl)pyridin-4-amine 1.41**

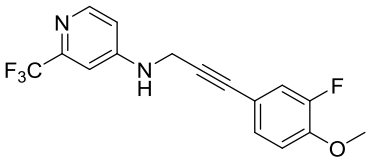

The compound was prepared according to **GP2**. *N*-(prop-2-yn-1-yl)-2-(trifluoromethyl)pyridin-4-amine **1.25** (40.0 mg, 0.200 mmol), 2-fluoro-4-iodo-1-methoxybenzene **1.21a** (50.4 mg, 0.200 mmol), DIPEA (712 µL, 54 mg 0.420 mmol), $Pd(PPh_3)_4$ (11.4 mg, 5 mol%) and CuI (1.90 mg 5 mol%) were used. Automated flash chromatography afforded the title compound as a yellow solid (3.24 mg, 0.010 mmol, 5%).

^{1}H-NMR (500 MHz, $CDCl_3$): δ [ppm] = 8.38 (d, *J* = 5.7 Hz, 1 H), 7.16 – 7.14 (m, 1 H), 7.13 – 7.11 (m, 1 H), 6.95 (d, *J* = 2.3 Hz, 1 H), 6.90 – 6.87 (m, 1 H), 6.70 (dd, *J* = 5.7 Hz, *J* = 2.3 Hz, 1 H), 4.79 (bs, 1 H), 4.23 (d, *J* = 5.8 Hz, 2 H), 3.90 (s, 3 H).

^{13}C-NMR (125 MHz, $CDCl_3$): δ [ppm] = 153.3, 152.6, 150.2, 148.5, 128.4, 119.4, 114.5,113.1, 109.6, 105.0, 83.38, 82.85, 56.18, 33.33, 29.68.

HRMS (ESI): $C_{16}H_{13}F_4N_2O^+$ $(M+H)^+$ calculated: 325.09585 found: 325.09537

***N*-(3-(3-chloro-4-methoxyphenyl)prop-2-yn-1-yl)-2-(trifluoromethyl)pyridin-4-amine 1.42**

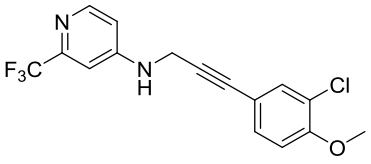

The compound was prepared according to **GP2**. *N*-(prop-2-yn-1-yl)-2-(trifluoromethyl)pyridin-4-amine **1.25** (40.0 mg, 0.200 mmol), 2-chloro-4-iodo-1-methoxybenzene **1.22a** (53.7 mg, 0.200 mmol), DIPEA (712 µL, 54 mg 0.420 mmol), $Pd(PPh_3)_4$ (11.4 mg, 5 mol%) and CuI (1.90 mg 5 mol%) were used.

Automated flash chromatography afforded the title compound as a yellow solid (16.3 mg, 0.048 mmol, 24%).

^{1}H-NMR (300 MHz, $CDCl_3$): δ [ppm] = 8.34 (d, *J* = 5.6 Hz, 1 H), 7.39 (s, 1 H), 7.24 (s, 1 H), 6.92-6.90 (m, 1 H), 6.83 (d, *J* = 8.4 Hz, 1 H), 6.66 (d, *J* = 5.6 Hz, 1 H), 4.82 (bs, 1 H), 4.19 (d, *J* = 5.6 Hz, 2 H), 3.88 (s, 3 H).

^{13}C-NMR (75 MHz, $CDCl_3$): δ [ppm] = 155.4, 153.2, 150.4, 150.2, 148.9, 133.3, 131.5, 122.3, 115.0, 111.7, 109.5, 105.0, 83.19, 83.08, 56.17, 33.31.

HRMS (ESI): $C_{16}H_{13}ClF_3N_2O^+$ $(M+H)^+$ calculated: 341.06630 found: 341.06564

***N*-(3-(4-ethoxy-3-fluorophenyl)prop-2-yn-1-yl)-2-(trifluoromethyl)pyridin-4-amine 1.43**

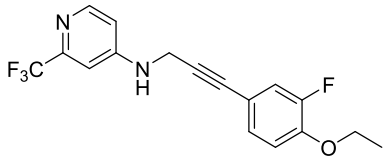

The compound was prepared according to **GP2**. *N*-(prop-2-yn-1-yl)-2-(trifluoromethyl)pyridin-4-amine **1.25** (40.0 mg, 0.200 mmol), 1-ethoxy-2-fluoro-4-iodobenzene **1.21b** (53.2 mg, 0.200 mmol), DIPEA (712 µL, 54 mg 0.420 mmol), $Pd(PPh_3)_4$ (11.4 mg, 5 mol%) and CuI (1.90 mg 5 mol%) were used. Automated flash chromatography afforded the title compound as a yellow solid (19.6 mg, 0.058 mmol, 29%).

^{1}H-NMR (500 MHz, $CDCl_3$): δ [ppm] = 8.36 (d, *J* = 5.7 Hz, 1 H), 7.10 – 7.12 (m, 2 H), 6.94 (d, *J* = 2.3 Hz, 1 H), 6.87 (dd, *J* = 8.4 Hz, 1 H), 6.69 (dd, *J* = 5.7 Hz, *J* = 2.3 Hz, 1 H), 4.82 (bs, 1 H), 4.22 (d, *J* = 5.8 Hz, 2 H), 4.11 (q, *J* = 7.0 Hz, 2 H), 1.46 (t, *J* = 7.0 Hz, 3 H).

^{13}C-NMR (126 MHz, $CDCl_3$): δ [ppm] = 153.0, 150.0, 147.6, 128.1, 122.5, 120.3, 119.1, 118.9, 114.3, 113.8, 104.6, 82.88, 82.56, 64.54, 33.05, 14.38.

HRMS (ESI): $C_{17}H_{15}F_4N_2O^+$ $(M+H)^+$ calculated: 339.11150 found: 339.11118

***N*-(3-(3-chloro-4-ethoxyphenyl)prop-2-yn-1-yl)-2-(trifluoromethyl)pyridin-4-amine 1.44**

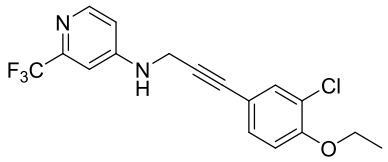

The compound was prepared according to **GP2**. *N*-(prop-2-yn-1-yl)-2-(trifluoromethyl)pyridin-4-amine **1.25** (40.0 mg, 0.200 mmol), 2-chloro-1-ethoxy-4-iodobenzene **1.22b** (56.5 mg, 0.200 mmol), DIPEA

(712 µL, 54 mg 0.420 mmol), $Pd(PPh_3)_4$ (11.4 mg, 5 mol%) and CuI (1.90 mg 5 mol%) were used. Automated flash chromatography afforded the title compound as a yellow solid (18.4 mg, 0.052 mmol, 26%).

^{1}H-NMR (300 MHz, $CDCl_3$): δ [ppm] = 8.37 – 8.33 (m, 1 H), 7.41 – 7.38 (m, 1 H), 7.24 (d, *J* = 8.4 Hz, 1 H), 6.94 – 6.91 (m, 1 H), 6.82 (d, *J* = 8.4 Hz, 1 H), 6.68 (d, *J* = 2.3 Hz, 1 H), 4.88 (bs, 1 H), 4.22 – 4.18 (m, 2 H), 4.10 (q, *J* = 6.71 Hz, 2 H), 1.46 (t, *J* = 6.7 Hz, 3 H).

^{13}C-NMR (75 MHz, $CDCl_3$): δ [ppm] = 154.9, 153.3, 150.2, 148.9, 133.3, 131.4, 122.6, 120.6, 114.8, 112.7, 109.5, 105.0, 83.1, 83.1, 64.8, 33.3, 14.5.

HRMS (ESI): $C_{17}H_{15}ClF_3N_2O^+$ $(M+H)^+$ calculated: 355.08195 found: 355.08127

***N*-(3-(3-fluoro-4-isopropoxyphenyl)prop-2-yn-1-yl)-2-(trifluoromethyl)pyridin-4-amine 1.45**

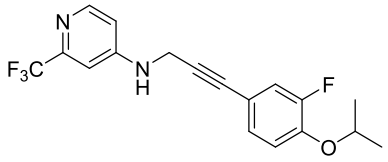

The compound was prepared according to **GP2**. *N*-(prop-2-yn-1-yl)-2-(trifluoromethyl)pyridin-4-amine **1.25** (40.0 mg, 0.200 mmol), 2-fluoro-4-iodo-1-isopropoxybenzene **1.21c** (56.0 mg, 0.200 mmol), DIPEA (712 µL, 54 mg 0.420 mmol), $Pd(PPh_3)_4$ (11.4 mg, 5 mol%) and CuI (1.90 mg 5 mol%) were used. Automated flash chromatography afforded the title compound as a yellow solid (19.0 mg, 0.054 mmol, 27%).

^{1}H-NMR (300 MHz, $CDCl_3$): δ [ppm] = 8.36 (d, *J* = 5.6 Hz, 1 H), 7.11 – 7.09 (m, 2 H), 6.93 (d, *J* = 1.8 Hz, 1 H), 6.90 – 6.85 (m, 1 H), 6.68 (dd, *J* = 5.6 Hz, *J* = 1.8 Hz, 1 H), 4.77 (bs, 1 H), 4.55 (dt, *J* = 12.1 Hz, *J* = 6.1 Hz, 1 H), 4.21 (d, *J* = 5.6 Hz, 2 H), 1.36 (d, *J* = 6.1 Hz, 6 H).

^{13}C-NMR (75 MHz, $CDCl_3$): δ [ppm] = 153.9, 153.5, 152.0, 150.5, 147.1, 128.5, 119.9, 119.8, 116.9, 116.8, 109.8, 105.3, 83.68, 83.10, 72.47, 33.60, 22.19.

HRMS (ESI): $C_{18}H_{17}F_4N_2O^+$ $(M+H)^+$ calculated: 353.12715 found: 353.12643

***N*-(3-(3-chloro-4-isopropoxyphenyl)prop-2-yn-1-yl)-2-(trifluoromethyl)pyridin-4-amine 1.46**

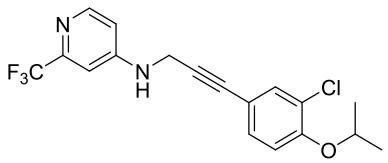

The compound was prepared according to **GP2**. *N*-(prop-2-yn-1-yl)-2-(trifluoromethyl)pyridin-4-amine **1.25** (40.0 mg, 0.200 mmol), 2-chloro-4-iodo-1-isopropoxybenzene **1.22c** (59.3 mg, 0.200 mmol), DIPEA (712 µL, 54 mg 0.420 mmol), $Pd(PPh_3)_4$ (11.4 mg, 5 mol%) and CuI (1.90 mg 5 mol%) were used. Automated flash chromatography afforded the title compound as a yellow solid (16.2 mg, 0.044 mmol, 22%).

^{1}H-NMR (300 MHz, $CDCl_3$): δ [ppm] = 8.38 – 8.33 (m, 1 H), 7.42 – 7.38 (m, 1 H), 7.22 (d, *J* = 8.2 Hz, 1 H), 6.94 – 6.91 (m, 1 H), 6.84 (d, *J* = 8.4 Hz, 1 H), 6.70 – 6.65 (m, 1 H), 4.81 (bs, 1 H), 4.59 – 4.53 (m, 1 H), 4.20 (d, *J* = 2.9 Hz, 2 H), 2.04 (s, 6 H).

^{13}C-NMR (75 MHz, $CDCl_3$): δ [ppm] = 154.4, 150.5, 149.2, 148.9, 133.8, 131.5, 124.1, 120.9, 115.1, 111.4, 109.8, 105.3, 83.49, 83.27, 72.26, 29.94, 22.15.

HRMS (ESI): $C_{18}H_{17}ClF_3N_2O$ $(M+H)^+$ calculated: 369.09760 found: 396.09705

***N*-(3-(4-fluorophenyl)propyl)-2-(trifluoromethyl)pyridin-4-amine 1.1**

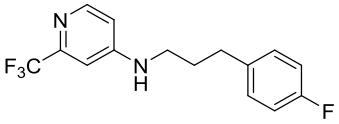

The compound was prepared according to **GP3**. (*E*)-*N*-(3-(4-fluorophenyl)allyl)-2-(trifluoromethyl)pyridin-4-amine **1.26** (5.4 mg, 0.018 mmol) was used and the title compound was isolated as a colorless solid (5.3 mg, 0.018 mmol, >98%).

^{1}H-NMR (300 MHz, $CDCl_3$): δ [ppm] = 8.27 (d, *J* = 5.6 Hz, 1 H), 7.37 – 7.31 (m, 2 H), 7.29 – 7.25 (m, 2 H), 6.74 (d, *J* = 2.3 Hz, 1 H), 6.48 (dd, *J* = 5.7 Hz, *J* = 2.4 Hz, 1 H), 4.42 (bs, 1 H), 3.25 (dd, *J* = 13.4 Hz, *J* = 6.9 Hz, 2 H), 2.76 (dd, *J* = 7.6 Hz, 2 H), 2.07 – 1.94 (m, 2 H).

^{13}C-NMR (75 MHz, $CDCl_3$): δ [ppm] = 159.3 154.2, 150.3, 149.1, 140.8, 135.6, 135.3, 132.3, 123.5, 108.9, 104.1, 42.15, 33.13, 30.29, 29.70.

HRMS (ESI): $C_{15}H_{15}F_4N_2^+$ $(M+H)^+$ calculated: 299.11659 found: 299.11591

***N*-(3-(6-chloropyridin-3-yl)propyl)-2-(trifluoromethyl)pyridin-4-amine 1.47**

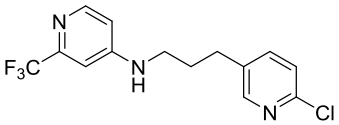

The compound was prepared according to **GP3**. *N*-(3-(6-chloropyridin-3-yl)prop-2-yn-1-yl)-2-(trifluoromethyl)pyridin-4-amine **1.32** (31.1 mg, 0.100 mmol) was used and the title compound was isolated as a yellow solid (30.2 mg, 0.959 mmol, 96%).

LC-MS: m/z: 316 $(M+H)^+$

***N*-(3-(3-methoxyphenyl)propyl)-2-(trifluoromethyl)pyridin-4-amine 1.48**

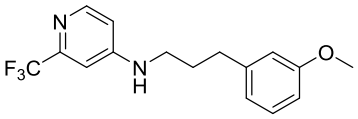

The compound was prepared according to **GP3**. *N*-(3-(3-methoxyphenyl)prop-2-yn-1-yl)-2-(trifluoromethyl)pyridin-4-amine **1.36** (30.6 mg, 0.100 mmol) was used and the title compound was obtained as colorless solid (30.1 mg, 0.971 mmol, 97%).

^{1}H-NMR (300 MHz, $CDCl_3$): δ [ppm] = 8.26 (d, *J* = 5.7 Hz, 1 H), 7.23 (d, *J* = 7.9 Hz, 1 H), 6.80 – 6.78 (m, 2 H), 6.74 – 6.73 (m, 2 H), 6.48 (dd, *J* = 5.8, *J* = 2.3 Hz, 1 H), 4.38 (bs, 1 H), 3.26 – 3.19 (m, 2 H), 2.73 (dd, *J* = 7.4 Hz, 2 H), 2.03 – 1.94 (m, 2 H).

HRMS (ESI): $C_{16}H_{18}F_3N_2O^+$ $(M+H)^+$ calculated: 311.13657 found: 311.13568

***N*-(3-(4-phenoxyphenyl)propyl)-2-(trifluoromethyl)pyridin-4-amine 1.49**

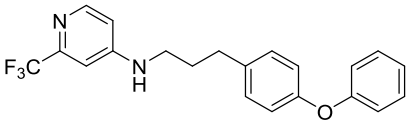

The compound was prepared according to **GP3**. *N*-(3-(4-phenoxyphenyl)prop-2-yn-1-yl)-2-(trifluoromethyl)pyridin-4-amine **1.39** (15.2 mg, 0.041 mmol) and the title compound was obtained as as a slight yellow solid (14.5 mg, 0.039 mmol, 95%).

^{1}H-NMR (300 MHz, $CDCl_3$): δ [ppm] = 8.27 (d, *J* = 5.6 Hz, 1 H), 7.37 – 7.31 (m, 2 H), 7.29 – 7.25 (m, 2 H), 6.74 (d, *J* = 2.3 Hz, 1 H), 6.48 (dd, *J* = 5.7 Hz, *J* = 2.4 Hz, 1 H), 4.42 (bs, 1 H), 3.25 (dd, *J* = 13.4 Hz, *J* = 6.9 Hz, 2 H), 2.76 (dd, *J* = 7.6 Hz, 2 H), 2.07 – 1.94 (m, 2 H).

^{13}C-NMR (75 MHz, $CDCl_3$): δ [ppm] = 158.4, 156.5, 156.4, 154.4, 150.2, 149.2, 140.9, 135.7, 135.5, 133.4, 123.5, 108.8, 104.1, 42.15, 33.13, 30.29, 29.70.

HRMS (ESI): $C_{21}H_{20}F_3N_2O^+$ $(M+H)^+$ calculated: 373.15222 found: 373.15161

(*Z*)-*N*-(3-(6-chloropyridin-3-yl)allyl)-2-(trifluoromethyl)pyridin-4-amine 1.50

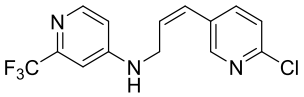

N-(3-(6-chloropyridin-3-yl)prop-2-yn-1-yl)-2-(trifluoromethyl)pyridin-4-amine **1.32** (20 mg, 0.064 mmol) was dissolved in EtOH (1.6 mL) and added under argon to a pre-stirred and degassesd suspension of Pd/C (0.6 mg, 10 mol%) in EtHOH (0.4 mL). The reaction mixture was stirred under an atmosphere of H_2 atfor 10 min at room temperature. The compound was filtered over silica gel and washed with EtOAc. The solvent was removed under reduced pressure and afforded the title compound as a colorless solid (19.7 mg, 0.063 mmol, > 98%).

^{1}H-NMR (300 MHz, $CDCl_3$): δ [ppm] = 8.74 (s, 1 H), 8.70 (d, *J* = 5.7 Hz, 1 H), 7.97 (dd, *J* = 8.2 Hz, *J* = 2.0 Hz, 1 H), 7.62 (d, *J* = 8.2 Hz, 1 H), 7.28 (s, 1 H), 7.02 (d, *J* = 5.6 Hz, 1 H), 5.32 (bs, 1 H), 4.60 (d, *J* = 5.8 Hz, 2 H).

^{13}C-NMR (76 MHz, $CDCl_3$): δ [ppm] = 153.6, 152.6, 151.4, 150.8, 149.6, 141.6, 124.4, 123.91, 118.6, 110.0, 105.4, 88.82, 80.37, 33.63, 30.10, 23.08.

HRMS (ESI): $C_{14}H_{12}ClF_3N_3^+$ $(M+H)^+$ calculated: 314.06664 found: 312.05041

***N*-((1-(2-fluorophenyl)-1*H*-1,2,3-triazol-4-yl)methyl)-2-(trifluoromethyl)pyridin-4-amine 3.16**

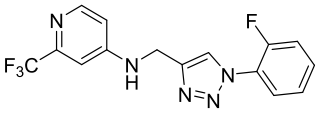

The compound was prepared according to **GP4.** 2-fluoroaniline (11.1 mg, 0.100 mmol) was used in the reaction and yielded 30.2 mg (89.5 µmol, 86%) of a slightly yellow solid after purification *via* automated flash chromatography (PE/EtOAc).

^{1}H-NMR (500 MHz, $CDCl_3$): δ [ppm] = 8.35 (bs, 1 H), 8.19 (bs, 1 H), 7.9 – 7.94 (m, 1 H), 7.48 – 7.44 (m, 1 H), 7.36 – 7.31 (m, 2 H), 6.97 (bs, 1 H), 6.72 (bs, 1 H), 5.43 (bs, 1 H), 4.64 (bs, 2 H).

^{13}C-NMR (126 MHz, $CDCl_3$): δ [ppm] = 154.1, 152.1, 153.3, 116.7, 116.9, 124.5, 125.1, 130.3, 38.14.

HRMS (ESI): $C_{15}H_{12}F_4N_5^+$ $(M+H)^+$ calculated: 338.10234 found: 338.10150

***N*-((1-(3-fluorophenyl)-1*H*-1,2,3-triazol-4-yl)methyl)-2-(trifluoromethyl)pyridin-4-amine 3.17**

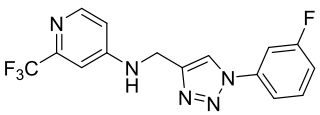

The compound was prepared according to **GP4.** 3-fluoroaniline (11.1 mg, 0.100 mmol) was used in the reaction and yielded 31.8 mg (94.2 µmol, 94%) of a yellow solid after purification *via* automated flash chromatography (PE/EtOAc).

^{1}H-NMR (500 MHz, $CDCl_3$): δ [ppm] = 8.34 (bs, 1 H), 8.02 (bs, 1 H), 7.52 – 7.49 (m, 3 H), 7.17 (bs, 1 H), 6.95 (bs, 1 H), 6.70 (bs, 1 H), 5.38 (bs, 1 H), 4.63 (bs, 2 H).

^{13}C-NMR (126 MHz, $CDCl_3$): δ [ppm] = 164.4, 162.4, 153.8, 138.4, 131.7, 116.4, 116.2, 116.1, 108.8, 108.5, 38.70.

HRMS (ESI): $C_{15}H_{12}F_4N_5^+$ $(M+H)^+$ calculated: 338.10234 found: 338.10144

***N*-((1-(4-fluorophenyl)-1*H*-1,2,3-triazol-4-yl)methyl)-2-(trifluoromethyl)pyridin-4-amine 3.18**

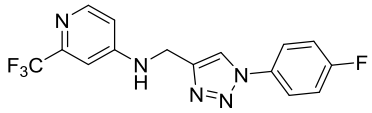

The compound was prepared according to **GP4.** 4-fluoroaniline (11.1 mg, 0.100 mmol) was used in the reaction and yielded 31.8 mg (94.3 µmol, 27%) of a yellow solid after purification *via* automated flash chromatography (PE/EtOAc).

^{1}H-NMR (500 MHz, acetone-d_6): δ [ppm] = 8.66 (bs, 1 H), 8.31 (bs, 1 H), 7.94 – 7.91 (m, 2 H), 7.39 – 7.35 (m, 2 H), 7.20 (bs, 1H), 6.92 (bs, 1 H), 6.83 (bs, 1 H), 4.66 (bs, 2 H).

^{13}C-NMR (126 MHz, acetone-d_6): δ [ppm] = 163.5, 161.6, 154.8, 122.9, 122.8, 117.1, 116.8, 38.20.

HRMS (ESI): $C_{15}H_{12}F_4N_5^+$ $(M+H)^+$ calculated: 338.10234 found: 338.10151

***N*-((1-(2-chlorophenyl)-1*H*-1,2,3-triazol-4-yl)methyl)-2-(trifluoromethyl)pyridin-4-amine 3.19**

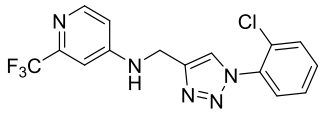

The compound was prepared according to **GP4.** 2-chloroaniline (12.8 mg, 0.100 mmol) was used in the reaction and yielded 9.36 mg (26.5 µmol, 94%) of a colorless solid after purification *via* automated flash chromatography (PE/EtOAc).

^{1}H-NMR (500 MHz, acetone-d_6): δ [ppm] = 8.36 (bs, 1 H), 8.23 (bs, 1 H), 7.71 (dd, *J* = 7.8 Hz, *J* = 1.7 Hz, 1 H), 7.66 – 7.64 (m, 1 H), 7.61 – 7. 63 (m, 1 H), 7.60– 7.57 (m, 1 H), 7.14 (bs, 1 H), 6.92 – 6.90 (m, 1 H), 6.86 (bs, 1 H), 4.70 (d, *J* = 5.7 Hz, 2 H).

^{13}C-NMR (126 MHz, acetone-d_6): δ [ppm] = 154.9, 135.6, 131.7, 131.0, 129.2, 128.7, 128.5, 38.15.

HRMS (ESI): $C_{15}H_{12}ClF_3N_5^+$ $(M+H)^+$ calculated: 354.07278 found: 354.07205

***N*-((1-(3-chlorophenyl)-1*H*-1,2,3-triazol-4-yl)methyl)-2-(trifluoromethyl)pyridin-4-amine 3.20**

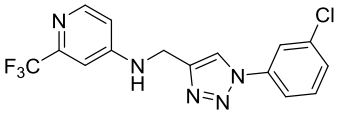

The compound was prepared according to **GP4.** 3-chloroaniline (12.8 mg, 0.100 mmol) was used in the reaction and yielded 30.1 mg (85.1 µmol, 85%) of a colorless solid after purification *via* automated flash chromatography (PE/EtOAc).

^{1}H-NMR (500 MHz, acetone-d_6): δ [ppm] = 8.64 (s, 1 H), 8.22 (d, *J* = 5.7 Hz, 1 H), 7.95 (dd, *J* = 2.0 Hz, 1 H), 7.88 – 7.886(m, 1 H), 7.61 (dd, *J* = 8.1 Hz, 1 H), 7.52 – 7.50 (m, 1 H), 7.13 (d, *J* = 2.1 Hz, 1 H), 6.88 (dd, *J* = 5.7 Hz, *J* = 2.3 Hz, 1 H), 6.83 (bs, 1 H), 4.68 (d, *J* = 5.8 Hz, 2 H).

^{13}C-NMR (126 MHz, acetone-d_6): δ [ppm] = 154.9, 150.5, 138.6, 153.2, 131.8, 128.8, 121.1, 120.4, 118.9, 109.4, 104.9, 38.23.

HRMS (ESI): $C_{15}H_{12}ClF_3N_5^+$ $(M+H)^+$ calculated: 354.07278 found: 354.07213

***N*-((1-(4-chlorophenyl)-1*H*-1,2,3-triazol-4-yl)methyl)-2-(trifluoromethyl)pyridin-4-amine 3.21**

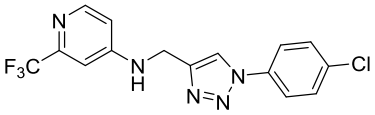

The compound was prepared according to **GP4.** 4-chloroaniline (12.8 mg, 0.100 mmol) was used in the reaction and yielded 24.4 mg (68.9 µmol, 69%) of an off-white solid after purification *via* automated flash chromatography (PE/EtOAc).

^{1}H-NMR (500 MHz, acetone-d_6): δ [ppm] = 8.58 (s, 1 H), 8.22 (d, *J* = 5.7 Hz, 1 H), 7.93 – 7.90 (m, 2 H), 7.63 – 7.60 (m, 2 H), 7.12 (d, *J* = 2.4 Hz, 1 H), 6.88 (dd, *J* = 7.9 Hz, *J* = 2.3 Hz, 1 H), 6.82 (bs, 1 H), 4.67 (d, *J* = 5.8 Hz, 2 H).

^{13}C-NMR (126 MHz, acetone-d_6): δ [ppm] = 154.9, 150.5, 146.1, 136.3, 133.9, 130.2, 122.1, 121.1, 109.5, 104.9, 38.23.

HRMS (ESI): $C_{15}H_{12}ClF_3N_5^+$ $(M+H)^+$ calculated: 354.07278 found: 354.07220

***N*-((1-(4-bromophenyl)-1*H*-1,2,3-triazol-4-yl)methyl)-2-(trifluoromethyl)pyridin-4-amine 3.22**

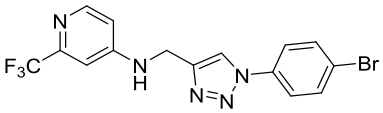

The compound was prepared according to **GP4.** 4-Bromoaniline (17.2 mg, 0.100 mmol) was used in the reaction and automated flash chromatography (PE/EtOAc) afforded the title compound as an orange solid (37.4 mg, 0.094 mmol, 94%).

^{1}H-NMR (300 MHz, $CDCl_3$): δ [ppm] = 8.35 (d, *J* = 5.0 Hz, 1 H), 7.91 (s, 1 H), 7.69 – 7.67 (m, 2 H), 7.63 – 7.61 (d, 2 H), 6.92 (s, 1 H), 6.68 (d, *J* = 3.6 Hz, 1 H), 5.18 (bs, 1 H), 4.63 (d, *J* = 5.3 Hz, 1 H).

^{13}C-NMR (76 MHz, $CDCl_3$): δ [ppm] = 153.8, 150.7, 135.9, 133.3, 123.1, 122.2, 109.6, 105.0, 38.77.

HRMS (ESI): $C_{15}H_{12}BrF_3N_5^+$ $(M+H)^+$ calculated: 398.02226 found: 398.02173

4-(4-(((2-(Trifluoromethyl)pyridin-4-yl)amino)methyl)-1*H*-1,2,3-triazol-1-yl)phenol 3.23

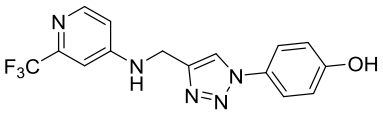

The compound was prepared according to **GP4.** 4-Aminophenol (10.9 g, 0.100 mmol) was used in the reaction and automated flash chromatography (PE/EtOAc) afforded the title compound as a yellow solid (11.5 mg, 34.3 µmol, 34%).

HRMS (ESI): $C_{15}H_{13}F_3N_5O^+$ $(M+H)^+$ calculated: 336.10667 found: 336.10596

***N*-((1-(4-methoxyphenyl)-1*H*-1,2,3-triazol-4-yl)methyl)-2-(trifluoromethyl)pyridin-4-amine 3.24**

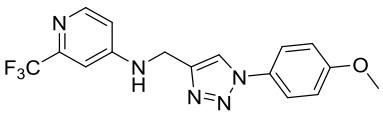

The compound was prepared according to **GP4.** 4-methoxyaniline was used in the reaction and yielded 11.2 mg (32.1 µmol, 32%) of a colorless solid after purification *via* automated flash chromatography (PE/EtOAc).

^{1}H-NMR (500 MHz, acetone-d_6): δ [ppm] = 8.44 (s, 1 H), 8.22 (d, *J* = 5.7 Hz, 1 H), 7.78 – 7.74 (m, 2 H), 7.12 – 7.11 (m, 2 H), 7.11 – 7.10 (m, 1 H), 6.88 (dd, *J* = 7.9 Hz, *J* = 2.3 Hz, 1 H), 6.78 (bs, 1 H), 4.64 (d, *J* = 5.7 Hz, 2 H), 3.87 (s, 1 H).

^{13}C-NMR (126 MHz, acetone-d_6): δ [ppm] = 160.2, 154.9, 150.5, 131.0, 122.2, 115.1, 109.5, 104.9, 55.48, 38.29.

LC-MS: m/z: 350 $(M+H)^+$

***N*-((1-(4-isopropoxyphenyl)-1*H*-1,2,3-triazol-4-yl)methyl)-2-(trifluoromethyl)pyridin-4-amine 3.25**

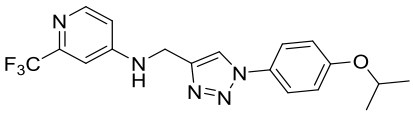

The compound was prepared according to **GP4.** 4-Isopropoxyaniline (15.1 mg, 0.100 mmol) was used. The title compound was obtained as a colorless solid (3.8 mg, 0.010 mmol, 10%) solid after purification *via* automated flash chromatography (PE/EtOAc).

^{1}H-NMR (500 MHz, $CDCl_3$): δ [ppm] = 8.34 (d, *J* = 5.7 Hz, 1 H), 7.83 (s, 1 H), 7.60 – 7.56 (m, 2 H), 7.02 – 6.99 (m, 2 H), 6.92 (d, *J* = 2.1 Hz, 1 H), 6.68 (d, *J* = 5.7 Hz, *J* = 2.1 Hz 1 H), 5.20 (bs, 1 H), 4.63 – 4.61 (m, 1 H), 4.61 (d, *J* = 5.7 Hz, 1 H), 1.36 (d, *J* = 6.1 Hz, 1 H).

^{13}C-NMR (76 MHz, $CDCl_3$): δ [ppm] = 158.7, 153.8, 150.6, 149.0, 144.42, 130.1, 122.5, 120.2, 116.8, 109.5, 104.9, 70.70, 38.81, 22.13.

HRMS (ESI): $C_{18}H_{19}F_3N_5O^+$ $(M+H)^+$ calculated: 378.15362 found: 378.15271

***N*-((1-(4-(trifluoromethoxy)phenyl)-1*H*-1,2,3-triazol-4-yl)methyl)-2-(trifluoromethyl)pyridin-4-amine 3.26**

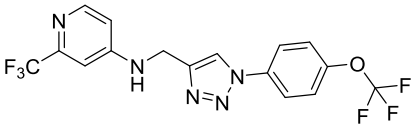

The compound was prepared according to **GP4.** 4-(trifluoromethoxy)aniline was used in the reaction and yielded 35.5 mg (88.0 µmol, 88%) of a colorless solid after purification *via* automated flash chromatography (PE/EtOAc).

^{1}H-NMR (500 MHz, acetone-d_6): δ [ppm] = 8.61 (s, 1 H), 8.21 (d, *J* = 5.7 Hz, 1 H), 8.04 – 8.01 (m, 2 H), 7.58 – 7.56 (m, 2 H), 7.13 (d, *J* = 2.3 Hz, 1 H), 6.88 (dd, *J* = 7.9 Hz, *J* = 2.3 Hz, 1 H), 6.83 (bs, 1 H), 4.68 (d, *J* = 5.7 Hz, 2 H).

HRMS (ESI): $C_{16}H_{12}F_6N_5O^+$ $(M+H)^+$ calculated: 404.09406 found: 404.09394

2-(Trifluoromethyl)-*N*-((1-(4-(trifluoromethyl)phenyl)-1*H*-1,2,3-triazol-4-yl)methyl)pyridin-4-amine 3.27

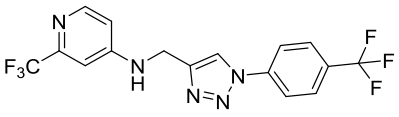

The compound was prepared according to **GP4.** 4-(trifluoromethyl)aniline was used in the reaction and yielded 32.2 mg (83.2 µmol, 83%) of a colorless solid after purification *via* automated flash chromatography (PE/EtOAc).

LC-MS: m/z: 388 $(M+H)^+$

4-(4-(((2-(Trifluoromethyl)pyridin-4-yl)amino)methyl)-1*H*-1,2,3-triazol-1-yl)benzonitrile 3.28

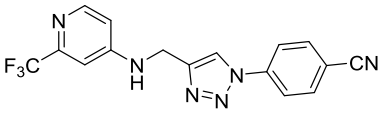

The compound was prepared according to **GP4.** 4-aminobenzonitrile was used in the reaction and yielded 23.9 mg (69.4 µmol, 69%) of a colorless solid after purification *via* automated flash chromatography (PE/EtOAc).

^{1}H-NMR (500 MHz, acetone-d_6): δ [ppm] = 8.72 (s, 1 H), 8.21 (d, *J* = 5.7 Hz, 1 H), 8.15 – 8.13 (m, 2 H), 8.03 – 8.01 (m, 2 H), 7.12 (d, *J* = 2.3 Hz, 1 H), 6.88 (dd, *J* = 7.9 Hz, *J* = 2.3 Hz, 1 H), 6.85 (bs, 1 H), 4.69 (d, *J* = 5.7 Hz, 2 H).

^{13}C-NMR (126 MHz, acetone-d_6): δ [ppm] = 154.9, 150.5, 146.5, 140.4, 134.4, 121.2, 120.9, 118.0, 109.5, 104.9, 38.18.

HRMS (ESI): $C_{16}H_{12}F_3N_6^+$ $(M+H)^+$ calculated: 345.10701 found: 345.10626

***N*-((1-(4-phenoxyphenyl)-1*H*-1,2,3-triazol-4-yl)methyl)-2-(trifluoromethyl)pyridin-4-amine 3.29**

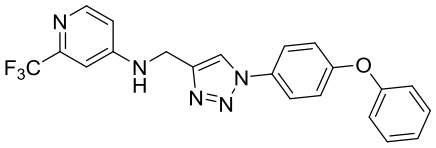

The compound was prepared according to **GP4.** 4-phenoxyaniline was used in the reaction and yielded 39.5 mg (96 µmol, 96%) of a colorless solid after purification *via* automated flash chromatography (PE/EtOAc).

^{1}H-NMR (300 MHz, DMSO-d_6): δ [ppm] = 8.72 (s, 1 H), 8.20 (d, *J* = 5.7 Hz, 1 H), 7.89 (m, 2 H), 7.64 (m, 1 H), 7.45 (m, 2 H), 7.21 (m, 3 H), 7.11 (m, 2 H), 7.06 (d, *J* = 2.2 Hz, 1 H), 6.83 (dd, *J* = 5.7 Hz, *J* = 2.2 Hz, 1 H), 4.53 (d, *J* = 5.7 Hz, 2 H).

^{13}C-NMR (75 MHz, DMSO-d_6): δ [ppm] = 156.9, 155.9, 154.3, 149.9, 145.1, 132.0, 130.2, 124.1, 122.1, 121.4, 119.3, 119.1, 37.26.

HRMS (ESI): $C_{21}H_{17}F_3N_5O^+$ $(M+H)^+$ calculated: 412.13797 found: 412.13705

***N*-((1-(4-phenoxyphenyl)-1*H*-1,2,3-triazol-4-yl)methyl)-2-(trifluoromethyl)pyridin-4-amine 3.30**

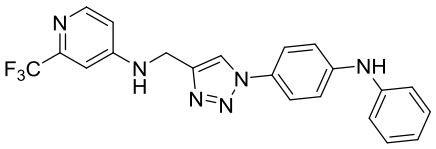

The compound was prepared according to **GP4.** N^1-Phenylbenzene-1,4-diamine (18.4 mg, 0.100 mmol) was used in the reaction and the title compound was afforded as an off-white solid (27.4 mg, 66.8 µmol, 67%) after purification *via* automated flash chromatography (PE/EtOAc).

HRMS (ESI): $C_{21}H_{17}F_3N_6^+$ $(M+H)^+$ calculated: 411.15396 found: 411.15317

***N*-((1-(3,4-dichlorophenyl)-1*H*-1,2,3-triazol-4-yl)methyl)-2-(trifluoromethyl)pyridin-4-amine 3.35**

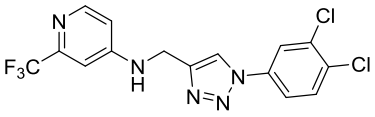

The compound was prepared according to **GP4.** 3,4-dichloroaniline and yielded 23.4 mg (60.0 µmol, 60%) of a colorless solid after purification *via* automated flash chromatography (PE/EtOAc).

^{1}H-NMR (500 MHz, acetone-d_6): δ [ppm] = 8.67 (s, 1 H), 8.21 (d, *J* = 5.8 Hz, 1 H), 8.13 (d, *J* = 2.4 Hz, 1 H), 7.92 (dd, *J* = 8.9 Hz, *J* = 2.6 Hz, 1 H), 7.79 (d, *J* = 8.7 Hz, 1 H), 7.12 (d, *J* = 2.3 Hz, 1 H), 6.88 (d, *J* = 5.7 Hz, *J* = 2.3 Hz, 1 H), 6.84 (bs, 1 H), 4.68 (d, *J* = 5.8 Hz, 2 H).

^{13}C-NMR (75 MHz, DMSO-d_6): δ [ppm] = 154.9, 150.5, 137.0, 132.1, 122.2, 120.3, 109.5, 104.9, 38.20.

HRMS (ESI): $C_{15}H_{11}Cl_2F_3N_5^+$ $(M+H)^+$ calculated: 388.03381 found: 388.03388

***N*-((1-(3-fluoro-4-methoxyphenyl)-1*H*-1,2,3-triazol-4-yl)methyl)-2-(trifluoromethyl)pyridin-4-amine 3.36**

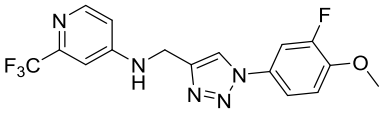

The compound was prepared according to **GP4.** 3-Fluoro-4-methoxyaniline was used in the reaction and yielded 25.7 mg (69.3 µmol, 69%) of a colorless solid after purification *via* automated flash chromatography (PE/EtOAc).

HRMS (ESI): $C_{16}H_{14}F_4N_5O^+$ $(M+H)^+$ calculated: 368.11290 found: 368.11224

***N*-((1-(3-chloro-4-methoxyphenyl)-1*H*-1,2,3-triazol-4-yl)methyl)-2-(trifluoromethyl)pyridin-4-amine 3.37**

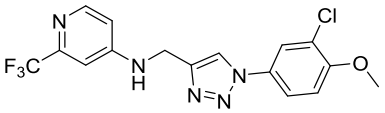

The compound was prepared according to **GP4.** 3-Chloro-4-methoxyaniline was used in the reaction and yielded 28.0 mg (73.0 µmol, 73%) of a colorless solid after purification *via* automated flash chromatography (PE/EtOAc).

^{1}H-NMR (500 MHz, acetone-d_6): δ [ppm] = 8.52 (s, 1 H), 8.22 (d, *J* = 5.6 Hz, 1 H), 7.90 (d, *J* = 2.6 Hz, 1 H), 7.80 (dd, *J* = 9.0 Hz, *J* = 2.8 Hz, 1 H), 7.31 (d, *J* = 8.9 Hz, 1 H), 7.12 (d, *J* = 2.3 Hz, 1 H), 6.88 (dd, *J* = 5.7 Hz, *J* = 2.2 Hz, 1 H), 6.81 (bs, 1 H), 4.65 (d, *J* = 5.6 Hz, 2 H), 3.98 (s, 3H).

^{13}C-NMR (75 MHz, DMSO-d_6): δ [ppm] = 155.6, 154.9, 150.5, 145.8, 131.1, 123.0, 122.4, 121.2, 120.4, 113.4, 109.5, 104.9, 56.44, 38.26.

HRMS (ESI): $C_{16}H_{14}ClF_3N_5O^+$ $(M+H)^+$ calculated: 384.08335 found: 384.08276

***N*-((1-(3-chloro-4-(trifluoromethoxy)phenyl)-1*H*-1,2,3-triazol-4-yl)methyl)-2-(trifluoromethyl) pyridine-4-amine 3.38**

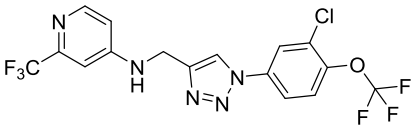

The compound was prepared according to **GP4.** 3-chloro-4-(trifluoromethoxy)aniline was used in the reaction and yielded 30.6 mg (69.9 µmol, 70%) of a colorless solid after purification *via* automated flash chromatography (PE/EtOAc).

^{1}H-NMR (500 MHz, acetone-d_6): δ [ppm] = 8.33 (d, *J* = 5.7 Hz, 1 H), 7.93 (m, 2 H), 7.69 (dd, *J* = 8.9 Hz, *J* = 2.6 Hz, 1 H), 7.51 (m, 1 H), 6.92 (d, *J* = 2.3 Hz, 1 H), 6.68 (dd, *J* = 5.7 Hz, *J* = 2.3 Hz, 1 H), 5.25 (m, 1 H), 4.63 (d, *J* = 5.6 Hz, 2 H).

^{13}C-NMR (75 MHz, DMSO-d_6): δ [ppm] = 153.5, 150.5, 149.2, 148.8, 145.3, 135.5, 130.0, 129.2, 123.7, 122.9, 122.0, 119.7, 118.63, 109.3, 107.8, 38.48.

HRMS (ESI): $C_{16}H_{11}ClF_6N_5O^+$ $(M+H)^+$ calculated: 438.05508 found: 438.05444

2-Chloro-1-isopropoxy-4-nitrobenzene 3.40a

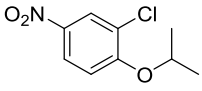

The compound was prepared according to **GP5**. Isopropanol (0.38 mL, 0.30 g, 5.00 mmol), 1,2-dichloro-4-nitrobenzene (960 mg, 5.00 mmol) and Cs_2CO_3 (4.89 g, 15.0 mmol) were used. The title compound was obtained as a yellowish solid (841 mg, 3.91 mmol, 78%).

LC-MS: m/z: 216 $(M+H)^+$

2-Chloro-1-cyclopropoxy-4-nitrobenzene 3.41a

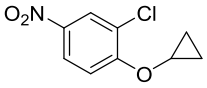

The compound was prepared according to **GP5**. Cyclopropanol (51 µL, 47 mg, 0.809 mmol), 1,2-dichloro-4-nitrobenzene (155 mg, 0.809 mmol) and Cs_2CO_3 (796 mg, 2.43 mmol) were used. The title compound was obtained as a colorless solid (117 mg, 0.548 mmol, 68%).

LC-MS: m/z: 214 $(M+H)^+$

^{1}H-NMR (300 MHz, $CDCl_3$): δ [ppm] = 8.29 (d, *J* = 2.6 Hz, 1 H), 8.18 (dd, *J* = 9.0 Hz, *J* = 2.8 Hz, 1 H), 7.40 (d, *J* = 9.1 Hz, 1 H), 3.94 – 3.90 (m, 1 H), 0.95 – 0.92 (m, 4 H).

2-Chloro-1-cyclobutoxy-4-nitrobenzene 3.42a

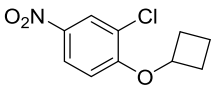

The compound was prepared according to **GP5**. Cyclopbutanol (34 µL, 31 mg, 0.430 mmol), 1,2-dichloro-4-nitrobenzene (83 mg, 0.430 mmol) and Cs_2CO_3 (423 mg, 1.29 mmol) were used. The title compound was obtained as a colorless solid (42 mg, 0.184 mmol, 43%).

LC-MS: m/z: 228 $(M+H)^+$

^{1}H-NMR (300 MHz, $CDCl_3$): δ [ppm] = 8.30 (d, *J* = 2.8 Hz, 1 H), 8.12 (dd, *J* = 9.2 Hz, *J* = 2.8 Hz, 1 H), 6.83 (d, *J* = 9.2 Hz, 1 H), 4.80 (quint, *J* = 7.2 Hz, 1 H), 2.57 – 2.52 (m, 2 H), 2.34 – 2.27 (m, 2 H), 1.98 – 1.94 (m, 1 H), 1.81 – 1.75 (m, 1 H).

3-(2-Chloro-4-nitrophenoxy)oxetane 3.43a

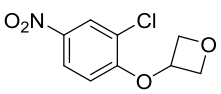

Oxetan-3-ol (64 µL, 74 mg, 1.00 mmol) was dissolved in anhydrous DMF (2 mL) and NaH (60 wt%, 55 mg, 1.50 mmol) was added at 0 °C. The mixture was stirred for 1 h and 1,2-dichloro-4-nitrobenzene (192 mg, 1.00 mmol) was added. The reaction mixture was stirred for 16 h at 80 °C. After cooling to

room temperature, H_2O was added and the mixture was extracted three times with EtOAc. The combined organic layers were washed with saturated LiCl solution, dried over Na_2SO_4 and concentrated *in vacuo*. Automated flash chromatography afforded the title compound as a yellow solid (147 mg, 0.642 mmol, 64%).

LC-MS: m/z: 244 $(M+H)^+$

^{1}H-NMR (300 MHz, $CDCl_3$): δ [ppm] = 8.35 (d, *J* = 2.6 Hz, 1 H), 8.12 (dd, *J* = 9.0 Hz, *J* = 2.6 Hz, 1 H), 6.55 (d, *J* = 9.1 Hz, 1 H), 5.36 (quint, *J* = 5.7 Hz, 1 H), 5.05 (dd, *J* = 7.1 Hz, 2 H), 4.86 (dd, *J* = 7.1 Hz, *J* = 5.7 Hz 2 H).

^{13}C-NMR (76 MHz, $CDCl_3$): δ [ppm] = 157.3, 141.9, 126.6, 123.9, 111.7, 71.38.

3-(2-Chloro-4-nitrophenoxy)tetrahydrofuran 3.44a

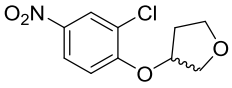

Tetrahydrofuran-3-ol (81 µL, 88 mg, 1.00 mmol) was dissolved in anhydrous DMF (2 mL) and NaH (60 wt%, 55 mg, 1.50 mmol) was added at 0 °C. The mixture was stirred for 1 h and 1,2-dichloro-4-nitrobenzene (192 mg, 1.00 mmol) was added. The reaction mixture was stirred for 16 h at 80 °C. After cooling to room temperature, H_2O was added and the mixture was extracted three times with EtOAc. The combined organic layers were washed with saturated LiCl solution, dried over Na_2SO_4 and concentrated *in vacuo*. Automated flash chromatography afforded the title compound as a yellow solid (129 mg, 0.530 mmol, 53%).

LC-MS: m/z: 244 $(M+H)^+$

^{1}H-NMR (300 MHz, $CDCl_3$): δ [ppm] = 8.32 (d, *J* = 2.6 Hz, 1 H), 8.16 (d, *J* = 9.0 Hz, *J* = 2.6 Hz, 1 H), 6.93 (d, *J* = 9.1 Hz, 1 H), 5.08 (bs, 1 h), 4.12 – 4.09 (m, 1 H), 4.06 – 4.02 (m, 2 H), 3.99 – 3.95 (m, 1 H), 2.34 – 2.28 (m, 1 H), 2.24 – 2.20 (m, 1 H).

^{13}C-NMR (76 MHz, $CDCl_3$): δ [ppm] = 158.2, 141.3, 126.4, 123.8, 112.6, 79.64, 72.70, 67.19, 33.01.

2-Chloro-4-nitro-1-phenoxybenzene 3.45a

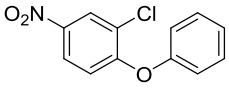

The compound was prepared according to **GP5**. Phenol (282 mg, 3.00 mmol), 1,2-dichloro-4-nitrobenzene (576 mg, 3.00 mmol) and Cs_2CO_3 (1.24 g, 2.98 mmol) were used. The title compound was obtained as a colorless solid (745 mg, 0.184 mmol, > 98%).

LC-MS: m/z: 250 $(M+H)^+$

^{1}H-NMR (300 MHz, $CDCl_3$): δ [ppm] = 8.41 (d, *J* = 2.7 Hz, 1 H), 8.06 (dd, *J* = 9.1 Hz, *J* = 2.7 Hz, 1 H), 7.50 – 7.44 (m, 2 H), 7.32 – 7.29 (m, 1 H), 7.13 – 7.10 (m, 2 H), 6.90 (d, *J* = 9.1 Hz, 1 H).

^{13}C-NMR (76 MHz, $CDCl_3$): δ [ppm] = 159.1, 154.5, 124.6, 130.4, 126.5, 125.7, 123.6, 120.2, 116.8.

3-Chloro-4-cyclopropoxyaniline 3.41b

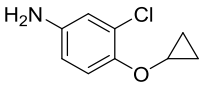

The compound was prepared according to **GP7** with toluene as solvent. 2-Chloro-1-cyclopropoxy-4-nitrobenzene **3.41a** (107 mg, 0.500 mmol) was used and the title compound was isolated as a brownish oil (98.1 mg, 0.468 mmol, 94%).

LC-MS: m/z: 184 $(M+H)^+$

^{1}H-NMR (300 MHz, $CDCl_3$): δ [ppm] = 7.09 (d, *J* = 8.7 Hz, 1 H), 6.76 (d, *J* = 2.8 Hz, 1 H), 8.59 (d, *J* = 8.6 Hz, *J* = 2.6 Hz, 1 H), 3.77 – 3.73 (m, 1 H), 0.85 – 0.80 (m, 2 H), 0.77 – 0.73 (m, 2 H).

3-Chloro-4-cyclobutoxyaniline 3.42b

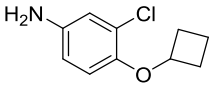

The compound was prepared according to **GP7** with THF as solvent. 2-Chloro-1-cyclobutoxy-4-nitrobenzene **3.42a** (114 mg, 0.500 mmol) was used and the title compound was isolated as a yellow oil (86 mg, 0.435 mmol, 87%).

LC-MS: m/z: 198 $(M+H)^+$

^{1}H-NMR (300 MHz, $CDCl_3$): δ [ppm] = 6.75 (d, *J* = 2.6 Hz, 1 H), 6.65 (d, *J* = 8.5 Hz, 1 H), 6.51 (dd, *J* = 8.7 Hz, *J* = 2.8 Hz 1 H), 4.56 (quint, *J* = 7.3 Hz, 1 H), 2.45 – 2.37 (m, 2 H), 2.25 – 2.17 (m, 2 H), 1.87 – 1.80 (m, 1 H), 1.68 – 1.85 (m, 1 H).

3-Chloro-4-(oxetan-3-yloxy)aniline 3.43b

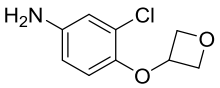

The compound was prepared according to **GP7** with THF as solvent. 3-(2-Chloro-4-nitrophenoxy)oxetane **3.43a** (115 mg, 0.500 mmol) was used and the title compound was isolated as a yellow oil (86 mg, 0.430 mmol, 86%).

LC-MS: m/z: 200 $(M+H)^+$

^{1}H-NMR (300 MHz, $CDCl_3$): δ [ppm] = 6.78 (d, *J* = 2.6 Hz, 1 H), 6.51 (dd, *J* = 8.7 Hz, *J* = 2.8 Hz, 1H), 8.42 (d, *J* = 8.7 Hz, 1 H), 5.13 (d, *J* = 5.7 Hz, 1 H), 4.92 (t, *J* = 6.9 Hz, 2 H), 4.83 (t, *J* = 5.7 Hz, 1 H).

^{13}C-NMR (76 MHz, $CDCl_3$): δ [ppm] = 145.5, 141.3, 124.1, 117.7, 115.7, 114.3, 71.98.

3-Chloro-4-((tetrahydrofuran-3-yl)oxy)aniline 3.44b

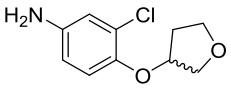

The compound was prepared according to **GP7** with THF as solvent. 3-(2-Chloro-4-nitrophenoxy)tetrahydrofuran **3.44a** (122 mg, 0.500 mmol) was used and the title compound was isolated as a yellow oil (107 mg, 0.498 mmol, > 98%).

LC-MS: m/z: 214 $(M+H)^+$

^{1}H-NMR (300 MHz, $CDCl_3$): δ [ppm] = 6.77 – 6.75 (m, 2 H), 6.54 (dd, *J* = 8.5 Hz, *J* = 2.6 Hz, 1 H), 4.83 (bs, 1 H), 4.07 – 4.00 (m, 2 H), 3.97 – 3.90 (m, 2 H), 2.21 – 2.17 (m, 1 H), 2.13 – 2.07 (m, 1 H).

^{13}C-NMR (76 MHz, $CDCl_3$): δ [ppm] = 145.7, 141.3, 125.1, 118.1, 116.9, 113.9, 80.03, 72.64, 66.93, 32.72.

3-Chloro-4-phenoxyaniline 3.45b

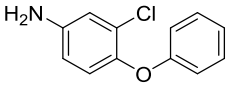

The compound was prepared according to **GP7** with EtOH as solvent. 2-Chloro-4-nitro-1-phenoxybenzene **3.45a** (100 mg, 0.400 mmol) was used and the title compound was obtained as a colorless solid (85 mg, 0.387 mmol, 97%).

LC-MS: m/z: 220 $(M+H)^+$

^{1}H-NMR (300 MHz, $CDCl_3$): δ [ppm] = 7.31 (d, *J* = 8.1 Hz, 1 H), 7.06 – 7.01 (m, 1 H), 6.93 – 6.88 (m, 3 H), 6.80 (d, *J* = 2.7 Hz, 1 H), 6.60 – 6.56 (m, 1 H), 3.68 (bs, 2 H).

^{13}C-NMR (76 MHz, $CDCl_3$): δ [ppm] = 150.1, 149.9, 141.6, 135.6, 130.1, 129.6, 127.8, 126.1, 124.8, 120.2, 84.89, 27.86.

***N*-((1-(3-chloro-4-isopropoxyphenyl)-1*H*-1,2,3-triazol-4-yl)methyl)-2-(trifluoromethyl)pyridin-4-amine 3.46**

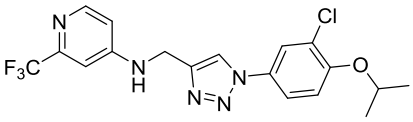

The compound was prepared according to **GP4.** 3-Chloro-4-isopropoxyaniline **3.40b** (8.6 mg, 0.046 mmol) was used. The title compound was obtained as a colorless solid (16.9 mg, 0.041, 89%).

^{1}H-NMR (300 MHz, $CDCl_3$): δ [ppm] = 8.33 (d, *J* = 5.7 Hz, 1 H), 7.84 (s, 1 H), 7.72 (s, 1 H), 7.54 (d, *J* = 8.9 Hz, 1 H), 7.05 (d, *J* = 8.9 Hz, 1 H), 6.92 (s, 1 H), 6.67 (d, *J* = 5.7 Hz, 1 H), 5.30 (bs, 1 H), 4.63 (quint, *J* = 6.0 Hz, 1 H), 4.61 (d, *J* = 5.3 Hz, 1 H), 1.43 (d, *J* = 6.0 Hz, 1 H).

^{13}C-NMR (126 MHz, $CDCl_3$): δ [ppm] = 154.2, 153.6, 150.4, 148.9, 144.5, 130.0, 125.1, 123.0, 120.6, 119.9, 115.6, 109.2, 104.8, 72.55, 38.48, 21.88.

HRMS (ESI): $C_{18}H_{18}ClF_3N_5O^+$ $(M+H)^+$ calculated: 412.11465 found: 412.11401

***N*-((1-(3-chloro-4-cyclopropoxyphenyl)-1*H*-1,2,3-triazol-4-yl)methyl)-2-(trifluoromethyl)pyridin-4-amine 3.47**

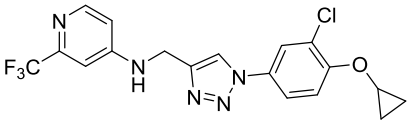

The compound was prepared according to **GP4.** 3-Chloro-4-cyclopropoxyaniline **3.41b** (10 mg, 0.050 mmol) was used. The title compound was obtained as yellowish solid (12.3 mg, 0.0.30 mmol, 60%).

^{1}H-NMR (500 MHz, $CDCl_3$): δ [ppm] = 8.32 (m, 1 H), 7.85 (bs, 1 H), 7.71 (d, *J* = 2.3 Hz, 1 H), 7.58 (dd, *J* = 8.9 Hz, *J* = 2.4 Hz, 1 H), 7.43 (d, *J* = 8.9 Hz, 1 H), 6.62 (s, 1 H), 6.68 – 6.67 (m, 1 H), 5.33 (bs, 1 H), 4.60 (d, *J* = 4.7 Hz, 2 H), 3.88 – 3.85 (m, 1 H), 0.90 (m, 4 H).

^{13}C-NMR (126 MHz, $CDCl_3$): δ [ppm] = 153.6, 152.8, 150.4, 149.0, 130.9, 124.3, 123.4, 122.8, 122.5, 120.1, 119.8, 115.5, 113.4, 109.2, 104.7, 51.8, 38.50. 5.04.

HRMS (ESI): $C_{18}H_{16}ClF_3N_5O^+$ $(M+H)^+$ calculated: 410.09899 found: 410.09859

***N*-((1-(3-hloro-4-cyclobutoxyphenyl)-1*H*-1,2,3-triazol-4-yl)methyl)-2-(trifluoromethyl)pyridin-4-amine 3.48**

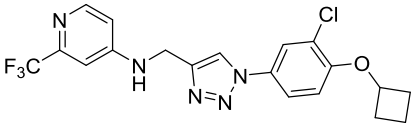

The compound was prepared according to **GP4.** 3-Chloro-4-cyclobutoxyaniline **3.42b** (27 mg, 0.120 mmol) was used. The title compound was obtained as a colorless solid (4.1 mg, 0.010 mmol, 12% brsm).

^{1}H-NMR (300 MHz, $CDCl_3$): δ [ppm] = 8.34 (d, *J* = 5.7 Hz, 1 H), 7.82 (s, 1 H), 7.73 (d, *J* = 2.6 Hz, 1 H), 7.52 (dd, *J* = 8.9 Hz, *J* = 2.7 Hz, 1 H), 6.92 (d, *J* = 2.3 Hz, 1 H), 6.89 (d, *J* = 8.9 Hz, 1 H), 6.67 (dd, *J* = 5.7 Hz, *J* = 2.3 Hz, 1 H), 5.17 (bs, 1 H), 4.75 (quint, *J* = 7.7 Hz, 1 H), 2.54 – 2.49 (m, 2 H), 2.32 – 2.26 (m, 2 H), 1.96 – 1.92 (m, 1 H) 1.79 – 1.73 (m, 1 H).

^{13}C-NMR (76 MHz, $CDCl_3$): δ [ppm] = 154.7, 153.1, 150.5, 149.2, 131.2, 124.5, 123.6, 123.0, 122.6, 120.1, 119.8, 115.5, 113.4, 109.2, 104.7, 77.1, 38.51, 14.1.

HRMS (ESI): $C_{19}H_{18}ClF_3N_5O^+$ $(M+H)^+$ calculated: 424.11465 found: 424.11386

***N*-((1-(3-chloro-4-(oxetan-3-yloxy)phenyl)-1H-1,2,3-triazol-4-yl)methyl)-2-(trifluoromethyl)pyridin-4-amine 3.49**

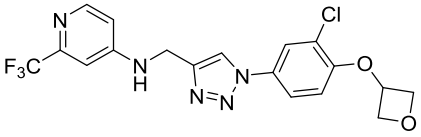

The compound was prepared according to **GP4.** 3-Chloro-4-(oxetan-3-yloxy)aniline **3.43b** (11 mg, 0.050 mmol) was used. The title compound was obtained as a colorless solid (10.9 mg, 0.026 mmol, 52%).

^{1}H-NMR (500 MHz, $CDCl_3$): δ [ppm] = 8.31 (d, *J* = 5.7 Hz, 1 H), 7.84 (s, 1 H), 7.78 (d, *J* = 2.4 Hz, 1 H), 7.54 (dd, *J* = 8.7 Hz, *J* = 2.4 Hz, 1 H), 6.91 (d, *J* = 2.0 Hz, 1 H), 6.66 (dd, *J* = 5.7 Hz, *J* = 2.0 Hz, 1 H), 6.61 (d, *J* = 8.7 Hz, 1 H), 5.32 – 5.27 (m, 1 H), 5.04 – 5.01 (m, 2 H), 4.86 – 4.84 (m, 2 H), 4.61 (d, *J* = 5.5 Hz, 2 H).

^{13}C-NMR (126 MHz, $CDCl_3$): δ [ppm] = 153.6, 152.8, 150.4, 149.0, 130.9, 124.3, 123.4, 122.8, 122.5, 120.1, 119.8, 115.5, 113.4, 109.2, 104.7, 77.41, 71.54, 38.48.

HRMS (ESI): $C_{18}H_{16}ClF_3N_5O_2^+$ $(M+H)^+$ calculated: 426.09391 found: 426.09294

***N*-((1-(3-chloro-4-((tetrahydrofuran-3-yl)oxy)phenyl)-1*H*-1,2,3-triazol-4-yl)methyl)-2 (trifluoromethyl)pyridin-4-amine 3.50**

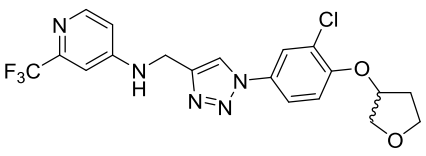

The compound was prepared according to **GP4.** 3-Chloro-4-((tetrahydrofuran-3-yl)oxy)aniline **3.44b** (12 mg, 0.050 mmol) was used. The title compound was obtained as a colorless solid (13.3 mg, 0.030 mmol, 61%).

^{1}H-NMR (500 MHz, $CDCl_3$): δ [ppm] = 8.31 (d, *J* = 5.7 Hz, 1 H), 7.85 (s, 1 H), 7.75 (d, *J* = 2.0 Hz, 1 H), 7.56 (dd, *J* = 8.3 Hz, *J* = 2.0 Hz, 1 H), 6.91 (d, *J* = 8.3 Hz, 1 H), 6.90 (d, *J* = 1.8 Hz, 1 H), 6.66 (dd, *J* = 5.7 Hz, *J* = 1.8 Hz, 1 H), 5.35 (m, 1 H), 5.02 (m, 1 H), 4.61 (d, *J* = 5.3 Hz, 2 H), 4.08 – 4.02 (m, 3 H), 3.98 – 3.94 (m, 1 H), 22.8 – 2.20 (m, 2 H).

^{1}H-NMR (126 MHz, $CDCl_3$): δ [ppm] = 153.7, 152.9, 150.5, 149.1, 131.2, 124.4, 123.5, 122.9, 122.6, 120.2, 119.9, 115.6, 113.5, 109.3, 104.8, 82.13, 80.12, 71.55, 38.49, 32.05.

HRMS (ESI): $C_{19}H_{18}ClF_3N_5O_2^+$ $(M+H)^+$ calculated: 440.10956 found: 440.10856

***N*-((1-(3-chloro-4-phenoxyphenyl)-1*H*-1,2,3-triazol-4-yl)methyl)-2-(trifluoromethyl)pyridin-4-amine 3.51**

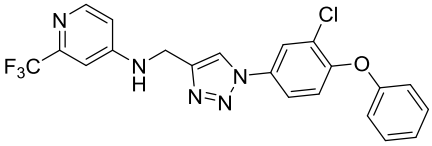

The compound was prepared according to **GP4.** 3-Chloro-4-phenoxyaniline **3.45b** (75 mg, 0.342 mmol) was used. The title compound was obtained as a colorless solid (43 mg, 0.337 mmol, > 98%).

^{1}H-NMR (500 MHz, acetone-d_6): δ [ppm] = 8.32 (d, *J* = 5.6 Hz, 1 H), 7.89 (s, 1 H), 7.85 (d, *J* = 2.6 Hz, 1 H), 7.54 (dd, *J* = 8.9 Hz, *J* = 2.6 Hz, 1 H), 7.39 (m, 2 H), 7.19 (m, 1 H), 7.05 (m, 3 H), 6.92 (d, *J* = 2.2 Hz, 1 H), 6.67 (d, *J* = 5.7 Hz, *J* = 2.3 Hz, 1 H), 5.34 – 5.31 (m, 1 H), 4.62 (d, *J* = 5.6 Hz, 2 H).

^{13}C-NMR (126 MHz, DMSO-d_6): δ [ppm] = 155.9, 153.7, 153.5, 150.3, 149.0, 148.6, 144.9, 132.4, 130.1, 126.5, 124.4, 123.5, 123.1, 120.3, 120.0, 119.9, 111.1, 109.2, 104.8, 38.43.

HRMS (ESI): $C_{21}H_{16}ClF_3N_5O^+$ $(M+H)^+$ calculated: 446.09899 found: 446.09830

2-chloro-4-iodo-6-(trifluoromethyl)pyridine 4.12/2-chloro-3-iodo-6-(trifluoromethyl)pyridine *iso*-4.12

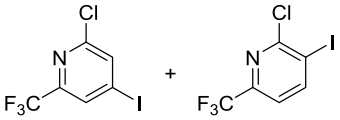

Freshly distilled DIPEA (2.86 mL, 2.06 g, 20.4 mmol) was dissolved in anhydrous THF (16 mL) and cooled to –100 °C, followed by the slow addition of *n*BuLi (2.5 M in THF, 8.0 mL, 20.0 mmol). The solution was

stirred for 30 minutes at this temperature and 2-chloro-6-(trifluoromethyl)pyridine (1.81 g, 10.0 mmol) in anhydrous THF (2.4 mL) was added slowly. The reaction mixture was stirred for 2 h and I_2 (2.53 g, 10.0 mmol) in anhydrous THF (2.4 mL) was added very slowly keeping the reaction temperature below –80 °C. The reaction mixture was stirred for 2 h at approximately –80 °C and then H_2O was added slowly. The reaction mixture was extracted with EtOAc and dried over Na_2SO_4. The solvent was evaporated under reduced pressure and automated column chromatography (PE/EtOAc) afforded a mixture of regioisomers (2:1, 2.14 g, 0.696 mmol, 70%).

LC-MS: m/z: 308 $(M+H)^+$

^{1}H-NMR (4.12) (300 MHz, acetone-d_6): δ [ppm] = 8.09 (d, *J* = 1.8 Hz, 1 H), 8.08 (d, *J* = 1.8 Hz, 1 H).

^{13}C-NMR (4.12) (76 MHz, acetone-d_6): δ [ppm] = 152.3, 148.5, 16.2, 128.5, 119.8, 107.5.

^{1}H-NMR (*iso*-4.12) (300 MHz, acetone-d_6): δ [ppm] = 8.50 (d, *J* = 8.0 Hz, 1 H), 7.47 (d, *J* = 8.0 Hz, 1 H).

^{13}C-NMR (*iso*-4.12) (76 MHz, acetone-d_6): δ [ppm] = 155.5, 150.5, 148.1, 120.7, 119.8, 99.21.

2-chloro-6-(trifluoromethyl)isonicotinic acid 4.13/2-chloro-6-(trifluoromethyl)nicotinic acid *iso*-4.13

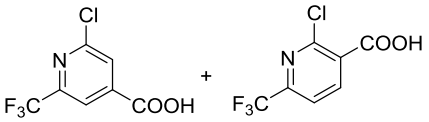

To a solution of $LiMg(nBu)_3$ (0.7 M in THF, 1.71 mL, 1.20 mmol) in anhydrous THF (2 mL) the mixture of 2-chloro-4-iodo-6-(trifluoromethyl)pyridine **4.12**/2-chloro-3-iodo-6-(trifluoromethyl)pyridine ***iso*-4.12** (308 mg, 1.00 mmol) in anhydrous THF (2 mL) was added slowly at 0 °C. After 15 minutes CO_2 was bubbled through the reaction mixture for 30 minutes. The reaction was quenched with 1 M HCl and extracted with EtOAc, dried over Na_2SO_4, filtered and the solvent was removed *in vacuo*. The crude product was directly used in the next step without further purification.

LC-MS: m/z: 224 $(M-H)^-$

^{1}H-NMR (4.13) (300 MHz, acetone-d_6): δ [ppm] = 8.23 (s, 1 H), 8.18 (s, 1 H).

^{13}C-NMR (4.13) (76 MHz, acetone-d_6): δ [ppm] = 167.5, 153.5, 149.8, 141.2, 128.0, 120.5, 119.1.

^{1}H-NMR (*iso*-4.13) (300 MHz, acetone-d_6): δ [ppm] = 8.60 – 8.59 (m, 1 H), 8.04 – 8.02 (m, 1 H).

^{13}C-NMR (*iso*-4.13) (76 MHz, acetone-d_6): δ [ppm] = 165.1, 150.5, 149.8, 134.6, 132.1, 121.7, 121.0.

***Tert*-butyl (2-chloro-6-(trifluoromethyl)pyridin-4-yl)carbamate 4.15**

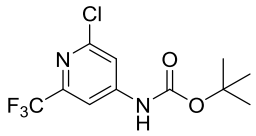

To a solution of 2-chloro-6-(trifluoromethyl)isonicotinic acid **4.13**/2-chloro-6-(trifluoromethyl)nicotinic acid ***iso*-4.13** was dissolved in anhydrous toluene (3 mL) and anhydrous NEt_3 (0.47 mL, 3.34 mmol) was added DPPA (0.45 mL, 1.67 mmol). The reaction mixture was stirred at 100 °C for 20 h and allowed to cool to room temperature. Then, KO*t*Bu (123 mg, 1.10 mmol) was suspended in anhydrous toluene (2 mL) and added to the reaction mixture at 0 °C. The reaction mixture was stirred for 30 minutes and allowed to warm to room temperature and was then extracted with EtOAc. The combined organic layers were washed with Brine and dried over Na_2SO_4. The solvent was removed under reduced pressure and automated flash chromatography (PE/EtOAc) afforded the title compound as a white solid (74.5 mg, 0.251 mmol, 25% over two steps).

LC-MS: m/z: 240 $(M+H-tBu)^+$

^{1}H-NMR (300 MHz, $CDCl_3$): δ [ppm] = 7.63 (bs, 1 H), 7.61 (bs, 1 H), 6.86 (bs, 1 H), 1.55 (s, 9 H).

***Tert*-butyl (2-chloro-6-(trifluoromethyl)pyridin-4-yl)(prop-2-yn-1-yl)carbamate 4.16**

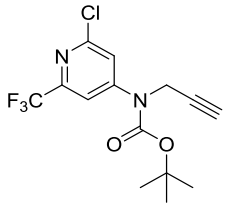

To a stirred solution of *tert*-butyl (2-chloro-6-(trifluoromethyl)pyridin-4-yl)carbamate **4.15** (593 mg, 2.00 mmol) in DMF (5 mL) at 0°C was added NaH (60 wt%) (92.1 mg, 2.40 mmol) propargyl bromide (72.17 mg, 2.4 mmol). The reaction was stirred for 1 h and then propargylbromide (182 µL, 2.40 mmol) was added dropwise and stirred for 5 h at r.t. The reaction was then added on ice water followed by extraction with EtOAc, dried over $MgSO_4$ and evaporated under reduced pressure. After automated flash chromatography (PE/EtOAc) the title compound was obtained as an orange solid (649 mg, 1.94 mmol, 97%).

LC-MS: m/z: 279 $(M+H-tBu)^+$

^{1}H-NMR (300 MHz, $CDCl_3$): δ [ppm] = 7.82 – 7.81 (m, 1 H), 7.63 – 7.62 (m, 1 H), 4.50 – 4.48 (m, 2 H), 2.40 – 2.39 (m, 1 H), 1.57 (s, 9 H).

2-Chloro-*N*-(prop-2-yn-1-yl)-6-(trifluoromethyl)pyridin-4-amine 4.17

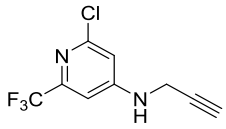

To *tert*-butyl (2-chloro-6-(trifluoromethyl)pyridin-4-yl)(prop-2-yn-1-yl)carbamate **4.16** (502 mg, 1.50 mmol) dissolved in DCM (9 mL) was added TFA (1 mL). After stirring at r.t. for 5 h the mixture was cooled to 0°C followed by the addition of saturated $NaHCO_3$ solution and extraction with DCM. The combined organic layers were dried over $MgSO_4$ and concentrated under reduced pressure. Automated flash chromatography (PE/EtOAc) gave the title compound as a white solid (346 mg, 1.48 mmol, > 98%).

LC-MS: m/z: 235 $(M+H)^+$

^{1}H-NMR (300 MHz, acetone-d_6): δ [ppm] = 7.09 (d, *J* = 2.0 Hz, 1 H), 7.03 (bs, 1 H), 6.87 (d, *J* = 2.0 Hz, 1 H), 4.19 (dd, *J* = 6.0 Hz, *J* = 2.6 Hz, 2 H), 2.88 (bs, 2 H), 2.82. (t, *J* = 2.5 Hz, 1 H).

^{13}C-NMR (76 MHz, acetone-d_6): δ [ppm] = 159.3, 156.7, 152.3, 122.8, 109.7, 105.8, 79.27, 73.12, 32.05.

2-Chloro-*N*-((1-(4-phenoxyphenyl)-1*H*-1,2,3-triazol-4-yl)methyl)-6-(trifluoromethyl)pyridin-4-amine 4.2

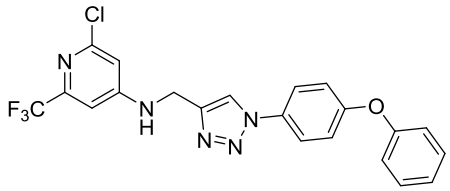

To a solution of 4-phenoxyaniline (18.5 mg, 0.100 mmol) in MeCN (1 mL) was added *tert*-butyl nitrite (0.110 mmol, 12.6 mg, 14.5 µL) at 0 °C. After stirring for 5 minutes trimethylsilylazide (0.110 mmol, 13.3 mg, 15.2 µL) was slowly added. The mixture was stirred for 1 h and 2-chloro-*N*-(prop-2-yn-1-yl)-6-(trifluoromethyl)pyridin-4-**amine 4.17** (28.2 mg, 0.120 mmol) was added at r.t. in one portion. After addition of DIPEA (0.120 mmol, 15.5 mg, 20.9 µL), the reaction mixture was purged with argon and $CuSO_4 \cdot 5\ H_2O$ (2.5 mg, 10 mol%) and Na-ascorbate (3.9 mg, 20 mol%) were added. The mixture was again purged with argon and stirred for 16 h at room temperature. Saturated NH_4Cl solution was added to the reaction mixture and stirred for 5 minutes. Then, EtOAc and saturated EDTA solution were added and the mixture was stirred for 15 minutes until the aqueous phase showed a clear blue color. The phases were separated and the aqueous phase was extracted with EtOAc three times. The combined organic layers were dried over $MgSO_4$, filtered and concentrated *in vacuo*. The crude product was purified *via* automated flash chromatography (PE/EtOAc) and afforded the title compound as a brownish solid (41.5 mg, 0.932 mmol, 93%).

^{1}H-NMR (300 MHz, $CDCl_3$): δ [ppm] = 7.90 (s, 1 H), 7.67 – 7.64 (m, 2 H), 7.42 – 7.38 (m, 2 H), 7.21 – 7.18 (m, 1 H), 7.15 – 7.12 (m 2 H), 7.08 – 7.06 (m, 2 H), 6.87 (d, *J* = 2.0 Hz, 1 H), 6.69 (d, *J* = 2.0 Hz, 1 H), 5.56 (bs, 1 H), 4.60 (s, 2 H).

^{13}C-NMR (76 MHz, $CDCl_3$): δ [ppm] = 158.3, 156.1, 155.3, 152.8, 148.5, 143.8, 131.7, 130.1, 124.3, 122.4, 120.0, 119.6, 119.2, 108.0, 104.7, 38.55.

HRMS (ESI): $C_{21}H_{16}ClF_3N_5O^+$ $(M+H)^+$ calculated: 446.09899 found: 446.09899

4-(((1-(4-Phenoxyphenyl)-1*H*-1,2,3-triazol-4-yl)methyl)amino)-6-(trifluoromethyl)pyridin-2-ol 4.19

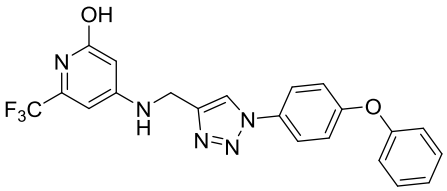

2-Chloro-*N*-((1-(4-phenoxyphenyl)-1H-1,2,3-triazol-4-yl)methyl)-6-(trifluoromethyl) pyridin-4-amine **4.2** (4.5 mg, 0.010 mmol) was dissolved in 1,4-dioxane (0.10 mL) and purged with argon. The solution was added to the pre-weighted catalyst (10 mol% of *t*BuBrettPhos Pd G3 or *t*BuXPhos Pd G3) under an argon atmosphere. NH_3 (0.5 M in 1,4-dioxane, 40 µL, 0.020 mmol) and NaO*t*Bu (2.0 M in 1,4-dioxane, 11 µL, 0.022 mmol) were added and the mixture was stirred for 24 h in a pre-heated sandbath at 80 °C. The reaction mixture was quenched with HOAc (0.01 mL) in MeCN (0.49 mL). Extraction with EtOAc

LC-MS: m/z: 428 $[M+H]^+$

2-((diphenylmethylene)amino)-*N*-((1-(4-phenoxyphenyl)-1*H*-1,2,3-triazol-4-yl)methyl)-6-(trifluoromethyl)pyridin-4-amine 4.20

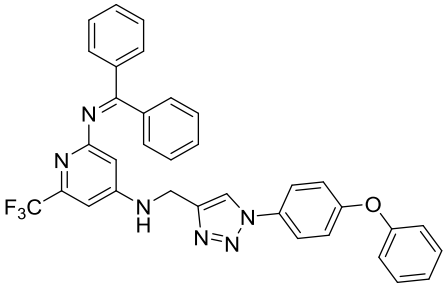

2-Chloro-*N*-((1-(4-phenoxyphenyl)-1*H*-1,2,3-triazol-4-yl)methyl)-6-(trifluoromethyl)pyridin-4-amine **4.2** (112 mg, 0.250 mmol) was dissolved in toluene (2.5 mL) and Cs_2CO_3 (326 mg, 1.00 mmol) was added. The reaction mixture was purged with argon and benzylamine (110 µL, 107 mg, 1.00 mmol), CataCXium A (10 mg, 10 mol%) and Pd_2dba_3 (23 mg, 10 mol%) were added. The reaction mixture was purged with argon for 15 min and was stirred in a pre-heated oil bath for 24 h at 120 °C. The mixture

was then filtered over silica gel and purified *via* automated flash chromatography (PE/EtOAc) and afforded the title compound as a yellow solid (101 mg, 0.171 mmol, 68%).

LC-MS: m/z: 591 $[M+H]^+$

^{1}H-NMR (300 MHz, $CDCl_3$): δ [ppm] = 7.67 (s, 1 H), 7.61 – 7.59 (m, 3 H), 7.42 – 7.39 (m, 3 H), 7.38 – 7.33 (m, 4 H), 7.33 – 7.27 (m, 2 H), 7.23 – 7.17 (m, 2 H), 7.16 – 7.12 (m, 2 H), 7.09 – 7.06 (m, 2 H), 6.84 – 6.83 (m, 1 H), 6.56 – 6.54 (m, 1 H), 5.17 (bs, 1 H), 4.51 (d, *J* = 5.7 Hz, 2 H).

N^2-benzyl-N^4-((1-(4-phenoxyphenyl)-1H-1,2,3-triazol-4-yl)methyl)-6-(trifluoromethyl)pyridine-2,4-diamine 4.21

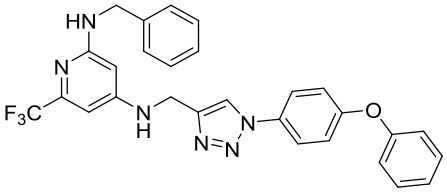

2-Chloro-*N*-((1-(4-phenoxyphenyl)-1*H*-1,2,3-triazol-4-yl)methyl)-6-(trifluoromethyl)pyridin-4-amine **4.2** (112 mg, 0.250 mmol) was dissolved in 1,4-dioxane (2.5 mL) and NaO*t*Bu (2 M in THF, 0.50 mL, 1.00 mmol) was added. The reaction mixture was purged with argon and benzylamine (110 µL, 107 mg, 1.00 mmol), $[Pd(cinnamyl)Cl]_2$ (13 mg, 10 mol%) and BippyPhos (25 mg, 20 mol%) were added. The reaction mixture was purged with argon for 15 min and was stirred in a pre-heated oil bath for 24 h at 80 °C. The mixture was then filtered over silica gel and purified *via* automated flash chromatography (PE/EtOAc) and afforded the title compound as a brown solid (45 mg, 0.087 mmol, 35%).

LC-MS: m/z: 517 $[M+H]^+$

^{1}H-NMR (300 MHz, $CDCl_3$): δ [ppm] = 7.67 (s, 1 H), 7.61 – 7.59 (m, 2 H), 7.42 – 7.39 (m, 2 H), 7.36 – 7.33 (m, 2 H), 7.31 – 7.28 (m, 2 H), 7.22 – 7.17 (m, 2 H), 7.15 – 7.11 (m, 2 H), 7.09 – 7.07 (m, 2 H), 5.64 (d, *J* = 1.4 Hz, 1 H), 5.17 (bs, 1 H), 4.89 (bs, 1 H), 4.51 (d, *J* = 5.7 Hz, 2 H), 4.44 (d, *J* = 5.7 Hz, 2 H).

N^2-(tert-butyl)-N^4-((1-(4-phenoxyphenyl)-1H-1,2,3-triazol-4-yl)methyl)-6-(trifluoromethyl)pyridine-2,4-diamine 4.22

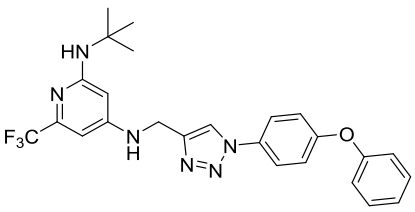

2-Chloro-*N*-((1-(4-phenoxyphenyl)-1*H*-1,2,3-triazol-4-yl)methyl)-6-(trifluoromethyl)pyridin-4-amine **4.2** (112 mg, 0.250 mmol) was dissolved in 1,4-dioxane (2.5 mL) and NaO*t*Bu (2 M in THF, 0.50 mL, 1.00 mmol) was added. The reaction mixture was purged with argon and *tert*-butyl amine (105 µL, 73 mg, 1.00 mmol), $[Pd(cinnamyl)Cl]_2$ (13 mg, 10 mol%) and BippyPhos (25 mg, 20 mol%) were added. The reaction mixture was purged with argon for 15 min and was stirred in a pre-heated oil bath for 24 h at 80 °C. The mixture was then filtered over silica gel.

LC-MS: m/z: 483 $[M+H]^+$

***N*^{4}-((1-(4-phenoxyphenyl)-1H-1,2,3-triazol-4-yl)methyl)-6-(trifluoromethyl)pyridine-2,4-diamine 4.1**

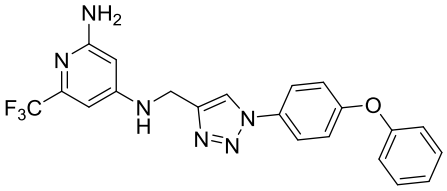

A crimp vial was charged with 2-chloro-*N*-((1-(4-phenoxyphenyl)-1*H*-1,2,3-triazol-4-yl)methyl)-6-(trifluoromethyl)pyridin-4-amine **4.2** (45 mg, 0.100 mmol), *tert*-butyl carbamate (23 mg, 0.200 mmol) and Cs_2CO_3 (72 mg, 0.220 mmol). 1,4-dioxane (1.1 mL) was added and the reaction mixture was purged with argon for 5 minutes. After addition of Pd-175 (3.9 mg, 5 mol%) the mixture was purged with argon for further 5 minutes and the vial was heated at 90 °C. After stirring for 16 hours the reaction mixture was filtered and subjected to automated flash chromatography using DCM/MeOH as an eluent which yielded the desired product as a beige solid (16.7 mg, 0.392 mmol, 39%).

^{1}H-NMR (500 MHz, acetone-d_6): δ [ppm] = 9.56 (bs, 1 H), 8.51 (s, 1 H), 7.89 – 7.86 (m, 2 H), 7.46 – 7.42 (m, 2 H), 7.22 – 7.20 (m, 1 H), 7.19 – 7.16 (m, 2 H), 7.11 – 7.09 (m, 2 H), 6.70 (d, *J* = 1.7 Hz, 1 H), 6.69 – 6.67 (m, 1 H), 6.03 (s, 1 H), 4.59 (d, *J* = 5.8 Hz, 2 H).

^{13}C-NMR (76 MHz, DMSO-d_6): δ [ppm] = 165.3, 157.9, 157.1, 156.9, 145.8, 133.0, 130.5, 124.5, 122.4, 121.1, 119.9, 100.7, 91.96, 38.45.

HRMS (ESI): $C_{21}H_{18}F_3N_6O^+$ $(M+H)^+$ calculated: 427.14887 found: 427.13721

1-Fluoro-2-(4-nitrophenoxy)benzene 5.1a

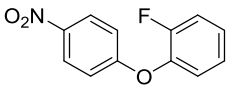

The compound was prepared according to **GP5**. 3-Fluorophenol (0.18 mL, 224 mg, 2.00 mmol), 1-chloro-4-nitrobenzene (315 mg, 2.00 mmol) and K_2CO_3 (828 mg, 6.00 mmol) were used. The title compound was obtained as a red solid (460 mg, 1.97 mmol, > 98%).

LC-MS: m/z: 234 $(M+H)^+$

^{1}H-NMR (300 MHz, $CDCl_3$): δ [ppm] = 8.24 – 8.20 (m, 2 H), 7.26 – 7.24 (m, 2 H), 7.22 – 7.21 (m, 1 H), 7.21 – 7.20 (m, 1 H), 7.03 – 7.00 (m, 2 H).

1-Fluoro-3-(4-nitrophenoxy)benzene 5.2a

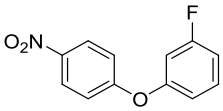

The compound was prepared according to **GP5**. 3-Fluorophenol (0.18 mL, 224 mg, 2.00 mmol), 1-chloro-4-nitrobenzene (315 mg, 2.00 mmol) and K_2CO_3 (828 mg, 6.00 mmol) were used. The title compound was obtained as a brown solid (462 mg, 1.98 mmol, > 98%).

LC-MS: m/z: 234 $(M+H)^+$

^{1}H-NMR (300 MHz, $CDCl_3$): δ [ppm] = cs954

4-(2-Fluorophenoxy)aniline 5.1b

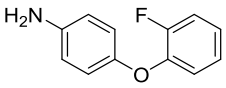

The compound was prepared according to **GP7** with EtOH as solvent. 1-Fluoro-2-(4-nitrophenoxy)benzene **5.1a** (117 mg, 0.500 mmol) was used and the title compound was isolated as a yellow solid (101 mg, 0.496 mmol, > 98%).

LC-MS: m/z: 204 $(M+H)^+$

^{1}H-NMR (300 MHz, $CDCl_3$): δ [ppm] = 7.17 – 7.13 (m, 1 H), 7.05 – 6.98 (m, 2 H), 6.94 – 6.90 (m, 1 H), 6.89 – 6.86 (m, 2 H), 6.69 – 6.66 (m, 2 H), 3.59 (bs, 2 H).

^{13}C-NMR (76 MHz, $CDCl_3$): δ [ppm] = 154.6, 152.6, 148.9, 145.8, 142.6, 124.4, 123.2, 119.9, 116.8, 116.2.

4-(3-Fluorophenoxy)aniline 5.2b

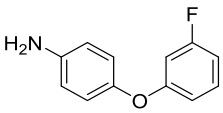

The compound was prepared according to **GP7** with EtOH as solvent. 1-Fluoro-3-(4-nitrophenoxy)benzene **5.2a** (117 mg, 0.500 mmol) was used and the title compound was isolated as a yellow solid (101 mg, 0.497 mmol, > 98%).

LC-MS: m/z: 204 $(M+H)^+$

^{1}H-NMR (300 MHz, $CDCl_3$): δ [ppm] = 7.24 – 7.19 (m, 1 H), 6.91 – 6.87 (m, 2 H), 6.73 – 6.69 (m, 4 H), 6.65 – 6.61 (m, 1 H), 3.63 (bs, 2 H).

^{13}C-NMR (76 MHz, $CDCl_3$): δ [ppm] = 162.5, 160.5, 147.7, 143.2, 130.3, 121.5, 116.2, 112.5, 108.8, 104.6.

***N*-((1-(4-(2-fluorophenoxy)phenyl)-1*H*-1,2,3-triazol-4-yl)methyl)-2-(trifluoromethyl)pyridin-4-amine 5.3**

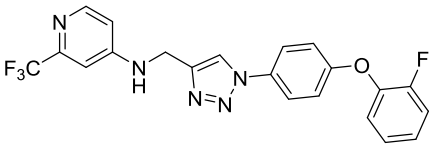

The compound was prepared according to **GP4.** 4-(2-Fluorophenoxy)aniline **5.1b** (20 mg, 0.100 mmol) was used. The title compound was obtained as yellow solid after purification *via* automated flash chromatography (4.1 mg, 0.095 mmol, 95%).

^{1}H-NMR (300 MHz, $CDCl_3$): δ [ppm] = 8.33 (d, *J* = 5.7 Hz, 1 H), 7.87 (s, 1 H), 7.66 – 7.63 (m, 2 H), 7.24 – 7.14 (m, 4 H), 7.12 – 7.09 (m, 2 H), 6.93 (d, *J* = 2.1 Hz, 1 H), 6.69 (dd, *J* = 5.8 Hz, *J* = 2.3 Hz, 1 H), 5.26 (bs, 1 H), 4.61 (d, *J* = 5.5 Hz, 2 H).

^{13}C-NMR (76 MHz, $CDCl_3$): δ [ppm] = 158.2, 153.7, 150.2, 144.4, 131.9, 125.9, 125.0, 122.4, 119.9, 117.7, 117.4, 109.3, 104.7, 38.56.

HRMS (ESI): $C_{21}H_{16}F_4N_5O^+$ $(M+H)^+$ calculated: 430.12855 found: 430.12795

***N*-((1-(4-(3-fluorophenoxy)phenyl)-1*H*-1,2,3-triazol-4-yl)methyl)-2-(trifluoromethyl)pyridin-4-amine 5.4**

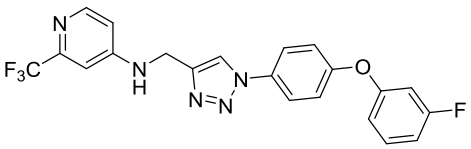

The compound was prepared according to **GP4.** 4-(3-Fluorophenoxy)aniline **5.2b** (20 mg, 0.100 mmol) was used. The title compound was obtained as yellow solid after purification *via* automated flash chromatography (4.0 mg, 0.093 mmol, 93%).

^{1}H-NMR (300 MHz, $CDCl_3$): δ [ppm] = 8.33 (d, *J* = 5.3 Hz, 1 H), 7.89 (s, 1 H), 7.71 – 7.69 (m, 2 H), 7.36 – 7.32 (m, 1 H), 7.19 – 7.16 (m, 2 H), 6.95 (d, *J* = 2.1 Hz, 1 H), 6.89 (ddd, *J* = 8.2 Hz, *J* = 2.3 Hz, *J* =

0.8 Hz, 1 H), 6.84 (dd, *J* = 8.2 Hz, *J* = 2.3 Hz, 1 H), 6.77 (ddd, *J* = 9.9 Hz, *J* = 2.4 Hz, 1 H), 6.70 (dd, *J* = 5.7 Hz, J = 1.9 Hz, 1 H), 5.33 (bs, 1 H), 4.63 (d, *J* = 5.3 Hz, 2 H).

^{13}C-NMR (76 MHz, $CDCl_3$): δ [ppm] = 157.2, 153.7, 150.1, 144.5, 132.5, 130.9, 122.5, 119.9, 114.7, 114.6, 111.0, 110.9, 109.3, 106.9, 106.7, 104.8, 38.58.

HRMS (ESI): $C_{21}H_{16}F_4N_5O^+$ $(M+H)^+$ calculated: 430.12855 found: 430.12796

2-Fluoro-3-(4-nitrophenoxy)pyridine 5.6a

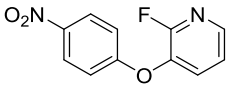

The compound was prepared according to **GP5**. 2-Fluoropyridin-3-ol (0.21 mL, 282 mg, 2.00 mmol), 1-fluoro-4-nitrobenzene (226 mg, 2.00 mmol) and K_2CO_3 (828 mg, 6.00 mmol) were used. The title compound was obtained as a brown solid (461 mg, 1.97 mmol, > 98%).

LC-MS: m/z: 235 $(M+H)^+$

^{1}H-NMR (300 MHz, DMSO-d_6): δ [ppm] = 8.29 – 8.26 (m, 2 H), 8.19 – 8.16 (m, 1 H), 8.02 – 7.98 (m, 1 H), 7.52 – 7.50 (m, 1 H), 7.26 – 7.23 (m, 2 H).

^{13}C-NMR (76 MHz, DMSO-d_6): δ [ppm] = 161.4, 155.6, 153.7, 143.8, 143.0, 136.4, 133.8, 126.3, 123.9, 116.9,

4-((2-Fluoropyridin-3-yl)oxy)aniline 5.6b

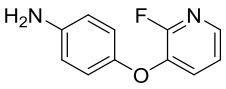

The compound was prepared according to **GP7** with DCM as solvent. 2-Fluoro-3-(4-nitrophenoxy)pyridine **5.6a** (76 mg, 0.325 mmol) was used and the title compound was isolated as a yellow solid (64 mg, 0.315 mmol, 97%).

LC-MS: m/z: 205 $(M+H)^+$

^{1}H-NMR (300 MHz, $CDCl_3$): δ [ppm] = 7.86 – 7.85 (m, 1 H), 7.25 – 7.21 (m, 1 H), 7.09 – 7.06 (m, 1 H), 6.90 – 6.87 (m, 2 H), 6.74 – 6.71 (m, 2 H), 3.60 (bs, 2 H).

^{13}C-NMR (76 MHz, $CDCl_3$): δ [ppm] = 153.8, 147.8, 143.2, 139.6, 127.3, 122.0, 120.8, 116.8.

***N*-((1-(4-((2-fluoropyridin-3-yl)oxy)phenyl)-1*H*-1,2,3-triazol-4-yl)methyl)-2-(trifluoromethyl)pyridin-4-amine 5.7**

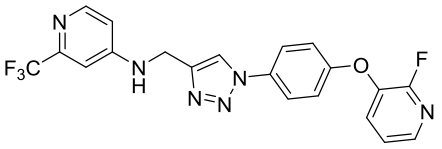

The compound was prepared according to **GP4.** 4-((2-Fluoropyridin-3-yl)oxy)aniline **5.6b** (20 mg, 0.100 mmol) was used. The title compound was obtained as yellowish solid (23 mg, 0.056 mmol, 56%).

^{1}H-NMR (500 MHz, acetone-d_6): δ [ppm] = 8.53 (s, 1 H), 8.22 – 8.21 (m, 1 H), 8.06 (m, 1 H), 7.91 – 7.89 (m, 2 H), 7.77 – 7.73 (m, 1 H), 7.42 – 7.40 (m, 1 H), 7.27 – 7.25 (m, 2 H), 7.12 (s, 1 H), 6.89 – 6.88 (m, 1 H), 6.80 (bs, 1 H), 4.66 (d, *J* = 5.7 Hz, 2 H).

^{13}C-NMR (126 MHz, acetone-d_6): δ [ppm] = 157.5, 157.1, 155.5, 155.2, 151.1, 146.4, 143.2, 143.1, 139.4, 139.7, 134.2, 132.3, 124.0, 123.1, 121.8, 119.5, 38.84.

HRMS (ESI): $C_{20}H_{15}F_4N_6O^+$ $(M+H)^+$ calculated: 431.12380 found: 431.12391

***N*-((1-(4-(pyridin-3-yloxy)phenyl)-1*H*-1,2,3-triazol-4-yl)methyl)-2-(trifluoromethyl)pyridin-4-amine 5.9**

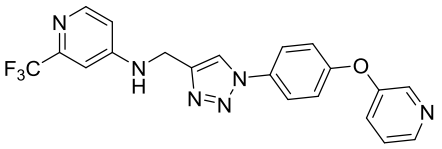

The compound was prepared according to **GP4.** 4-(pyridin-3-yloxy)aniline (19 mg, 0.100 mmol) was used. The title compound was obtained as yellowish solid (23 mg, 0.056 mmol, 56%).

^{1}H-NMR (300 MHz, acetone-d_6): δ [ppm] = 8.54 (s, 1 H), 8.43 – 8.41 (m, 2 H), 8.22 – 8.21 (m, 1 H), 7.91 – 7.90 (m, 2 H), 7.51 – 7.49 (m, 1 H), 7.45 – 7.43 (m, 1 H), 7.27 – 7.25 (m, 2 H), 7.14 (s, 1 H), 6.89 – 6.88 (m, 1 H), 6.81 (bs, 1 H), 4.66 (d, *J* = 5.7 Hz, 2 H).

^{13}C-NMR (126 MHz, acetone-d_6): δ [ppm] = 157.8, 155.5, 154.2, 151.1, 146.4, 146.2, 142.5, 134.2, 126.9, 125.5, 124.3, 123.1, 122.1, 121.8, 120.6, 38.85.

HRMS (ESI): $C_{20}H_{16}F_3N_6O^+$ $(M+H)^+$ calculated: 413.13322 found: 413.13245

***N*-((1-(4-(1*H*-indol-1-yl)phenyl)-1*H*-1,2,3-triazol-4-yl)methyl)-2-(trifluoromethyl)pyridin-4-amine 5.10**

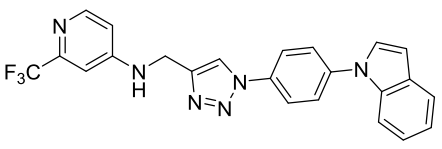

N-((1-(4-bromophenyl)-1*H*-1,2,3-triazol-4-yl)methyl)-2-(trifluoromethyl)pyridin-4-amine **3.22** (40 mg, 0.100 mmol), indole (42 mg, 0.100 mmol), K_2CO_3 (69 mg, 0.500 mmol) and L-proline (1.2 mg, 10 mol%) were dissolved in DMSO (0.5 mL). The reaction mixture was purged with argon and CuI (1.0 mg, 5 mol%) was added. The reaction mixture was heated at 80 °C for 3 d and was then allowed to cool to room temperature. H_2O was added and the mixture was extracted with EtOAc, dried over Na_2SO_4, filtered and concentrated *in vacuo*. The crude product was purified *via* automated flash chromatography (PE/EtOAc) and gave the title compound was a slightly yellow solid (35.4 mg, 0.082 mmol, 82%)

^{1}H-NMR (300 MHz, acetone-d_6): δ [ppm] = 8.36 (d, *J* = 5.7 Hz, 1 H), 7.97 (s, 1 H), 7.90 – 7.88 (m, 2 H), 7.73 (s, 1 H), 7.71 – 7.69 (m, 2 H), 7.60 (d, *J* = 8.2 Hz, 1 H), 7.38 (d, *J* = 3.4 Hz, 1 H), 7.28 (dd, *J* = 7.3 Hz, 1 H), 7.22 (d, *J* = 8.2 Hz, 1 H), 6.95 (d, *J* = 2.3 Hz, 1 H), 6.76 (d, *J* = 3.2 Hz, 1 H), 670 (dd, *J* = 5.7 Hz, *J* = 2.3 Hz, 1 H), 5.21 (bs, 1 H), 4.66 (d, *J* = 5.7 Hz, 2 H).

^{13}C-NMR (76 MHz, $CDCl_3$) δ [ppm] = 153.8, 143.7, 138.6, 135.0, 132.6, 129.7, 122.4, 119.1, 118.9, 116.5, 116.3, 116.2, 110.7, 109.5, 109.3, 108.9, 108.5, 102.6, 38.90.

HRMS (ESI): $C_{23}H_{18}F_3N_6^+$ $(M+H)^+$ calculated: 435.15396 found: 435.15339

1-(4-nitrophenyl)-1*H*-pyrrolo[2,3-c]pyridine 5.12a

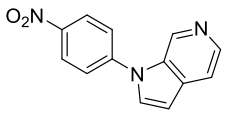

The compound was prepared according to **GP6.** 1*H*-pyrrolo[2,3-c]pyridine (236 mg, 2.00 mmol), 1-chloro-4-nitrobenzene (316 mg, 2.00 mmol), Cs_2CO_3 (1.97 g, 6.00 mmol) in DMF (4 mL) were used. The title compound was obtained as a yellow solid (473 mg, 1.98 mmol, > 98%).

LC-MS: m/z: 240 $(M+H)^+$

^{1}H-NMR (300 MHz, $CDCl_3$) δ [ppm] = 9.05 (s, 1 H), 8.48 – 8.45 (m, 2 H), 8.40 (d, *J* = 5.3 Hz, 1 H), 7.75 – 7.72 (m, 2 H), 7.61 (dd, *J* = 5.3 Hz, *J* = 1.1 Hz, 1 H), 7.55 (d, *J* = 3.2 Hz, 1 H), 6.81 (dd, *J* = 3.3 Hz, *J* = 0.8 Hz, 1 H).

1-(4-Nitrophenyl)-1*H*-pyrrolo[2,3-b]pyridine 5.13a

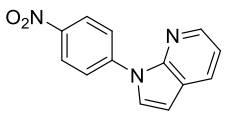

The compound was prepared according to **GP6.** 1*H*-pyrrolo[2,3-b]pyridine (236 mg, 2.00 mmol), 1-chloro-4-nitrobenzene (316 mg, 2.00 mmol) and Cs_2CO_3 (1.97 g, 6.00 mmol) in DMF (4 mL) were used. The title compound was obtained as a yellow solid (471 mg, 1.97 mmol, > 98%).

LC-MS: m/z: 240 $(M+H)^+$

^{1}H-NMR (300 MHz, $CDCl_3$) δ [ppm] = 8.42 (dd, *J* = 4.7 Hz, *J* = 1.5 Hz, 1 H), 8.41 – 8.39 (m, 2 H), 8.16 – 8.13 (m, 2 H), 8.01 (dd, *J* = 7.9 Hz, *J* = 1.5 Hz, 1 H), 7.61 (d, *J* = 3.8 Hz, 1 H), 7.22 (dd, *J* = 7.8 Hz, *J* = 4.7 Hz, 1 H), 6.74 (d, *J* = 3.8 Hz, 1 H).

1-(4-nitrophenyl)-1*H*-benzo[d]imidazole 5.14a

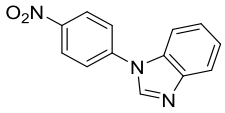

The compound was prepared according to **GP6.** Benzimidazole (236 mg, 2.00 mmol), 1-chloro-4-nitrobenzene (316 mg, 2.00 mmol) and Cs_2CO_3 (1.97 g, 6.00 mmol) in DMF (4 mL) were used. The title compound was obtained as a yellow solid (382 mg, 1.60 mmol, 80%).

LC-MS: m/z: 240 $(M+H)^+$

^{1}H-NMR (300 MHz, $CDCl_3$) δ [ppm] = 8.51 – 8.48 (m, 2 H), 8.20 (s, 1 H), 7.94 – 7.91 (m, 1 H), 7.78 – 7.75 (m, 2 H), 7.64 – 7.61 (m, 1 H), 7.44 – 7.40 (m, 2 H).

1-(4-Nitrophenyl)-1*H*-indazole 5.15a

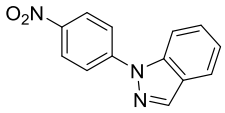

The compound was prepared according to **GP6.** Indazole (236 mg, 2.00 mmol), 1-chloro-4-nitrobenzene (316 mg, 2.00 mmol) and Cs_2CO_3 (1.97 g, 6.00 mmol) in DMF (4 mL) were used. The title compound was obtained as a yellow solid (418 mg, 1.75 mmol, 88%).

LC-MS: m/z: 240 $(M+H)^+$

^{1}H-NMR (300 MHz, $CDCl_3$) δ [ppm] = 8.45 – 8.42 (m, 2 H), 8.29 (d, *J* = 0.8 Hz, 1 H), 8.02 – 7.98 (m, 2 H), 7.89 – 7.85 (m, 2 H), 7.57 – 7.53 (m, 1 H), 7.35 – 7.32 (m, 1 H).

4-(1*H*-pyrrolo[2,3-c]pyridin-1-yl)aniline 5.12b

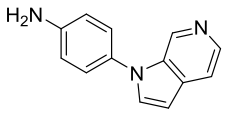

The compound was prepared according to **GP7**. 1-(4-nitrophenyl)-1*H*-pyrrolo[2,3-c]pyridine **5.12a** (473 mg, 1.98 mmol) was used and the title compound was obtained as a yellow solid (266 mg, 1.27 mmol, 64%).

LC-MS: m/z: 210 $(M+H)^+$

^{1}H-NMR (300 MHz, $CDCl_3$) δ [ppm] = 8.81 – 8.75 (m, 1 H), 8.28 (d, *J* = 6.1 Hz, 1 H), 7.63 – 7.59 (m, 1 H), 7.47 – 7.43 (m, 1 H), 7.38 – 7.34 (m, 1 H), 7.26 – 7.25 (m, 1 H), 7.20 – 7.17 (m, 1 H), 6.84 – 6.80 (m, 1 H), 6.68 – 6.65 (m, 1 H).

4-(1*H*-pyrrolo[2,3-b]pyridin-1-yl)aniline 5.13b

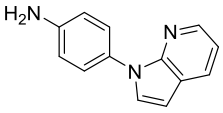

The compound was prepared according to **GP7**. 1-(4-nitrophenyl)-1*H*-pyrrolo[2,3-b]pyridine **5.13a** (120 mg, 0.500 mmol) was used and the title compound was obtained as a yellowish solid (104 mg, 0.498 mmol, > 98%).

LC-MS: m/z: 210 $(M+H)^+$

4-(1*H*-benzo[d]imidazol-1-yl)aniline 5.14b

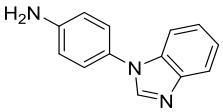

The compound was prepared according to **GP7.** 1-(4-nitrophenyl)-1*H*-benzo[d]imidazole **5.14a** (120 mg, 0.500 mmol) was used and the title compound was obtained as an orange solid (103 mg, 0.492 mmol, > 98%).

LC-MS: m/z: 210 $(M+H)^+$

4-(1*H*-indazol-1-yl)aniline 5.15b

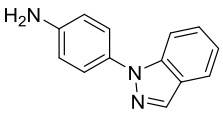

The compound was prepared according to **GP7**. 1-(4-nitrophenyl)-1*H*-indazole **5.15a** (120 mg, 0.500 mmol) was used and the title compound was obtained as a brownish solid (91.5 mg, 0.438 mmol, 88%).

LC-MS: m/z: 210 $(M+H)^+$

***N*-((1-(4-(1*H*-pyrrolo[2,3-c]pyridin-1-yl)phenyl)-1*H*-1,2,3-triazol-4-yl)methyl)-2-(trifluoromethyl) pyridin-4-amine 5.16**

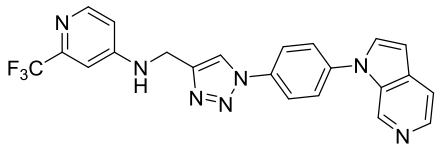

The title compound was prepared according to **GP4**. 4-(1*H*-pyrrolo[2,3-c]pyridin-1-yl)aniline **5.12b** (21 mg, 0.100 mmol) was used in the reaction and the title compound was obtained as a yellow solid (43.2 mg, 0.099 mmol, > 98%).

LC-MS: m/z: 437 $(M+H)^+$

^{1}H-NMR (300 MHz, $CDCl_3$) δ [ppm] = 9.00 (bs, 1 H), 8.41 (bs, 1 H), 8.36 (d, *J* = 5.7 Hz, 1 H), 8.00 (s, 1 H), 7.97 – 7.93 (m, 2 H), 7.75 – 7.71 (m, 2 H), 7.53 (d, *J* = 2.9 Hz, 1 H), 6.95 (d, *J* = 2.3 Hz, 1 H), 6.78 (d, *J* = 3.2 Hz, 1 H), 6.72 – 6.70 (m, 1 H), 5.19 (bs, 1 H), 4.66 (d, *J* = 5.5 Hz, 1 H).

^{13}C-NMR (76 MHz, $CDCl_3$) δ [ppm] = 153.7, 143.6, 139.7, 138.5, 134.9, 132.6, 129.7, 122.4, 119.1, 118.9, 116.4, 116.2, 116.1, 110.6, 108.9, 108.4, 102.5, 38.90.

***N*-((1-(4-(1*H*-pyrrolo[2,3-b]pyridin-1-yl)phenyl)-1*H*-1,2,3-triazol-4-yl)methyl)-2-(trifluoromethyl) pyridin-4-amine 5.17**

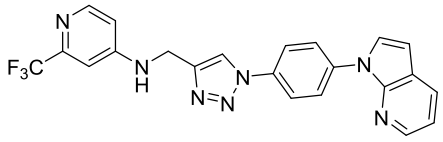

The title compound was prepared according to **GP4**. 4-(1*H*-pyrrolo[2,3-b]pyridin-1-yl)aniline **5.13b** (21 mg, 0.100 mmol) was used in the reaction and the title compound was obtained as a yellow solid (43.1 mg, 0.099 mmol, > 98%).

^{1}H-NMR (300 MHz, $CDCl_3$) δ [ppm] = 8.41 (dd, *J* = 4.6 Hz, *J* = 1.4 Hz, 1 H), 8.36 (d, *J* = 5.7 Hz, 1 H), 8.03 – 8.02 (m, 2 H), 8.02 – 8.00 (m, 1 H), 7.95, (s, 1 H), 7.90 – 7.86 (m, 2 H), 7.58 (d, *J* = 3.7 Hz, 1 H), 7.21 – 7.18 (m, 1 H), 6.95 (d, *J* = 2.4 Hz, 1 H), 6.71 – 6.70 (m, 2 H), 5.20 (bs, 1 H), 4.65 (d, *J* = 5.5 Hz, 1 H).

^{13}C-NMR (76 MHz, $CDCl_3$) δ [ppm] = 153.7, 147.9, 140.3, 138.5, 134.8, 132.6, 129.8, 122.6, 119.4, 119.2, 116.5, 116.4, 116.3, 111.6, 108.8, 108.3, 102.4, 38.89.

HRMS (ESI): $C_{22}H_{17}F_3N_7^+$ $(M+H)^+$ calculated: 436.14921 found: 436.14862

***N*-((1-(4-(1*H*-benzo[d]imidazol-1-yl)phenyl)-1*H*-1,2,3-triazol-4-yl)methyl)-2-(trifluoromethyl) pyridin-4-amine 5.18**

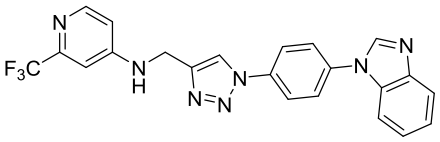

The title compound was prepared according to **GP4**. 4-(1*H*-benzo[d]imidazol-1-yl)aniline **5.14b** (21 mg, 0.100 mmol) was used in the reaction and the title compound was obtained as a yellow solid (37.6 mg, 0.086 mmol, 86%).

^{1}H-NMR (300 MHz, $CDCl_3$) δ [ppm] = 8.37 (d, *J* = 5.7 Hz, 1 H), 8.18 (bs, 1 H), 8.00 (s, 1 H), 7.99 – 7.96 (m, 2 H), 7.94 – 7.92 (m, 1 H), 7.76 – 7.72 (m, 2 H), 7.58 (bs, 1 H), 7.41 – 7.39 (m, 2 H), 6.95 (d, *J* = 2.4 Hz, 1 H), 6.70 (dd, *J* = 5.7 Hz, *J* = 2.3 Hz, 1 H), 5.17 (bs, 1 H), 4.68 (d, *J* = 5.5 Hz, 1 H).

^{13}C-NMR (76 MHz, $CDCl_3$) δ [ppm] = 153.6, 150.5, 145.1, 136.9, 136.0, 130.7, 125.3, 124.4, 122.2, 121.0 119.7, 109.4, 104.8, 38.60.

HRMS (ESI): $C_{22}H_{17}F_3N_7^+$ $(M+H)^+$ calculated: 436.14921 found: 436.14860

***N*-((1-(4-(1*H*-indazol-1-yl)phenyl)-1*H*-1,2,3-triazol-4-yl)methyl)-2-(trifluoromethyl)pyridin-4-amine 5.19**

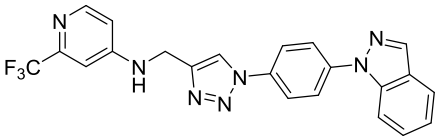

The title compound was prepared according to **GP4**. 4-(1*H*-indazol-1-yl)aniline **5.15b** (21 mg, 0.100 mmol) was used in the reaction and the title compound was obtained as a yellow solid (43.0 mg, 0.099 mmol, > 98%).

^{1}H-NMR (300 MHz, $CDCl_3$) δ [ppm] = 8.36 (d, *J* = 5.7 Hz, 1 H), 8.26 (s, 1 H), 7.99 (s, 1 H), 7.98 – 7.95 (m, 2 H), 7.93 – 7.90 (m, 2 H), 7.85 (d, *J* = 8.0 Hz, 1 H), 7.80 (d, *J* = 8.7 Hz, 1 H), 7.52 – 7.49 (m, 1 H), 7.30 (dd, *J* = 7.5 Hz, 1 H), 6.95 (d, *J* = 2.1 Hz, 1 H), 6.70 (dd, *J* = 5.7 Hz, *J* = 2.4 Hz, 1 H), 5.20 (bs, 1 H), 4.66 (d, *J* = 5.5 Hz, 1 H).

^{13}C-NMR (76 MHz, $CDCl_3$) δ [ppm] = 153.6, 150.4, 145.1, 136.8, 130.7, 125.3, 124.4, 122.2, 121.0, 120.4, 119.9, 118.7, 109.3, 104.7, 38.59.

HRMS (ESI): $C_{22}H_{17}F_3N_7^+$ $(M+H)^+$ calculated: 436.14921 found: 436.14886

***N*-((1-(4-(1*H*-pyrazolo[4,3-b]pyridin-1-yl)phenyl)-1*H*-1,2,3-triazol-4-yl)methyl)-2-(trifluoromethyl) pyridin-4-amine 5.20**

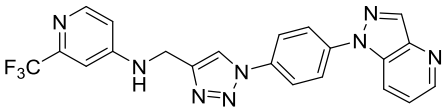

N-((1-(4-bromophenyl)-1*H*-1,2,3-triazol-4-yl)methyl)-2-(trifluoromethyl)pyridin-4-amine **3.22** (25 mg, 0.063 mmol), 1*H*-pyrazolo[4,3-b]pyridine (7.5 mg, 0.063 mmol) and K_3PO_4 (26 mg, 0.122 mmol) were suspended in DMSO (0.32 mL) and the solution was purged with argon for 10 minutes. DMEDA (10 µL, 7.3 mg, 0.083 mmol) and CuI (6.3 mg 0.032 mmol) were added and the mixture was purged with argon for another 15 minutes. The reaction mixture was then heated for 25 h in a pre-heated oil bath at 80 °C. After cooling to room temperature H_2O was added and the mixture was extracted three times with EtOAc, dried over $MgSO_4$, filtered and concentrated *in vacuo*. Automated flash chromatography (PE/EtOAc) afforded the title compound as a yellow solid (10 mg, 0.023 mmol, 37%)

^{1}H-NMR (500 MHz, acetone-d_6): δ [ppm] = 8.07 (bs, 1 H), 7.84 (s, 1 H), 7.68 – 7.67 (m, 1 H), 7.49 – 7.47 (m, 1 H), 7.36 – 7.35 (m, 2 H), 7.29 – 7.27 (m, 2 H), 6.78 – 6.77 (m, 1 H), 6.62 – 6.61 (m, 1 H), 6.30 (s, 1 H), 6.05 – 6.04 (m, 1 H), 4.77 (bs, 1 H), 4.00 (s, *J* = 5.0 Hz, 2 H).

^{13}C-NMR (125 MHz, acetone-d_6): δ [ppm] = 159.8, 155.3, 150.9, 145.4, 145.4, 144.7, 140.8, 139.9, 134.8, 128.4, 127.6, 126.7, 126.6, 120.3, 120.2, 114.4, 43.11.

HRMS (ESI): $C_{21}H_{16}F_3N_8^+$ $(M+H)^+$ calculated: 437.14445 found: 437.14371

***N*-((1-(4-(1*H*-pyrazolo[3,4-c]pyridin-1-yl)phenyl)-1*H*-1,2,3-triazol-4-yl)methyl)-2-(trifluoromethyl) pyridin-4-amine 5.21**

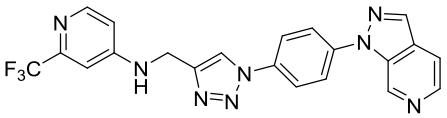

N-((1-(4-bromophenyl)-1*H*-1,2,3-triazol-4-yl)methyl)-2-(trifluoromethyl)pyridin-4-amine **3.22** (25 mg, 0.063 mmol), 1*H*-pyrazolo[3,4-c]pyridine (7.5 mg, 0.063 mmol) and K_3PO_4 (26 mg, 0.122 mmol) were suspended in DMSO (0.32 mL) and the solution was purged with argon for 10 minutes. DMEDA (10 µL, 7.3 mg, 0.083 mmol) and CuI (6.3 mg 0.032 mmol) were added and the mixture was purged with argon for another 15 minutes. The reaction mixture was then heated for 25 h in a pre-heated oil bath at 80 °C. After cooling to room temperature H_2O was added and the mixture was extracted three times with EtOAc, dried over $MgSO_4$, filtered and concentrated *in vacuo*. Automated flash chromatography (PE/EtOAc) afforded the title compound as a yellow solid (9.2 mg, 0.021 mmol, 33%)

^{1}H-NMR (500 MHz, acetone-d_6): δ [ppm] = 9.42 (s, 1 H), 8.69 – 8.68 (m, 1 H), 8.47 – 8.46 (m, 1 H), 8.42 – 8.41 (m, 1 H), 8.26 – 8.23 (m, 2 H), 8.17 – 8.13 (m, 2 H), 7.89 – 7.88 (m, 1 H), 7.75 – 7.74 (m, 1 H), 7.16 – 7.13 (m, 1 H), 6.92 – 6.87 (m, 2 H), 4.71 – 4.70 (m, 2 H).

^{13}C-NMR (125 MHz, acetone-d_6): δ [ppm] = 159.8, 151.3, 145.3, 144.6, 140.7, 139.8, 137.6, 137.1, 134.7, 128.3, 127.5, 126.6, 126.5, 120.3, 120.1, 114.3, 43.11.

HRMS (ESI): $C_{21}H_{16}F_3N_8^+$ $(M+H)^+$ calculated: 437.14445 found: 437.14392

***N*-((1-(4-(4-fluoro-1*H*-indazol-1-yl)phenyl)-1*H*-1,2,3-triazol-4-yl)methyl)-2-(trifluoromethyl)pyridin-4-amine 5.22**

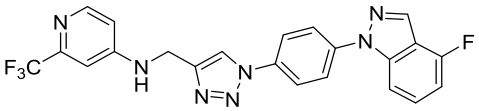

The compound was prepared according to **GP8**. *N*-((1-(4-bromophenyl)-1*H*-1,2,3-triazol-4-yl)methyl)-2-(trifluoromethyl)pyridin-4-amine (20 mg, 0.050 mmol), 4-fluoro-1*H*-indazole (7 mg, 0.050 mmol) and Cs_2CO_3 (18 mg, 0.055 mmol) were used and the title compound was obtained as a yellow solid (8.2 mg, 0.018 mmol, 36%).

^{1}H-NMR (500 MHz, acetone-d_6): δ [ppm] = 8.67 (s, 1 H), 8.43 (s, 1 H), 8.24 (d, *J* = 5.8 Hz, 1 H), 8.14 – 8.11 (m, 2 H), 8.05 – 8.02 (m, 2 H), 7.76 (d, *J* = 8.6 Hz, 1 H), 7.56 – 7.52 (m, 1 H), 7.15 (d, *J* = 2.3 Hz, 1 H), 7.04 – 7.00 (m, 1 H), 6.90 (dd, *J* = 5.8 Hz, *J* = 2.3 Hz, 1 H), 6.86 (bs, 1 H), 4.70 (d, *J* = 5.8 Hz, 1 H).

^{13}C-NMR (125 MHz, $CDCl_3$): δ [ppm] = 156.9, 154.9, 153.6, 150.4, 144.9, 141.1, 140.4, 134.9, 132.7, 128.9, 123.6, 121.7, 119.8, 116.0, 109.3, 106.4, 106.3, 104.8, 38.56.

HRMS (ESI): $C_{22}H_{16}F_4N_7^+$ $(M+H)^+$ calculated: 454.13978 found: 454.13922

***N*-((1-(4-(5-fluoro-1*H*-indazol-1-yl)phenyl)-1*H*-1,2,3-triazol-4-yl)methyl)-2-(trifluoromethyl)pyridin-4-amine 5.23**

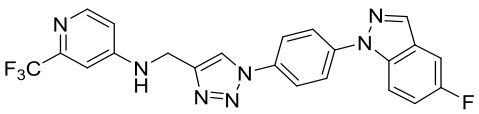

The compound was prepared according to **GP8**. *N*-((1-(4-bromophenyl)-1*H*-1,2,3-triazol-4-yl)methyl)-2-(trifluoromethyl)pyridin-4-amine (20 mg, 0.050 mmol), 5-fluoro-1*H*-indazole (7 mg, 0.050 mmol) and Cs_2CO_3 (18 mg, 0.055 mmol) were used and the title compound was obtained as a yellow solid (9.1 mg, 0.020 mmol, 40%).

^{1}H-NMR (500 MHz, acetone-d_6): δ [ppm] = 8.66 (s, 1 H), 8.34 (s, 1 H), 8.24 (d, *J* = 5.8 Hz, 1 H), 8.13 – 8.10 (m, 2 H), 8.05 – 8.01 (m, 2 H), 7.98 (dd, *J* = 9.2 Hz, *J* = 4.1 H, 1 H), 7.63 (dd, *J* = 8.7 Hz, *J* = 2.1 H, 1 H), 7.37 (ddd, *J* = 9.2 Hz, *J* = 2.4 H, 1 H), 7.15 (d, *J* = 2.3 Hz, 1 H), 6.90 (dd, *J* = 5.1 Hz, *J* = 2.7 H, 1 H), 6.86 (bs, 1 H), 4.70 (d, *J* = 5.7 Hz, 1 H).

^{13}C-NMR (125 MHz, $CDCl_3$): δ [ppm] = 159.3, 157.4, 153.6, 150.4, 148.8, 144.8, 140.5, 135.9, 135.6, 134.8, 125.9, 123.3, 121.7, 119.7, 117.0, 111.3, 109.3, 105.7, 104.8, 38.56.

HRMS (ESI): $C_{22}H_{16}F_4N_7^+$ $(M+H)^+$ calculated: 454.13978 found: 454.13940

***N*-((1-(4-(6-fluoro-1*H*-indazol-1-yl)phenyl)-1*H*-1,2,3-triazol-4-yl)methyl)-2-(trifluoromethyl)pyridin-4-amine 5.24**

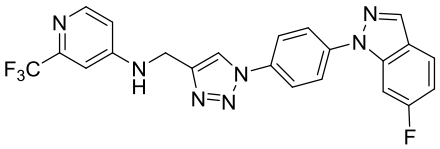

The compound was prepared according to **GP8**. *N*-((1-(4-bromophenyl)-1*H*-1,2,3-triazol-4-yl)methyl)-2-(trifluoromethyl)pyridin-4-amine (20 mg, 0.050 mmol), 6-fluoro-1*H*-indazole (7 mg, 0.050 mmol) and Cs_2CO_3 (18 mg, 0.055 mmol) were used and the title compound was obtained as a yellow solid (13.5 mg, 0.030 mmol, 60%).

^{1}H-NMR (500 MHz, acetone-d_6): δ [ppm] = 8.66 (s, 1 H), 8.35 (d, *J* = 0.9 Hz, 1 H), 8.24 (d, *J* = 5.8 Hz, 1 H), 8.12 – 8.09 (m, 2 H), 8.05 – 8.01 (m, 2 H), 7.95 (dd, *J* = 8.9 Hz, *J* = 5.3 Hz, 1 H), 7.69 – 7.66 (m, 1 H), 7.16 – 7.15 (m, 2 H), 7.13 (dd, *J* = 9.0 Hz, *J* = 2.0 Hz, 1 H), 6.90 (dd, *J* = 5.7 Hz, *J* = 2.3 Hz, 1 H), 6.86 (bs, 1 H), 4.70 (d, *J* = 5.8 Hz, 1 H).

^{13}C-NMR (126 MHz, acetone-d_6): δ [ppm] = 164.7, 162.8, 155.5, 151.1, 149.1, 146.6, 140.9, 139.8, 139.7, 137.3, 136.2, 124.3, 124.1, 123.7, 122.3, 121.7, 112.4, 112.2, 97.64, 38.86.

HRMS (ESI): $C_{22}H_{16}F_4N_7^+$ $(M+H)^+$ calculated: 454.13978 found: 454.13939

***N*-((1-(4-(7-fluoro-1*H*-indazol-1-yl)phenyl)-1*H*-1,2,3-triazol-4-yl)methyl)-2-(trifluoromethyl)pyridin-4-amine 5.25**

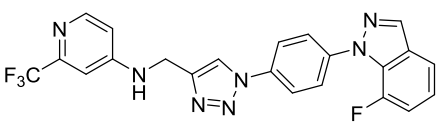

The compound was prepared according to **GP8**. *N*-((1-(4-bromophenyl)-1*H*-1,2,3-triazol-4-yl)methyl)-2-(trifluoromethyl)pyridin-4-amine (20 mg, 0.050 mmol), 7-fluoro-1*H*-indazole (7 mg, 0.050 mmol)

and Cs_2CO_3 (18 mg, 0.055 mmol) were used and the title compound was obtained as a yellow solid (9.4 mg, 0.021 mmol, 42%).

^{1}H-NMR (500 MHz, acetone-d_6): δ [ppm] = 8.67 (s, 1 H), 8.41 (d, *J* = 2.0 Hz, 1 H), 8.24 (d, *J* = 5.7 Hz, 1 H), 8.08 – 8.06 (m, 2 H), 7.91 – 7.89 (m, 2 H), 7.74 – 7.73 (m, 1 H), 7.29 – 7.26 (m, 2 H), 7.15 (d, *J* = 2.1 Hz, 1 H), 6.91 (dd, *J* = 5.7 Hz, *J* = 2.1 Hz, 1 H), 6.86 (bs, 1 H), 4.70 (d, *J* = 5.8 Hz, 1 H).

^{13}C-NMR (126 MHz, acetone-d_6): δ [ppm] = 155.5, 151.1, 150.0, 148.9, 146.6, 141.3, 137.6, 136.9, 130.6, 128.8, 126.6, 124.3, 121.8, 121.5, 118.4, 113.5, 109.9, 105.5, 38.87.

HRMS (ESI): $C_{22}H_{16}F_4N_7^+$ $(M+H)^+$ calculated: 454.13978 found: 454.13934

***N*-((1-(4-((2-fluorophenyl)amino)phenyl)-1*H*-1,2,3-triazol-4-yl)methyl)-2-(trifluoromethyl)pyridin-4-amine 5.26**

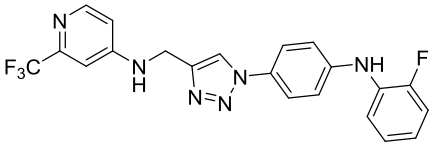

N-((1-(4-bromophenyl)-1*H*-1,2,3-triazol-4-yl)methyl)-2-(trifluoromethyl)pyridin-4-amine (20 mg, 0.050 mmol), 2-fluoroaniline (5 µL, 5.6 mg, 0.050 mmol) and NaO*t*Bu (2 M in THF, 75 µL, 0.150 mmol) were dissolved in 1,4-dioxane (0.5 mL). The solution was purged with argon for 10 minutes and $[Pd(cinammyl)Cl]_2$ (1.3 mg, 5 mol%) and BippyPhos (2.5 mg, 10 mol%) were added. The reaction mixture was purged with argon for another 15 minutes and stirred for 27 h in pre-heated oil bath at 80 °C. The reaction mixture was allowed to cool to room temperature and H_2O was added. The mixture was extracted three times with EtOAc, dried over $MgSO_4$, filtered and concentrated *in vacuo*. Automated flash chromatography (DCM/MeOH) afforded the title compound as a colorless solid (9.4 mg, 0.022 mmol, 44%)

^{1}H-NMR (300 MHz, $CDCl_3$): δ [ppm] = 7.85 (s, 1 H), 7.60 – 7.58 (m, 2 H), 7.38 – 7.35 (m, 1 H), 7.19 – 7.17 (m, 2 H), 7.17 – 7.13 (m, 1 H), 7.12 – 7.09 (m, 1 H), 7.00 – 6.96 (m, 1 H), 6.94 – 6.93 (m, 1 H), 6.71 – 6.69 (m, 1 H), 5.95 (s, 1 H), 5.24 (bs, 1 H), 4.61 (d, *J* = 5.5 Hz, 2 H).

^{13}C-NMR (76 MHz, $CDCl_3$): δ [ppm] = 156.2, 152.8, 150.2, 148.6, 144.1, 138.5, 135.8, 134.2, 130.2, 124.5, 122.5, 122.1, 119.8, 119.1, 117.8, 116.0, 115.8, 109.3, 38.62.

HRMS (ESI): $C_{21}H_{17}F_4N_6^+$ $(M+H)^+$ calculated: 429.14453 found: 429.14380

***N*-((1-(3-bromophenyl)-1*H*-1,2,3-triazol-4-yl)methyl)-2-(trifluoromethyl)pyridin-4-amine 5.28**

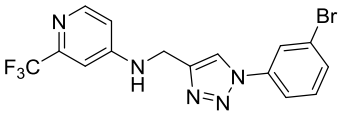

The compound was prepared according to **GP4.** 3-Bromoaniline (17.2 mg, 0.100 mmol) was used in the reaction and afforded the title compound as a brownish solid (38.7 mg, 0.097 mmol, 97%).

LC-MS: m/z: 399 $(M+H)^+$

^{1}H-NMR (300 MHz, $CDCl_3$): δ [ppm] = 8.35 (d, *J* = 5.7 Hz, 1 H), 7.94 – 7.93 (m, 1 H), 7.93 – 7.92 (m, 1 H), 7.68 (ddd, *J* = 8.1 Hz, *J* = 2.0 Hz, *J* = 0.8 Hz, 1 H), 7.60 (ddd, *J* = 8.1 Hz, *J* = 1.8 Hz, *J* = 0.9 Hz, 1 H), 7.42 (dd, *J* = 8.1 Hz, 1 H), 6.93 (d, *J* = 2.3 Hz, 1 H), 6.68 (dd, *J* = 5.7 Hz, *J* = 2.3 Hz, 1 H), 5.20 (bs, 1 H), 4.64 (d, *J* = 5.5 Hz, 1 H).

^{13}C-NMR (76 MHz, $CDCl_3$): δ [ppm] = 153.6, 150.3, 148.9, 144.9, 137.6, 123.1, 131.1, 124.9, 123.6, 122.7, 120.6, 119.8, 118.9, 109.2, 104.8, 56.48.

***N*-((1-(3-(phenylamino)phenyl)-1*H*-1,2,3-triazol-4-yl)methyl)-2-(trifluoromethyl)pyridin-4-amine 5.27**

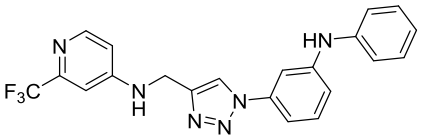

N-((1-(3-bromophenyl)-1*H*-1,2,3-triazol-4-yl)methyl)-2-(trifluoromethyl)pyridin-4-amine **5.28** (36 mg, 0.091 mmol), aniline (9 µL, 0.099 mmol) and NaO*t*Bu (2 M in THF, 0.10 mL, 0.200 mmol) were dissolved in 1,4-dioxane (0.91 mL) and the solution was purged with argon for 10 minutes. $[Pd(cinammyl)Cl]_2$ (2.4 mg, 5 mol%) and BippyPhos (4.6 mg, 10 mol%) were and the mixture was again purged with argon for 15 minutes. And stirred for 18 h in pre-heated oil bath at 80 °C. The reaction mixture was cooled to room temperature and then filtered over silica gel and subsequently washed with EtOAc. Automated flash chromatography (DCM/MeOH) afforded the title compound as a brownish solid (16.1 mg, 0.039 mmol, 43%).

^{1}H-NMR (300 MHz, $CDCl_3$): δ [ppm] = 8.31 (d, *J* = 5.7 Hz, 1 H), 7.88 (s, 1 H), 7.43 – 7.41 (m, 1 H), 7.37 – 7.31 (m, 3 H), 7.16 – 7.14 (m, 2 H), 7.12 – 7.10 (m, 1 H), 7.10 – 7.08 (m, 1 H), 7.06 – 7.03 (m, 1 H), 6.91 – 6.90 (m, 1 H), 6.67 – 6.66 (m, 1 H), 6.03 (s, 1 H), 5.36 (s, 1 H), 4.59 (d, *J* = 5.3 Hz, 2 H).

^{13}C-NMR (76 MHz, $CDCl_3$): δ [ppm] = 153.7, 150.26, 148.9, 145.4, 144.3, 141.5, 137.8, 130.7, 129.6, 122.7, 119.9, 119.6, 116.8, 111.8, 109.3, 108.3, 104.8, 38.48.

HRMS (ESI): $C_{21}H_{18}F_3N_6^+$ $(M+H)^+$ calculated: 411.15396 found: 411.15338

***N*-((1-(3-((4-fluorophenyl)amino)phenyl)-1*H*-1,2,3-triazol-4-yl)methyl)-2-(trifluoromethyl)pyridin-4-amine 5.30**

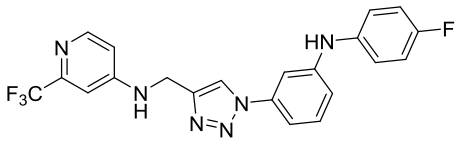

N-((1-(3-bromophenyl)-1*H*-1,2,3-triazol-4-yl)methyl)-2-(trifluoromethyl)pyridin-4-amine **5.28** (20 mg, 0.050 mmol), 4-fluoro-aniline (5 µL, 0.053 mmol) and NaO*t*Bu (2 M in THF, 75 µL, 0.150 mmol) were dissolved in 1,4-dioxane (0.5 mL) and the solution was purged with argon for 10 minutes. $[Pd(cinammyl)Cl]_2$ (2.4 mg, 5 mol%) and BippyPhos (4.6 mg, 10 mol%) were and the mixture was again purged with argon for 15 minutes. And stirred for 18 h in pre-heated oil bath at 80 °C. The reaction mixture was cooled to room temperature and then filtered over silica gel, subsequently washed with EtOAc and the solvent was removed under reduced pressure. Automated flash chromatography (DCM/MeOH) afforded the title compound as a brownish solid (11.7 mg, 0.016 mmol, 32%).

^{1}H-NMR (300 MHz, $CDCl_3$): δ [ppm] = 8.32 – 8.30 (m, 1 H), 7.87 (d, *J* = 4.7 Hz, 1 H), 7.36 – 7.32 (m, 2 H), 7.27 – 7.25 (m, 1 H), 7.15 – 7.13 (m, 3 H), 7.08 – 7.03 (m, 1 H), 6.99-6.90 (m, 2 H), 6.66 (s, 1 H), 5.88 (s, 1 H), 5.27 (bs, 1 H), 4.59 (bs, 2 H).

^{13}C-NMR (76 MHz, $CDCl_3$): δ [ppm] = 159.9, 157.9, 153.6, 150.4, 148.9, 146.1, 144.3, 137.8, 137.2, 130.7, 129.9, 122.8, 122.6, 120.6, 119.9, 116.4, 116.2 115.9, 111.3, 109.2, 107.4, 104.7, 38.49.

HRMS (ESI): $C_{21}H_{17}F_4N_6^+$ $(M+H)^+$ calculated: 429.14453 found: 429.14378

***N*-((1-(3-((2-fluorophenyl)amino)phenyl)-1*H*-1,2,3-triazol-4-yl)methyl)-2-(trifluoromethyl)pyridin-4-amine 5.31**

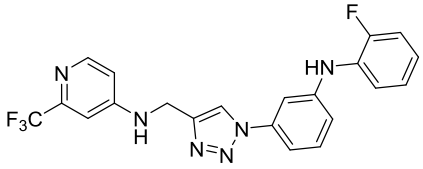

N-((1-(3-bromophenyl)-1*H*-1,2,3-triazol-4-yl)methyl)-2-(trifluoromethyl)pyridin-4-amine **5.28** (40 mg, 0.100 mmol), 2-fluoroaniline 10 µL, 0.104 mmol) and Cs_2CO_3 (36 mg, 0.110 mmol) were dissolved in 1,4-dioxane (1.15 mL). The reaction mixture was purged with argon for 10 minutes and Pd-175 (3.9 mg, 5 mol%) was added. After 15 minutes of argon purge the reaction mixture was stirred for 24 h in a pre-heated metal block at 90 °C. The reaction mixture was cooled to room temperature, filtered over silica gel and concentrated *in vacuo*. The crude product was purified *via* automated flash

chromatography (DCM/MeOH) and yielded the title compound as a brownish solid (30.4 mg, 0.071 mmol, 71%).

^{1}H-NMR (300 MHz, $CDCl_3$): δ [ppm] = 8.49 (s, 1 H), 8.32 (d, *J* = 5.7 Hz, 1 H), 7.60 – 7.57 (m, 2 H), 7.48 – 7.46 (m, 1 H), 7.43 (dd, *J* = 8.1 Hz, 1 H), 7.30 (dd, *J* = 8.9 Hz, *J* = 2.0 Hz, 1 H), 7.22 – 7.18 (m, 1 H), 7.17 – 7.14 (m, 2 H), 7.13 (d, *J* = 2.3 Hz, 1 H), 7.07 – 7.04 (m, 1 H), 6.88 (*J* = 5.7 Hz, *J* = 2.3 Hz, 1 H), 6.80 (bs, 1 H), 4.64 (d, *J* = 5.7 Hz, 2 H).

^{13}C-NMR (76 MHz, $CDCl_3$): δ [ppm] = 156.5, 155.5, 154.6, 151.1, 146.4, 146.2, 139.1, 131.4, 131.2, 125.7, 124.3, 123.9, 123.8, 121.9, 121.7, 117.3, 116.9, 116.8, 112.3, 108.8, 38.83.

HRMS (ESI): $C_{21}H_{17}F_4N_6^+$ $(M+H)^+$ calculated: 429.14453 found: 429.14453

***N*-((1-(3-((3-fluorophenyl)amino)phenyl)-1*H*-1,2,3-triazol-4-yl)methyl)-2-(trifluoromethyl)pyridin-4-amine 5.32**

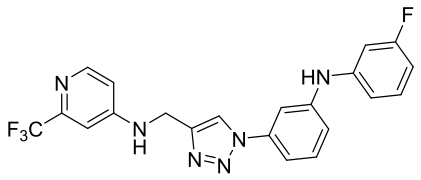

N-((1-(3-bromophenyl)-1*H*-1,2,3-triazol-4-yl)methyl)-2-(trifluoromethyl)pyridin-4-amine **5.28** (40 mg, 0.100 mmol), 3-fluoroaniline 10 µL, 0.104 mmol) and Cs_2CO_3 (36 mg, 0.110 mmol) were dissolved in 1,4-dioxane (1.15 mL). The reaction mixture was purged with argon for 10 minutes and Pd-175 (3.9 mg, 5 mol%) was added. After 15 minutes of argon purge the reaction mixture was stirred for 24 h in a pre-heated metal block at 90 °C. The reaction mixture was cooled to room temperature, filtered over silica gel and concentrated *in vacuo*. The crude product was purified *via* automated flash chromatography (DCM/MeOH) and yielded the title compound as a brownish solid (42.5 mg, 0.991 mmol, > 98%).

^{1}H-NMR (300 MHz, $CDCl_3$): δ [ppm] = 8.52 (s, 1 H), 8.21 (d, *J* = 5.8 Hz, 1 H), 8.01 (bs, 1 H), 7.66 (dd, *J* = 2.0 Hz, 1 H), 7.46 (dd, *J* = 8.1 Hz, 1 H), 7.35 – 7.33 (m, 1 H), 7.33 – 7.29 (m, 1 H), 7.23 (dd, *J* = 8.1 Hz, *J* = 2.3 Hz, 1 H), 7.12 (d, *J* = 2.3 Hz, 1 H), 7.01 (dd, *J* = 8.2 Hz, *J* = 1.4 Hz, 1 H), 6.68 (dd, *J* = 5.8 Hz, *J* = 2.4 Hz, 1 H), 6.81 (bs, 1 H), 6.66 (dd, *J* = 8.2 Hz, *J* = 2.4 Hz, 1 H), 4.64 (d, *J* = 5.8 Hz, 2 H).

^{13}C-NMR (76 MHz, $CDCl_3$): δ [ppm] = 165.6, 163.7, 155.5, 151.1, 146.3, 145.9, 145.5, 139.2, 131.8, 131.7, 124.3, 122.1, 121.7, 118.3, 114.3, 122.9, 110.1, 109.7, 108.2, 105.1, 38.83.

HRMS (ESI): $C_{21}H_{17}F_4N_6^+$ $(M+H)^+$ calculated: 429.14453 found: 429.14435

_N_-((1-(3-((2,5-difluorophenyl)amino)phenyl)-1_H_-1,2,3-triazol-4-yl)methyl)-2-(trifluoromethyl) pyridin-4-amine 5.33

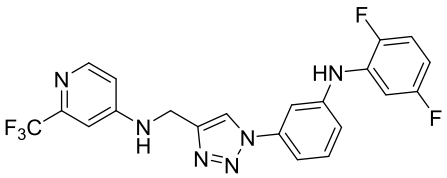

_N_-((1-(3-bromophenyl)-1_H_-1,2,3-triazol-4-yl)methyl)-2-(trifluoromethyl)pyridin-4-amine **5.28** (40 mg, 0.100 mmol), 2,5-_di_fluoroaniline 11 µL, 0.110 mmol) and Cs_2CO_3 (36 mg, 0.110 mmol) were dissolved in 1,4-dioxane (1 mL). The reaction mixture was purged with argon for 10 minutes and Pd-175 (3.9 mg, 5 mol%) was added. After 15 minutes of argon purge the reaction mixture was stirred for 24 h in a pre-heated metal block at 90 °C. The reaction mixture was cooled to room temperature, filtered over silica gel and concentrated _in vacuo_. The crude product was purified _via_ automated flash chromatography (DCM/MeOH) and yielded the title compound as a brownish solid (44.3 mg, 0.993 mmol, > 98%).

^{1}H-NMR (500 MHz, $CDCl_3$): δ [ppm] = 8.33 (d, _J_ = 5.8 Hz, 1 H), 7.92 (s, 1 H), 7.53 (dd, _J_ = 2.1 Hz, 1 H), 7.46 (dd, _J_ = 8.1 Hz, 1 H), 7.28 (dd, _J_ = 2.1 Hz, _J_ = 0.9 Hz, 1 H), 7.20 (ddd, _J_ = 8.2 Hz, _J_ = 2.3 Hz, _J_ = 0.8 Hz, 1 H), 7.10 – 7.08 (m, 1 H), 7.07 – 7.04 (m, 1 H), 6.94 (d, _J_ = 2.3 Hz, 1 H), 6.69 (dd, _J_ = 5.7, _J_ = 2.3 Hz, 1 H), 6.65 – 6.63 (m, 1 H), 6.07 (s, 1 H), 5.26 (bs, 1 H), 4.63 (d, _J_ 5.5 Hz, 2 H).

^{13}C-NMR (126 MHz, $CDCl_3$): δ [ppm] = 159.7, 157.7, 153.6, 149.9, 144.2, 142.7, 137.6, 131.3, 130.7, 122.4, 119.6, 118.4, 116.1, 115.8, 113.5, 110.2, 109.0, 107.3, 104.6, 104.4, 38.30.

HRMS (ESI): $C_{21}H_{16}F_5N_6^+$ $(M+H)^+$ calculated: 447.13511 found: 447.13476

_N_-((1-(3-(1_H_-indazol-1-yl)phenyl)-1_H_-1,2,3-triazol-4-yl)methyl)-2-(trifluoromethyl)pyridin-4-amine 5.34

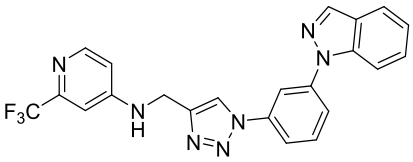

_N_-((1-(3-bromophenyl)-1_H_-1,2,3-triazol-4-yl)methyl)-2-(trifluoromethyl)pyridin-4-amine **5.28** (20 mg, 0.050 mmol), 1_H_-indazole (5.9 mg, 0.050 mmol) and K_3PO_4 (20 mg, 0.094 mmol) were suspended in 1,4-dioxane (0.5 mL). The reaction mixture was purged with argon and CuI (5 mg, 0.026 mmol) and DMEDA (8 µL, 6.5 mg, 0.074 mmol) were added. After purging the reaction mixture for 15 minutes with argon, the mixture was stirred at 80 °C for 16 h, cooled to room temperature and filtered over

silica gel. The crude product was purified *via* automated flash chromatography (DCM/MeOH) and the title compound was obtained as a colorless solid (8.1 mg, 0.018 mmol, 37%).

^{1}H-NMR (300 MHz, $CDCl_3$): δ [ppm] = 8.34 – 8.33 (m, 1 H), 8.25 (s, 1 H), 8.18 (s, 1 H), 8.04 (s, 1 H), 7.88 – 7.87 (m, 1 H), 7.85 – 7.83 (m 2 H), 7.71 – 7.70 (m, 2 H), 7.52 – 7.49 (m, 1 H), 7.31 – 7.28 (m, 1 H), 6.94 (s, 1 H), 6.70 – 6.68 (m, 1 H), 5.35 (bs, 1 H), 4.64 (d, *J* = 5.2 Hz, 2 H).

^{13}C-NMR (76 MHz, $CDCl_3$): δ [ppm] = 153.6, 150.4, 141.6, 138.6, 137.6, 136.5, 130.9, 129.9, 127.9, 125.7, 122.2, 121.8, 121.7, 119.9, 117.8, 114.3, 110.3, 109.2, 104.8, 38.51.

HRMS (ESI): $C_{22}H_{17}F_3N_7^+$ $(M+H)^+$ calculated: 436.14921 found: 436.14842

2-Chloro-*N*-((1-(3-chloro-4-isopropoxyphenyl)-1*H*-1,2,3-triazol-4-yl)methyl)-6-(trifluoromethyl) pyridin-4-amine 5.35

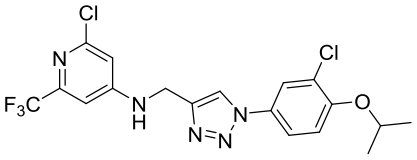

The compound was prepared according to **GP4.** 2-Chloro-*N*-(prop-2-yn-1-yl)-6-(trifluoromethyl)pyridin-4-amine **4.17** (20 mg, 0.085 mmol) and 3-Chloro-4-isopropoxyaniline **3.40b** (16 mg, 0.085 mmol) were used. The title compound was obtained as a red solid (4.9 mg, 0.011 mmol, 13%).

^{1}H-NMR (300 MHz, $CDCl_3$): δ [ppm] = 7.85 (s, 1 H), 7.74 (d, *J* = 2.6 Hz, 1 H), 7.56 (dd, *J* = 8.9 Hz, *J* = 2.6 Hz, 1 H), 7.07 (d, *J* = 8.9 Hz, 1 H), 6.86 (d, *J* = 2.0 Hz, 1 H), 6.69 (d, *J* = 2.0 Hz, 1 H), 5.37 (bs, 1 H), 4.64 (quint, *J* = 6.1 Hz, 1 H), 4.60 (d, *J* = 5.3 Hz, 1 H), 1.44 (d, *J* = 6.1 Hz, 1 H).

^{13}C-NMR (76 MHz, $CDCl_3$): δ [ppm] = 115.3, 154.4, 152.9, 143.8, 129.9, 125.2, 123.1, 120.0, 119.9, 115.7, 72.59, 38.62, 21.90.

HRMS (ESI): $C_{18}H_{17}Cl_2F_3N_5O^+$ $(M+H)^+$ calculated: 446.07568 found: 446.07511

2-Chloro-*N*-((1-(4-(2-fluorophenoxy)phenyl)-1*H*-1,2,3-triazol-4-yl)methyl)-6-(trifluoromethyl) pyridin-4-amine 5.36

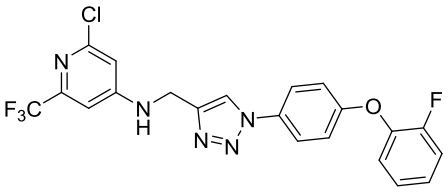

The compound was prepared according to **GP4.** 2-Chloro-*N*-(prop-2-yn-1-yl)-6-(trifluoromethyl)pyridin-4-amine **4.17** (35 mg, 0.148 mmol) and 4-(2-Fluorophenoxy)aniline **5.1b** (30 mg, 0.148 mmol). The title compound was obtained as a colorless solid (63 mg, 0.136 mmol, 92%).

^{1}H-NMR (500 MHz, $CDCl_3$): δ [ppm] = 7.68 (s, 1 H), 7.66 – 7.63 (m, 2 H), 7.26 – 7.15 (m, 4 H), 7.11 – 7.10 (m, 2 H), 6.86 (s, 1 H), 6.69 (s, 1 H), 5.45 (bs, 1 H), 4.59 (s, 2 H).

^{13}C-NMR (76 MHz, $CDCl_3$): δ [ppm] = 158.2, 155.3, 153.5, 152.8, 143.8, 131.8, 126.0, 125.9, 122.35, 119.9, 117.7, 117.5, 117.3, 115.8, 108.0, 104.8, 38.59.

HRMS (ESI): $C_{21}H_{15}ClF_4N_5O^+$ $(M+H)^+$ calculated: 464.08958 found: 464.08963

2-Chloro-*N*-((1-(4-((2-fluoropyridin-3-yl)oxy)phenyl)-1*H*-1,2,3-triazol-4-yl)methyl)-6-(trifluoromethyl)pyridin-4-amine 5.37

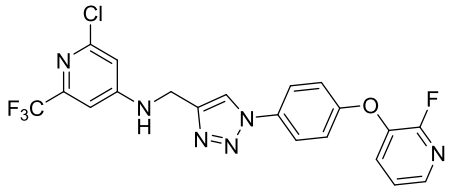

The compound was prepared according to **GP4.** 2-Chloro-*N*-(prop-2-yn-1-yl)-6-(trifluoromethyl)pyridin-4-amine **4.17** (50 mg, 0.213 mmol) and 4-((2-Fluoropyridin-3-yl)oxy)aniline **5.6b** (43 mg, 0.213 mmol) were used. The crude product was purified using automated flash chromatography (DCM/MeOH) and yielded the title compound as a colorless solid (71.0 mg, 0.153 mmol, 72%).

^{1}H-NMR (300 MHz, $CDCl_3$): δ [ppm] = 8.08 – 8.07 (m, 1 H), 7.96 (bs, 1 H), 7.72 – 7.70 (m, 2 H), 7.57 – 7.53 (m, 1 H), 7.26 – 7.24 (m, 1 H), 7.15 – 7.13 (m, 2 H), 6.87 (s, 1 H), 6.70, (s, 1 H), 5.41 (bs, 1 H), 4.61 (s, 1 H).

^{13}C-NMR (76 MHz, $CDCl_3$): δ [ppm] = 159.9, 156.3, 155.3, 154.4, 152.4, 148.6, 142.5, 138.5, 132.7, 131.2, 122.6, 121.9, 121.6, 119.8, 118.4, 108.1, 104.7, 38.62.

HRMS (ESI): $C_{20}H_{14}ClF_4N_6O^+$ $(M+H)^+$ calculated: 465.08483 found: 465.08417

2-Chloro-*N*-((1-(4-(pyridin-3-yloxy)phenyl)-1H-1,2,3-triazol-4-yl)methyl)-6-(trifluoromethyl)pyridin-4-amine 5.38

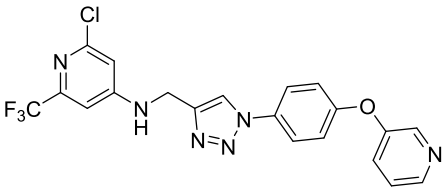

The compound was prepared according to **GP4.** 2-Chloro-*N*-(prop-2-yn-1-yl)-6-(trifluoromethyl)pyridin-4-amine **4.17** (89 mg, 0.380 mmol) and 4-(pyridin-3-yloxy)aniline (71 mg, 0.380 mmol) were used. The crude product was purified using automated flash chromatography (DCM/MeOH) and yielded the title compound as a colorless solid (141 mg, 0.315 mmol, 83%).

^{1}H-NMR (500 MHz, acetone-d_6): δ [ppm] = 8.57 (s, 1 H), 8.43 (bs, 2 H), 7.92 – 7.89 (m, 2 H), 7.52 – 7.49 (m, 1 H), 7.46 – 7.43 (m, 1 H), 7.27 – 7.25 (m, 2 H), 7.21 (bs, 1 H), 7.16 (d, *J* = 2.0 Hz, 1 H), 6.94 (d, *J* = 2.0 Hz, 1 H), 4.70 (d, 5.8 Hz, 2 H).

^{13}C-NMR (126 MHz, acetone-d_6): δ [ppm] = 157.9, 157.7, 146.2, 145.9, 142.5, 134.1, 126.9, 125.5, 123.2, 121.9, 120.6, 38.49.

HRMS (ESI): $C_{20}H_{15}ClF_3N_6O^+$ $(M+H)^+$ calculated: 447.09425 found: 447.09366

***N*-((1-(4-(1*H*-pyrrolo[2,3-b]pyridin-1-yl)phenyl)-1*H*-1,2,3-triazol-4-yl)methyl)-2-chloro-6-(trifluoromethyl)pyridin-4-amine 5.39**

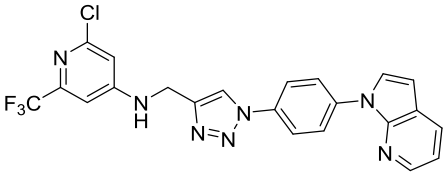

The compound was prepared according to **GP4.** 2-Chloro-*N*-(prop-2-yn-1-yl)-6-(trifluoromethyl)pyridin-4-amine **4.17** (42 mg, 0.178 mmol) and 4-(1*H*-pyrrolo[2,3-b]pyridin-1-yl)aniline **5.13b** (37 mg, 0.178 mmol) were used. The title compound was obtained as colorless solid (54 mg, 0.115 mmol, 65%).

^{1}H-NMR (500 MHz, DMSO-d_6): δ [ppm] = 9.00 (bs, 1 H), 8.90 (s, 1 H), 8.27 (d, *J* = 4.7 Hz, 1 H), 8.15 – 8.11 (m, 2 H), 8.08 – 8.06 (m, 1 H), 8.03 (d, *J* = 3.4 Hz, 1 H), 7.11 (s, 1 h), 6.92 (s, 1 H), 6.85 (d, *J* = 3.2 Hz, 1 H), 4.61 (d, *J* = 5.7 Hz, 1 H).

^{13}C-NMR (126 MHz, DMSO-d_6): δ [ppm] = 156.6, 144.9, 139.9, 139.4, 138.2, 134.9, 134.0, 133.5, 132.3, 125.1, 122.3, 121.6, 121.5, 120.1, 115.6, 103.5, 37.40.

HRMS (ESI): $C_{22}H_{16}ClF_3N_7^+$ $(M+H)^+$ calculated: 470.11023 found: 470.11002

***N*-((1-(4-(1*H*-pyrrolo[2,3-c]pyridin-1-yl)phenyl)-1*H*-1,2,3-triazol-4-yl)methyl)-2-chloro-6-(trifluoromethyl)pyridin-4-amine 5.40**

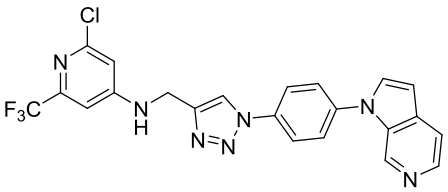

The compound was prepared according to **GP4.** 2-Chloro-*N*-(prop-2-yn-1-yl)-6-(trifluoromethyl)pyridin-4-amine **4.17** (42 mg, 0.178 mmol) and 4-(1*H*-pyrrolo[2,3-c]pyridin-1-yl)aniline **5.12b** (42 mg, 0.178 mmol) and 4-(1*H*-pyrrolo[2,3-b]pyridin-1-yl)aniline **5.13b** (37 mg, 0.178 mmol) were used. The title compound was obtained as colorless solid (56 mg, 0.119 mmol, 67%).

^{1}H-NMR (500 MHz, DMSO-d_6): δ [ppm] = 8.86 (s, 1 H), 8.36 (dd, *J* = 4.6 Hz, *J* = 1.5 Hz, 1 H), 8.24 – 8.21 (m, 2 H), 8.12 (dd, *J* = 7.8 Hz, *J* = 1.5 Hz, 1 H), 8.09 – 8.08 (m, 2 H), 8.08 – 8.06 (m, 1 H), 8.06 – 8.04 (m, 1 H), 7.26 (dd, *J* = 7.9 Hz, *J* = 4.7 Hz, 1 H), 7.12 (bs, 1 H), 6.93 (bs, 1 H), 6.80 (d, *J* = 7.8 Hz, 1 H), 4.61 (d, *J* = 5.5 Hz, 1 H).

^{13}C-NMR (126 MHz, DMSO-d_6): δ [ppm] = 162.4, 156.6, 146.9, 144.8, 143.4, 138.2, 13.9, 129.5, 128.1, 123.9, 121.6, 120.9, 117.3, 102.6, 37.43.

HRMS (ESI): $C_{22}H_{16}ClF_3N_7^+$ $(M+H)^+$ calculated: 470.11023 found: 470.11002

***N*-((1-(4-(1*H*-indazol-1-yl)phenyl)-1*H*-1,2,3-triazol-4-yl)methyl)-2-chloro-6-(trifluoromethyl)pyridin-4-amine 5.41**

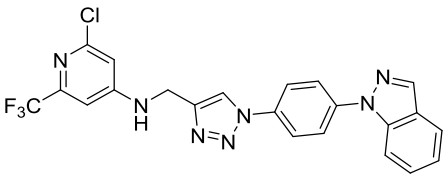

The compound was prepared according to **GP4.** 2-Chloro-*N*-(prop-2-yn-1-yl)-6-(trifluoromethyl)pyridin-4-amine **4.17** (54 mg, 0.115 mmol) and 4-(1*H*-indazol-1-yl)aniline (24 mg, 0.115 mmol) were used. Automated flash chromatography (PE/EtOAc) afforded the title compound as a colorless solid (35.4 mg, 0.076 mmol, 67%).

^{1}H-NMR (500 MHz, acetone-d_6): δ [ppm] = 8.69 (s, 1 H), 8.34 (s, 1 H), 8.11 – 8.09 (m, 2 H), 8.06 – 8.04 (m, 2 H), 7.96 – 7.94 (m, 1 H), 7.92 – 7.91 (m, 1 H), 7.55 – 7.52 (m, 1 H), 7.32 – 7.29 (m, 1 H), 7.21 (bs, 1 H), 7.18 (d, *J* = 2.0 Hz, 1 H), 6.96 (d, *J* = 2.0 Hz, 1 H), 4.75 (d, *J* = 5.8 Hz, 2 H).

^{13}C-NMR (126 MHz, DMSO-d_6): δ [ppm] = 157.7, 153.1, 146.1, 139.5, 137.2, 135.9, 128.6, 126.9, 123.9, 122.9, 122.5, 122.3, 121.8, 111.41, 38.97.

HRMS (ESI): $C_{22}H_{16}ClF_3N_7^+$ $(M+H)^+$ calculated: 470.11023 found: 470.11282

***N*-((1-(4-bromophenyl)-1*H*-1,2,3-triazol-4-yl)methyl)-2-chloro-6-(trifluoromethyl)pyridin-4-amine 5.42**

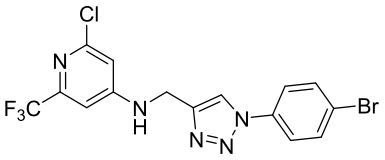

The compound was prepared according to **GP4.** 2-Chloro-*N*-(prop-2-yn-1-yl)-6-(trifluoromethyl)pyridin-4-amine **4.17** (117 mg, 0.500 mmol) and 4-bromoaniline (99 mg, 0.500 mmol) were used. The title compound was obtained as a brownish solid (210 mg, 0.486 mmol, 97%).

LC-MS: m/z: 433 $(M+H)^+$

^{1}H-NMR (500 MHz, $CDCl_3$): δ [ppm] = 7.96 (bs, 1 H), 7.68 – 7.66 (m, 2 H), 7.62 – 7.60 (m, 2 H), 6.87 (d, *J* = 1.8 Hz, 1 H), 6.68 (d, *J* = 1.8 Hz, 1 H), 5.66 (bs, 1 H), 4.61 (d, *J* = 5.3 Hz, 2 H).

^{13}C-NMR (126 MHz, $CDCl_3$): δ [ppm] = 155.4, 152.8, 148.2, 135.6, 133.0, 122.9, 121.9, 119.8, 110.2, 107.9, 105.8, 104.8, 38.48.

***N*-((1-(3-bromophenyl)-1*H*-1,2,3-triazol-4-yl)methyl)-2-chloro-6-(trifluoromethyl)pyridin-4-amine 5.43**

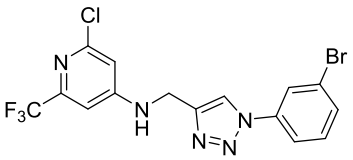

The compound was prepared according to **GP4.** 2-Chloro-*N*-(prop-2-yn-1-yl)-6-(trifluoromethyl)pyridin-4-amine **4.17** (117 mg, 0.500 mmol) and 3-bromoaniline (99 mg, 0.500 mmol) were used. The title compound was obtained as a yellow solid (204 mg, 472 mmol, 94%).

LC-MS: m/z: 433 $(M+H)^+$

^{1}H-NMR (500 MHz, $CDCl_3$): δ [ppm] = 7.95 (s, 1 H), 7.93 – 7.92 (m, 1 H), 7.69 – 7.67 (m, 1 H), 7.62 – 7.60 (m, 1 H), 7.44 – 7.41 (m, 1 H), 6.87 (d, *J* = 2.0 Hz, 1 H), 6.69 (d, *J* = 2.0 Hz, 1 H), 5.50 (bs, 1 H), 4.61 (s, 2 H).

^{13}C-NMR (126 MHz, $CDCl_3$): δ [ppm] = 157.9, 151.1, 149.4, 146.7, 135.9, 132.8, 121.9, 121.1, 120.1, 108.8, 105.3, 54.95

2-Chloro-*N*-((1-(4-(4-fluoro-1*H*-indazol-1-yl)phenyl)-1H-1,2,3-triazol-4-yl)methyl)-6-(trifluoromethyl)pyridin-4-amine 5.44

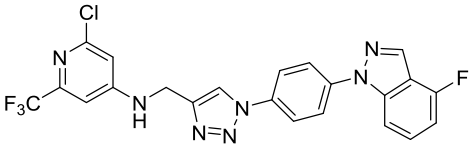

N-((1-(4-bromophenyl)-1*H*-1,2,3-triazol-4-yl)methyl)-2-chloro-6-(trifluoromethyl)pyridin-4-amine **5.42** (22 mg, 0.051 mmol), 4-fluoro-1*H*-indazole (7.6 mg, 0.056mmol) and NaO*t*Bu (7.0 mg, 0.076 mmol) were dissolved in toluene (0.51 mL). The mixture was purged with argon and *t*BuXPhos Pd G3 (2 mg, 5 mol%) was added. The mixture was degassed again with argon and heated for 18 h in a pre-heated oil bath at 100 °C. The reaction mixture was allowed to cool to room temperature and saturated NH_4Cl solution was added. The mixture was then extracted three times with EtOAc, dried over Na_2SO_4, filtered and concentrated under reduced pressure. Purification *via* automated flash chromatography afforded the title compound as a colorless solid (14.4 mg, 0.032 mmol, 58%).

^{1}H-NMR (500 MHz, DMSO-d_6): δ [ppm] = 8.87 (s, 1 H), 8.59 – 8.57 (m, 1 H), 8.14 – 8.11 (m, 2 H), 7.77 – 7.75 (m, 1 H), 8.03 – 8.01 (m, 2 H), 7.57 – 7.53 (m, 1 H), 7.13 – 7.09 (m, 1 H), 6.91 (bs, 1 H), 4.69 (d, *J* = 5.5 Hz, 2 H).

^{13}C-NMR (126 MHz, DMSO-d_6): δ [ppm] = 156.6. 155.9, 153.9, 153.7, 145.3, 144.9, 140.7, 139.2, 134.9, 132.4, 129.3, 123.5, 121.6, 121.4, 115.1, 111.4, 107.3, 106.6, 106.4, 37.41.

HRMS (ESI): $C_{22}H_{15}ClF_4N_7^+$ $(M+H)^+$ calculated: 488.10081 found: 488.10014

***N*-((1-(4-(1*H*-pyrazolo[3,4-c]pyridin-1-yl)phenyl)-1*H*-1,2,3-triazol-4-yl)methyl)-2-chloro-6-(trifluoromethyl)pyridin-4-amine 5.45**

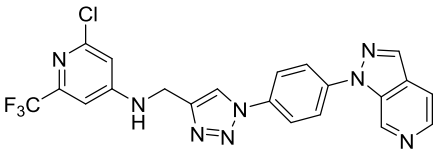

N-((1-(4-bromophenyl)-1*H*-1,2,3-triazol-4-yl)methyl)-2-chloro-6-(trifluoromethyl)pyridin-4-amine **5.42** (22 mg, 0.051 mmol), 1*H*-pyrazolo[4,3-*b*]pyridine (7 mg, 0.056 mmol), and NaO*t*Bu (7.0 mg, 0.076 mmol) were dissolved in toluene (0.51 mL) and the reaction mixture was degassed with argon. Then, *t*BuXPhos Pd G3 (2 mg, 5 mol%) was added and the reaction mixture was purged with argon

again before stirring the mixture at a pre-heated oil bath at 100 °C for 18 h. The reaction mixture was allowed to cool to room temperature and saturated NH_4Cl solution was added. The mixture was then extracted three times with EtOAc, dried over Na_2SO_4, filtered and concentrated under reduced pressure. Purification *via* automated flash chromatography afforded the title compound as a colorless solid (8.9 mg, 0.019 mmol, 37%)

^{1}H-NMR (500 MHz, acetone-d_6): δ [ppm] = 8.70 (s, 1 H), 8.67 (dd, *J* = 4.3 Hz, *J* = 1.1 Hz, 1 H), 8.50 (s, 1 H), 8.40 (d, *J* = 8.6 Hz, 1 H), 8.14 – 8.11 (m, 2 H), 8.09 – 8.06 (m, 2 H), 7.53 (dd, *J* = 8.7 Hz, *J* = 4.3 Hz, 1 H), 7.23 (bs, 1 h), 7.18 (d, *J* = 1.8 Hz, 1 H), 6.96 (d, *J* = 1.8 Hz, 1 H), 4.75 (d, *J* = 5.7 Hz, 1 H).

HRMS (ESI): $C_{21}H_{15}ClF_3N_8^+$ $(M+H)^+$ calculated: 471.10548 found: 471.10509

2-Chloro-*N*-((1-(3-((2,5-difluorophenyl)amino)phenyl)-1H-1,2,3-triazol-4-yl)methyl)-6-(trifluoromethyl)pyridin-4-amine 5.46

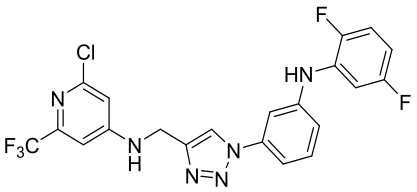

N-((1-(3-bromophenyl)-1*H*-1,2,3-triazol-4-yl)methyl)-2-chloro-6-(trifluoromethyl)pyridin-4-amine **5.43** (43 mg, 0.100 mmol) was dissolved in 1,4-dioxane (1 mL) and Cs_2CO_3 (36 mg, 0.110 mmol) was added, followed by the addition of 2,5-difluoroaniline (10 µL, 13 mg, 0.100 mmol). The mixture was purged with argon and Pd-175 (7.8 mg, 10 mol%) was added. After degassing the solution for 10 minutes with argon, the mixture was stirred in a pre-heated oil bath at 80 °C for 3 h. The reaction mixture was cooled to room temperature and filtered over SiO_2. The crude product was purified *via* automated flash chromatography (DCM/MeOH) and afforded the title compound as a colorless solid (26.0 mg, 0.054 mmol, 54%).

LC-MS: m/z: 482 $(M+H)^+$

^{1}H-NMR (500 MHz, acetone-d_6): δ [ppm] = 8.53 (s, 1 H), 7.76 (bs, 1 H), 7.69 (dd, *J* = 2.0 Hz, 1 H), 7.49 (dd, *J* = 8.1 Hz, 1 H), 7.42 (ddd, *J* = 7.9 Hz, *J* = 2.0 Hz, *J* = 0.9 Hz, 1 H), 7.26 (d, *J* = 8.1 Hz, *J* = 2.4 Hz, 1 H), 7.22 – 7.16 (m, 2 H), 6.70 – 6.63 (m, 3 H), 6.01 (d, *J* = 1.7 Hz, 1 H), 4.60 (d, *J* = 5.7 Hz, 2 H).

^{13}C-NMR (126 MHz, acetone-d_6): δ [ppm] = 165.9, 162.8, 160.9, 157.7, 151.8, 149.9, 146.3, 144.8, 139.2, 133.14, 131.6, 121.7, 118.8, 117.4, 113.6, 110.4, 108.0, 106.4, 101.3, 92.66, 39.03.

6-Chloro-*N*-(prop-2-yn-1-yl)-2-(trifluoromethyl)pyrimidin-4-amine 5.48

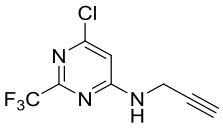

Propargylamine (35 µLm 30 mg, 0.550 mmol), 4,6-dichloro-2-(trifluoromethyl)pyrimidine (108 mg, 0.500 mmol) and Cs_2CO_3 (178 mg, 0.550 mmol) were mixed in DMF (1 mL). The reaction mixture was then heated for 1 h at 75 °C (microwave) and H_2O was added. The mixture was extracted with EtOAc, dried over Na_2SO_4, filtered and the solvent was removed under reduced pressure. The crude product was purified *via* automated flash chromatography (PE/EtOAC) and yielded the title compound as a colorless solid (69 mg, 0.292 mmol, 58%).

LC-MS: m/z: 236 $(M+H)^+$

^{1}H-NMR (300 MHz, $CDCl_3$): δ [ppm] = 6.51 (s, 1 H), 4.42 (bs, 1 H), 3.27 – 3.09 (m, 2 H), 2.34 (s, 1 H).

6-Chloro-*N*-((1-(4-phenoxyphenyl)-1*H*-1,2,3-triazol-4-yl)methyl)-2-(trifluoromethyl)pyrimidin-4-amine 5.49

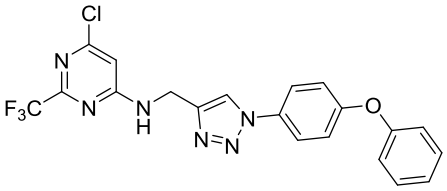

The compound was prepared according to **GP4.** 4-Phenoxyaniline (55 mg, 0.297 mmol) and 6-Chloro-*N*-(prop-2-yn-1-yl)-2-(trifluoromethyl)pyrimidin-4-amine **5.48** (70 mg, 0.297 mmol) were used in the reaction and afforded the title compound as a colorless solid (108 mg, 0.242 mmol, 81%).

^{1}H-NMR (300 MHz, $CDCl_3$): δ [ppm] = 8.06 (bs, 1 H), 7.65 – 7.64 (m, 2 H), 7.42 _ 7.39 (m, 2 H), 7.21 – 7.18 (m, 1 H), 7.15 – 7.13 (m, 2 H), 7.08 – 7.07 (m, 2 H), 6.70 – 6.68 (m, 1 H), 4.82 (bs, 2 H).

^{13}C-NMR (76 MHz, $CDCl_3$): δ [ppm] = 163.2, 158.3, 156.1, 144.3, 131.8, 130.1, 124.3, 122.2, 119.6, 119.2, 106.5, 36.09.

HRMS (ESI): $C_{20}H_{15}ClF_3N_6O^+$ $(M+H)^+$ calculated: 447.09425 found: 447.09369

***N*-((1-(4-phenoxyphenyl)-1*H*-1,2,3-triazol-4-yl)methyl)-2-(trifluoromethyl)pyrimidin-4-amine 5.50**

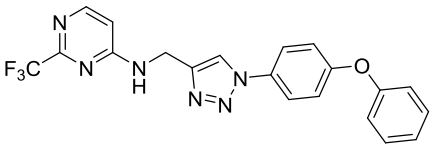

6-Chloro-*N*-((1-(4-phenoxyphenyl)-1*H*-1,2,3-triazol-4-yl)methyl)-2-(trifluoromethyl)pyrimidin-4-amine **5.49** (27 mg, 0.06 mmol) was dissolved in MeOH (2 mL). The mixture was degassed with argon for 10 minutes and Pd black (0.7 mg, 10 mol%) was added. The reaction mixture was purged with argon for 10 minutes and stirred at room temperature for 2 d. The mixture was then filtered over silica gel, washed with EtOAc and concentrated *in vacuo*. Automated flash chromatography afforded the title compound was a colorless solid (24 mg, 0.059 mmol, > 98%).

^{1}H-NMR (300 MHz, $CDCl_3$): δ [ppm] = 8.84 – 8.83 (m, 1 H), 8.64 – 8.65 (m, 1 H), 7.87 – 7.86 (m, 2 H), 7.46 – 7.42 (m, 2 H), 7.22 – 7.17 (m, 3 H), 7.12 – 7.09 (m, 2 H), 4.68 – 4.66 (m, 2 H).

^{13}C-NMR (76 MHz, $CDCl_3$): δ [ppm] = 157.1, 155.9, 154.1, 147.9, 144.9, 142.5, 132.0, 130.3, 124.2 122.0, 119.3, 108.5, 37.10.

HRMS (ESI): $C_{20}H_{16}F_3N_6O^+$ $(M+H)^+$ calculated: 413.13322 found: 413.13266

***N*-((1-(4-phenoxyphenyl)-1*H*-1,2,3-triazol-4-yl)methyl)-2-(1*H*-pyrazol-4-yl)-6-(trifluoromethyl) pyridin-4-amine 5.52**

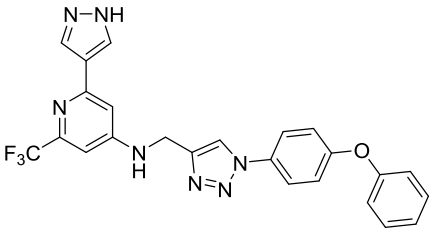

2-Chloro-*N*-((1-(4-phenoxyphenyl)-1*H*-1,2,3-triazol-4-yl)methyl)-6-(trifluoromethyl)pyridin-4-amine **4.2** (446 mg, 1.00 mmol), 4-(4,4,5,5-Tetramethyl-1,3,2-dioxaborolan-2-yl)-1*H*-pyrazole (786 mg, 4.00 mmol) and Cs_2CO_3 (1.64 g, 5.00 mmol) were suspended in toluene (5 mL). The reaction mixture was purged with argon and cataCXium A (36 mg, 10 mol%) and Pd_2dba_3 (4.6 mg, 5 mol%) were added. The mixture was degassed with argon for 10 minutes and then stirred for 2 h at 100 °C (microwave). After cooling to room temperature, H_2O was added and the mixture was extracted three times with EtOAc, dried over Na_2SO_4, filtered and concentrated *in vacuo*. Automated flash chromatography (DCM/MeOH) afforded the title compound as a colorless solid (402 mg, 0.842 mmol, 84%).

^{1}H-NMR (500 MHz, $CDCl_3$): δ [ppm] = 7.90 (s, 1 H), 7.67 – 7.64 (m, 2 H), 7.42 – 7.38 (m, 2 H), 7.21 – 7.18 (m, 1 H), 7.15 – 7.12 (m, 2 H), 7.09 – 7.06 (m, 2 H), 6.87 (d, *J* = 2.0 Hz, 1 H), 6.69 (d, *J* = 2.0 Hz, 1 H), 5.56 (bs, 1 H), 4.60 (bs, 2 H).

^{13}C-NMR (126 MHz, $CDCl_3$): δ [ppm] = 158.6, 156.3, 155.6, 153.0, 148.5, 144.1, 131.9, 130.3, 128.9, 125.4, 124.6, 122.6, 120.3, 119.8, 119.5, 108.3, 104.9, 38.81.

HRMS (ESI): $C_{24}H_{19}F_3N_7O^+$ $(M+H)^+$ calculated: 478.15977 found: 478.15872

2-(1*H*-imidazol-1-yl)-*N*-((1-(4-phenoxyphenyl)-1*H*-1,2,3-triazol-4-yl)methyl)-6-(trifluoromethyl) pyridin-4-amine 5.53

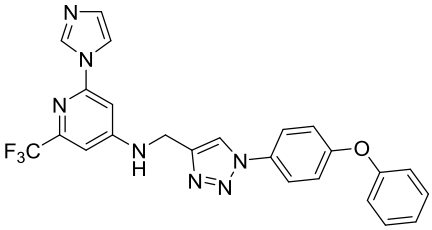

2-Chloro-*N*-((1-(4-phenoxyphenyl)-1*H*-1,2,3-triazol-4-yl)methyl)-6-(trifluoromethyl)pyridin-4-amine **4.2** (45 mg, 0.100 mmol), imidazole (21 mg, 0.300 mmol) and Cs_2CO_3 (108 mg, 0.300 mmol) were suspended in toluene (1 mL). The reaction mixture was heated at 120 °C for 16 h, cooled to room temperature, filtered and concentrated *in vacuo*. The crude product was purified *via* automated flash chromatography (DCM/MeOH) and yielded the title compound as a slightly brownish solid (10.8 mg, 0.023 mmol, 8%).

^{1}H-NMR (500 MHz, DMSO-d_6): δ [ppm] = 8.59 (s, 1 H), 8.40 (s, 1 H), 7.88 – 7.85 (m, 2 H), 7.83 (s, 1 H), 7.46 – 7.43 (m, 2 H), 7.25 – 7.22 (m, 2 H), 7.21 – 7.20 (m, 1 H), 7.19 – 7.16 (m, 2 H), 7.15 (d, *J* = 1.7 Hz, 1 H), 7.11 – 7.10 (m, 2 H), 7.09 (m, 1 H), 4.79 (d, *J* = 5.7 Hz, 2 H).

^{13}C-NMR (126 MHz, acetone-d_6): δ [ppm] = 158.2, 156.5, 155.3, 152.9, 133.93, 131.2, 128.6, 125.2, 123.2, 122.0, 116.4, 108.8, 92.05, 39.19.

HRMS (ESI): $C_{24}H_{19}F_3N_7O^+$ $(M+H)^+$ calculated: 478.15977 found: 478.15920

***N*-((1-(4-phenoxyphenyl)-1*H*-1,2,3-triazol-4-yl)methyl)-2-(1*H*-1,2,4-triazol-1-yl)-6-(trifluoromethyl) pyridin-4-amine 5.54**

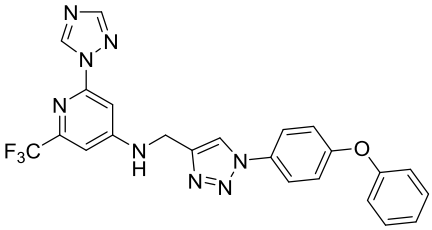

2-Chloro-*N*-((1-(4-phenoxyphenyl)-1*H*-1,2,3-triazol-4-yl)methyl)-6-(trifluoromethyl)pyridin-4-amine **4.2** (45 mg, 0.100 mmol), 1*H*-1,2,4-triazole (21 mg, 0.300 mmol) and Cs_2CO_3 (108 mg, 0.300 mmol) were suspended in 1,4-dioxane (1 mL). The reaction mixture was heated at 100 °C for 16 h (microwave), cooled to room temperature, filtered and concentrated *in vacuo*. The crude product was

purified *via* automated flash chromatography (DCM/MeOH) and yielded the title compound as a slightly brownish solid (16.6 mg, 0.035 mmol, 35%).

^{1}H-NMR (500 MHz, acetone-d_6): δ [ppm] = 9.15 (s, 1 H), 8.57 (s, 1 H), 8.13 (s, 1 H), 7.87 – 7.85 (m, 2 H), 7.46 – 7.42 (m, 2 H), 7.35 (bs, 1 H), 7.22 (d, *J* = 2.1 Hz, 1 H), 7.21 (s, 1 H), 7.19 – 7.16 (m, 2 H), 7.11 – 7.09 (m, 2 H), 7.09 – 7.08 (m, 1 H), 4.79 (d, *J* = 5.7 Hz, 2 H).

^{13}C-NMR (126 MHz, acetone-d_6): δ [ppm] = 158.8, 158.4, 154.1, 146.1, 133.6, 131.2, 127.6, 125.2, 123.2, 122.0, 120.4, 93.66, 39.29.

HRMS (ESI): $C_{23}H_{18}F_3N_8O^+$ $(M+H)^+$ calculated: 479.15502 found: 479.15436

***N*-((1-(4-(2-fluorophenoxy)phenyl)-1*H*-1,2,3-triazol-4-yl)methyl)-2-(1*H*-pyrazol-4-yl)-6-(trifluoromethyl)pyridin-4-amine 5.55**

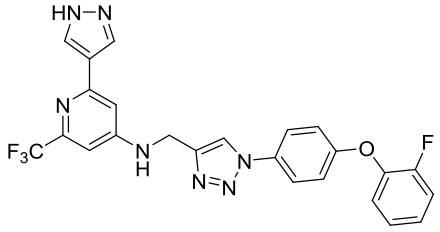

2-Chloro-*N*-((1-(4-(2-fluorophenoxy)phenyl)-1*H*-1,2,3-triazol-4-yl)methyl)-6-(trifluoromethyl)pyridin-4-amine (16.2 mg, 0.035 mmol), 4-(4,4,5,5-Tetramethyl-1,3,2-dioxaborolan-2-yl)-1*H*-pyrazole (14 mg, 0.070 mmol) and Cs_2CO_3 (25 mg, 0.077 mmol) were suspended in toluene (0.35 mL). The mixture was degassed with argon and cataCXium A (1.3 mg, 10 mol%) and Pd_2dba_3 (1.6 mg, 5 mol%) were added. The reaction mixture was purged with argon for 10 minutes and stirred for 2 h at 100 °C (microwave). After cooling to room temperature, H_2O was added and the mixture was extracted three times with EtOAc, dried over Na_2SO_4, filtered and concentrated *in vacuo*. Automated flash chromatography (DCM/MeOH) afforded the title compound as a colorless solid (10.7 mg, 0.022 mmol, 63%)

LC-MS: m/z: 497 $(M+H)^+$

^{1}H-NMR (300 MHz, $CDCl_3$): δ [ppm] = 7.88 (s, 1 H), 7.67 – 7.64 (m, 2 H), 7.25 – 7.15 (m, 5 H), 7.11 – 7.09 (m, 2 H), 6.87 (s, 1 H), 6.69 (s, 1 H), 5.54 (bs, 1 H), 4.59 (s, 2 H).

^{13}C-NMR (76 MHz, $CDCl_3$): δ [ppm] = 158.2, 155.4, 155.3, 153.5, 152.8, 148.5, 148.3, 143.8, 142.5, 131.8, 128.8, 125.9, 125.0, 122.6, 122.4, 121.9, 119.9, 117.7, 117.3, 108.0, 104.7, 38.59.

2-Chloro-*N*-((1-(4-isopropoxyphenyl)-1*H*-1,2,3-triazol-4-yl)methyl)-6-(trifluoromethyl)pyridine-4-amine 5.56

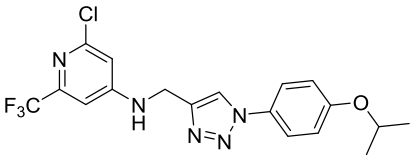

The compound was prepared according to **GP4.** 2-Chloro-*N*-(prop-2-yn-1-yl)-6-(trifluoromethyl)pyridin-4-amine **4.17** (54 mg, 0.115 mmol) and 4-isopropoxyaniline (17 mg, 0115 mmol) were used. The title compound was obtained as a colorless solid (46.7 mg, 0.114 mmol, > 98%).

^{1}H-NMR (300 MHz, acetone-d_6): δ [ppm] = 8.34 (s, 1 H), 7.62 - 7.59 (m, 2 H), 7.05 (bs, 1 H), 7.03 (d, *J* = 1.9 Hz, 1 H), 6.97 – 6.95 (m, 2 H), 6.81 (d, *J* = 1.8 Hz, 1 H), 4.58 (dq, *J* = 6.0 Hz, 1 H), 4.50 (d, *J* = 5.8 Hz, 2 H), 1.21 (d, *J* = 6.0 Hz, 6 H).

^{13}C-NMR (126 MHz, acetone-d_6): δ [ppm] = 159.2, 157.7, 145.5, 131.3, 123.5, 122.8, 121.8, 121.3, 117.4, 70.94, 38.69, 22.22.

HRMS (ESI): $C_{18}H_{18}ClF_3N_5O^+$ $(M+H)^+$ calculated: 412.11465 found: 412.11368

***N*-((1-(4-isopropoxyphenyl)-1*H*-1,2,3-triazol-4-yl)methyl)-2-(1*H*-pyrazol-4-yl)-6-(trifluoromethyl) pyridin-4-amine 5.57**

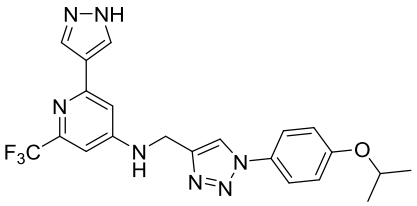

2-Chloro-*N*-((1-(4-isopropoxyphenyl)-1*H*-1,2,3-triazol-4-yl)methyl)-6-(trifluoromethyl)pyridine-4-amine **5.55** (10 mg, 0.024 mmol), 4-(4,4,5,5-Tetramethyl-1,3,2-dioxaborolan-2-yl)-1*H*-pyrazole (20 mg, 0.103 mmol) and Cs_2CO_3 (26 mg, 0.079 mmol) were suspended in toluene (0.5 mL). The reaction mixture was purged with argon and cataCXium A (0.9 mg, 10 mol%) and Pd_2dba_3 (1.1 mg, 5 mol%) were added. The mixture was degassed with argon for 10 minutes and then stirred for 16 h at 120 °C (microwave). After cooling to room temperature, H_2O was added and the mixture was extracted three times with EtOAc, dried over Na_2SO_4, filtered and concentrated *in vacuo*. Automated flash chromatography (DCM/MeOH) afforded the title compound as a colorless solid (9.8 mg, 0.022 mmol, 92%).

^{1}H-NMR (500 MHz, acetone-d_6): δ [ppm] = 10.82 (bs, 1 H), 8.09 (s, 2 H), 7.88 (s, 1 H), 7.60 – 7.56 (m, 2 H), 7.00 – 6.98 (m, 2 H), 6.88 (s, 1 H), 6.80 (d, *J* = 2.0 Hz, 1 H), 5.47 (bs, 1 H), 4.64 (d, *J* = 5.5 Hz, 2 H), 4.61 (dq, *J* = 6.1 Hz, 1 H), 1.36 (d, *J* = 6.0 Hz, 6 H).

HRMS (ESI): $C_{21}H_{21}F_3N_7O^+$ $(M+H)^+$ calculated: 444.17542 found: 444.17468

***N*-((1-(4-isopropoxyphenyl)-1*H*-1,2,3-triazol-4-yl)methyl)-2-(1*H*-1,2,4-triazol-1-yl)-6-(trifluoromethyl)pyridin-4-amine 5.59**

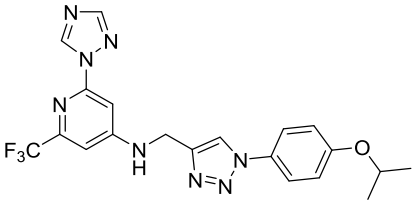

2-Chloro-*N*-((1-(4-isopropoxyphenyl)-1*H*-1,2,3-triazol-4-yl)methyl)-6-(trifluoromethyl)pyridine-4-amine **5.55** (10 mg, 0.024 mmol), 1*H*-1,2,4-triazole (5 mg, 0.032 mmol) and Cs_2CO_3 (26 mg, 0.079 mmol) were suspended in 1,4-dioxane (0.5 mL). The reaction mixture was heated at 100 °C for 16 h (microwave), cooled to room temperature, filtered and concentrated *in vacuo*. The crude product was purified *via* automated flash chromatography (DCM/MeOH) and yielded the title compound as a slightly brownish solid (7.5 mg, 0.017 mmol, 70%).

^{1}H-NMR (500 MHz, acetone-d_6): δ [ppm] = 9.15 (s, 1 H), 8.48 (s, 1 H), 8.13 (s, 1 H), 7.74 – 7.72 (m, 2 H), 7.41 (d, *J* = 1.8 Hz, 1 H), 7.32 (bs, 1 H), 7.21 (d, *J* = 2.0 Hz, 1 H), 7.11 – 7.07 (m, 2 H), 4.78 (d, *J* = 5.7 Hz, 2 H), 4.70 (dq, *J* = 6.1 Hz, 1 H), 1.32 (d, *J* = 6.0 Hz, 6 H).

^{13}C-NMR (126 MHz, acetone-d_6): δ [ppm] = 159.2, 158.3, 153.8, 1245.6, 142.8, 131.3, 122.8, 121.8, 70.94, 39.15, 22.22.

HRMS (ESI): $C_{20}H_{20}F_3N_8O^+$ $(M+H)^+$ calculated: 445.17067 found: 445.16989

(*E*)-4-phenoxybenzaldehyde oxime 5.70

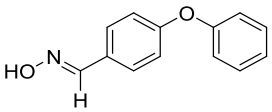

4-Phenoxybenzaldehyde (337 mg, 1.70 mmol) and $NH_2OH{\cdot}HCl$ (119 mg, 1.71 mmol) were dissolved in MeOH/H_2O (1:3, 10 mL) and stirred for 10 min until the reaction mixture was a clear solution. Then, Na_2CO_3 (90 mg, 1.54 mmol) was added and the reaction mixture was stirred at room temperature for 3 h. The mixture was extracted with DCM three times, dried over Na_2SO_4, filtered and the solvent was removed under reduced pressure. The title compound was obtained as an off-white solid (215 mg, 1.01 mmol, 59%) The crude product was used in the next step without further purification.

^{1}H-NMR (300 MHz, $CDCl_3$): δ [ppm] = 8.04 (s, 1 H), 7.55 (bs, 1 H), 7.48 – 7.44 (m, 2 H), 7.32 – 7.29 (m, 2 H), 7.20 – 7.18 (m, 2 H), 7.17 – 7.14 (m, 2 H), 7.10 – 7.05 (m, 1 H).

_N_-((3-(4-phenoxyphenyl)isoxazol-5-yl)methyl)-2-(trifluoromethyl)pyridin-4-amine 5.67

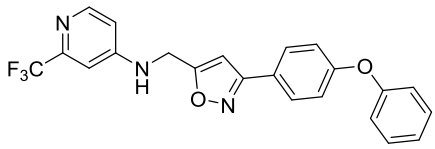

Step 1: (*E*)-4-phenoxybenzaldehyde oxime (197 mg, 0.982 mmol) was dissolved in DCM (3 mL) and *N*-chlorosuccinimide (122 mg, 0.924 mmol) was added. The reaction mixture was stirred at room temperature for 6 h until the starting material was fully consumed (TLC, PE/EtOAc). The reaction mixture was concentrated *in vacuo* and the colorless solid (*E/Z*)-*N*-hydroxy-4-phenoxybenzimidoyl chloride **5.69** was used in the next step without further purification.

Step 2: (*E*)-*N*-hydroxy-4-phenoxybenzimidoyl chloride **5.69** (120 mg, 0.850 mmol) and *N*-(prop-2-yn-1-yl)-2-(trifluoromethyl)pyridin-4-amine **1.25** (187 mg, 0.935 mmol) were dissolved in *t*BuOH/H_2O (1:1, 10 mL). Na_2CO_3 (397 mg, 3.75 mmol) was added and the mixture was degassed with argon and stirred for 10 min at room temperature. Then, Na-ascorbate (17 mg, 10 mol%) and $CuSO_4 \cdot 5\ H_2O$ (4.3 mg, 2 mol%) were added. The mixture was stirred for 16 h at room temperature and H_2O was added, followed by extraction with EtOAc. The combined organic layers were washed with brine, dried over Na_2SO_4, filtered and concentrated *in vacuo*. The crude product was purified *via* automated flash chromatography (DCM/MeOH) and yielded the title compound as a colorless solid (7.2 mg, 0.018 mmol, 2%).

^{1}H-NMR (300 MHz, $CDCl_3$): δ [ppm] = 8.36 (d, *J* = 5.7 Hz, 1 h), 7.76 – 7.71 (m, 2 H), 7.41 – 7.36 (m, 2 H), 7.20 – 7.15 (m, 1 H), 7.07 – 7.04 (m, 4 H), 6.93 (d, *J* = 2.2 Hz, 1 H), 6.66 (dd, *J* = 5.7 Hz, *J* = 2.3 Hz, 1 H), 6.46 (s, 1 H), 5.04 (bs, 1 H), 4.62 (d, *J* = 6.0 Hz, 2 H).

HRMS (ESI): $C_{22}H_{17}F_3N_3O_2^+$ $(M+H)^+$ calculated: 412.12674 found: 412.12633

4-Phenoxybenzohydrazide 5.77

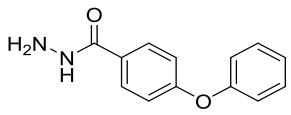

4-Phenoxybenzoic acid (536 mh, 2.50 mmol) was dissolved in THF (3 mL) and CDI was added (527 mg, 3.25 mmol). Upon stirring at room temperature for 2 h, the colorless suspension turned to a clear yellow solution and $N_2H_4 \cdot H_2O$ (0.38 mL, 7.50 mmol) in THF (2 mL) was added. The mixture was stirred for 3 h and saturated NH_4Cl solution was added. After extraction with EtOAc, the combined organic layers were washed with H_2O, dried over Na_2SO_4 and concentrated *in vacuo*. The title compound was obtained as a colorless solid (566 mg, 2.48 mmol, > 98%).

LC-MS: m/z: 229 $(M+H)^+$

^{1}H-NMR (300 MHz, DMSO-d_6): δ [ppm] = 7.89 – 7.84 (m, 2 H), 7.49 – 7.42 (m, 2 H), 7.25 – 7.18 (m, 1 H), 7.12 – 7.02 (m, 4 H).

Ethyl 2-oxo-2-(2-(4-phenoxybenzoyl)hydrazinyl)acetate 5.76

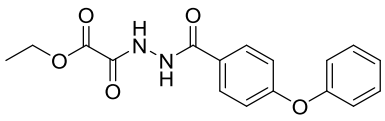

4-Phenoxybenzohydrazide **5.77** (114 mg, 0.500 mmol) was dissolved in DCM (2.5 mL) and DIPEA (93 µL 70.7 mg, 0.550 mmol) was added. The mixture was cooled to 0 °C and ethyl 2-chloro-2-oxoacetate (67 µL, 82 mg, 0.600 mmol) in DCM (2.5 mL) was added slowly. The mixture was allowed to warm to room temperature and was stirred for 5 h. The reaction was quenched with saturated NH_4Cl solution and extracted with EtOAc. The combined organic layers were washed with brine and dried over Na_2SO_4. The solvent was evaporated under reduced pressure and the title compound was obtained as a colorless solid (136 mg, 0.415 mmol, 83%). The crude product was used in the next step without further purification.

LC-MS: m/z: 329 $(M+H)^+$

^{1}H-NMR (300 MHz, $CDCl_3$): δ [ppm] = 9.90 (bs, 1 H), 9.19 (s, 1 H), 7.85 – 7.81 (m, 2 H), 7.41 – 7.38 (m, 2 H), 7.22 – 7.19 (m, 1 H), 7.08 – 7.05 (m, 2 H), 7.03 – 6.99 (m, 2 H), 4.42 (q, *J* = 7.1 Hz, 2 H), 1.41 (t, *J* = 7.1 Hz, 3 H).

^{13}C-NMR (76 MHz, $CDCl_3$): δ [ppm] = 163.5, 161.8, 158.4, 155.4, 152.6, 130.1, 129.4, 124.7, 120.1, 117.7, 63.74, 13.96.

Ethyl 5-(4-phenoxyphenyl)-1,3,4-oxadiazole-2-carboxylate 5.75

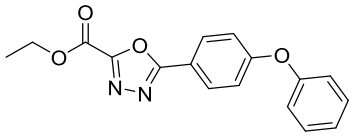

Ethyl 2-oxo-2-(2-(4-phenoxybenzoyl)hydrazinyl)acetate **5.76** (153 mg, 0.640 mmol) was dissolved in anhydrous DCM (4.5 mL) and anhydrous NEt_3 (98 µL, 0.704 mmol) was added. The reaction mixture was cooled to 0 °C and TsCl (52 µL, 77 mg, 0.704 mmol) was added. After warming up to room temperature the reaction mixture was stirred for 13 h and quenched with saturated $NaHCO_3$ solution, followed by extraction with DCM. The combined organic layers were dried over Na_2SO_4 and the solvent

was removed *in vacuo*. The title compound was obtained as a colorless solid (140 mg, 0.454 mmol, 71%). The crude product was used in the next step without further purification.

LC-MS: m/z: 311 $(M+H)^+$

^{1}H-NMR (300 MHz, $CDCl_3$): δ [ppm] = 8.14 – 8.11 (m, 2 H), 7.44 – 7.41 (m, 2 H), 7.24 – 7.22 (m, 1 H), 7.11 – 7.10 (m, 4 H), 4.57 (q, *J* = 6.9 Hz, 2 H), 1.49 (t, *J* = 6.9 Hz, 3 H).

(5-(4-Phenoxyphenyl)-1,3,4-oxadiazol-2-yl)methanol 5.74

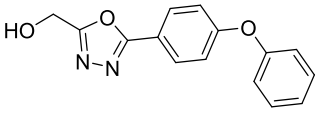

Ethyl 5-(4-phenoxyphenyl)-1,3,4-oxadiazole-2-carboxylate **5.75** (140 mg, 0.454 mmol) was dissolved in THF (3 mL) and $NaBH_4$ (121 mg, 3.20 mmol) was added at 0 °C, followed by slow addition of MeOH (3 mL). The reaction mixture was stirred at room temperature for 3 h and then quenched with saturated NH_4Cl solution. The mixture was then extracted with EtOAc and the combined organic layers were dried over Na_2SO_4 concentrated under reduced pressure. Automated flash chromatography (PE/EtOAc) afforded the title compound as a yellow solid (74 mg, 0.276 mmol, 61%).

LC-MS: m/z: 296 $(M+H)^+$

^{1}H-NMR (300 MHz, $CDCl_3$): δ [ppm] = 8.03 – 8.02 (m, 2 H), 7.43 – 7.40 (m, 2 H), 7.23 – 7.20 (m, 1 H), 7.10 – 7.08 (m, 4 H), 4.95 (s, 2 H), 2.45 (bs, 1 H).

^{13}C-NMR (76 MHz, $CDCl_3$): δ [ppm] = 164.9, 164.5, 155.3, 129.8, 128.7, 124.4, 119.8, 117.9, 117.6, 55.22.

2-(Bromomethyl)-5-(4-phenoxyphenyl)-1,3,4-oxadiazole 5.73

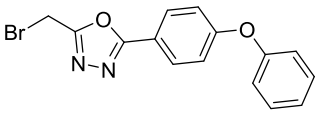

(5-(4-Phenoxyphenyl)-1,3,4-oxadiazol-2-yl)methanol **5.74** (67 mg, 0.248 mmol) was dissolved in DCM (1 mL) and PBr_3 (26 µL, 74 mg, 0.273 mmol) was added at 0 °C. The reaction mixture was stirred at room temperature for 3 h and H_2O was added, followed by extraction with EtOAc. The combined organic layers were dried over Na_2SO_4 and the solvent was removed under reduced pressure. The title compound was obtained as a colorless solid (80 mg, 0.241 mmol, 98%) and was used in the next step without further purification.

LC-MS: m/z: 332 $(M+H)^+$

^{1}H-NMR (300 MHz, $CDCl_3$): δ [ppm] = 8.03 – 8.02 (m, 2 H), 7.43 – 7.40 (m, 2 H), 7.23 – 7.20 (m, 1 H), 7.10 – 7.08 (m, 4 H), 4.60 (s, 2 H).

^{13}C-NMR (76 MHz, $CDCl_3$): δ [ppm] = 161.9, 160.9, 155.2, 129.9, 128.8, 124.4, 119.85, 117.9, 117.4, 16.42.

***Tert-butyl*((5-(4-phenoxyphenyl)-1,3,4-oxadiazol-2-yl)methyl)(2-(trifluoromethyl)pyridin-4-yl) carbamate 5.79**

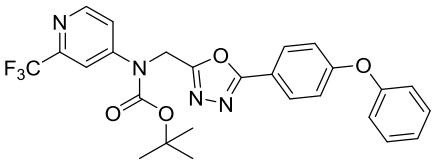

Tert-butyl (2-(trifluoromethyl)pyridin-4-yl)carbamate **1.8** (21 mg, 0.080 mmol) was dissolved in anhydrous DMF (0.4 mL) and NaH (60 wt%, 4 mg, 0.110 mmol) was added at 0 °C. The reaction mixture was stirred for 1 h and then added dropwise to a solution of 2-(Bromomethyl)-5-(4-phenoxyphenyl)-1,3,4-oxadiazole **5.73** (24 mg, 0.073 mmol) in anhydrous DMF (0.4 mL) at 0 °C. After stirring for 2 h at room temperature, the reaction was quenched with saturated NH_4Cl solution and extracted with EtOAc. The combined organic layers were washed with saturated LiCl solution, dried over Na_2SO_4 and the solvent was removed under reduced pressure. Automated flash chromatography (PE/EtOAc) afforded the title compound as a colorless solid (19 mg, 0.037 mmol, 51%).

LC-MS: m/z: 456 $(M\text{-}t\text{Bu}+H)^+$

^{1}H-NMR (300 MHz, $CDCl_3$): δ [ppm] = 8.67 (d, *J* = 5.6 Hz, 1 H), 7.99 – 7.95 (m, 2 H), 7.91 (d, *J* = 2.1 Hz, 1 H), 7.58 (dd, *J* = 5.6 Hz, *J* = 2.1 Hz, 1 H), 7.43 – 7.40 (m, 2 H), 7.23 – 7.21 (m, 1 H), 7.10 – 7.07 (m, 4 H), 5.17 (s, 2 H), 1.53 (s, 9 H).

^{13}C-NMR (76 MHz, $CDCl_3$): δ [ppm] = 165.1, 162.3, 161.2, 155.4, 152.2, 150.9, 150.5, 148.9, 130.1, 128.8, 124.7, 122.4, 120.2, 120.1, 118.2, 117.6, 115.6, 84.17, 43.87, 28.03.

***N*-((5-(4-phenoxyphenyl)-1,3,4-oxadiazol-2-yl)methyl)-2-(trifluoromethyl)pyridin-4-amine 5.72**

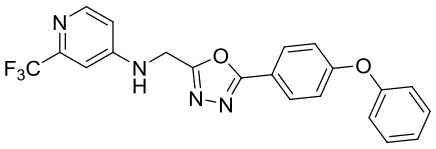

Tert-butyl((5-(4-phenoxyphenyl)-1,3,4-oxadiazol-2-yl)methyl)(2-(trifluoromethyl)pyridin-4-yl) carbamate **5.79** (19 mg, 0.037 mmol) was dissolved in DCM (0.36 mL) and TFA (0.04 mL) was added. The reaction mixture was stirred at room temperature for 18 h, followed by slow addition of saturated

$NaHCO_3$. The mixture was extracted with DCM and the combined organic layers were dried over Na_2SO_4 and concentrated *in vacuo*. The crude product was purified using automated flash chromatography (PE/EtOAc) and the title compound was isolated as a colorless solid (13.3 mg, (0.032 mmol, 87%).

^{1}H-NMR (300 MHz, $CDCl_3$): δ [ppm] = 8.38, (d, *J* = 5.8 Hz, 1 H), 7.98 – 7.94 (m, 2 H), 7.43 – 7.39 (m, 2 H), 7.23 – 7.20 (m, 1 H), 7.09 – 7.06 (m, 4 H), 7.02 (d, *J* = 2.4 Hz, 1 H), 6.77 (dd, *J* = 5.8 Hz, *J* = 2.4 Hz, 1 H), 5.41 (bs, 1 H), 4.73 (d, *J* = 5.9 Hz, 2 H).

^{13}C-NMR (76 MHz, $CDCl_3$): δ [ppm] = 165.3, 162.3, 161.2, 155.4, 153.1, 150.6, 149.2, 130.1, 128.9, 124.7, 122.7, 120.5, 120.1, 118.2, 117.4, 109.4, 104.9, 53.41.

HRMS (ESI): $C_{21}H_{16}F_3N_4O_2^+$ $(M+H)^+$ calculated: 413.12199 found: 413.12099

Methyl 3-chloro-4-isopropoxybenzoate 5.81

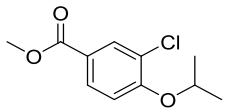

Methyl 3-chloro-4-hydroxybenzoate (746 mg, 4.00 mmol) was dissolved in acetone (8 mL) and Cs_2CO_3 (1.43 g, 4.40 mmol) was added. The mixture was stirred for 5 minutes at room temperature and then isopropylbromide (0.83 mL, 1.08 g, 8.80 mmol) was added. The reaction mixture was subjected to microwave-aided heating at 50 °C for 3 h. The mixture was cooled to room temperature and H_2O was added. After extraction with EtOAc, the combined organic layers were dried over Na_2SO_4 and the solvent was removed under reduced pressure. The crude product was purified *via* automated flash chromatography (PE/EtOAc) and the title compound was isolated as a colorless oil (745 mg, 3.27 mmol, 82%).

LC-MS: m/z: 229 $(M+H)^+$

^{1}H-NMR (300 MHz, $CDCl_3$): δ [ppm] = 8.06 (s, 1 H), 7.90 (d, *J* = 8.5 Hz, 1 H), 6.95 (d, *J* = 8.5 Hz, 1 H), 4.70 – 4.65 (m, 1 H), 3.90 (s, 3 H), 1.43 (d, *J* = 4.1 Hz, 6 H).

^{13}C-NMR (76 MHz, $CDCl_3$): δ [ppm] = 165.9, 157.4, 131.9, 129.6, 123.6, 122.9, 113.6, 71.91, 52.09, 21.88.

3-Chloro-4-isopropoxybenzohydrazide 5.82

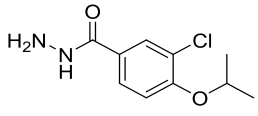

Methyl 3-chloro-4-isopropoxybenzoate **5.81** (330 mg, 1.44 mmol) was dissolved in EtOH (4 mL) and $N_2H_4 \cdot H_2O$ (0.70 mL, 14.4 mmol) was added. The reaction mixture was stirred at 80 °C for 5 h and after cooling to room temperature, saturated NH_4Cl solution was added. The mixture was extracted three times with EtOAc and the combined organic layers were washed with brine. The combined organic layers were then dried over Na_2SO_4 and concentrated under reduced pressure, affording the title compound as a colorless solid (278 mg, 1.21 mmol, 87%).

LC-MS: m/z: 229 $(M+H)^+$

^{1}H-NMR (300 MHz, $CDCl_3$): δ [ppm] = 7.79 (s, 1 H), 7.62 (d, *J* = 8.4 Hz, 1 H), 7.23 (bs, 1 H), 6.97 (d, *J* = 8.4 Hz, 1 H), 4.68 – 4.64 (m, 1 H), 1.69 (bs, 2 H), 1.42 (d, *J* = 4.0 Hz, 1 H).

^{13}C-NMR (76 MHz, $CDCl_3$): δ [ppm] = 166.1, 151.1, 129.5, 126.8, 125.5, 124.4, 114.5, 72.28, 22.13.

Ethyl 5-(3-chloro-4-isopropoxyphenyl)-1,3,4-oxadiazole-2-carboxylate 5.83

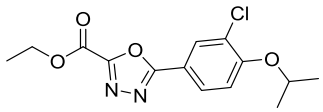

3-Chloro-4-isopropoxybenzohydrazide **5.82** (278 mg, 1.21 mmol) was dissolved in anhydrous DCM (8 mL) and anhydrous NEt_3 (0.34 mL, 2.42 mmol, 244 mg) was added. The mixture was cooled to 0 °C, ethyl 2-chloro-2-oxoacetate (0.15 mL, 181 mg, 1.33 mmol) was added and the mixture was allowed to warm to room temperature overnight. After 15 h starting material was fully consumed (TLC, PE/EtOAc 7:3) and anhydrous NEt_3 (0.17 mL, 122 mg, 1.21 mmol) was added. The reaction mixture was cooled to 0 °C and TsCl (231 mg, 1.21 mmol) was added. The mixture was stirred for 4 h at room temperature and then carefully quenched with saturated $NaHCO_3$ solution. After extraction with DCM, the combined organic layers were washed with 1 M HCl and dried over Na_2SO_4. The solvent was removed *in vacuo* and the crude product was used in the next step without further purification. The title compound was obtained as a yellow oil (355 mg, 1.14 mmol, 94%).

LC-MS: m/z: 311 $(M+H)^+$

^{1}H-NMR (300 MHz, $CDCl_3$): δ [ppm] = 8.18 (s, 1 H), 8.03 (d, *J* = 8.5 Hz, 1 H), 7.06 (d, *J* = 8.5 Hz, 1 H), 4.73 – 4.69 (m, 1 H), 4.56 (q, *J* = 6.7 Hz, 2 H), 1.49 (t, *J* = 6.8 Hz, 3 H), 1.44 (d, *J* = 5.7 Hz, 6 H).

^{13}C-NMR (76 MHz, $CDCl_3$): δ [ppm] = 165.5, 157.3, 156.2, 154.4, 129.7, 127.5, 124.7, 115.3, 114.4, 72.16, 63.52, 21.86, 14.09.

2-(Bromomethyl)-5-(3-chloro-4-isopropoxyphenyl)-1,3,4-oxadiazole 5.84

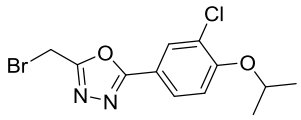

Step 1: Ethyl 5-(3-chloro-4-isopropoxyphenyl)-1,3,4-oxadiazole-2-carboxylate **5.83** (193, 0.622 mmol) was dissolved in MeOH and $NaBH_4$ (235 mg, 6.22 mmol) was added slowly at 0 °C. The reaction mixture was stirred for 14 h at room temperature and saturated NH_4Cl solution was added. The mixture was extracted three times with EtOAc and the combined organic layers were dried over Na_2SO_4. The solvent was removed under reduced pressure and the crude product was used in the next step without further purification.

LC-MS: m/z: 269 $(M+H)^+$

Step 2: The crude product from step 1 (94 mg, 0.350 mmol) was dissolved in DCM (1.4 mL) and PBr_3 (37 µL, 0.385 mmol) was added at 0 °C. The reaction was stirred for 3 h and H_2O was added, followed by extraction with EtOAc. The combined organic layers were driver over Na_2SO_4 and the solvent was removed under reduced pressure. The crude product was used without further purification and the title compound was obtained as a colorless solid (100 mg, 302 µmol, 94%).

LC-MS: m/z: 332 $(M+H)^+$

^{1}H-NMR (500 MHz, $CDCl_3$): δ [ppm] = 8.08 (d, *J* = 2.1 Hz, 1 H), 7.93 (dd, *J* = 8.7 Hz, *J* = 2.1 Hz, 1 H), 7.04 (d, *J* = 8.7 Hz, 1 H), 4.69 (sept, *J* = 6.1 Hz, 1 H), 1.44 (d, *J* = 6.1 Hz, 6 H).

***Tert*-butyl but-2-yn-1-yl(2-(trifluoromethyl)pyridin-4-yl)carbamate 5.86**

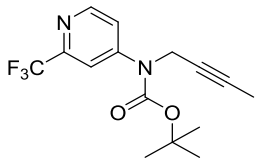

Tert-butyl prop-2-yn-1-yl(2-(trifluoromethyl)pyridin-4-yl)carbamate **1.24** (80 mg, 0.267 mmol) was dissolved in anhydrous THF (1.3 mL) and LDA (1.0 M in THF, 0.27 mL, 0.270 mmol) was added at –78 °C. The resulting yellow solution was stirred for 1 h at this temperature and MeI (19 µL, 42 mg, 0.297 mmol) was added. The reaction mixture was allowed to warm to room temperature and stirred for 18 h. Saturated NH_4Cl solution was added and the mixture was extracted with EtOAc three times, dried over Na_2SO_4 and concentrated *in vacuo*. The crude product was purified using automated flash chromatography (PE/EtOAc). The title compound was obtained as a colorless solid (70 mg, 0.223 mmol, 83%.

^{1}H-NMR (300 MHz, $CDCl_3$): δ [ppm] = 8.63 (d, *J* = 5.7 Hz, 1 H), 7.87 (d, *J* = 2.1 Hz, 1 H), 7.57 (dd, *J* = 5.7 Hz, *J* = 2.1 Hz, 1 H), 4.44 – 4.43 (m, 2 H), 1.58 (s, 9 H).

^{13}C-NMR (76 MHz, $CDCl_3$): δ [ppm] = 152.4, 150.6, 150.4, 146.8, 119.1, 113.3, 111.2, 103.5, 8.31, 81.07, 8.71, 28.15, 3.51.

_N_-((5-methyl-1-(4-phenoxyphenyl)-1_H_-1,2,3-triazol-4-yl)methyl)-2-(trifluoromethyl)pyridin-4-amine 5.87

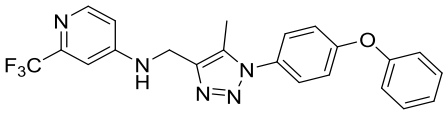

Tert-butyl but-2-yn-1-yl(2-(trifluoromethyl)pyridin-4-yl)carbamate **5.86** (20 mg, 0.064 mmol) and 1-azido-4-phenoxybenzene (14 mg, 0.064 mmol) were dissolved in MeCN and stirred at 80 °C for 3 d. The solvent was removed under reduced pressure and the crude product was purified *via* automated flash chromatography (PE/EtOAc). The title compound was obtained as a colorless solid (2.6 mg, 0.006 mmol, 10%).

^{1}H-NMR (300 MHz, $CDCl_3$): δ [ppm] = 8.35 (d, *J* = 5.7 Hz, 1 H), 7.43 – 7.42 (m, 2 H), 7.42 – 7.43 (m, 2 h), 7.23 – 7.20 (m, 1 H), 7.16 – 7,14 (m, 2 H), 7.11 – 7.09 (m, 2 H), 6.93 (d, *J* = 2.3 Hz, 1 H), 6.71 (dd, *J* = 5.7 Hz, *J* = 2.3 Hz, 1 H), 5.19 (bs, 1 H), 4.48 (d, *J* = 4.9 Hz, 2 H), 2.35 (s, 3 H).

^{13}C-NMR (76 MHz, $CDCl_3$): δ [ppm] = 158.9, 155.9, 153.7, 150.3, 148.8, 140.5, 130.9, 130.1, 128.2, 127.6, 126.6, 124.5, 119.8, 118.8, 109.4, 104.5, 38.18, 8.82.

HRMS (ESI): $C_{22}H_{19}F_3N_5O^+$ $(M+H)^+$ calculated: 426.15362 found: 426.15282

5-(4-(((2-Chloro-6-(trifluoromethyl)pyridin-4-yl)amino)methyl)-1_H_-1,2,3-triazol-1-yl)-2-hydroxy benzonitrile 5.92

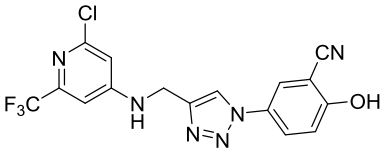

The compound was prepared according to **GP4.** 2-Chloro-*N*-(prop-2-yn-1-yl)-6-(trifluoromethyl)pyridin-4-amine **4.17** (30 mg, 0.125 mmol) and 5-amino-2-hydroxybenzonitrile (20 mg, 0.125 mmol) were used. Automated flash chromatography (DCM/MeOH) afforded the title compound as a colorless solid (17.4 mg, 0.044 mmol, 36%).

LC-MS: m/z: 395 $(M+H)^+$

4-(4-(((2-Chloro-6-(trifluoromethyl)pyridin-4-yl)amino)methyl)-1*H*-1,2,3-triazol-1-yl)-3-fluorophenol 5.93

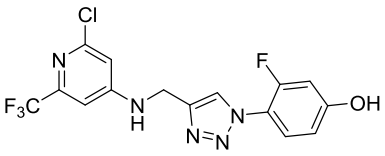

The compound was prepared according to **GP4.** 2-Chloro-*N*-(prop-2-yn-1-yl)-6-(trifluoromethyl)pyridin-4-amine **4.17** (30 mg, 0.125 mmol) and 4-amino-3-fluorophenol (19 mg, 0.125 mmol) were used. Automated flash chromatography (DCM/MeOH) afforded the title compound as a colorless solid (47.7 mg, 0.123 mmol, > 98%).

LC-MS: m/z: 388 $(M+H)^+$

5-(4-(((2-Chloro-6-(trifluoromethyl)pyridin-4-yl)amino)methyl)-1*H*-1,2,3-triazol-1-yl)-2-isopropoxy benzonitrile 5.94

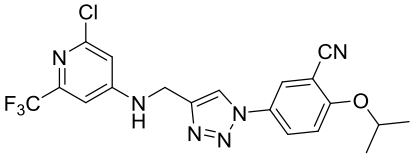

5-(4-(((2-Chloro-6-(trifluoromethyl)pyridin-4-yl)amino)methyl)-1*H*-1,2,3-triazol-1-yl)-2-hydroxy benzonitrile **5.92** (17 mg, 0.044 mmol) was dissolved in acetone (0.44 mL) and Cs_2CO_3 (16 mg, 0.048 mmol) was added. The mixture was stirred for 10 minutes at room temperature and isopropylbromide (12 µL, 16 mg, 0.132 mmol) was added. The mixture was then stirred at 60 °C for 2 d and after cooling to room temperature, saturated NH_4Cl solution was added. EtOAc was added and the mixture was extracted three times. The combined organic layers were washed with saturated Na_2CO_3 solution, dried over Na_2SO_4, filtered and concentrated *in vacuo*. Automated flash chromatography afforded the title compound as a colorless solid (8.7 mg, 0.020 mmol, 45%).

^{1}H-NMR (500 MHz, acetone-d_6): δ [ppm] = 8.60 (s, 1 H), 8.14 (s, 1 H), 7.47 – 7.46 (m, 1 H), 7.22 – 7.18 (m, 1 H), 7.15 (s, 1 H), 6.93 (s, 1 H), 4.92 (sept, *J* = 5.7 Hz, 1 H), 4.71 (d, *J* = 5.8 Hz, 2 H), 1.42 (d, *J* = 6.1 Hz, 6 H).

^{13}C-NMR (126 MHz, acetone-d_6): δ [ppm] = 160.6, 157.7, 146.1, 11.2, 127.6, 126.4, 121.9, 116.1, 104.2, 73.38, 38.90, 22.05.

HRMS (ESI): $C_{19}H_{17}ClF_3N_6O^+$ $(M+H)^+$ calculated: 437.10989 found: 437.10955

2-Chloro-*N*-((1-(2-fluoro-4-isopropoxyphenyl)-1*H*-1,2,3-triazol-4-yl)methyl)-6-(trifluoromethyl) pyridin-4-amine 5.95

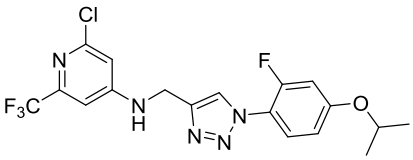

4-(4-(((2-Chloro-6-(trifluoromethyl)pyridin-4-yl)amino)methyl)-1*H*-1,2,3-triazol-1-yl)-3-fluorophenol **5.93** (53 mg, 0.137 mmol) was dissolved in acetone 1.37 mL) and Cs_2CO_3 (49 mg, 0.151 mmol) was added. The mixture was stirred for 10 minutes at room temperature and isopropylbromide (39 µL, 50 mg, 0.411 mmol) was added. The mixture was then stirred at 60 °C for 2 d and after cooling to room temperature, saturated NH_4Cl solution was added. EtOAc was added and the mixture was extracted three times. The combined organic layers were washed with saturated Na_2CO_3 solution, dried over Na_2SO_4, filtered and concentrated *in vacuo*. Automated flash chromatography afforded the title compound as a colorless solid (50.5 mg, 0.117 mmol, 86%).

^{1}H-NMR (500 MHz, acetone-d_6): δ [ppm] = 8.32 (s, 1 H), 7.68 (dd, *J* = 8.9 Hz, 1 H), 7.17 – 7.16 (m, 2 H), 7.01 – 6.69 (m, 1 H), 6.95 (bs, 2 H), 4.76 (dt, *J* = 6.0 Hz, 1 H), 4.71 (d, *J* = 5.7 Hz, 2 H), 1.36 (d, *J* = 6.0 Hz, 6 H).

^{13}C-NMR (126 MHz, acetone-d_6): δ [ppm] = 160.9, 157.8, 157.3, 155.3, 145.2, 127.6, 125.2, 113.4,

HRMS (ESI): $C_{18}H_{17}ClF_4N_5O^+$ $(M+H)^+$ calculated: 430.10523 found: 430.10503

***Tert*-butyl (4-cyano-3-(trifluoromethyl)phenyl)carbamate 6.2**

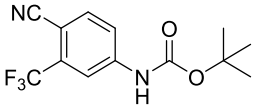

4-Amino-2-(trifluoromethyl)benzonitrile (500 mg, 2.68 mmol) was dissolved in THF (4.5 mL) and DMAP (33 mg, 0.27 mmol) was added. The mixture was cooled to 0 °C and Boc_2O (645 mg, 2.96 mmol) in THF (1.5 mL) was added. The reaction mixture was allowed to warm to room temperature and was then stirred for 15 h. After addition of H_2O, the mixture was extracted three times with Et_2O and the combined organic layers were washed with brine, dried over Na_2SO_4 and the solvent was removed under reduced pressure. The crude product was purified *via* automated flash chromatography (PE/EtOAc) and afforded the title compound as a colorless solid (530 mg, 1.85 mmol, 69%).

LC-MS: m/z: 230 $(M-t\text{Bu}+H)^+$

^{1}H-NMR (300 MHz, $CDCl_3$): δ [ppm] = 7.89 (d, *J* = 1.8 Hz, 1 H), 7.74 (d, *J* = 8.5 Hz, 1 H), 7.66 (dd, *J* = 8.5 Hz, *J* = 1.8 Hz, 1 H), 6.96 (bs, 1 H), 1.54 (s, 9 H).

^{13}C-NMR (76 MHz, $CDCl_3$): δ [ppm] = 151.6, 142.9, 135.2, 131.5, 126.6, 123.9, 120.2, 115.7, 102.3, 84.49, 28.13.

***Tert*-butyl (4-cyano-3-(trifluoromethyl)phenyl)(prop-2-yn-1-yl)carbamate 6.3**

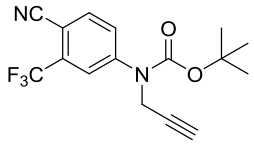

Tert-butyl (4-cyano-3-(trifluoromethyl)phenyl)carbamate **6.2** (300 mg, 1.05 mmol) was dissolved in DMF and NaH (60 wt%, 54 mg, 1.26 mmol) was added at 0 °C. After stirring for 10 min, propargyl bromide (0.61 mL, 1.26 mmol) was added dropwise and the mixture was allowed to warm to room temperature and was stirred for 3 h. Then, 0.1 M HCl was added and the reaction mixture was extracted with Et_2O three times. The combined organic layers were dried over Na_2SO_4, filtered and concentrated *in vacuo*. The title compound was obtained as a brownish oil (325 mg, 1.00 mmol. 96%) and was used in the next step without further purification.

LC-MS: m/z: 268 $(M\text{-}t\text{Bu}+H)^+$

^{1}H-NMR (300 MHz, $CDCl_3$): δ [ppm] = 7.90 (d, *J* = 1.7 Hz, 1 H), 7.81 (d, *J* = 8.5 Hz, 1 H), 7.71 (dd *J* = 8.4 Hz, *J* = 2.0 Hz, 1 H), 4.46 (d, *J* = 2.6 Hz, 2 H), 1.52 (s, 9 H).

^{13}C-NMR (76 MHz, $CDCl_3$): δ [ppm] = 152.5, 146.2, 144.2, 153.1, 133.1, 131.6, 129.7, 127.0, 122.9, 115.4, 107.5, 83.38, 73.21, 39.02, 28.12.

4-(Prop-2-yn-1-ylamino)-2-(trifluoromethyl)benzonitrile 6.4

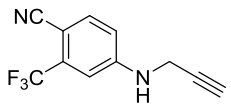

Tert-butyl (4-cyano-3-(trifluoromethyl)phenyl)(prop-2-yn-1-yl)carbamate **6.3** (65 mg, 0.200 mmol) was dissolved in DCM (2 mL), TFA was added (1 mL) and the mixture was stirred at room temperature for 16 h. The reaction was quenched with water and extracted three times with DCM. The combined organic layers were carefully washed with saturated $NaHCO_3$ solution, dried over Na_2SO_4, concentrated *in vacuo* and purified *via* automated flash chromatography (PE/EtOAc). The title compound was obtained as a slightly yellow solid (43 mg, 0.192 mmol, 96%).

LC-MS: m/z: 225 $(M+H)^+$

^{1}H-NMR (300 MHz, $CDCl_3$): δ [ppm] = 7.63 (d, *J* = 8.6 Hz, 1 H), 6.97 (d, *J* = 2.2 Hz, 1 H), 6.82 (dd, *J* = 8.6 Hz, *J* = 2.3 Hz, 1 H), 4.86 (bs, 1 H), 4.03 (dd, *J* = 5.8 Hz, *J* = 2.4 Hz, 2 H), 2.30 (t, *J* = 2.4 Hz, 1 H).

4-(((1-(4-Phenoxyphenyl)-1*H*-1,2,3-triazol-4-yl)methyl)amino)-2-(trifluoromethyl)benzonitrile 6.5

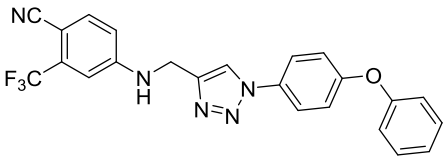

4-(Prop-2-yn-1-ylamino)-2-(trifluoromethyl)benzonitrile **6.4** (16 mg, 0.071 mmol) and 1-azido-4-phenoxybenzene (15 mg, 0.071 mmol) were dissolved in H_2O/*t*BuOH (1:1, 1 mL) and DIPEA was added (0.1 mL, 76 mg, 0.589 mmol). The reaction mixture was purged with argon for 10 min and Na ascorbate (1.2 mg, 0.006 mmol) and $CuSO_4 \cdot 5\ H_2O$ (1.5 mg, 0.006 mmol) were added. The mixture was then purged with argon for 5 min and stirred at 40 °C for 18 h. Then, 1 M HCl was added and the mixture was extracted with EtOAc three times. The combined organic layers were washed with brine, dried over Na_2SO_4 and concentrated *in vacuo*. The crude product was purified *via* automated flash chromatography (PE/EtOAc) and afforded the title compound as a colorless solid (8.6 mg, 0.020 mmol, 28%).

^{1}H-NMR (300 MHz, $CDCl_3$): δ [ppm] = 7.87 (s, 1 H), 7.67 – 7.63 (m, 2 H), 7.61 (d, *J* = 8.7 Hz, 1 H), 7.43 – 7.39 (m, 2 H), 7.22 – 7.17 (m, 1 H), 7.16 – 7.11 (m, 2 H), 7.10 – 7.13 (m, 2 H), 6.99 (d, *J* = 2.2 Hz, 1 H), 8.83 (dd, *J* = 8.7 Hz, *J* = 2.2 Hz, 1 H), 5.25 (bs, 1 H), 4.61 (d, *J* = 5.5 Hz, 2 H).

^{13}C-NMR (76 MHz, $CDCl_3$): δ [ppm] = 158.3, 156.1, 150.3, 144.3, 136.3, 131.8, 130.1, 124.3, 122.4, 119.9, 119.5, 119.2, 116.8, 114.2, 110.6, 96.74, 39.00.

HRMS (ESI): $C_{23}H_{17}F_3N_5O^+$ $(M+H)^+$ calculated: 436.13797 found: 436.13721

6-Bromo-2-(trichloromethyl)-4-(trifluoromethyl)-1*H*-benzo[d]imidazole 6.8

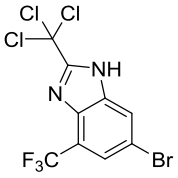

5-Bromo-3-(trifluoromethyl)benzene-1,2-diamine (2.55 g, 10.0 mmol) was dissolved in HOAc (26 mL) and methyl 2,2,2-trichloroacetimidate (1.49 mL, 2.12 g, 12.0 mmol) was added. The mixture was stirred at room temperature for 2 h and H_2O was added. After extraction with EtOAc, the combined organic layers were washed with brine and saturated $NaHCO_3$ solution. The organic layer was dried

over Na_2SO_4 and the solvent was removed *in vacuo*. The title compound was obtained as a white solid (3.81, 9.97 mmol, > 98%).

LC-MS: m/z: 383 $(M+H)^+$

Methyl 6-bromo-4-(trifluoromethyl)-1*H*-benzo[d]imidazole-2-carboxylate 6.7

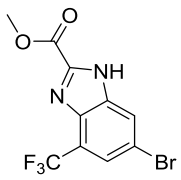

6-Bromo-2-(trichloromethyl)-4-(trifluoromethyl)-1*H*-benzo[d]imidazole **6.8** (3.81 g, 9.97 mmol) was dissolved in MeOH (100 mL) and Na_2CO_3 (1.69 g, 18.5 mmol) was added. The mixture was stirred for 28 h at room temperature. Then, 1 M HCl was added slowly and the mixture was stirred for 30 min at room temperature. The reaction mixture was extracted with Et_2O three times, dried over Na_2SO_4, filtered and the solvent was removed under reduced pressure. The title compound was obtained as a yellow solid (3.16 g, 9.78 mmol, 98%) and was used in the next step without further purification.

LC-MS: m/z: 324 $(M+H)^+$

^{1}H-NMR (300 MHz, $CDCl_3$): δ [ppm] = 8.19 (bs, 1 H), 7.82 (bs, 1 H), 4.11 (s, 3 H).

1-(*Tert*-butyl) 2-methyl 6-bromo-4-(trifluoromethyl)-1*H*-benzo[d]imidazole-1,2-dicarboxylate 6.14

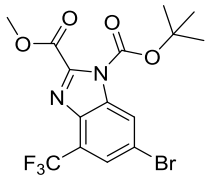

Methyl 6-bromo-4-(trifluoromethyl)-1*H*-benzo[d]imidazole-2-carboxylate **6.7** (1.05 g, 3.25 mmol) was dissolved in DCM followed by the addition of NEt_3 (0.92 mL, 656 mg, 6.50 mmol), DMAP (40 mg, 0.325 mmol) and Boc_2O (1.50 g, 6.50 mmol). The reaction mixture was stirred for 2 h at room temperature and saturated NH_4Cl solution was added. The mixture was extracted with DCM and the combined organic layers were washed with brine and dried over Na_2SO_4. The solvent was removed under reduced pressure and afforded the title compound as a yellow solid (1.37 g, 3.24 mmol, > 98%). The compound was used in the next step without further purification.

LC-MS: m/z: 367 $(M-t\text{Bu}+H)^+$

^{1}H-NMR (300 MHz, $CDCl_3$): δ [ppm] = 8.43 (d, *J* = 1.7 Hz, 1 H), 7.82 (d, *J* = 1.7 Hz, 1 H), 4.05 (s, 3 H), 1.67 (s, 9 H).

^{13}C-NMR (76 MHz, $CDCl_3$): δ [ppm] = 159.3, 151.2, 145.9, 135.5, 125.4, 121.2, 118.7, 87.83, 53.19, 27.29.

2,4-Dinitro-6-(trifluoromethyl)aniline 6.12

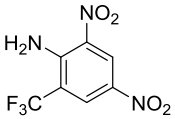

2-Chloro-1,5-dinitro-3-(trifluoromethyl)benzene (540 mg, 2.00 mmol) was dissolved in DMSO (10 mL) and NH_4OH (10 mL) was added. The mixture was degassed with argon for 10 minutes and Cu_2O (28 mg, 20 mol%) and 1,10-phenanthroline (72 mg, 40 mol%) were added. The reaction mixture was then stirred for 21 h at 80 °C (microwave). After cooling to room temperature, H_2O was added and the mixture was extracted three times with EtOAc. The combined organic layers were washed three times with half-saturated NaCl solution, dried over $MgSO_4$, filtered and concentrated *in vacuo*. The title compound was obtained as a colorless solid The crude product was used in the next step without further purification. (465 mg, 1.85 mmol, 93%).

LC-MS: m/z: 252 $(M+H)^+$

^{1}H-NMR (300 MHz, DMSO-d_6): δ [ppm] = 9.31 (s, 1 H), 8.64 (s, 1 H).

Methyl 2-((2,4-dinitro-6-(trifluoromethyl)phenyl)amino)-2-oxoacetate 6.11

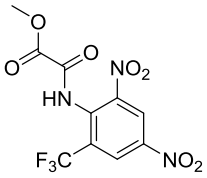

2,4-Dinitro-6-(trifluoromethyl)aniline **6.12** (25 mg, 0.100 mmol) was dissolved in anhydrous DCM (1 mL) followed by the addition of DIPEA (19 µL, 25 mg, 0.110 mmol), and DMAP (1.2 mg, 0.010 mmol). The mixture was cooled to 0 °C and methyl 2-chloro-2-oxoacetate (11 µL, 13.4 mg, 0.110 mmol) was added dropwise. The reaction mixture was stirred for 30 minutes and was allowed to warm to room temperature. Then, saturated NH_4Cl solution was added and the mixture was extracted with EtOAc three times and the combined organic layers were washed with brine, dried over Na_2SO_4, filtered and concentrated under reduced pressure. The title compound was obtained as a colorless solid (332 mg, 0.986 mmol, > 98%). The crude product was used in the next step without further purification.

LC-MS: m/z: 338 $(M+H)^+$

^{1}H-NMR (300 MHz, $CDCl_3$): δ [ppm] = 9.47 (bs, 1 H), 9.05 (d, *J* = 2.4 Hz, 1 H), 8.84 (d, *J* = 2.4 Hz, 1 H), 4.04 (s, 3 H).

^{13}C-NMR (76 MHz, $CDCl_3$): δ [ppm] = 159.2, 154.1, 145.0, 131.9, 128.3, 125.8, 124.6, 122.5, 120.3, 54.82.

Methyl 6-amino-4-(trifluoromethyl)-1*H*-benzo[d]imidazole-2-carboxylate 6.10

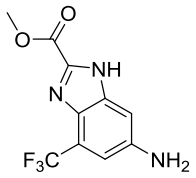

Methyl 2-((2,4-dinitro-6-(trifluoromethyl)phenyl)amino)-2-oxoacetate **6.11** (345 mg, 1.02 mmol) was dissolved in EtOH (5 mL) and the solution was purged with argon for 10 minutes followed by the addition of Pd/C (5.4 mg, 5 mol%). After degassing the mixture for further 10 minutes, H_2 was bubbled through the mixture for 5 minutes. The reaction mixture was then stirred under an H_2 atmosphere for 5 h. Upon filtration over SiO_2 the solvent was removed under reduced pressure and automated flash chromatography (DCM/MeOH) afforded the title compound as a colorless solid (179 mg, 0.690 mmol, 68%).

LC-MS: m/z: 305 $(M+HCOOH)^+$

Mixture of tautomers (1:1)

Tautomer 1:

^{1}H-NMR (300 MHz, $CDCl_3$): δ [ppm] = 8.71 (bs, 1 H), 7.01 – 7.00 (m, 1 H), 6.81 – 6.79 (m, 1 H), 3.17 (s, 3 H).

^{13}C-NMR (76 MHz, $CDCl_3$): δ [ppm] = 163.1, 154.5, 145.3, 143.8, 136.9, 130.3, 111.2, 106.8, 100.5, 53.01

Tautomer 2:

^{1}H-NMR (300 MHz, $CDCl_3$): δ [ppm] = 8.18 (bs, 1 H), 6.81 – 6.80 (m, 1 H), 6.79 – 6.78 (m, 1 H), 3.07 (s, 3 H).

^{13}C-NMR (76 MHz, $CDCl_3$): δ [ppm] = 163.1, 154.5, 145.3, 143.8, 136.9, 130.3, 111.2, 106.8, 100.5, 48.60.

Ethyl 2,4-dihydroxy-6-(trifluoromethyl)nicotinate 6.32

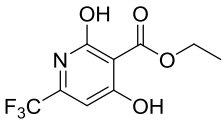

Step 1:

(*E*/*Z*)-3-amino-4,4,4-trifluorobut-2-enoate **6.29** (18.0 g, 98.3 mmol) was dissolved in DCM/pyridine (9:1, 98 mL) and 3-chloro-3-oxopropanoate **6.30** (15.1 mL, 17.8 g, 118 mmol) was added dropwise at 0 °C over a period of 30 minutes. The reaction mixture was stirred at room temperature for 18 h and 1 M HCl was added, followed by extraction with EtOAc. The combined organic layers were dried over $MgSO_4$ and concentrated under reduced pressure.

LC-MS: m/z: 298 $(M+H)^+$

Step 2:

The crude product was then dissolved in EtOH (172 mL) and KO*t*Bu (18.0 g, 0.160 mmol) was added. The mixture was stirred at 80 °C for 18 h. After cooling to room temperature the solvent was evaporated and the title compound was obtained as a colorless solid. The crude product was used in the next step without further purification.

LC-MS: m/z: 252 $(M+H)^+$

^{1}H-NMR (300 MHz, DMSO-d_6): δ [ppm] = 11.97 (bs, 1 H), 9.82 (bs, 1 H), 6.77 (s, 1 H), 4.23 (q, *J* = 7.1 Hz, 2 H), 1.23 (t, *J* = 7.2 Hz, 3 H).

^{13}C-NMR (76 MHz, DMSO-d_6): δ [ppm] = 165.4, 165.0, 162.6, 144.3, 121.1, 106.0, 102.3, 61.05, 14.11.

6-(Trifluoromethyl)pyridine-2,4-diol 6.33

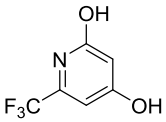

Ethyl 2,4-dihydroxy-6-(trifluoromethyl)nicotinate **6.32** was dissolved in 6 M HCl (210 mL) and stirred at 100 °C for 23 h. After cooling to room temperature, H_2O was added and the reaction mixture was extracted five times with Et_2O. The combined organic layers were dried over $MgSO_4$ and the solvent was removed under reduced pressure. The title compound was obtained as colorless solid (96.9 g, 54.1 mmol, 55% over 3 steps).

LC-MS: m/z: 180 $(M+H)^+$

^{1}H-NMR (300 MHz, DMSO-d_6): δ [ppm] = 11.57 (bs, 2 H), 6.70 (d, *J* = 1.8 Hz, 1 H), 6.15 (d, *J* = 1.8 Hz, 1 H).

^{13}C-NMR (76 MHz, DMSO-d_6): δ [ppm] = 168.6, 165.9, 144.5, 121.6, 103.1, 98.06.

3-Nitro-6-(trifluoromethyl)pyridine-2,4-diol 6.34

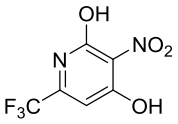

6-(Trifluoromethyl)pyridine-2,4-diol **6.33** (3.92 g, 21.9 mmol) was dissolved in concentrated H_2SO_4 and HNO_3 (70%) was added dropwise. The resulting dark brown solution was stirred for 16 h. The reaction mixture was then poured onto ice and H_2O was added carefully. The mixture was stirred for 30 minutes, followed by extraction with Et_2O. The combined organic layers were washed with brine, dried over $MgSO_4$ and concentrated *in vacuo*. The title compound was obtained as a yellow solid (4.84 g, 21.6 mmol, > 98%) and used in the next step without further purification.

LC-MS: m/z: 225 $(M+H)^+$

^{1}H-NMR (300 MHz, DMSO-d_6): δ [ppm] = 6.81 (s, 1 H).

^{13}C-NMR (76 MHz, DMSO-d_6): δ [ppm] = 159.4, 157.2, 143.1, 126.9, 120.5, 102.4.

4-Chloro-3-nitro-6-(trifluoromethyl)pyridin-2-ol 6.28

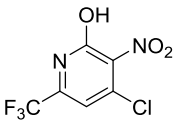

3-Nitro-6-(trifluoromethyl)pyridine-2,4-diol **6.34** (4.84 g, 21.6 mmol) was dissolved in $PhPOCl_2$ (15 mL, 108 mmol) and stirred for 5 h at 100 °C. The reaction mixture was allowed to cool to room temperature and carefully poured onto ice. After stirring for 30 minutes the mixture was extracted with Et_2O and the combined organic layers were washed with brine, dried over Na_2SO_4, filtered and concentrated *in vacuo*. Automated flash chromatography (PE/EtOAc) afforded the title compound as a yellow solid (4.66 g, 19.2 mmol, 89%)

LC-MS: m/z: 243 $(M+H)^+$

^{1}H-NMR (300 MHz, DMSO-d_6): δ [ppm] = 7.75 (s, 1 H).

^{13}C-NMR (76 MHz, DMSO-d_6): δ [ppm] = 156.7, 144.7, 137.6, 136.5, 120.0, 113.4.

3-Nitro-4-(prop-2-yn-1-ylamino)-6-(trifluoromethyl)pyridin-2-ol 6.27

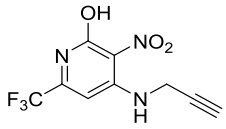

4-Chloro-3-nitro-6-(trifluoromethyl)pyridin-2-ol **6.28** (945 mg, 3.89 mmol) was dissolved in anhydrous THF (10 mL) and DIPEA (0.73 mL, 552 mg, 4.30 mmol) was added. After stirring at room temperature for 30 minutes, propargylamine (0.55 mL, 471 mg, 8.56 mmol) was added. The reaction mixture was stirred for 18 h at room temperature and then, saturated NH_4Cl solution was added. The mixture was extracted three times with EtOAc and the combined organic layers were washed with brine, dried over Na_2SO_4 and concentrated *in vacuo*. Automated flash chromatography (PE/EtOAc) afforded the title compound as an off-white solid (486 mg, 1.86 mmol, 48%).

LC-MS: m/z: 262 $(M+H)^+$

^{1}H-NMR (300 MHz, DMSO-d_6): δ [ppm] = 8.65 (bs, 1 H), 6.47 (s, 1 H), 4.27 (dd, *J* = 5.8 Hz, *J* = 2.4 Hz, 2 H), 3.34 (t, *J* = 2.4 Hz, 1 H).

^{13}C-NMR (76 MHz, DMSO-d_6): δ [ppm] = 161.7, 150.3, 146.9, 132.6, 121.2, 119.9, 99.75, 79.47, 75.06, 32.18.

3-Nitro-4-(((1-(4-phenoxyphenyl)-1*H*-1,2,3-triazol-4-yl)methyl)amino)-6-(trifluoromethyl)pyridin-2-ol 6.35

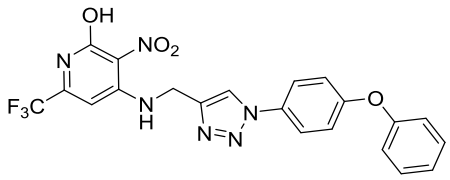

3-Nitro-4-(prop-2-yn-1-ylamino)-6-(trifluoromethyl)pyridin-2-ol **6.27** (275 mg, 1.05 mmol) was dissolved in H_2O/*t*BuOH (1:1, 10 mL) and DIPEA (0.36 mL, 274 mg, 2.10 mmol) was added. The reaction was purged with argon and 1-azido-4-phenoxybenzene (222 mg, 1.05 mmol), Na ascorbate (42 mg, 20 mol%) and $CuSO_4 \cdot 5\ H_2O$ (26 mg, 10 mol%) were added. The reaction mixture was stirred for 15 h and 1 M HCl was added, followed by extraction with EtOAc. The combined organic layers were washed with brine, dried over Na_2SO_4 and the solvent was removed *in vacuo*. Automated flash chromatography (DCM/MeOH) afforded the title compound as a brownish solid (317 mg, 0.672 mmol, 64%).

LC-MS: m/z: 473 $(M+H)^+$

^{1}H-NMR (300 MHz, DMSO-d_6): δ [ppm] = 8.68 (s, 1 H), 8.54 (t, *J* = 5.8 Hz, 1 H), 7.88 – 7.85 (m, 2 H), 7.61 (s, 1 H), 7.46 – 7.41 (m, 2 H), 7.22 – 7.20 (m, 1 H), 7.19 – 7.17 (m, 2 H), 7.11 – 7.08 (m, 2 H), 4.75 (d, *J* = 5.8 Hz, 2 H).

^{13}C-NMR (76 MHz, DMSO-d_6): δ [ppm] = 156.9, 155.9, 148.4, 145.9, 144.1, 142.6, 132.7, 131.9, 131.6, 130.3, 129.8, 128.9, 128.8, 124.2, 122.1, 121.6, 120.6, 119.3, 119.2, 106.7, 37.97.

2-Chloro-3-nitro-*N*-((1-(4-phenoxyphenyl)-1*H*-1,2,3-triazol-4-yl)methyl)-6-(trifluoromethyl)pyridin-4-amine 6.26

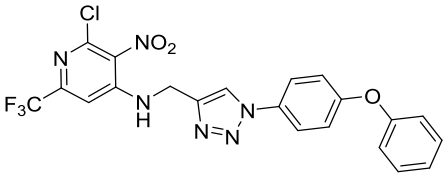

3-Nitro-4-(((1-(4-phenoxyphenyl)-1*H*-1,2,3-triazol-4-yl)methyl)amino)-6-(trifluoromethyl)pyridin-2-ol **6.35** (130 mg, 0.275 mmol) was dissolved in $PhPOCl_2$ (1.5 mL) and stirred for 5 h at 80 °C. The mixture was allowed to cool to room temperature and then carefully poured onto ice. EtOAc was added and the mixture was stirred for 15 min. The phases were separated and the aqueous phase was extracted twice with EtOAc. The combined organic layers were washed with brine and dried over Na_2SO_4, filtered and concentrated *in vacuo*. The crude product was purified using automated flash chromatography (DCM/MeOH) and afforded the title compound as a yellowish solid (108 mg, 0.220 mmol, 80%).

LC-MS: m/z: 491 $(M+H)^+$

^{1}H-NMR (300 MHz, acetone-d_6): δ [ppm] = 8.56 (s, 1 H), 7.87 (bs, 1 H), 7.86 – 7.83 (m, 2 H), 7.73 (s, 1 H), 7.46 – 7.42 (m, 2 H), 7.22 – 7.20 (m, 1 H), 7.19 – 7.15 (m, 2 H), 7.11 – 7.09 (m, 2 H), 4.96 (s, 2 H).

^{13}C-NMR (76 MHz, acetone-d_6): δ [ppm] = 158.8, 150.1, 145.1, 144.9, 131.1, 125.1, 123.1, 122.1, 120.3, 120.2, 107.3, 39.48.

3-Nitro-N^4-((1-(4-phenoxyphenyl)-1*H*-1,2,3-triazol-4-yl)methyl)-6-(trifluoromethyl)pyridine-2,4-diamine 6.36

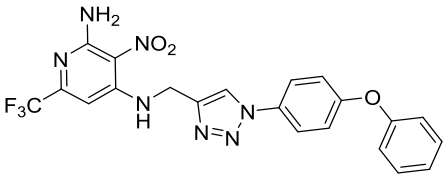

2-Chloro-3-nitro-*N*-((1-(4-phenoxyphenyl)-1*H*-1,2,3-triazol-4-yl)methyl)-6-(trifluoromethyl)pyridin-4-amine **6.26** (98 mg, 0.200 mmol) were dissolved in 1,4-dioxane (1 mL) and NH_4OH (1 mL). The reaction

mixture was purged with argon and Cu_2O (2.9 mg, 10 mol%) and 1,10-phenanthroline (7.2 mg, 20 mol%) were added. The mixture was purged with argon and stirred for 1 h at 100 °C (microwave). The crude mixture was filtered over SiO_2 and automated flash chromatography (DCM/MeOH) afforded the title compound as an off-white solid (68.3 mg, 0.145 mmol, 72%).

LC-MS: m/z: 472 $(M+H)^+$

^{1}H-NMR (300 MHz, $CDCl_3$): δ [ppm] = 9.61 (bs, 1 H), 7.91 (s, 1 H), 7.69 – 7.65 (m, 2 H), 7.42 – 7.38 (m, 2 H), 7.21 – 7.18 (m, 1 H), 7.16 – 7.12 (m, 2 H), 7.10 – 7.06 (m, 2 H), 6.59 (s, 1 H), 4.78 (d, *J* = 5.3 Hz).

^{13}C-NMR (76 MHz, acetone-d_6): δ [ppm] = 158.8, 156.4, 150.1, 144.8, 144.2, , 125.1, 123.1, 122.1, 120.3, 120.2, 112.6, 107.3, 39.49.

Methyl 2-((3-nitro-4-(((1-(4-phenoxyphenyl)-1H-1,2,3-triazol-4-yl)methyl)amino)-6-(trifluoromethyl)pyridin-2-yl)amino)-2-oxoacetate 6.39

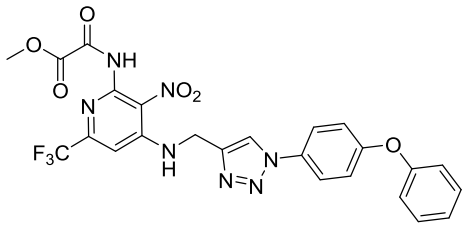

3-Nitro-*N*^{4}-((1-(4-phenoxyphenyl)-1*H*-1,2,3-triazol-4-yl)methyl)-6-(trifluoromethyl)pyridine-2,4-diamine **6.36** (77 mg, 0.163 mmol) was dissolved in anhydrous DCM (1.6 mL) followed by the addition of DIPEA (33 µL, 0.196 mmol) and DMAP (2.4 mg, 0.020 mmol). The mixture was cooled to 0 °C and methyl 2-chloro-2-oxoacetate (18 µL, 0.196 mmol) was added slowly to the solution. While stirring for 3 h, the mixture was allowed to warm to room temperature and H_2O was added. The mixture was extracted with EtOAc and the combined organic layers were washed with saturated NH_4Cl solution and brine. The organic layer was dried over Na_2SO_4, filtered and the solvent was removed under reduced pressure. The title compound was afforded as an off-white solid (72.7 mg, 0.130 mmol, 80%).

LC-MS: m/z: 558 $(M+H)^+$

^{1}H-NMR (300 MHz, $CDCl_3$): δ [ppm] = 9.61 (bs, 1 H), 7.91 (s, 1 H), 7.69 – 7.65 (m, 2 H), 7.42 – 7.38 (m, 2 H), 7.21 – 7.18 (m, 1 H), 7.16 – 7.12 (m, 2 H), 7.10 – 7.06 (m, 2 H), 6.59 (s, 1 H), 4.78 (d, *J* = 5.3 Hz).

7. References

(1) Kraker, M. E. A. de; Stewardson, A. J.; Harbarth, S. Will 10 Million People Die a Year due to Antimicrobial Resistance by 2050? *PLoS Medicine* **2016**, *13*.

(2) Lakemeyer, M.; Zhao, W.; Mandl, F. A.; Hammann, P.; Sieber, S. A. Thinking Outside the Box-Novel Antibacterials To Tackle the Resistance Crisis. *Angewandte Chemie (International ed. in English)* **2018**, *57*, 14440–14475.

(3) Lyddiard, D.; Jones, G. L.; Greatrex, B. W. Keeping it simple: lessons from the golden era of antibiotic discovery. *FEMS microbiology letters* **2016**, *363*.

(4) Cooper, M. A.; Shlaes, D. Fix the antibiotics pipeline. *Nature* **2011**, *472*, 32.

(5) Renwick, M.; Mossialos, E. What are the economic barriers of antibiotic R&D and how can we overcome them? *Expert opinion on drug discovery* **2018**, *13*, 889–892.

(6) Årdal, C.; Balasegaram, M.; Laxminarayan, R.; McAdams, D.; Outterson, K.; Rex, J. H.; Sumpradit, N. Antibiotic development - economic, regulatory and societal challenges. *Nature reviews. Microbiology* [Online early access]. DOI: 10.1038/s41579-019-0293-3.

(7) CVM, F. D.A. 2015 Summary Report on Antimicrobials Sold or Distributed for Use in Food-Producing Animals.

(8) CVM/FDA/DS. 2018 Summary Report On Antimicrobials Sold or Distributed for Use in Food-Producing Animals.

(9) Cdc. What Exactly is Antibiotic Resistance? https://www.cdc.gov/drugresistance/about.html (accessed June 8, 2020).

(10) Davies, J.; Davies, D. Origins and evolution of antibiotic resistance. *Microbiology and molecular biology reviews : MMBR* **2010**, *74*, 417–433.

(11) Crofts, T. S.; Gasparrini, A. J.; Dantas, G. Next-generation approaches to understand and combat the antibiotic resistome. *Nature reviews. Microbiology* **2017**, *15*, 422–434.

(12) D'Costa, V. M.; McGrann, K. M.; Hughes, D. W.; Wright, G. D. Sampling the antibiotic resistome. *Science (New York, N.Y.)* **2006**, *311*, 374–377.

(13) Perry, J. A.; Westman, E. L.; Wright, G. D. The antibiotic resistome: what's new? *Current opinion in microbiology* **2014**, *21*, 45–50.

(14) Blair, J. M. A.; Webber, M. A.; Baylay, A. J.; Ogbolu, D. O.; Piddock, L. J. V. Molecular mechanisms of antibiotic resistance. *Nature reviews. Microbiology* **2015**, *13*, 42–51.

(15) Flemming, H.-C.; Wingender, J. The biofilm matrix. *Nature reviews. Microbiology* **2010**, *8*, 623–633.

(16) Wagner, S.; Sommer, R.; Hinsberger, S.; Lu, C.; Hartmann, R. W.; Empting, M.; Titz, A. Novel Strategies for the Treatment of Pseudomonas aeruginosa Infections. *Journal of medicinal chemistry* **2016**, *59*, 5929–5969.

(17) Flemming, H.-C.; Wingender, J. Relevance of microbial extracellular polymeric substances (EPSs) - Part I: Structural and ecological aspects. *Water Science and Technology* **2001**, *43*, 1–8.

(18) Drenkard, E. Antimicrobial resistance of Pseudomonas aeruginosa biofilms. *Microbes and infection* **2003**, *5*, 1213–1219.

(19) MacLeod, D. L.; Nelson, L. E.; Shawar, R. M.; Lin, B. B.; Lockwood, L. G.; Dirk, J. E.; Miller, G. H.; Burns, J. L.; Garber, R. L. Aminoglycoside-resistance mechanisms for cystic fibrosis Pseudomonas aeruginosa isolates are unchanged by long-term, intermittent, inhaled tobramycin treatment. *The Journal of infectious diseases* **2000**, *181*, 1180–1184.

(20) Prickett, M. H.; Hauser, A. R.; McColley, S. A.; Cullina, J.; Potter, E.; Powers, C.; Jain, M. Aminoglycoside resistance of Pseudomonas aeruginosa in cystic fibrosis results from convergent evolution in the mexZ gene. *Thorax* **2017**, *72*, 40–47.

(21) Wilton, M.; Charron-Mazenod, L.; Moore, R.; Lewenza, S. Extracellular DNA Acidifies Biofilms and Induces Aminoglycoside Resistance in Pseudomonas aeruginosa. *Antimicrobial agents and chemotherapy* **2016**, *60*, 544–553.

(22) Shigeta, M.; Tanaka, G.; Komatsuzawa, H.; Sugai, M.; Suginaka, H.; Usui, T. Permeation of antimicrobial agents through Pseudomonas aeruginosa biofilms: a simple method. *Chemotherapy* **1997**, *43*, 340–345.

(23) Rehman, A.; Patrick, W. M.; Lamont, I. L. Mechanisms of ciprofloxacin resistance in Pseudomonas aeruginosa: new approaches to an old problem. *Journal of medical microbiology* **2019**, *68*, 1–10.

(24) Suci, P. A.; Mittelman, M. W.; Yu, F. P.; Geesey, G. G. Investigation of ciprofloxacin penetration into Pseudomonas aeruginosa biofilms. *Antimicrobial agents and chemotherapy* **1994**, *38*, 2125–2133.

(25) Vrany, J. D.; Stewart, P. S.; Suci, P. A. Comparison of recalcitrance to ciprofloxacin and levofloxacin exhibited by Pseudomonas aeruginosa bofilms displaying rapid-transport characteristics. *Antimicrob. Agents Chemother.* **1997**, *41*, 1352–1358.

(26) Walters, M. C.; Roe, F.; Bugnicourt, A.; Franklin, M. J.; Stewart, P. S. Contributions of antibiotic penetration, oxygen limitation, and low metabolic activity to tolerance of Pseudomonas aeruginosa biofilms to ciprofloxacin and tobramycin. *Antimicrob. Agents Chemother.* **2003**, *47*, 317–323.

(27) Brooun, A.; Liu, S.; Lewis, K. A dose-response study of antibiotic resistance in Pseudomonas aeruginosa biofilms. *Antimicrob. Agents Chemother.* **2000**, *44*, 640–646.

(28) Calvert, M. B.; Jumde, V. R.; Titz, A. Pathoblockers or antivirulence drugs as a new option for the treatment of bacterial infections. *Beilstein journal of organic chemistry* **2018**, *14*, 2607–2617.

(29) Clatworthy, A. E.; Pierson, E.; Hung, D. T. Targeting virulence: a new paradigm for antimicrobial therapy. *Nature chemical biology* **2007**, *3*, 541–548.

(30) Dickey, S. W.; Cheung, G. Y. C.; Otto, M. Different drugs for bad bugs: antivirulence strategies in the age of antibiotic resistance. *Nature reviews. Drug discovery* **2017**, *16*, 457–471.

(31) Empting, M. Trendbericht Biochemie 2017: Pathoblocker - Ein neues Konzept gegen bakterielle Infektionen. *Nachr. Chem.* **2018**, *66*, 290–294.

(32) Garland, M.; Loscher, S.; Bogyo, M. Chemical Strategies To Target Bacterial Virulence. *Chemical reviews* **2017**, *117*, 4422–4461.

(33) Fleitas Martínez, O.; Cardoso, M. H.; Ribeiro, S. M.; Franco, O. L. Recent Advances in Anti-virulence Therapeutic Strategies With a Focus on Dismantling Bacterial Membrane Microdomains, Toxin Neutralization, Quorum-Sensing Interference and Biofilm Inhibition. *Frontiers in cellular and infection microbiology* **2019**, *9*, 74.

(34) Heras, B.; Scanlon, M. J.; Martin, J. L. Targeting virulence not viability in the search for future antibacterials. *British journal of clinical pharmacology* **2015**, *79*, 208–215.

(35) Rasko, D. A.; Sperandio, V. Anti-virulence strategies to combat bacteria-mediated disease. *Nature reviews. Drug discovery* **2010**, *9*, 117–128.

(36) Ruer, S.; Pinotsis, N.; Steadman, D.; Waksman, G.; Remaut, H. Virulence-targeted Antibacterials: Concept, Promise, and Susceptibility to Resistance Mechanisms. *Chemical biology & drug design* **2015**, *86*, 379–399.

(37) Bilitewski, U.; Blodgett, J. A. V.; Duhme-Klair, A.-K.; Dallavalle, S.; Laschat, S.; Routledge, A.; Schobert, R. Chemical and Biological Aspects of Nutritional Immunity-Perspectives for New Anti-Infectives that Target Iron Uptake Systems. *Angewandte Chemie (International ed. in English)* **2017**, *56*, 14360–14382.

(38) Defoirdt, T. Quorum-Sensing Systems as Targets for Antivirulence Therapy. *Trends in microbiology* **2018**, *26*, 313–328.

(39) Johnson, B. K.; Abramovitch, R. B. Small Molecules That Sabotage Bacterial Virulence. *Trends in pharmacological sciences* **2017**, *38*, 339–362.

(40) Allen, R. C.; Popat, R.; Diggle, S. P.; Brown, S. P. Targeting virulence: can we make evolution-proof drugs? *Nature reviews. Microbiology* **2014**, *12*, 300–308.

(41) García-Contreras, R.; Martínez-Vázquez, M.; Velázquez Guadarrama, N.; Villegas Pañeda, A. G.; Hashimoto, T.; Maeda, T.; Quezada, H.; Wood, T. K. Resistance to the quorum-quenching compounds

brominated furanone C-30 and 5-fluorouracil in Pseudomonas aeruginosa clinical isolates. *Pathogens and disease* **2013**, *68*, 8–11.

(42) Navalkele, B. D.; Chopra, T. Bezlotoxumab: an emerging monoclonal antibody therapy for prevention of recurrent Clostridium difficile infection. *Biologics : targets & therapy* **2018**, *12*, 11–21.

(43) Aridis Pharmaceuticals | AR-301 (Salvecin®). https://www.nobelprize.org/uploads/2018/06/press-10.pdf (accessed June 8, 2020).

(44) Rezzoagli, C.; Archetti, M.; Baumgartner, M.; Kümmerli, R. *Combining antibiotics with antivirulence compounds is effective and can reverse selection for antibiotic resistance in Pseudomonas aeruginosa* 9, 2019.

(45) Lewis, K. Platforms for antibiotic discovery. *Nature reviews. Drug discovery* **2013**, *12*, 371–387.

(46) Lewis, K. Antibiotics: Recover the lost art of drug discovery. *Nature* **2012**, *485*, 439–440.

(47) Brown, E. D.; Wright, G. D. Antibacterial drug discovery in the resistance era. *Nature* **2016**, *529*, 336–343.

(48) Nathan, C.; Goldberg, F. M. Outlook: the profit problem in antibiotic R&D. *Nature reviews. Drug discovery* **2005**, *4*, 887–891.

(49) Waring, M. J.; Arrowsmith, J.; Leach, A. R.; Leeson, P. D.; Mandrell, S.; Owen, R. M.; Pairaudeau, G.; Pennie, W. D.; Pickett, S. D.; Wang, J.*; et al.* An analysis of the attrition of drug candidates from four major pharmaceutical companies. *Nature reviews. Drug discovery* **2015**, *14*, 475–486.

(50) Prentis, R. A.; Lis, Y.; Walker, S. R. Pharmaceutical innovation by the seven UK-owned pharmaceutical companies (1964-1985). *British journal of clinical pharmacology* **1988**, *25*, 387–396.

(51) Kola, I.; Landis, J. Can the pharmaceutical industry reduce attrition rates? *Nature reviews. Drug discovery* **2004**, *3*, 711–715.

(52) Campbell, I. B.; Macdonald, S. J. F.; Procopiou, P. A. Medicinal chemistry in drug discovery in big pharma: past, present and future. *Drug discovery today* **2018**, *23*, 219–234.

(53) Kerns, E. Pharmaceutical profiling in drug discovery. *Drug discovery today* **2003**, *8*, 316–323.

(54) Kerns, E. H.; Di, L. *Drug-like properties: Concepts, structure design and methods ; from ADME to toxicity optimization*; Academic Press: Amsterdam, Boston, 2008.

(55) Waring, M. J. Lipophilicity in drug discovery. *Expert opinion on drug discovery* **2010**, *5*, 235–248.

(56) Di, L.; Kerns, E. H. Profiling drug-like properties in discovery research. *Current Opinion in Chemical Biology* **2003**, *7*, 402–408.

(57) Wright, P. M.; Seiple, I. B.; Myers, A. G. The evolving role of chemical synthesis in antibacterial drug discovery. *Angewandte Chemie (International ed. in English)* **2014**, *53*, 8840–8869.

(58) Lombardino, J. G.; Lowe, J. A. The role of the medicinal chemist in drug discovery--then and now. *Nature reviews. Drug discovery* **2004**, *3*, 853–862.

(59) Nwaka, S.; Ridley, R. G. Virtual drug discovery and development for neglected diseases through public-private partnerships. *Nature reviews. Drug discovery* **2003**, *2*, 919–928.

(60) Noble Prize in Chemistry 2010.

(61) Torborg, C.; Beller, M. Recent Applications of Palladium-Catalyzed Coupling Reactions in the Pharmaceutical, Agrochemical, and Fine Chemical Industries. *Adv. Synth. Catal.* **2009**, *351*, 3027–3043.

(62) Wu, X.-F.; Anbarasan, P.; Neumann, H.; Beller, M. From noble metal to Nobel Prize: palladium-catalyzed coupling reactions as key methods in organic synthesis. *Angewandte Chemie (International ed. in English)* **2010**, *49*, 9047–9050.

(63) Ruiz-Castillo, P.; Buchwald, S. L. Applications of Palladium-Catalyzed C-N Cross-Coupling Reactions. *Chemical reviews* **2016**, *116*, 12564–12649.

(64) Dorel, R.; Grugel, C. P.; Haydl, A. M. The Buchwald-Hartwig Amination After 25 Years. *Angewandte Chemie (International ed. in English)* **2019**, *58*, 17118–17129.

(65) Brown, D. G.; Boström, J. Analysis of Past and Present Synthetic Methodologies on Medicinal Chemistry: Where Have All the New Reactions Gone? *Journal of medicinal chemistry* **2016**, *59*, 4443–4458.

(66) Boström, J.; Brown, D. G.; Young, R. J.; Keserü, G. M. Expanding the medicinal chemistry synthetic toolbox. *Nature reviews. Drug discovery* **2018**, *17*, 709–727.

(67) Nicolaou, K. C.; Jain, N. F.; Natarajan, S.; Hughes, R.; Solomon, M. E.; Li, H.; Ramanjulu, J. M.; Takayanagi, M.; Koumbis, A. E.; Bando, T. Total Synthesis of Vancomycin Aglycon—Part 2: Synthesis of Amino Acids 1-3 and Construction of the AB-COD-DOE Ring Skeleton. *Angewandte Chemie International Edition* **1998**, *37*, 2714–2716.

(68) Nicolaou, K. C.; Li, H.; Boddy, C. N. C.; Ramanjulu, J. M.; Yue, T.-Y.; Natarajan, S.; Chu, X.-J.; Bräse, S.; Rübsam, F. Total Synthesis of Vancomycin—Part 1: Design and Development of Methodology. *Chem. Eur. J.* **1999**, *5*, 2584–2601.

(69) Nicolaou, K. C.; Mitchell, H. J.; Jain, N. F.; Winssinger, N.; Hughes, R.; Bando, T. Total Synthesis of Vancomycin. *Angewandte Chemie International Edition* **1999**, *38*, 240–244.

(70) Uehling, M. R.; King, R. P.; Krska, S. W.; Cernak, T.; Buchwald, S. L. Pharmaceutical diversification via palladium oxidative addition complexes. *Science (New York, N.Y.)* **2019**, *363*, 405–408.

(71) Kolb, H. C.; Finn, M. G.; Sharpless, K. B. Click Chemistry: Diverse Chemical Function from a Few Good Reactions. *Angewandte Chemie International Edition* **2001**, *40*, 2004–2021.

(72) Hein, C. D.; Liu, X.-M.; Wang, D. Click chemistry, a powerful tool for pharmaceutical sciences. *Pharmaceutical research* **2008**, *25*, 2216–2230.

(73) Kolb, H. C.; Sharpless, K.B. The growing impact of click chemistry on drug discovery. *Drug discovery today* **2003**, *8*, 1128–1137.

(74) Boutureira, O.; Bernardes, G. J. L. Advances in chemical protein modification. *Chemical reviews* **2015**, *115*, 2174–2195.

(75) Hou, J.; Liu, X.; Shen, J.; Zhao, G.; Wang, P. G. The impact of click chemistry in medicinal chemistry. *Expert opinion on drug discovery* **2012**, *7*, 489–501.

(76) Jiang, X.; Hao, X.; Jing, L.; Wu, G.; Kang, D.; Liu, X.; Zhan, P. Recent applications of click chemistry in drug discovery. *Expert opinion on drug discovery* **2019**, *14*, 779–789.

(77) Thirumurugan, P.; Matosiuk, D.; Jozwiak, K. Click chemistry for drug development and diverse chemical-biology applications. *Chemical reviews* **2013**, *113*, 4905–4979.

(78) Gehringer, M.; Laufer, S. A. Click Chemistry: Novel Applications in Cell Biology and Drug Discovery. *Angewandte Chemie International Edition* **2017**, *56*, 15504–15505.

(79) Blakemore, D. C.; Castro, L.; Churcher, I.; Rees, D. C.; Thomas, A. W.; Wilson, D. M.; Wood, A. Organic synthesis provides opportunities to transform drug discovery. *Nature chemistry* **2018**, *10*, 383–394.

(80) Russell, M. G.; Jamison, T. F. Seven-Step Continuous Flow Synthesis of Linezolid Without Intermediate Purification. *Angewandte Chemie (International ed. in English)* **2019**, *58*, 7678–7681.

(81) Webb, T. R. Improving the Efficiency of the Drug Development by Expanding the Scope of the Role of Medicinal Chemists in Drug Discovery. *ACS medicinal chemistry letters* **2018**, *9*, 1153–1155.

(82) Lu, C.; Kirsch, B.; Zimmer, C.; Jong, J. C. de; Henn, C.; Maurer, C. K.; Müsken, M.; Häussler, S.; Steinbach, A.; Hartmann, R. W. Discovery of antagonists of PqsR, a key player in 2-alkyl-4-quinolone-dependent quorum sensing in Pseudomonas aeruginosa. *Chemistry & biology* **2012**, *19*, 381–390.

(83) Storz, M. P.; Maurer, C. K.; Zimmer, C.; Wagner, N.; Brengel, C.; Jong, J. C. de; Lucas, S.; Müsken, M.; Häussler, S.; Steinbach, A.*; et al.* Validation of PqsD as an anti-biofilm target in Pseudomonas aeruginosa by development of small-molecule inhibitors. *J. Am. Chem. Soc.* **2012**, *134*, 16143–16146.

(84) Lu, C.; Maurer, C. K.; Kirsch, B.; Steinbach, A.; Hartmann, R. W. Overcoming the unexpected functional inversion of a PqsR antagonist in Pseudomonas aeruginosa: an in vivo potent antivirulence agent targeting pqs quorum sensing. *Angewandte Chemie (International ed. in English)* **2014**, *53*, 1109–1112.

(85) Thomann, A.; Mello Martins, A. G. G. de; Brengel, C.; Empting, M.; Hartmann, R. W. Application of Dual Inhibition Concept within Looped Autoregulatory Systems toward Antivirulence Agents against Pseudomonas aeruginosa Infections. *ACS chemical biology* **2016**, *11*, 1279–1286.

(86) Zender, M.; Witzgall, F.; Kiefer, A.; Kirsch, B.; Maurer, C. K.; Kany, A. M.; Xu, N.; Schmelz, S.; Börger, C.; Blankenfeldt, W.*; et al.* Flexible Fragment Growing Boosts Potency of Quorum-Sensing Inhibitors against Pseudomonas aeruginosa Virulence. *ChemMedChem* **2020**, *15*, 188–194.

(87) Sheldrake, H. M.; Travica, S.; Johansson, I.; Loadman, P. M.; Sutherland, M.; Elsalem, L.; Illingworth, N.; Cresswell, A. J.; Reuillon, T.; Shnyder, S. D.*; et al.* Re-engineering of the duocarmycin structural architecture enables bioprecursor development targeting CYP1A1 and CYP2W1 for biological activity. *Journal of medicinal chemistry* **2013**, *56*, 6273–6277.

(88) Miyaura, N.; Ishiyama, T.; Sasaki, H.; Ishikawa, M.; Sato, M.; Suzuki, A. Palladium-catalyzed inter- and intramolecular cross-coupling reactions of B-alkyl-9-borabicyclo[3.3.1]nonane derivatives with 1-halo-1-alkenes or haloarenes. Syntheses of functionalized alkenes, arenes, and cycloalkenes via a hydroboration-coupling sequence. *J. Am. Chem. Soc.* **1989**, *111*, 314–321.

(89) Prediger, P.; Barbosa, L. F.; Génisson, Y.; Correia, C. R. D. Substrate-directable Heck reactions with arenediazonium salts. The regio- and stereoselective arylation of allylamine derivatives and applications in the synthesis of naftifine and abamines. *The Journal of organic chemistry* **2011**, *76*, 7737–7749.

(90) Kamal, A. A. M.; Petrera, L.; Eberhard, J.; Hartmann, R. W. Structure-functionality relationship and pharmacological profiles of Pseudomonas aeruginosa alkylquinolone quorum sensing modulators. *Organic & biomolecular chemistry* **2017**, *15*, 4620–4630.

(91) Brennan, R. J.; Schiestl, R. H. Aniline and its metabolites generate free radicals in yeast. *Mutagenesis* **1997**, *12*, 215–220.

(92) Bomhard, E. M.; Herbold, B. A. Genotoxic activities of aniline and its metabolites and their relationship to the carcinogenicity of aniline in the spleen of rats. *Critical reviews in toxicology* **2005**, *35*, 783–835.

(93) Khan, M.F.; Wu, X.; Kaphalia, B. S.; Boor, P. J.; Ansari, G.A.S. Acute hematopoietic toxicity of aniline in rats. *Toxicology Letters* **1997**, *92*, 31–37.

(94) M. Firoze Khan, G. A. S. A. CONTRIBUTION OF NITROSOBENZENE TO SPLENIC TOXICITY OF ANILINE. *Journal of Toxicology and Environmental Health, Part A* **2000**, *60*, 263–273.

(95) Doiron, J. E.; Le, C. A.; Ody, B. K.; Brace, J. B.; Post, S. J.; Thacker, N. L.; Hill, H. M.; Breton, G. W.; Mulder, M. J.; Chang, S.*; et al.* Evaluation of 1,2,3-Triazoles as Amide Bioisosteres In Cystic Fibrosis Transmembrane Conductance Regulator Modulators VX-770 and VX-809. *Chem. Eur. J.* **2019**, *25*, 3662–3674.

(96) Ballard, T. E.; Richards, J. J.; Wolfe, A. L.; Melander, C. Synthesis and antibiofilm activity of a second-generation reverse-amide oroidin library: a structure-activity relationship study. *Chem. Eur. J.* **2008**, *14*, 10745–10761.

(97) Tischler, M.; Nasu, D.; Empting, M.; Schmelz, S.; Heinz, D. W.; Rottmann, P.; Kolmar, H.; Buntkowsky, G.; Tietze, D.; Avrutina, O. Braces for the peptide backbone: insights into structure-activity relationships of protease inhibitor mimics with locked amide conformations. *Angewandte Chemie International Edition* **2012**, *51*, 3708–3712.

(98) Goddard-Borger, E. D.; Stick, R. V. An efficient, inexpensive, and shelf-stable diazotransfer reagent: imidazole-1-sulfonyl azide hydrochloride. *Organic letters* **2007**, *9*, 3797–3800.

(99) Barral, K.; Moorhouse, A. D.; Moses, J. E. Efficient conversion of aromatic amines into azides: a one-pot synthesis of triazole linkages. *Organic letters* **2007**, *9*, 1809–1811.

(100) Müller, K.; Faeh, C.; Diederich, F. Fluorine in pharmaceuticals: looking beyond intuition. *Science (New York, N.Y.)* **2007**, *317*, 1881–1886.

(101) Talele, T. T. The "Cyclopropyl Fragment" is a Versatile Player that Frequently Appears in Preclinical/Clinical Drug Molecules. *Journal of medicinal chemistry* **2016**, *59*, 8712–8756.

(102) Lewis, R. V.; Lofthouse, C. Adverse Reactions with β-Adrenoceptor Blocking Drugs. https://link.springer.com/article/10.2165/00002018-199309040-00005 (accessed June 7, 2020).

(103) AR Human Androgen NHR Binding (Agonist Radioligand) Assay, Cerep. https://www.eurofinsdiscoveryservices.com/catalogmanagement/viewitem/AR-Human-Androgen-NHR-Binding-Agonist-Radioligand-Assay-Cerep/933 (accessed June 7, 2020).

(104) alpha1A Human Adrenoceptor GPCR Binding (Antagonist Radioligand) Assay, Cerep. https://www.eurofinsdiscoveryservices.com/catalogmanagement/viewitem/alpha1A-Human-Adrenoceptor-GPCR-Binding-Antagonist-Radioligand-Assay-Cerep/2338 (accessed June 7, 2020).

(105) Stevens, M.; Peigneur, S.; Tytgat, J. Neurotoxins and their binding areas on voltage-gated sodium channels. *Frontiers in pharmacology* **2011**, *2*, 71.

(106) Tyloxapol. https://www.tacholiquin.de/tacholiquin/beratung/tyloxapol (accessed June 8, 2020).

(107) Connon, S. J.; Hegarty, A. F. Stabilised 2,3-Pyridyne Reactive Intermediates of Exceptional Dienophilicity. *Eur. J. Org. Chem.* **2004**, *2004*, 3477–3483.

(108) Searls, T.; McLaughlin, L. W. Synthesis of the analogue nucleoside 3-deaza-2′-deoxycytidine and its template activity with DNA polymerase. *Tetrahedron* **1999**, *55*, 11985–11996.

(109) Cottet, F.; Schlosser, M. Three Chloro(trifluoromethyl)pyridines as Model Substrates for Regioexhaustive Functionalization. *Eur. J. Org. Chem.* **2004**, *2004*, 3793–3798.

(110) Cheung, C. W.; Surry, D. S.; Buchwald, S. L. Mild and highly selective palladium-catalyzed monoarylation of ammonia enabled by the use of bulky biarylphosphine ligands and palladacycle precatalysts. *Organic letters* **2013**, *15*, 3734–3737.

(111) Surry, D. S.; Buchwald, S. L. Selective palladium-catalyzed arylation of ammonia: synthesis of anilines as well as symmetrical and unsymmetrical di- and triarylamines. *J. Am. Chem. Soc.* **2007**, *129*, 10354–10355.

(112) Wolfe, J. P.; Åhman, J.; Sadighi, J. P.; Singer, R. A.; Buchwald, S. L. An Ammonia Equivalent for the Palladium-Catalyzed Amination of Aryl Halides and Triflates. *Tetrahedron Letters* **1997**, *38*, 6367–6370.

(113) Bremer, P. T.; Janda, K. D. Investigating the effects of a hydrolytically stable hapten and a Th1 adjuvant on heroin vaccine performance. *Journal of medicinal chemistry* **2012**, *55*, 10776–10780.

(114) Wentland, M. P.; Lu, Q.; Ganorkar, R.; Zhang, S.-Z.; Jo, S.; Cohen, D. J.; Bidlack, J. M. Redefining the structure-activity relationships of 2,6-methano-3-benzazocines. Part 7: syntheses and opioid receptor properties of cyclic variants of cyclazocine. *Bioorganic & medicinal chemistry letters* **2009**, *19*, 365–368.

(115) Leahy, D. K.; Desai, L. V.; Deshpande, R. P.; Mariadass, A. V.; Rangaswamy, S.; Rajagopal, S. K.; Madhavan, L.; Illendula, S. Development of Two Complementary Syntheses for a Privileged CGRP Receptor Antagonist Substructure. *Org. Process Res. Dev.* **2012**, *16*, 244–249.

(116) Crawford, S. M.; Lavery, C. B.; Stradiotto, M. BippyPhos: a single ligand with unprecedented scope in the Buchwald-Hartwig amination of (hetero)aryl chlorides. *Chem. Eur. J.* **2013**, *19*, 16760–16771.

(117) Young, I. S.; Glass, A.-L.; Cravillion, T.; Han, C.; Zhang, H.; Gosselin, F. Palladium-Catalyzed Site-Selective Amidation of Dichloroazines. *Organic letters* **2018**, *20*, 3902–3906.

(118) DeAngelis, A. J.; Gildner, P. G.; Chow, R.; Colacot, T. J. Generating Active "L-Pd(0)" via Neutral or Cationic π-Allylpalladium Complexes Featuring Biaryl/Bipyrazolylphosphines: Synthetic, Mechanistic, and Structure-Activity Studies in Challenging Cross-Coupling Reactions. *The Journal of organic chemistry* **2015**, *80*, 6794–6813.

(119) Beutner, G. L.; Coombs, J. R.; Green, R. A.; Inankur, B.; Lin, D.; Qiu, J.; Roberts, F.; Simmons, E. M.; Wisniewski, S. R. Palladium-Catalyzed Amidation and Amination of (Hetero)aryl Chlorides under Homogeneous Conditions Enabled by a Soluble DBU/NaTFA Dual-Base System. *Org. Process Res. Dev.* **2019**, *23*, 1529–1537.

(120) Gildner, P. G.; DeAngelis, A.; Colacot, T. J. Palladium-Catalyzed N-Arylation of Cyclopropylamines. *Organic letters* **2016**, *18*, 1442–1445.

(121) Gillis, E. P.; Eastman, K. J.; Hill, M. D.; Donnelly, D. J.; Meanwell, N. A. Applications of Fluorine in Medicinal Chemistry. *Journal of medicinal chemistry* **2015**, *58*, 8315–8359.

(122) Hagmann, W. K. The many roles for fluorine in medicinal chemistry. *Journal of medicinal chemistry* **2008**, *51*, 4359–4369.

(123) Zhou, Y.; Wang, J.; Gu, Z.; Wang, S.; Zhu, W.; Aceña, J. L.; Soloshonok, V. A.; Izawa, K.; Liu, H. Next Generation of Fluorine-Containing Pharmaceuticals, Compounds Currently in Phase II-III Clinical Trials of Major Pharmaceutical Companies: New Structural Trends and Therapeutic Areas. *Chemical reviews* **2016**, *116*, 422–518.

(124) Wang, J.; Sánchez-Roselló, M.; Aceña, J. L.; del Pozo, C.; Sorochinsky, A. E.; Fustero, S.; Soloshonok, V. A.; Liu, H. Fluorine in pharmaceutical industry: fluorine-containing drugs introduced to the market in the last decade (2001-2011). *Chemical reviews* **2014**, *114*, 2432–2506.

(125) Meanwell, N. A. Fluorine and Fluorinated Motifs in the Design and Application of Bioisosteres for Drug Design. *Journal of medicinal chemistry* **2018**, *61*, 5822–5880.

(126) Swallow, S. Fluorine in medicinal chemistry. *Progress in medicinal chemistry* **2015**, *54*, 65–133.

(127) Böhm, H.-J.; Banner, D.; Bendels, S.; Kansy, M.; Kuhn, B.; Müller, K.; Obst-Sander, U.; Stahl, M. Fluorine in medicinal chemistry. *Chembiochem : a European journal of chemical biology* **2004**, *5*, 637–643.

(128) Ma, D.; Cai, Q. l -Proline Promoted Ullmann-Type Coupling Reactions of Aryl Iodides with Indoles, Pyrroles, Imidazoles or Pyrazoles. *Synlett* **2004**, 128–130.

(129) Zhao, C.-r.; Wang, R.-q.; Li, G.; Xue, X.-x.; Sun, C.-j.; Qu, X.-j.; Li, W.-b. Synthesis of indazole based diarylurea derivatives and their antiproliferative activity against tumor cell lines. *Bioorganic & medicinal chemistry letters* **2013**, *23*, 1989–1992.

(130) Anderson, K. W.; Tundel, R. E.; Ikawa, T.; Altman, R. A.; Buchwald, S. L. Monodentate phosphines provide highly active catalysts for Pd-catalyzed C-N bond-forming reactions of heteroaromatic halides/amines and (H)N-heterocycles. *Angewandte Chemie International Edition* **2006**, *45*, 6523–6527.

(131) Brown, D. G.; May-Dracka, T. L.; Gagnon, M. M.; Tommasi, R. Trends and exceptions of physical properties on antibacterial activity for Gram-positive and Gram-negative pathogens. *Journal of medicinal chemistry* **2014**, *57*, 10144–10161.

(132) Ebejer, J.-P.; Charlton, M. H.; Finn, P. W. Are the physicochemical properties of antibacterial compounds really different from other drugs? *Journal of cheminformatics* **2016**, *8*, 30.

(133) da Rosa, R.; Moraes, M. H. de; Zimmermann, L. A.; Schenkel, E. P.; Steindel, M.; Bernardes, L. S. C. Design and synthesis of a new series of 3,5-disubstituted isoxazoles active against Trypanosoma cruzi and Leishmania amazonensis. *European journal of medicinal chemistry* **2017**, *128*, 25–35.

(134) Li, Z.; Bai, X.; Deng, Q.; Zhang, G.; Zhou, L.; Liu, Y.; Wang, J.; Wang, Y. Preliminary SAR and biological evaluation of antitubercular triazolothiadiazine derivatives against drug-susceptible and drug-resistant Mtb strains. *Bioorganic & medicinal chemistry* **2017**, *25*, 213–220.

(135) Kumar, N. N. B.; Kuznetsov, D. M.; Kutateladze, A. G. Intramolecular cycloadditions of photogenerated azaxylylenes with oxadiazoles provide direct access to versatile polyheterocyclic ketopiperazines containing a spiro-oxirane moiety. *Organic letters* **2015**, *17*, 438–441.

(136) Miller, J. F.; Chong, P. Y.; Shotwell, J. B.; Catalano, J. G.; Tai, V. W.-F.; Fang, J.; Banka, A. L.; Roberts, C. D.; Youngman, M.; Zhang, H.*; et al.* Hepatitis C replication inhibitors that target the viral NS4B protein. *Journal of medicinal chemistry* **2014**, *57*, 2107–2120.

(137) Adam, F. M.; Bish, G.; Calo, F.; Carr, C. L.; Castro, N.; Hay, D.; Hodgson, P. B.; Jones, P.; Knight, C. J.; Paradowski, M.*; et al.* Development of a Practical Synthesis of Toll-like Receptor Agonist PF-4171455: 4-Amino-1-benzyl-6-trifluoromethyl-1,3-dihydroimidazo [4,5- c] pyridin-2-one. *Org. Process Res. Dev.* **2011**, *15*, 788–796.

(138) A. S. A. Ahmed, M. Empting, M. Hamed, R. W. Hartmann, J. Haupenthal, T. Hesterkamp, A. A. M. Kamal, C. K. Maurer, T. Röhrig, C. Schütz, S. Yahiaoui, M. Zender. PqsR Inverse Agonists, EP18181475.

(139) C. Schütz, M. Empting, A. S. A. Ahmed, M. Hamed, R. W. Hartmann, T. Röhrig, A. M. Kany, A. K.H. Hirsch. New PqsR Inverse Agonists, EP20150104.

(140) M. Hamed, A. S. A. Ahmed, M. Empting, C. Schütz, R. W. Hartmann, T. Röhrig, A. M. Kany, A. K.H. Hirsch. Novel PqsR Inverse Agonists, EP20150119.

(141) Ho, D.-K.; Murgia, X.; Rossi, C. de; Christmann, R.; Hüfner de Mello Martins, A. G.; Koch, M.; Andreas, A.; Herrmann, J.; Müller, R.; Empting, M.*; et al.* Squalenyl Hydrogen Sulfate Nanoparticles for Simultaneous Delivery of Tobramycin and an Alkylquinolone Quorum Sensing Inhibitor Enable the Eradication of P. aeruginosa Biofilm Infections. *Angewandte Chemie International Edition* [Online early access]. DOI: 10.1002/anie.202001407.

(142) OMPTA – new antibiotics platform - Polyphor. https://www.nobelprize.org/uploads/2018/06/press-10.pdf (accessed June 8, 2020).

(143) Schönauer, E.; Kany, A. M.; Haupenthal, J.; Hüsecken, K.; Hoppe, I. J.; Voos, K.; Yahiaoui, S.; Elsässer, B.; Ducho, C.; Brandstetter, H.*; et al.* Discovery of a Potent Inhibitor Class with High Selectivity toward Clostridial Collagenases. *J. Am. Chem. Soc.* **2017**, *139*, 12696–12703.

(144) Sommer, R.; Wagner, S.; Rox, K.; Varrot, A.; Hauck, D.; Wamhoff, E.-C.; Schreiber, J.; Ryckmans, T.; Brunner, T.; Rademacher, C.*; et al.* Glycomimetic, Orally Bioavailable LecB Inhibitors Block Biofilm Formation of Pseudomonas aeruginosa. *J. Am. Chem. Soc.* **2018**, *140*, 2537–2545.

(145) Wagner, S.; Hauck, D.; Hoffmann, M.; Sommer, R.; Joachim, I.; Müller, R.; Imberty, A.; Varrot, A.; Titz, A. Covalent Lectin Inhibition and Application in Bacterial Biofilm Imaging. *Angewandte Chemie (International ed. in English)* **2017**, *56*, 16559–16564.